

BLOCK COPOLYMERS: SYNTHESIS,  
CHARACTERIZATION AND PROPERTIES

A thesis submitted in accordance with the requirements  
of the University of Liverpool  
for the degree of Doctor in Philosophy

KEVIN JOHN PARR

September 1986

The Donnan Laboratories  
Chemistry Department  
The University of  
Liverpool

TO MY PARENTS

## ACKNOWLEDGEMENTS

The work described in this thesis was carried out under the supervision of Dr G C Eastmond in the Department of Inorganic, Physical and Industrial Chemistry at the University of Liverpool during the period October 1982 to September 1985.

I wish to express my thanks to Dr G C Eastmond for his guidance and encouragement throughout the period of this work and to the members of the Chemistry Department for their help and sometimes witty comments. I would also like to thank the late Dr D H Richards and his colleagues at PERME, Waltham Abbey for valuable discussions and help with the setting up of anionic polymerization methods used in this thesis.

My thanks are also due to Dr J Fergie-Woods for his comments on the manuscript and to Mrs M Foley for typing the manuscript so speedily and efficiently.

Finally I gratefully acknowledge the Ministry of Defence for supporting me financially throughout the period of this study.

## SUMMARY

During the course of the work presented here, it has been shown that it is feasible to use the anionic to free-radical transformation process to produce novel block copolymers, using larger preformed polymer blocks than previously used, to ensure conditions which will impart microphase separation of the blocks in the copolymer. The range of possible monomer combinations that could be used to prepare block copolymers was successfully extended to include various acrylate and methacrylate monomers. The general kinetics of the free-radical carbonyl-halide initiating system were found to be simple under certain conditions. It was observed that the initial activity of the preformed polymer depended on the method of synthesis; high vacuum conditions being the most favourable for the synthesis of high-activity preformed polymers.

A recent approach to block copolymer characterization by gel permeation chromatography proposed by Eastmond and Woo was discussed in relation to the characterization of copolymer synthesis during this work. It was shown that the methacrylate copolymers studied, appeared to have smaller hydrodynamic volumes than expected. These results might indicate the presence of added AB copolymer or homomethacrylate through transfer or a process not yet understood, if the model is applicable to these block

copolymers. If experimental data were compared to a theoretical 'ideal', then it may be possible to study the shrinkage of the copolymer chains in solution by this model. Alternatively, the results might have arisen because the molecular weight distributions for polymethylmethacrylate deviate from that applicable to free-radical polymerization with the simple kinetic model.

A method for determining GPC calibration data for homopolymer was devised, which showed encouraging results based on Eastmond's model. It was concluded that the general concepts used to construct the model were valid, assuming polymer interactions and shrinkage effects are negligible.

From visual, infrared and rheovibron studies, it was found that the cast films of the copolymer prepared had a laminate structure, due to the macroscopic phase separation of the preformed polymer residue and the copolymer, which seemed to vindicate Meier's theoretical and Eastmond's conceptual arguments of macrophase separation. Dynamic mechanical and DSC data, indicated the presence of microphase separation in the copolymers. Rheovibron and dielectric data were also used to determine activation energies of the  $\alpha$ -transition processes for acrylate and methacrylate components.

Tensile experiments showed some interesting features and from these it was concluded that the copolymers studied did not behave as ideal thermoplastic elastomers and that in conjunction with other evidence, it was concluded that there may possibly be processes occurring during the free-radical polymerization which are not fully understood.

## CONTENTS

	<u>PAGE</u>
<u>CHAPTER I</u>	
GENERAL INTRODUCTION	
1.1 Multicomponent Copolymers	1
1.2 Phase Separation and Morphology	3
1.2.1 Thermodynamics of mixing of homo- polymer blends and copolymer blocks	3
1.2.2 Morphology	5
1.2.3 Addition of homopolymer to an AB or ABA block copolymer	8
1.3 Synthesis of Block Copolymers	9
1.3.1 Ionic Polymerization	
a) Anionic Polymerizations	12
b) Cationic Polymerizations	13
1.3.2 Free-Radical Polymerization	14
1.3.3 Traditional Methods for Synthesis of Block Copolymers	18
1.4 Transformation Reactions	23
1.4.1 Anion to Cation Transformation	26
1.4.2 Cation to Anion Transformation	28
1.4.3 Anion to Ziegler-Natta Transformation	29
1.4.4 Anion to Free-Radical Transformation	29
1) Use of Lead Salts	30
2) Use of Mercury Salts	31
3) Use of Metal Carbonyl and Organic Halide Systems	32
1.4.5 Other Metal Carbonyl based Systems	35
1.4.6 Other Transformations	35

PAGE

1.5	Characterization	36
1.5.1	Molecular Weight and Molecular Weight Distributions	39
1.6	General Properties	41
1.6.1	The Glass Transition Temperature (T <sub>g</sub> )	42
1.6.2	Properties of Block Copolymers	43
1.6.3	Applications	45
1.7	Gel Permeation Chromatography (GPC)	46
1.7.1	Separation Process	47
1.7.2	Retention	48
1.7.3	Solute Detection	49
1.7.4	Calibration	49
1.7.5	Calculation of Molecular Weight	50
1.7.6	Applications	51
1.8	Aims of Present Work	52

CHAPTER II

COPOLYMER SYNTHESIS		54
2.1	Experimental	
2.1.1	Purification of Materials	55
i)	Monomers	55
ii)	Initiators	57
iii)	Solvents	57
iv)	Other Materials	58
2.2	Preparation and Purification of brominated Polystyrenes	58
i)	Preparation of the Grignard Reagent	59



	<u>PAGE</u>
ii) Anionic Polymerization of Styrene	
a) Nitrogen Technique	59
b) High Vacuum Technique	60
2.3 Free-radical Homopolymerizations	63
2.3.1 Small Scale Preparations	64
2.4 Copolymerizations	65
2.4.1 Large Scale Preparations	67
2.5 Photoinitiation Apparatus	69
2.6 The High Vacuum System	69
2.7 Concentration of Dimanganese decacarbonyl used in Reaction mixtures	70
2.8 Measurement of Polymerization Rate	71
2.9 Kinetic Studies	
2.9.1 Homopolymerizations	72
2.9.2 Copolymerizations	75

### CHAPTER III

IDENTIFICATION AND CHARACTERIZATION OF BLOCK COPOLYMERS BY GEL PERMEATION CHROMATOGRAPHY	79
3.1 The GPC Instrument	80
3.2 Sample Preparation	80
3.3 Calibration	81
3.4 Detector Response	82
3.5 Copolymer Identification	83
3.6 Chromatogram Analysis	88
3.6.1 Characterization	
3.6.1.1 Copolymer Composition	89
3.6.1.2 Molecular Weight Calibration	89
3.6.1.3 Results and Discussion	92



## GENERAL INTRODUCTION

### 1.1 Multicomponent Copolymers

For a number of years now interest has been growing in the synthesis of multicomponent copolymers, with the aim of tailor-making new polymeric materials that may have desirable properties. The term multicomponent polymer is generally used to describe polymers, which have been prepared from two or more different types of monomer unit and in which like monomer units are attached in long sequences (blocks). Such materials include blends of homopolymers, certain types of copolymer and their blends with one or more homopolymers.

Early attempts at copolymer synthesis resulted in random copolymers formed by the simultaneous polymerization of two or more monomers. The sequential arrangement of monomer units in a random copolymer is statistical and the lengths of these sequences of the different monomers are determined by reaction kinetics; the lengths depend on the reactivity ratios of the monomers and the monomer concentrations.

Later developments in polymer chemistry allowed the synthesis of multicomponent polymers with long sequences of like monomer units to be achieved; these have been

called block copolymers. The simplest copolymer structures based on two different monomers, denoted A and B are given in table 1:1.

Table 1:1

Designation	Monomer Sequence
AB random copolymer	-AABBBBABBAAAB-
AB block copolymer	-AAAABBBB-
ABA block copolymer	-AAABBB-BBAAA-
AB graft copolymer (A <sub>2</sub> B block copolymer)	-AAAAA- B B BBBB-
AB crosslinked polymer (A <sub>2</sub> BA <sub>2</sub> block copolymer)	-AAAAAAA- B B · B B -AAAAAAA-

The main reason for the interest in multicomponent polymers is the manner in which the properties of the final polymer reflect and combine the properties of the homopolymer constituents. Often block copolymers exhibit unique properties that result from the segregation of the components, because of the immiscibility of most different polymers and the fact that blocks are covalently bonded to each other.

The sequential arrangement of the individual blocks is very important, as the overall properties depend on the molecular architecture. The actual arrangement of

the sequential blocks is dictated by the synthetic technique used to prepare block copolymers. Providing microphase separation of the constituents has occurred in the block copolymer, some properties are essentially independent of block sequences, eg, thermal transition and electrical behaviour, while others, eg, elastomeric behaviour and melt rheology are greatly influenced.

## 1.2 Phase Separation and Morphology

### 1.2.1 Thermodynamics of mixing of homopolymer blends and copolymer blocks

The most important factor affecting the thermodynamics of polymer blends and copolymer blocks with respect to other systems is the large molecular weights involved for the respective blocks or polymers. Generally polymers have limited miscibility even when the polymers concerned are chemically similar.

Consider the free energy of mixing  $\Delta G$ , of two monomers A and B in a volume, V,

$$\Delta G = \Delta H - T\Delta S \quad 1.1$$

where  $\Delta H$  and  $\Delta S$  are the enthalpy and entropy of mixing respectively and T is the absolute temperature. For two monomers,  $\Delta S$  is often large and positive due to the large number of molecules present, while the positive  $\Delta H$  is usually small. Since  $\Delta S$  is large and  $\Delta H$  is small, it can be seen from equation 1.1 that  $\Delta G$  is negative

and so mixing is favourable. Here  $\Delta S$  is given by the equation,

$$\Delta S = -R(N_A \ln V_A + N_B \ln V_B) \quad 1.2$$

where  $V_A$  and  $V_B$  are the volume fractions of each component, while  $N_A$  and  $N_B$  are the number of moles of each component. When the monomers are polymerized, the  $\Delta H$  for two non-polar homopolymers is given by

$$\Delta H = V(\delta_A - \delta_B)^2 V_A V_B \quad 1.3$$

where  $\delta_A$ ,  $\delta_B$  are the solubility parameters of the homopolymers involved, owing to the reduction in the number of molecules as the molecular weight of the resulting polymers increases, (giving a reduction in the number of degrees of freedom that each molecule has), the entropy term,  $\Delta S$  must be greatly reduced, ie,  $N_A$  and  $N_B$  become small. This results in  $\Delta G$  being controlled by  $\Delta H$  and not  $\Delta S$ , as was the case with the two monomers alone. The enthalpy term,  $\Delta H$  is positive when  $\delta_A \neq \delta_B$ , therefore with few exceptions, phase separation occurs in homopolymers because they are not miscible, ie,  $\Delta G$  mixing is positive. Exceptions do occur usually when very low molecular weight polymers are added together or there are specific interactions (ie, dipole-dipole interactions between pendant groups on the polymers) between the polymers that can affect the  $\Delta H$  term, and so give  $\Delta G$  mix a negative value. Similar arguments apply to the case of block copolymers (1, 2, 3) where segregation of unlike blocks occurs. The major difference between blends and block copolymers being that in the block copolymers the A and B blocks are chemically bonded to each other and so large scale separation is limited, the domain size is reduced to a similar level as

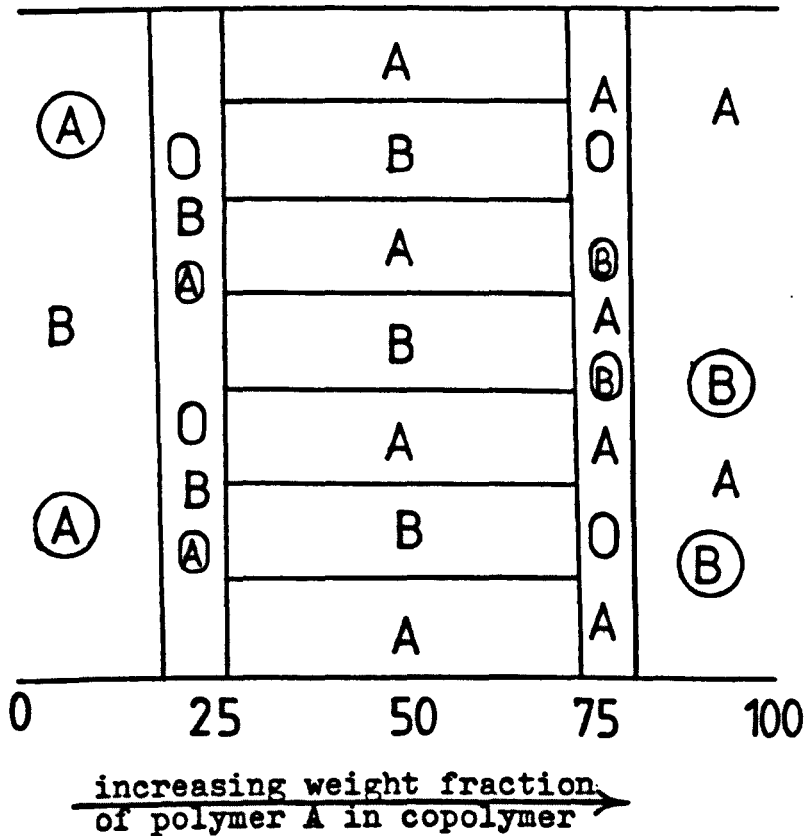
that of molecular dimensions of the copolymer species. This small scale separation of component polymers is given the name 'microphase separation'.(1)

During the last 15-20 years there has been considerable evidence for the occurrence of microphase separation and it is now an accepted phenomenon in many copolymer systems (4, 5, 6).

### 1.2.2 Morphology

Morphology is the term used for the study of the shapes and arrangements of heterogeneities, which have arisen from the microphase separation of the individual components of the system. For an AB or ABA block copolymer there are three basic morphologies, ie, spherical or cylindrical dispersion of a minor component in a matrix of the major component and alternating domains, often referred to as lamellae. If A and B are used to denote the components of the copolymer, figure 1.1 shows the types of morphology clearly.

Figure 1.1



The morphology found in any given sample is dependent on the volume fraction of each block, solvent casting conditions and the thermal history. Meier has predicted the relative compositions of polymers at which the different morphologies would appear, assuming that the chain flexibilities of the polymers A, B were the same and that the two polymers were mutually immiscible.

Changes in morphology can be effected by using preferential casting solvents. The block least soluble in the casting solvent will tend to be the first to 'come out of solution' as the solvent evaporates away. Depending on their volume fraction the block segments will form

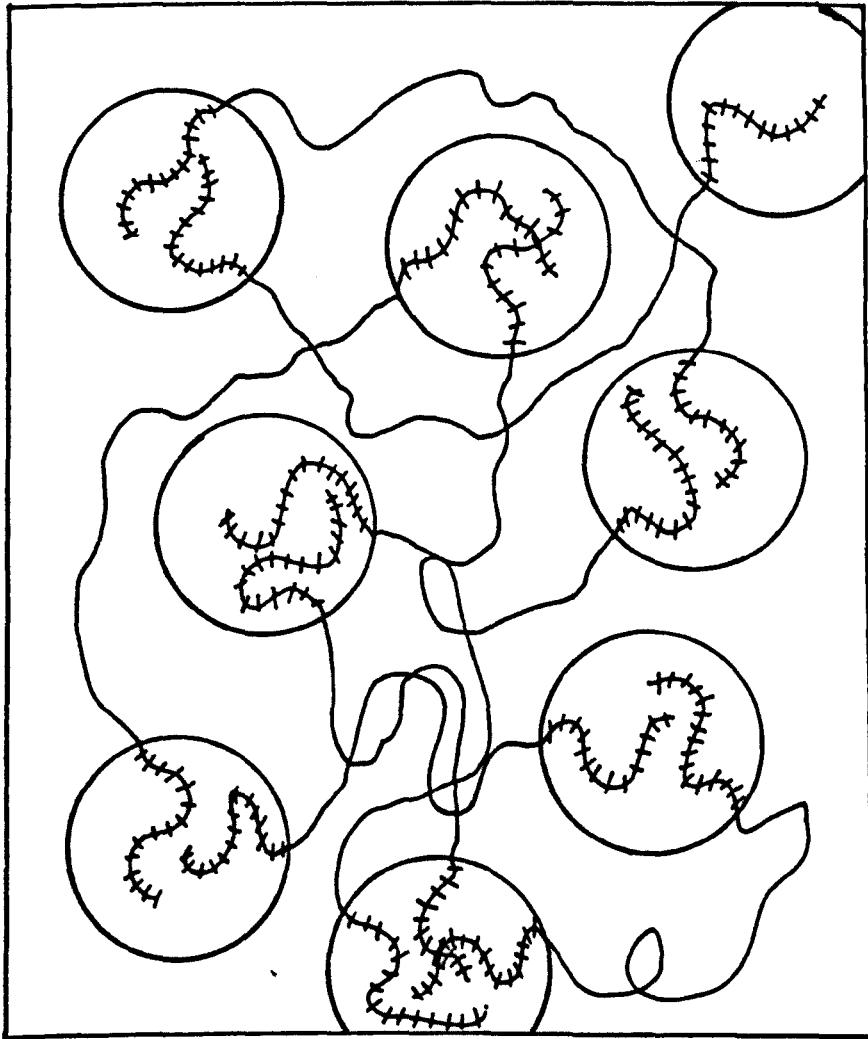


rods or spheres in a continuous matrix of the second block. This effect can be reversed by using a solvent in which the first block is more soluble than the second.

The existence of two phases in a diblock copolymer can be found by using differential scanning calorimetry, modulus-temperature relationships and dielectric relaxations, but the different types of morphology cannot easily be identified. Electron microscopy can be used to identify the type of morphology existing in a block copolymer, in which there are large differences in the electron density of the segments or whose segments can be selectively stained (usually by osmium tetroxide (7), if one constituent polymer has carbon-carbon double bonds in its backbone).

The unique elastomeric properties of some ABA block copolymers are a direct result of the morphologies which they exhibit and these properties have led to the development of some commercially important copolymers. Such materials, where the components have undergone microphase separation require a two phase physical network as in figure 1.2. If the A block is the minor component (spheres) and is 'hard' (ie,  $T_g$  greater than room temperature) and the B block is the major component and 'soft' (ie,  $T_g$  less than room temperature), the polymer would show thermoplastic elastomeric properties. If the positions were reversed with 'hard' polymer A becoming the matrix and the 'soft' polymer B becoming the spheres, the properties

FIG. 1.2



Phase Arrangement in ABA Block Copolymers.

xxxxxx A BLOCKS  
~~~~~ B BLOCKS

would be dramatically different from the first case. The second case would give a copolymer that was hard, but could withstand impact, eg, impact resistant polystyrene.

The two cases above are the extremes, but it can be seen that the fraction of hard and soft chains are critical. For an elastomer there must be sufficient cross-links to give satisfactory recovery properties, but as the composition changes and goes through other morphologies the elastomeric properties deteriorate.

AB copolymers do not have the same elastomeric properties because only one end of each soft chain is linked to a domain of hard chains, ie, there are no 'soft' cross-links between 'hard' domains. Thus AB impurities in ABA copolymers may adversely affect the mechanical properties of thermo-plastic elastomers. There is however interest in AB copolymers as surfactants and emulsifiers (particularly as a means of compatibilising homopolymers).

### 1.2.3 Addition of homopolymer to an AB or ABA block copolymer

It has been reported by Inoue (4), that on the addition of polystyrene to a block copolymer of styrene-isoprene, the homopolystyrene is solubilised into the polystyrene microphase of the copolymer. This phenomenon was found to occur when the molecular weight of the homopolymer ( $M_H$ ) was less than the molecular weight of the corresponding block in the copolymer ( $M_A$ ).

Meier (8) later predicted from theory, that if homo-polymer A or B was of higher molecular weight than the blocks of A and B in an AB block copolymer, then the added homopolymer would be immiscible with the copolymer and phase separation of homopolymer and copolymer would occur. Meier's theories agreed with the observations of Inoue in that the mixing of homopolymer A or B with an AB or ABA block copolymer becomes favourable as the ratio  $M_H/M_A$  decreases, resulting in the added homopolymer being solubilised in the appropriate microphase of the copolymer.

### 1.3 Synthesis of Block Copolymers

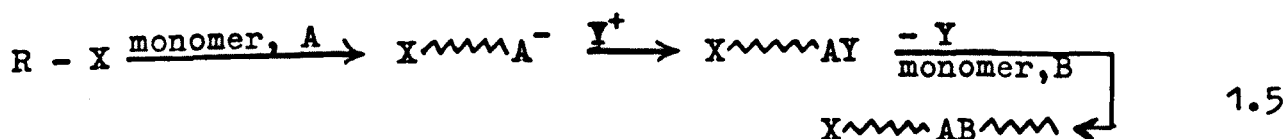
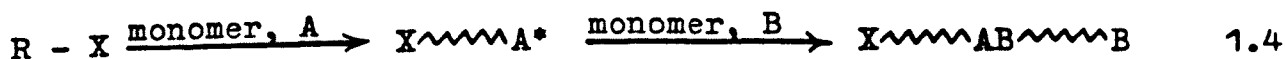
Most polymerization mechanisms (8-16) can be used in the synthesis of block copolymers and on closer examination all the mechanisms tend to use one of two general approaches:-

- 1) the sequential polymerization of the constituent monomers;
- 2) the end-to-end coupling of homopolymer chains.

Both approaches involve the incorporation of reactive sites into the homopolymer chain (usually as end-groups), but this is not always true as block copolymers can be made by direct sequential addition of the second monomer to the first polymer.

- 1) Sequential polymerization requires the polymerization of the first monomer A to give polymer A, followed by the polymerization of monomer B onto the end of polymer

A as shown in equations 1.4 and 1.5



In equation 1.4 the addition of monomer B to polymer A can be a direct sequential addition or make use of an end-group on polymer A that can be used to initiate the polymerization of monomer B. In equation 1.5,  $Y^+$  is used to terminate polymer A which may be isolated as an intermediate, removal of Y will give a macroinitiator molecule (polymer A) that can then be used for the polymerization of monomer B.

2) The end-to-end coupling of homopolymers (eg, 1.6) requires



the synthesis of homopolymers with potentially reactive end groups, eg, hydroxyl, amino, isocyanate or acyl halide groups. The only requirement being that they can interact with one another to couple the homopolymers.

Addition mechanisms are often used for the polymerization of the homopolymers that are to be used to prepare the block copolymer. In these processes there are usually three well defined and individual stages:-

1) Initiation, where an initiator molecule first forms the reactive species and then initiates polymerization of the monomer molecules.

2) Propagation, the growth of the chain carriers by the addition of monomer molecules.

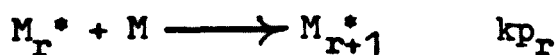
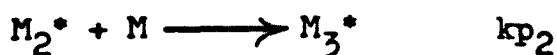
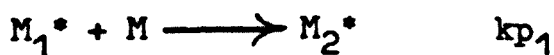
3) Termination, where the growing chains of polymer are stopped from further growth by a bimolecular reaction that destroys the active ends of the polymer chains, giving rise to unreactive polymer. Under some conditions another bimolecular reaction can take place called transfer, which normally involves the transfer of a proton from one molecule to another and often results in the termination of the growing polymer chain. A generalised reaction scheme for addition polymerization is summarised below.

SCHEME 1.1

Initiation



Propagation



Termination



Transfer



(S\* is often a new active species)

where I, X<sub>0</sub><sup>\*</sup> and M are the initiator, initiating species derived from I, and the monomer respectively, while M<sub>r</sub><sup>\*</sup>, P<sub>r</sub>,

S - H, represent the propagating species of monomer chain length  $r$ , the polymer of chain length  $r$ , and the transfer agent respectively ( $r$  is an arbitrary value).  $M^*$  can be a variety of different species in addition polymerizations, but the most commonly used species are free-radicals and ions. Y is a terminating agent, that can be a monomer or polymer radical in radical polymerizations. If the polymerization were of a free-radical nature,  $M^*$  would be a radical that could be denoted  $R^*$ . If the polymerization were of an ionic nature,  $M^*$  could either be denoted  $M^+$  or  $M^-$  depending on the mechanism.

### 1.3.1 Ionic Polymerization

#### a) Anionic Polymerizations

The discovery by Szwarc in the 1950's of 'living' anionic polymerization (16, 17) opened up the way for the synthesis of homopolymers and block copolymers by an anionic mechanism. The active species is a macroanion derived from an initiator molecule and the subsequent addition of monomer. The term 'living' was given to this type of polymerization, because the propagating species do not terminate by mutual interaction and will only terminate with species that will destroy the anions to give 'dead' polymer, ie, no termination process. To synthesize polymers with narrow molecular weight distributions using a 'living' system requires a rapid initiation step,

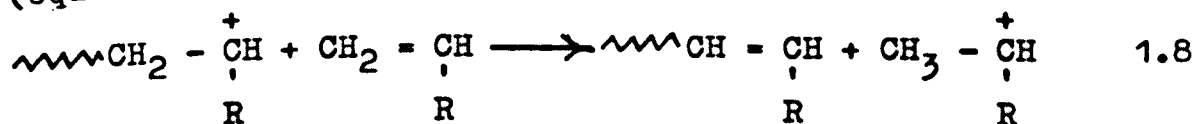
so that essentially all the initiator molecules present will initiate, followed by a relatively slow propagation step. To avoid termination it is important to remove any impurities from the system that are capable of reacting with the macroanions. Propagation continues until an equilibrium situation exists between the macroanions and the monomer, (eg, 1.7) which will depend on the conditions used .



Using this method of polymerization it is possible to prepare polymers that have near monodisperse block lengths, while controlling the actual block lengths, providing the rate of propagation is constant and all the initiator molecules actually initiate polymerization.

### b) Cationic Polymerization

Formally, the situation is exactly analogous to anionic polymerization except that the polymeric species participating in the propagation reaction are positively charged. In cationic systems problems arise because of transfer processes occurring often with the monomer (equation 1.8).



Often this transfer to monomer is the dominant reaction which prevents the possibility of a 'living' system developing.



However, under suitable conditions, the cationic ring opening of strained cyclic ethers can be considered as 'living' system (18).

### 1.3.2 Free-Radical Polymerization

The free-radical process by which some vinyl compounds of the types  $\text{CH}_2 = \text{CHY}$ ,  $\text{CH}_2 = \text{CXY}$  are polymerized is basically similar to the processes in scheme 1.1 except for the termination process. In the ionic system it was possible to remove the termination step, but in a free-radical system the termination step is always present and can be effected in two different processes:-

- a) combination termination where two radicals combine to give one polymer molecule and
- b) disproportionation termination where two radicals terminate to give two polymer molecules. The following scheme for termination can be substituted into scheme 1.1 for the termination process.

Termination a) by combination



b) by disproportionation



where  $\text{R}^\bullet$  and  $\text{P}$  represent the propagating radical and the polymer respectively ( $m$  and  $n$  are arbitrary values). The overall reaction scheme 1.1 with the added termination process can be used to derive some simple kinetic relationships, if some basic assumptions are made.

1) Radical reactivity is independent of chain length so that

$$k_{p1} = k_{p2} = k_{p3} = k_{p_r} = k_p \quad 1.11$$

and similarly for values of  $k_{tc}$  and  $k_{td}$ .

2) A steady state in radical concentration is set up, ie, the rate of termination is equal to the rate of initiation. This is only an approximation, but is applicable as long as the initiator concentration remains effectively constant, the concentration of the radicals at this state of balance will remain constant. This situation only persists for a finite period of time.

3) The length of the propagating chain is large, so that the consumption of monomer is primarily due to propagation and not initiation, ie, the total rate of monomer consumption may be equated to the rate of consumption in propagation alone.

It can be shown that the rate of polymerization,  $\omega$ , is given by

$$-\frac{d[M]}{dt} = \omega = k_p[M] \left( \frac{f}{k_{tc} + k_{td}} \right)^{\frac{1}{2}} \quad 1.12$$

where  $f$  is the rate of formation of primary radicals  $R_0^\cdot$  which give rise to the propagating species (rate of initiation) and  $[M]$  is the monomer concentration. The average degree of polymerization,  $\bar{P}_n$ , (average number of monomer units in a polymer molecule) is defined by

$$\bar{P}_n = \frac{\text{rate of monomer consumption to form polymer}}{\text{rate of formation of polymer molecules}} \quad 1.13$$

$$\therefore \bar{P}_n = \frac{k_p[M]}{(k_{tc}/2 + k_{td})} \cdot \left( \frac{k_{tc} + k_{td}}{f} \right)^{\frac{1}{2}} \quad 1.13$$

The 2 in  $(k_{tc}/2 + k_{td})$  comes in because on termination by combination, two radicals give only one polymer molecule. The termination process is a major factor that will dictate to some extent the eventual molecular size of the polymer and because termination can occur at any time, the result is a distribution of molecule sizes and so the quantities so far defined are averages.

Another important kinetic parameter can be obtained from  $\omega$  and  $\bar{P}_n$

$$\frac{k_p}{(k_{tc}/2 + k_{td})^{\frac{1}{2}}} = \left( \frac{\omega \bar{P}_n}{[M]^2} \right)^{\frac{1}{2}} \quad 1.14$$

The left hand side of equation 1.14 is often considered a constant for free-radical polymerizations of a given monomer at a given temperature and is denoted  $k_{pkt}^{-\frac{1}{2}}$ .

Complications occur when transfer, inhibition or retardation occur during a polymerization and give rise to kinetic problems. A common feature of all three processes is that they interrupt the normal growth of the polymer chains, thereby reducing  $\bar{P}_n$ .

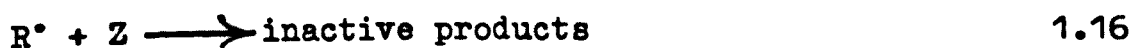
The effect of transfer on the kinetics depends on the reactivity of the new radical (denoted  $S^*$  in scheme 1.1). Often this new radical will reinitiate polymerization and

so reduce  $\bar{P}_n$ , although  $\omega$  is not affected. It can be shown that

$$\frac{1}{\bar{P}_n} = \frac{1}{\bar{P}_{n_0}} + C_s \frac{[S]}{[M]} \quad 1.15$$

where  $\bar{P}_{n_0}$  is  $\bar{P}_n$  if the polymer is formed in the absence of any transfer reaction,  $C_s$  is the transfer to solvent constant which is the ratio  $k_s/k_p$  where  $k_s$  is the rate coefficient for the transfer process,  $C_m$ , the constant for transfer to monomer and is accounted for in  $\bar{P}_{n_0}$ .

Inhibition and retardation are both processes in which an added substance Z, reacts with active radicals,  $R^\bullet$ , to form inactive products only.



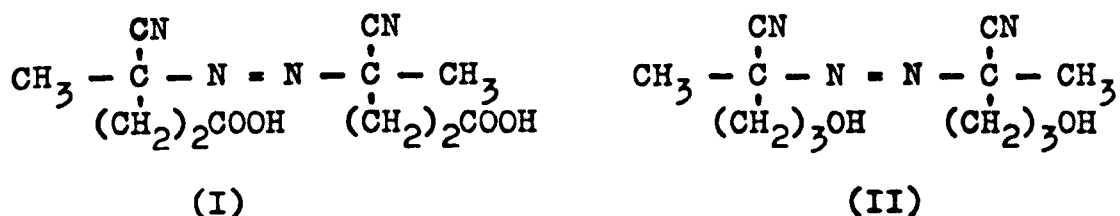
The major difference between the two is that inhibitors react with the primary radicals ( $R_0^\bullet$ ), while retarders usually react with the propagating radicals  $R_r^\bullet$ . The two processes can be separated by looking at the kinetic parameters  $k_p k_t^{-1/2}$ ,  $\omega_\lambda^{\text{and}}$ ,  $\bar{P}_n$  for a reaction. With inhibition, there is an induction period where the inhibitor is used up, giving a zero rate of polymerization. After the induction period the polymerization would continue as expected, giving the anticipated values of  $\bar{P}_n$ ,  $k_p k_t^{-1/2}$  and  $\omega$ , except that the average  $\omega$  for the total time of reaction would be low. With retardation all the parameters considered previously are reduced.

### 1.3.3 Traditional Methods for Synthesis of Block Copolymers

Much of the early work on the preparation of multi-component polymers was based on free radical polymerization techniques. The first reported synthesis (19) was a sequential free-radical polymerization of methylmethacrylate (MMA) and chloroprene. The monomer MMA was polymerized first and the second stage initiation of the second monomer, chloroprene being effected by poly (MMA) radicals trapped in a poly (MMA) matrix.

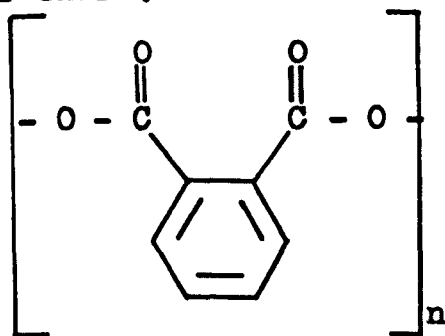
Bamford and Jenkins (8) made use of the fact that polyacrylonitrile is insoluble in acrylonitrile monomer. Macroradicals of polyacrylonitrile were trapped in the insoluble polymer and by increasing the temperature of the mixture the stability of the aggregated polymer decreases and so the trapped radicals became accessible to further polymerization. The radicals were used to polymerize other acrylonitrile and styrene units.

Bamford, Jenkins and Wayne (9) also developed a coupling technique for free radically prepared polymers, which involved incorporating terminal carboxyl and hydroxyl groups into homopolymers, that were then coupled to form copolymers of styrene, methylmethacrylate and acrylonitrile. The incorporation of the potentially active groups was achieved by initiating the homopolymerizations with 4,4'-azo-bis-(4-cyanopentanoic acid) (I) and 4,4'-azo-bis (4-cyanopentan-1-ol) (II).



The main problem with this technique for block copolymer synthesis was that low conversions (less than 25%) of monomer was found to be necessary in order to avoid the formation of homopolymer with inactive end groups.

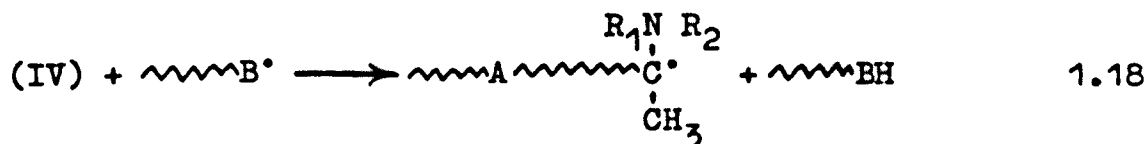
In the 1950's it was shown by Woodward and Smets (10, 11) that polymeric phthaloyl peroxide (III) could be used to initiate the polymerization of styrene thermally. The resulting polystyrene (at low conversions) contained phthaloyl peroxide sequences as end groups and/or within the polymer chain.



(III)

On heating, the peroxide groups in the polystyrene chain would decompose giving two radicals, one of which would be a macroradical capable of initiating polymerization. In the presence of methylmethacrylate, these macroradicals initiated the free-radical polymerization of the methylmethacrylate, so producing a block copolymer. This synthetic route to block copolymers illustrates some common and undesirable features.





The polymeric radical produced can then polymerize monomer B and so produce copolymers. To prevent excessive homopolymerization of the second monomer by the radical formed in the transfer reaction (equation 1.18), the polymerization must be carried out under conditions of high transfer. Methylmethacrylate and acrylonitrile block copolymers have been synthesised in this way.

The redox reaction between transition metal species, eg, Fe(II) and hydroperoxides can also be used to prepare block copolymers. If a polymer is produced with hydroperoxide end groups, the following reaction (eg, 1.19) could be used to initiate polymerization of a second monomer, thus giving a copolymer.



where R is the polymer chain. Unfortunately the oxidised species found (Fe(III)) may terminate the polymerization (20) and so prevent good kinetics.

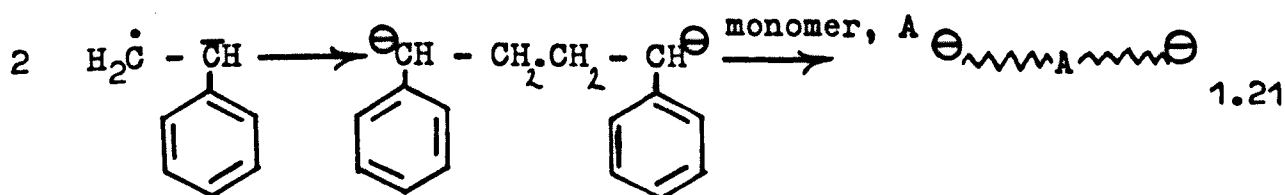
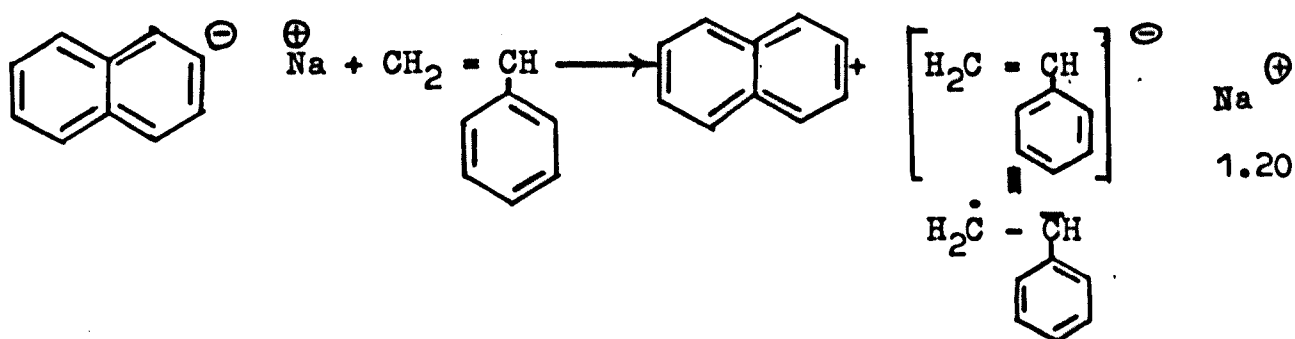
Mechanical methods have also been used to prepare block copolymers. Here free radicals are produced by the mechanical cleavage of bonds along a polymer chain either in the presence of another polymer, which may also be mechanically ruptured to form free-radicals or in the



presence of a vinyl monomer. In either case, block and graft copolymers are formed, but the type and distribution of species formed in the final product is largely unknown.

Use of 'living' anionic polymerization techniques proved to be useful in preparing block copolymers. These techniques also had the advantages of being able to control the block sizes and architecture, while not producing homopolymer contaminants, if care is taken.

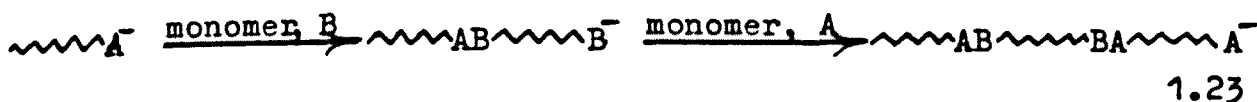
If an initiator like sodium naphthalene is used which forms radical-anion species with styrene that can dimerise in the presence of monomer to form a bifunctional anionic species (VI) then the polymer formed can be incorporated as the middle unit of an ABA block copolymer (21-23) as shown in equation 1.21-1.23.



(VI)



If a monoanion-forming initiator is used, eg, n-butyl lithium (24), both AB and ABA block copolymers can be synthesised by the sequential addition of different monomers (equation 1.23).



Coupling techniques have been used to form ABA block copolymers by the joining of 'living' AB copolymers, using a suitable difunctional coupling agent (23, 25) and are often used when the monomer B is too weak a nucleophile to initiate the anionic polymerization of monomer A in the sequential method.

Unfortunately, anionic methods of block copolymer synthesis are limited to a relatively small number of monomers, eg, styrene,  $\alpha$ -methylstyrene, butadiene and isoprene, so the different combinations of polymers that can be incorporated in block copolymers is severely restricted by this synthetic method.

New methods of synthesis are being developed for AB and ABA block copolymers that can overcome the problems that are faced when using free-radical and anionic techniques to some extent.

#### 1.4 Transformation Reactions

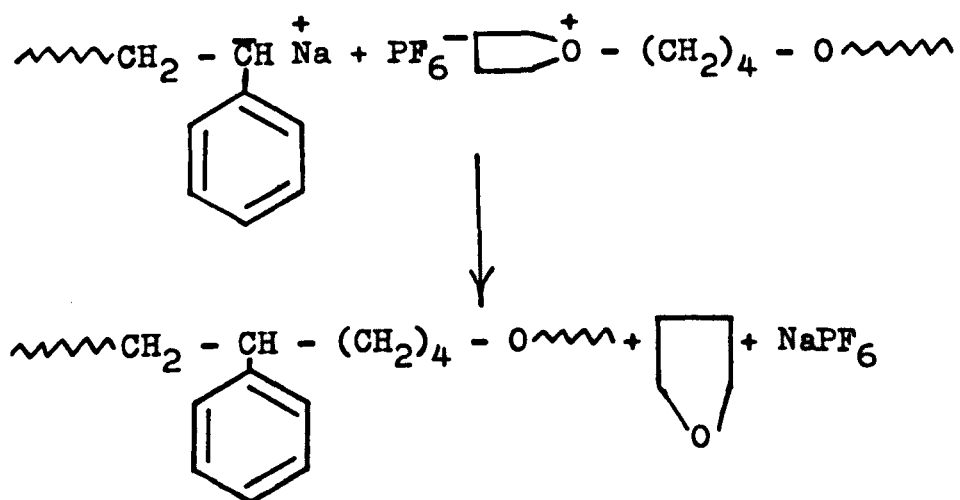
Most synthetic routes to block copolymers involve the use of one propagation mechanism, which can limit the number

and types of available monomer combinations.

When using traditional free-radical techniques, contamination of block copolymer often occurs, *owing* to transfer reactions giving homopolymers of the monomers being used. With a trapping method for the synthesis of block copolymer, only a small percentage of radicals formed can be used to produce block copolymer, so giving a small quantity of copolymer in a large mass of homopolymer. Also the molecular weight distribution of each component block will be broad and this may not be desired. The use of 'living' ionic techniques has somewhat improved the situation by allowing greater control of the molecular weight, molecular weight distribution and homopolymer contamination. *Owing* to this control, great interest has been shown in ionic techniques.

The one major draw back with these anionic and cationic techniques is the small number of monomers that can be used to great effect. Anionic mechanisms are generally restricted to diene and alkenyl aromatic monomers, while the cationic mechanism is generally restricted to tetrahydrofuran, if some degree of control is to be afforded. Another associated problem is that polymeric ions of one monomer, must be capable of initiating polymerization of the second monomer to give a block copolymer and vice versa, if more than two blocks are envisaged. This severely limits the monomer combinations possible, but there are ways of increasing these limits considerably.

One method is the mutual termination of an anionic species with a cationic species; this has been successfully done and high efficiencies have been reported (26, 27), equation 1.24



1.24

Another method would be to devise processes by which the polymerization mechanism can be changed at will to suit the monomers being polymerised sequentially. In the late 1970's Richards (28, 29) proposed a series of conversion processes that were loosely referred to as 'transformation reactions'. These reactions involve the interconversion of the propagating step from one mechanism to another, in order to increase the number of monomer combinations possible. Initially Richards proposed transformation reactions involving free-radical, anionic and cationic mechanisms, but later extended the process to include Ziegler-Natta catalysis mechanisms.

To effect a transformation reaction and so generate a block copolymer, it was suggested that a transformation reaction would require at least three distinct stages,

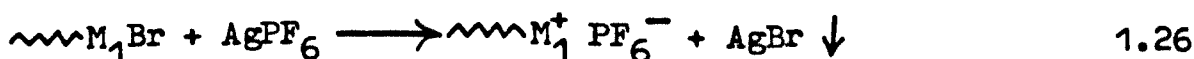
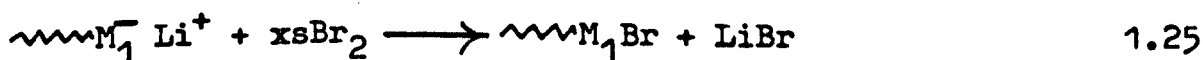
these stages being:-

- 1) Polymerization of monomer A by mechanism I and capping of the propagating end with a stable but potentially reactive functional group.
- 2) Isolation of polymer A, dissolution in a solvent suitable for mechanism II and the addition of monomer B.
- 3) Reaction or change of conditions to transform the functionalised end into propagating species B which will polymerize monomer B by mechanism II.

Richards and co-workers have investigated anion to cation (28-31), cation to anion (32, 33), anion to free-radical (34-37) and anion to Ziegler-Natta (38) transformation processes.

#### 1.4.1 Anion to Cation Transformation

The process investigated by Richards was based on the reaction between organic halides and the silver salts of strong acids, eg,  $\text{AgPF}_6$ ,  $\text{AgClO}_4$ ,  $\text{AgSbF}_6$ . The steps involved in this transformation process are given in equations 1.25 and 1.26



The sequence of reactions used involved 'living' polystyrene', denoted  $\sim\sim\sim\text{M}_1^- \text{Li}^+$ , produced via an anionic mechanism,

which was reacted with bromine to give a terminal benzylic bromide on the polystyrene molecule. The polymeric bromide was then reacted with silver salts to create a species, denoted  $\sim\sim\sim\text{M}^+\text{PF}_6^-$ , which would initiate the polymerization of tetrahydrofuran (THF) via a cationic mechanism. The reaction for the generation of the bromine terminated polymer (equation 1.25) resulted in a maximum efficiency of 60%, the remaining material being Wurtz coupled polymer (equation 1.27).



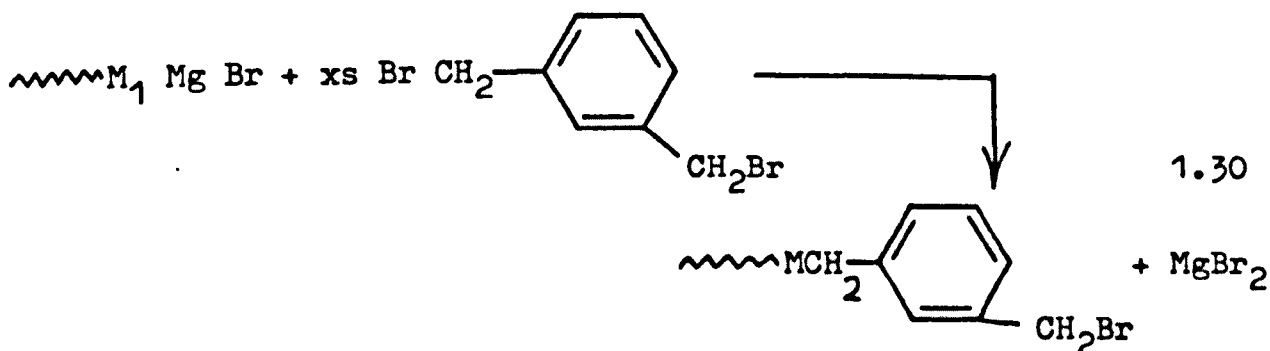
The product yield was found to be independent of the excess bromine used, which indicated that the coupling reaction was so fast that reaction occurred at the interface of the solutions, before mixing had been effected.

The coupling reaction was reduced by reacting the 'living' polystyryl anion with excess magnesium bromide to give a 'Grignard intermediate' (39), which was less reactive than the polystyryl anion (equation 1.28). The lower reactivity of the Grignard considerably reduced the coupling reaction when excess bromine was added (equation 1.29).



$\alpha, \alpha'$ -dibromo-m-xylene has also been used in these reactions

instead of bromine to give polystyrene functionalised with terminal bromine (equation 1.30).

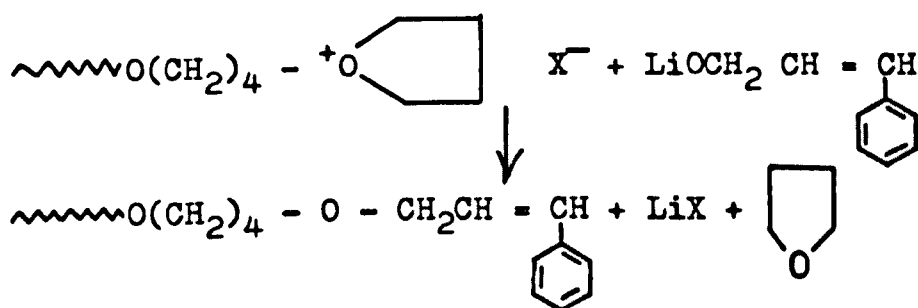


Bromine terminated polystyrene and a suitable silver salt were then used to initiate the polymerization of tetrahydrofuran, which acted both as solvent and monomer for the subsequent cationic polymerization.

Following the methods described for the anion to cation transformation process, styrene, butadiene and tetrahydrofuran have been used to prepare block copolymers. The efficiency of the copolymerization was found to be approximately 80%.

#### 1.4.2 Cation to Anion Transformation

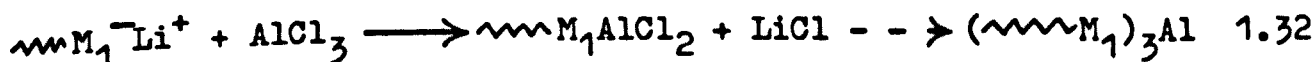
In order to effect this transformation, living poly-(tetrahydrofuran) was reacted with lithium cinnamate to form a polymer that possessed a terminal styryl double bond (equation 1.31). The polymer was isolated, dissolved in benzene and reacted with n-butyl lithium to create a terminal anion. Addition of monomer such as styrene or isoprene resulted in the formation of block copolymer. The reported efficiency of this transformation polymerization is 10%.



1.31

#### 1.4.3 Anion to Ziegler-Natta Transformation

In this transformation process 'living' polymer was produced via an anionic method, which was then reacted with aluminium chloride. Depending on the relative concentrations of reactants it was possible to gain adducts up to the fully alkylated product (equation 1.32). These products were then



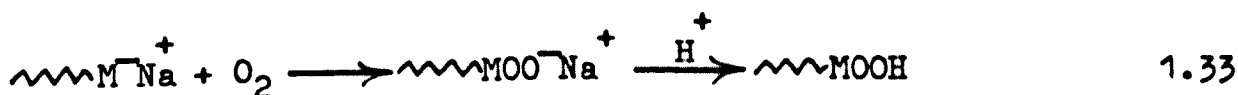
reacted with suitable transition metal salts, eg,  $\text{TiCl}_4$  and  $\text{TiCl}_3$ , and a second monomer added. Initial indications were found to be encouraging for this route to block copolymers, but initial results showed low efficiencies in the region of 10%.

#### 1.4.4 Anionic to Free-Radical Transformations

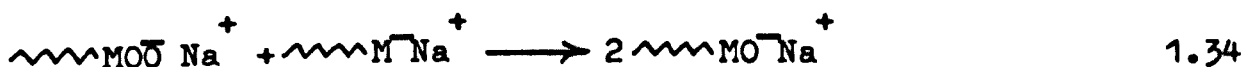
The transformation of polymeric anions to polymeric



radicals has been used by a number of workers to produce block copolymers because of the large number of monomers that can be incorporated into copolymers at the free-radical stage of the polymerization. Brossas (40) used molecular oxygen to terminate a living polymer to give terminal hydroperoxide groups (equation 1.33),



by using a large excess of oxygen the major competing reaction (equation 1.34) can be minimised.



Polymeric radicals were then produced by titration with ferrous sulphate.

Richards and co-workers defined three methods by which the above transformation could be effected. These methods involved the use of

- 1) lead salts (34),
  - 2) mercury salts (35) and
  - 3) the reaction between organic halides and transition metal carbonyls (41, 42);
- this last method was used entirely during the course of this work.

#### 1) Use of Lead Salts

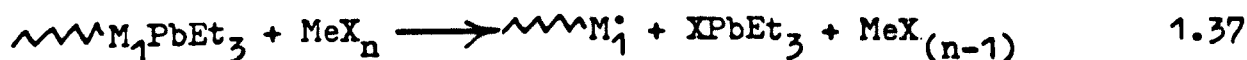
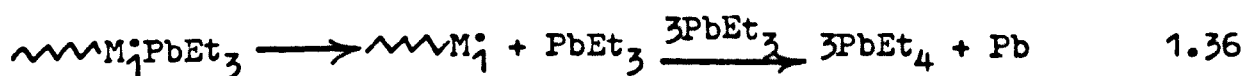
Living polystyrene was reacted with triethyl lead

chloride to yield the adduct (PSt:PbEt<sub>3</sub>) quantitatively (equation 1.35)



The lead adduct was isolated and was later used to produce polymeric radicals, by thermal decomposition (equation 1.36) or by reacting it chemically with salts of certain variable valency metals (equation 1.37), eg,

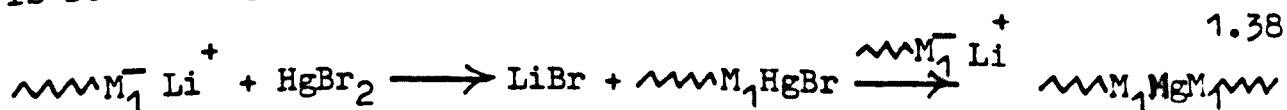
AgNO<sub>3</sub>, AgClO<sub>4</sub>, FeCl<sub>3</sub>



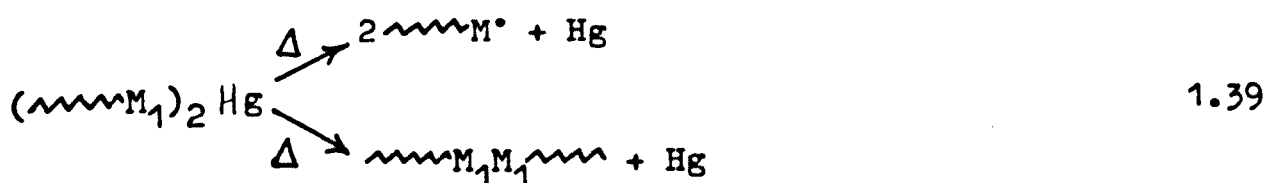
Styrene-methylmethacrylate block copolymers have been prepared by thermal decomposition of the adduct in the presence of methylmethacrylate, but yields were poor (5-10%). The yield was significantly improved when a silver salt was initially complexed with 18C6 crown ether, because the rate of radical production was slowed and the radical life time was increased.

## 2) Use of Mercury Salts

Mercury salts are used as terminating agents for anionically prepared living polymer, the concentration being important in determining whether the mono or diadduct is formed (equation 1.38).



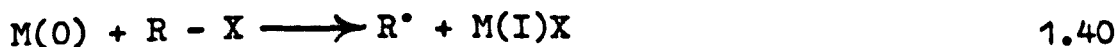
Both adducts are thermally unstable and are easily decomposed to give polymeric radicals, although the diadduct is prone to a coupling process (equation 1.39) via a radical cage recombination



reaction. Styrene and methylmethacrylate block copolymers have been prepared by this method, but yields were low.

### 3) Use of Metal Carbonyl and Organic Halide Systems

The transformation process used here is a development from work done by Bamford and Finch (43), who found that metal carbonyls reacted with carbon tetrachloride were sources of radicals. Subsequent studies showed that other organo-metallic complex halide combinations were possible initiators for free-radical polymerizations (44). Bamford and Eastmond recognised that by incorporating the organic halide into a polymer chain as terminal or pendant side groups, it would be possible to initiate polymerization from preformed polymers and hence form block and graft copolymers respectively. The overall radical forming reaction can be summarised by equation 1.40

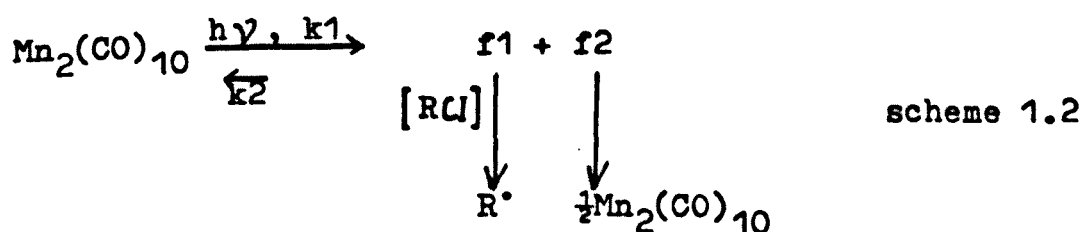


where M(O) is the transition metal with an oxidation state of zero, X is the halogen and R represents a preformed

polymer chain in this case. In the presence of a suitable monomer,  $R^\bullet$  will initiate polymerization.

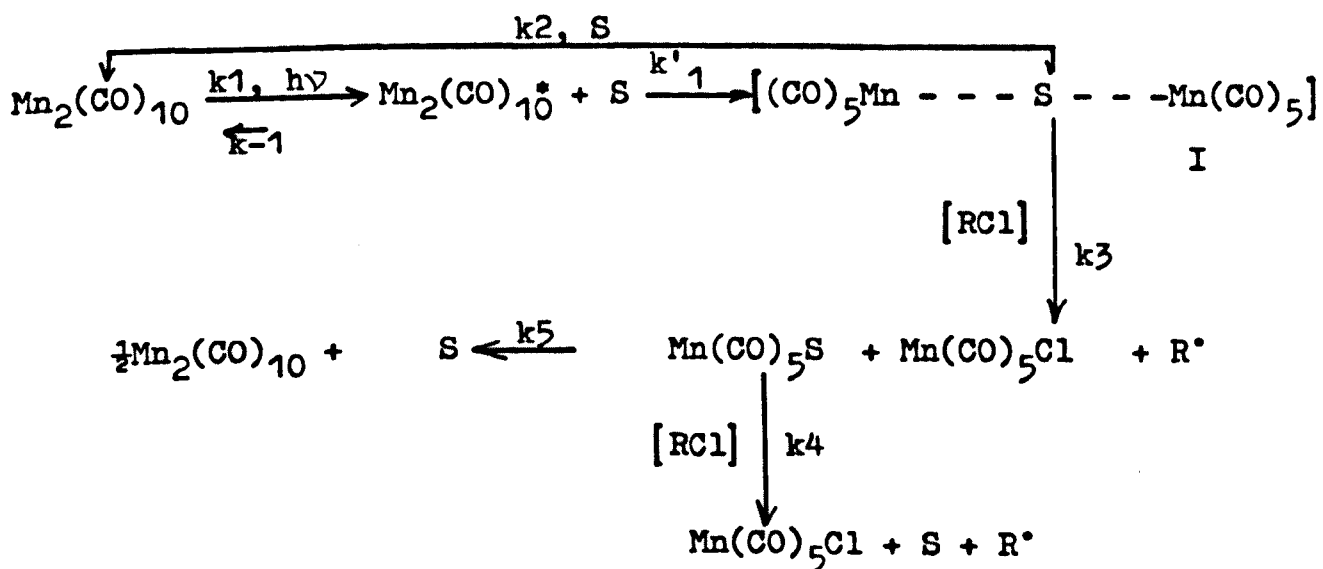
These techniques were applied to the bromine terminated polystyrene that had previously been prepared for the anion to cation transformation process (section 1.4.1). Eastmond and Woo (42) found these techniques to be successful in preparing a variety of copolymers, that had relatively low molecular weight A blocks, the prepolymer being 2000 molecular weight polystyrene terminated by  $\alpha, \alpha'$ -dibromo-*m*-xylene.

The photolysis of dimanganese decacarbonyl,  $Mn_2(CO)_{10}$ , ( $\lambda = 438.5$  nm), in the presence of an organic halide (prepolymer) was used as the initiating system for the free-radical step in producing block copolymers. Bamford et al (45, 46) found that the quantum efficiency for this initiation process was unity and proposed the following simplified kinetic scheme for initiation (1.2)



$f_1$  and  $f_2$  being fragmentation products of  $Mn_2(CO)_{10}$ , were assumed to be unequal, one of which reacts with organic halide to give a radical, while the other, it was suggested reforms  $\frac{1}{2} Mn_2(CO)_{10}$ . Bamford proposed that  $f_1$  and  $f_2$  may be  $Mn(CO)_6$  and  $Mn(CO)_4$  respectively, based on chemical considerations.

Eastmond and Harvey later did work on improving the scheme in the light of discrepancies that were found, based on data on quantum efficiencies of initiation in different monomers (47) and known solvent effects (48). The following mechanism was proposed



where S is the solvent.

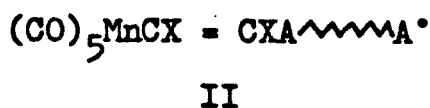
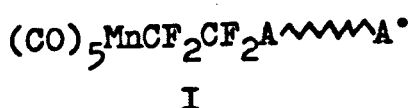
Bamford et al used isotopically labelled halides to show that radical formation occurs exclusively by abstraction of halogen from the halide by species (I). Despite the complexity of the initiation mechanism, the dimanganese decacarbonyl-halide system is a specific initiating system, in that, at high halide concentrations the kinetics are simple and if a polymeric halide is used, the only initiating radicals produced are attached to the preformed polymer.

Bamford, Crowe and Wayne (45) showed that the rate of polymerization of methylmethacrylate (photoinitiated by

$\text{Mn}_2(\text{CO})_{10}$  and  $\text{CCl}_4$  at  $25^\circ \text{C}$ ) was independent of the halide concentration at concentrations greater than about  $10^{-3} \text{ mol l}^{-1}$ , but falls away at lower concentrations to a zero rate at zero halide concentration (figure 1.3). Above the limiting halide concentration, the rate of polymerization ( $-\frac{d[\text{M}]}{dt}$ ) is proportional to  $I^{\frac{1}{2}}$ , monomer and  $[\text{carbonyl}]^{\frac{1}{2}}$  concentrations. ( $I = \text{incident light intensity}$ ).

#### 1.4.5 Other metal carbonyl based systems

Bamford and Mullik (49) found that photoinitiation by dimanganese decacarbonyl and fluoro-olefins did not proceed by halogen atom abstraction from the fluoro-olefin, but resulted in the incorporation of a terminal manganese atom in the polymer chain. If tetrafluoroethylene was used with monomer A, the propagating species would be I. It was found that certain

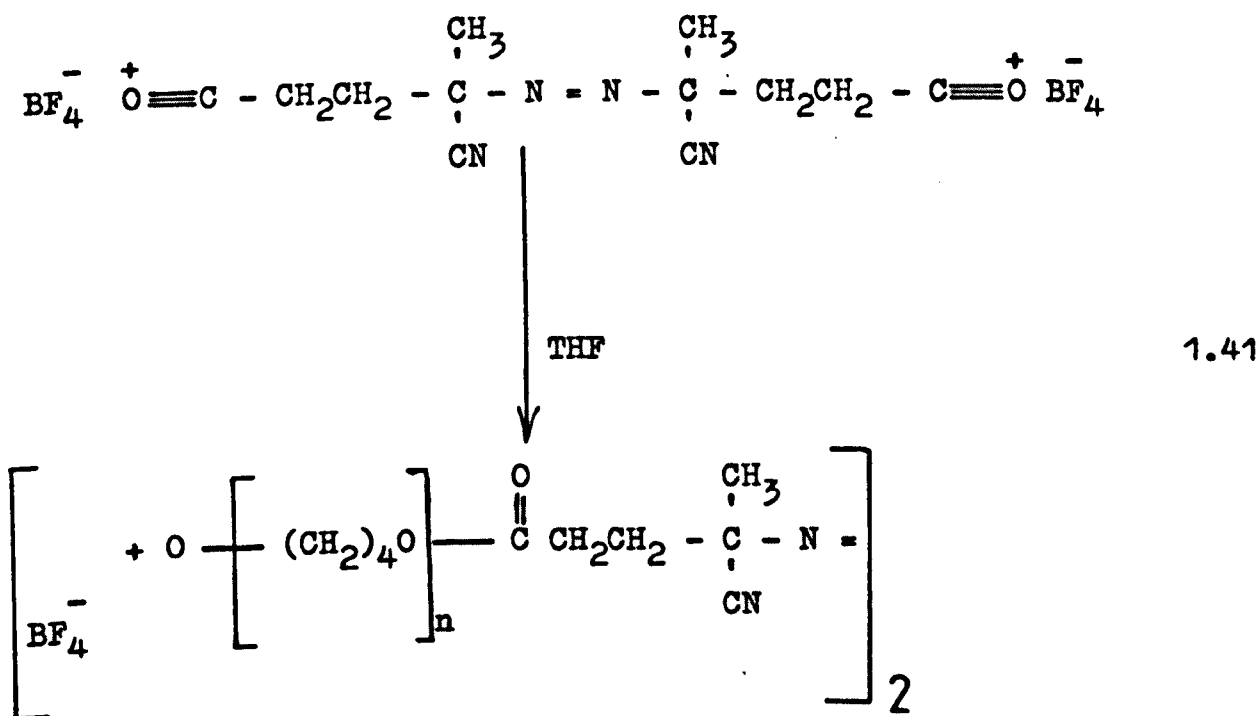


substituted acetylenes would undergo a similar process to give II. Structures I and II were found to be thermally unstable and would initiate the polymerization of methyl methacrylate at  $100^\circ \text{C}$ .

#### 1.4.6 Other transformations

Recently Yağci (50) reported a reaction scheme for block copolymer synthesis that approximated to a cation to free-radical transformation. The cationic stage involves

polymerizing tetrahydrofuran (THF) with a difunctional azo-oxocarbenium salt (equation 1.41)



Thermal decomposition of the azolinkage in the presence of suitable monomers, would give rise to block copolymer formation.

### 1.5 Characterization

The different solubility characteristics of homopolymers and block copolymers can be used to isolate the copolymer, often dissolving the homopolymers in suitable solvents to leave the copolymer fraction. This fraction can then be analysed spectroscopically to confirm the

presence of units derived from different monomers in the block copolymer. Once the overall composition has been determined, there is still the problem, that the block copolymer has a composition distribution coupled with molecular weight distributions of the blocks and often some fraction of the copolymer will be soluble in the solvent used in the extraction process (usually low molecular weight polymer). So the isolated copolymer may not accurately reflect the true composition of the copolymer originally formed.

The mutual immiscibility of most pairs of chemically different homopolymers may allow homopolymer mixtures and block copolymers to be distinguished by the clarity of polymer films (amorphous systems only). Blends of immiscible homopolymers give rise to opaque films owing to changes in refractive index at the phase boundaries. Block copolymers can, however, produce transparent films if their blocks have undergone microphase separation, the reason being that the domains produced are too small to scatter visible light effectively.

Gel permeation chromatography (GPC) is probably the quickest and most convenient method of identifying block copolymers, providing there are at least two detectors in use on the equipment and that the components concerned have different detector responses. The methods involved in GPC analysis of block copolymers are described later in Chapter 3.



Defining the structure of a block copolymer can be difficult and often requires knowledge of the polymerization mechanism employed. For elastomeric materials, it may be possible to qualitatively distinguish AB from ABA block copolymer structures by their different elastomeric properties. Interpretation of results could be hampered if the copolymer is contaminated by homopolymer of either one or both constituent polymers. GPC and ultracentrifuge procedures may be used to separate and identify the presence of more than one polymeric species, if there is a large difference in molecular weight and density between species.

Separation of the block copolymer and the homopolymer contaminant can sometimes be effected when the molecular weight of the homopolymer is sufficiently high as to allow phase separation to occur between the homopolymer and the copolymer.

Overall molecular weights of the copolymer can be found using membrane and vapour pressure osmometry, viscometry and light-scattering (depending on the solvent used, as some solvents may only 'show' one of the components), but interpretation of data is complicated where there are broad distributions and homopolymer contaminants present.

The size of individual blocks is very important with respect to microphase separation and so, if the sizes could

be determined, a structure may possibly be assigned with the help of knowledge of the mechanism involved, in producing the block copolymer.

### 1.5.1 Molecular Weight and Molecular Weight Distribution

Molecular weight is a very important parameter in polymer chemistry, as it can have an enormous influence on physical properties of polymers, such as hardness, brittleness, melt viscosity and solubility. The synthesis of polymeric materials however always produces a range of molecules of different chain lengths, giving a distribution of molecular weights. The molecular weight distribution can be found experimentally via fractionation of the polymer and characterizing the fractions or by use of gel permeation chromatography. It is possible to predict the distribution of sizes or molecular weights by using a statistical approach providing the chemistry of the polymerization process being used is known (51).

During the characterization of a polymeric material, the values gained for the molecular weight of the polymer will be averages gained from the whole distribution. The average molecular weights that are most often used are the number average molecular weight and the weight average molecular weight,  $\bar{M}_n$  and  $\bar{M}_w$  respectively.  $\bar{M}_n$  and  $\bar{M}_w$  are defined as

$$\bar{M}_n = \frac{\sum N_i M_i}{\sum N_i} = \frac{\sum W_i}{\sum W_i / M_i} \quad 1.42$$

$$\bar{M}_w = \frac{\sum N_i M_i^2}{\sum N_i M_i} = \frac{\sum W_i M_i}{\sum W_i} \quad 1.43$$

where  $N_i$  is the number of molecules with a molecular weight  $M_i$ ,  $W_i$  is the total weight of molecules with molecular weight  $M_i$ ; the summation is carried out over the range  $i = 0$  to  $i = \infty$ . Using the quantities  $\bar{M}_n$  and  $\bar{M}_w$  it is possible to get some indication of the breadth of the distribution. The ratio  $\bar{M}_w/\bar{M}_n$  is used as a measure of the dispersity of the polymer and is often called 'polydispersity'. A polymer is monodisperse if  $\bar{M}_w/\bar{M}_n = 1$ .

Other molecular weight averages exist and are defined by

$$\bar{M} = \frac{\sum N_i M_i^{n+1}}{\sum N_i M_i^n} \quad 1.44$$

in which  $n \geq 0$  and is not necessarily integral. Equations 1.4 and 1.5 give  $\bar{M}_n$  and  $\bar{M}_w$  for  $n = 0$  and  $n = 1$  respectively.

Although the use of average molecular weights to describe a molecular weight distribution is often convenient, care must be taken as they do not always provide sufficient information about the molecular weight distribution. For example, it is possible for polymers to have the same or similar molecular weights, but have totally different molecular weight distributions and hence possibly have different physical properties.

## 1.6 General Properties

Polymeric materials have gained widespread use in industry over the past few decades, mainly due to their versatile mechanical properties. The general principles of mechanical properties have been established in terms of viscoelasticity, ie, polymers are examples of viscoelastic materials, inferring that they exhibit properties in between those of a perfect elastic material and those of a viscous liquid.

Consider a perfectly elastic material, such as a steel spring. When a load is applied to the material, it is deformed by the load and all the energy of deformation is stored and can therefore be retrieved by removing the load. If a periodic deformation is employed, the stress will be exactly in phase with the strain.

A viscous liquid on the other hand behaves differently from an elastic material, in that the energy of deformation when a load is applied is lost and is not recoverable on removal of the load; this situation can be represented by a dash pot. If a periodic deformation were to be applied, then the stress would be out of phase with the applied strain.

All polymers show characteristics of both the elastic and viscous behaviour, thus giving potentially interesting mechanical properties.

### 1.6.1 The Glass Transition Temperature, $T_g$

The properties of polymers are a function of temperature and it has been found that the coefficient of thermal expansion of amorphous polymers undergoes rapid change in the region of the glass transition; the temperature at which the rapid change occurs is called the glass transition temperature,  $T_g$ . Below  $T_g$  many polymers are hard, brittle materials, having moduli greater than  $10^{10}$  dynes/cm<sup>2</sup> (in SI units this is  $10^9$  Nm<sup>-2</sup>) and is often termed the "glassy region".

In the glassy region, thermal energy is insufficient to surmount the potential barriers for rotational motions of segments of the polymer molecules and so the molecules are in effect frozen (cannot move). Above  $T_g$ , the amorphous polymer is soft and flexible, having a modulus in the region of  $10^7$  dynes/cm<sup>2</sup> ( $10^6$  Nm<sup>-2</sup>). The change in the moduli (and properties) through the polymer transition region, is due to the onset of micro-Brownian motion of the molecular chains from the frozen state with increasing temperature, ie, the thermal energy has overcome the potential energy barriers to segmental motion.

In the glass transition region, the polymer has short-range diffusional motion along with micro-Brownian motion. The polymer segments are capable of moving in a co-operative manner from one lattice site to another, so a hard polymer becomes soft and rubbery.

Lower energy transitions do exist, but it is difficult to define their origins, but it is thought that they may possibly be due to rotation of pendant groups on the polymer backbone.

### 1.6.2 Properties of Block Copolymers

Block copolymers, as previously stated, can show mechanical properties in the bulk state which are different from those of the component homopolymers or random copolymers. These different and sometimes desirable properties are often attributed to the microphase separation of the component polymers and the accompanying morphology. An example is that of an ABA block copolymer that has undergone microphase separation, whose properties could range from a thermoplastic elastomer to a toughened thermoplastic. The range in properties is affected by the changes in composition of the component polymers and the attendant morphology.

When measurements of Tg's are made on block copolymers, transitions due to both component polymers can normally be seen. Since, in general, the component polymers are completely immiscible and so give microphase separation, the transitions seen in the copolymer will correspond to those of the component homopolymers, ie, the transitions (Tg's) will occur at the same temperatures as those of the homopolymers.

If the component polymers are in fact slightly miscible then the properties of the copolymer may be modified slightly from those expected. In particular, if there is mixing between two polymers A and B, then the transitions (Tg's) occurring may be shifted, so that they do not occur at the temperatures expected for pure A and pure B. Therefore measurements of Tg's for block copolymers can give indications as to whether or not the component polymers are miscible or not and, if they do exhibit miscibility, the extent to which they are miscible.

ABA thermoplastic elastomers at service temperatures possess high tensile strength but at higher temperatures they can undergo a transition to a melt and so be industrially processed like thermoplastic materials. This transition between melt-like and elastomer-like behaviour is reversible and can be repeated many times. In these copolymers A and B are chosen so the A is hard and B is soft at use temperatures. The morphology is important in that the A component must be the minor component and aggregate into spheres of A in a matrix of B. With increase in the proportion of one or other of the polymeric components the stress-strain response will change, so giving a range of properties in between the plastic and elastic extremes.

Block copolymers lose strength rapidly as the temperature is raised to approach the glass transition temperature of

the dispersed hard phase. Conversely, the modulus and hardness will increase rapidly as the temperature is lowered approaching the glass transition temperature of the soft matrix.

In the melt state, block copolymers often behave slightly differently from thermoplastics in that, they have a limiting melt viscosity and have anomalous relationships of melt viscosity to shear stress. The anomalous melt behaviour of ABA block copolymers has been attributed to the phase structure which persists in the melt.

Block copolymers when dissolved in solvents display behaviour which is unusual, when compared to that of the corresponding homopolymers. Each component of the copolymer will tend to dissolve in a solvent or solvent blend which will dissolve the corresponding homopolymer, giving rise to solubility problems. In dilute solutions, using a solvent system good for all component blocks, problems are not usually found, but with highly concentrated solutions, micellization can occur, especially if the solvent is a poor one for at least one of the component blocks.

### 1.6.3 Applications

Because the individual blocks in a block copolymer exhibit selective solution properties, a block copolymer may act as a surface active agent, as it can be accommodated at an interface between two phases of other materials, if



it contains blocks compatible with each phase respectively. Thus it can act as an emulsifier between two incompatible solvents or other liquids.

Those block copolymers which are thermoplastic elastomers can be formed into useful rubber articles by conventional plastics processing methods such as extrusion, blow moulding and injection moulding. They can be blended with various additives to give materials designed for specific applications.

Other applications of block copolymers are in adhesives, sealants and coatings.

### 1.7 Gel Permeation Chromatography (GPC)

GPC is a relatively new offspring of the more conventional and widely used liquid chromatography which was first reported about 1900. Since the introduction of GPC in the 1960's, it has become a very important technique in polymer science, because of its ability to separate molecules according to their size and so molecular weight. This separation allows the determination of molecular weight and molecular weight distribution of polymers. Previously, time consuming bulk fractionation methods were used to obtain the molecular weight distribution of a polymer.

GPC often allows the determination of the molecular weight distribution and requires considerably less time

(minutes as opposed to days or weeks) and less sample (milligram as opposed to grams) than the bulk fractionation methods. By judicious use of various detectors (eg, ultraviolet, refractive index) attached to the GPC equipment, mixtures of polymers and block copolymers can sometimes be qualitatively analysed. GPC can give information on polymers just by inspection of the relevant chromatograms supplied by the detectors.

### 1.7.1 Separation Process

GPC is a form of size exclusion chromatography (SEC) (52) ie, separating molecules according to their size in dilute solution. The separation is achieved by passing the polymer solution through a column packed with porous particles. This separation of molecules is in accordance to their molecular weight (size) with the high molecular weight molecules being eluted first. The sample components (ie, polymers of different molecular weight) migrate through the column at different velocities and elute separately from the column at different times. As a solute moves along with the carrier solvent (mobile phase), it is at times momentarily held back, either by the surface, the column packing or a stagnant phase (within the pores) in the column packing (stationary phase). Since solutes move only when they are in the mobile phase, the distribution of solute molecules between the mobile and stationary phases determines the average solute migration velocity. Molecules that favour the stationary phase (low molecular weight) will migrate more slowly and so elute from the column later.

### 1.7.2 Retention

In GPC the retention of molecules of various molecular weight is determined by the size of the pores in the column packing and the size of the polymer molecules involved.

This retention can be considered thermodynamically:- as molecules migrate through the column they transfer back and forth between phases to satisfy thermodynamic equilibrium. The thermodynamic equilibrium of the solute distribution can be defined as the condition in which the chemical potential of each solute component is the same in the two phases. For dilute solutions at equilibrium the solute distribution can be related to the standard free energy different,  $\Delta G^\circ$  between the phases at constant temperature and pressure,  $\Delta G^\circ$  can be given by equations 1.45-1.46.

$$\Delta G^\circ = - RT \ln K_{GPC} \quad 1.45$$

$$\Delta G^\circ = \Delta H^\circ - T\Delta S^\circ \quad 1.46$$

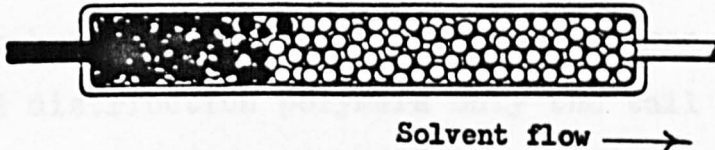
where  $K_{GPC}$  is the solute distribution coefficient,  $T$  is the absolute temperature,  $\Delta H^\circ$  is the enthalpy and  $\Delta S^\circ$  is the entropy difference between phases. For GPC,  $\Delta H^\circ$  is approximately zero. Since solute mobility becomes more limited inside the pores of the column, solute permeation is associated with a decrease in entropy as shown in equation 1.47, figure (1.4)

$$K_{GPC} \approx e^{\Delta S^\circ/R} \quad 1.47$$

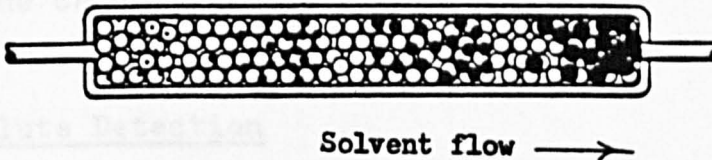
shows the retention process diagrammatically.

FIG. 1.4

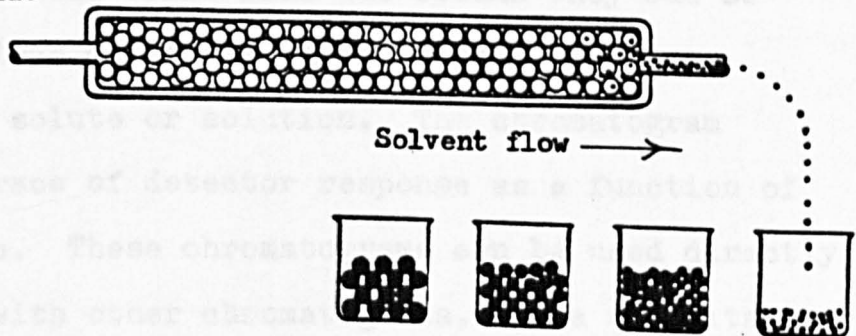
Injection of mixed sizes



Separation by size



Collection by size



Molecules of various sizes elute from the column at different rates. The column retains low molecular weight material (small black dots) longer than high molecular weight material (large black dots). The time it takes for a specific fraction to elute is called its "retention" time.

During the separation process, a small amount of mixing and dilution occurs while travelling through the column and 'instrumental' or 'peak' broadening effects are observed in the resulting chromatogram. The broadening effect can affect calculations of molecular weight and molecular weight distributions especially for monodisperse polymers. With broad distribution polymers only the tail of the chromatogram is affected, and is normally insignificant compared with the rest of the chromatogram.

### 1.7.3 Solute Detection

As the fractions elute from the column they can be detected by various detectors which respond to some property of the solute or solution. The chromatogram obtained is a trace of detector response as a function of retention volume. These chromatograms can be used directly for comparison with other chromatograms. If a quantitative analysis of the curves is required, then the variation of the detector response with molecular weight may have to be taken into account, if the molecular weights involved are very low, *owing* to possible end-group effects on the detector response.

### 1.7.4 Calibration

GPC is a secondary method for determining molecular weights and as such requires calibration. The simplest method of calibration involves measuring peak retention

volumes of monodisperse polymer fractions of known molecular weight (often calculated by osmometry or light scattering). From this information a graph can be drawn of  $\ln \eta$  (molecular weight) against retention volume, within the limits of total exclusion and total permeation this is approximately linear, see figure 1.5. The linear part of the graph can conveniently be described by a straight line equation 1.48

$$\log M = i - sV \quad 1.48$$

where  $M$ ,  $i$ ,  $s$  and  $V$  are the molecular weight of the polymer, the intercept, the slope and the retention volume of the peak respectively.

Molecular weight calibration is an experimental approach, that is only valid for one particular polymer/solvent system and also is dependant on the columns in use at the time, ie, it can only apply to a given set of columns.

Until recently polymer standards other than polystyrene were not commercially available and so measured molecular weights were usually given as 'polystyrene equivalent molecular weights'. One of the recent additions is the commercial availability of poly methylmethacrylate standards. Other methods do exist for calibration and have had varying degrees of success. These methods include the 'Q-factor' method proposed by Moore and Hendrickson (53) and the more widely accepted 'Universal Calibration Curve' method (53-55).

### 1.7.5 Calculation of Molecular Weight

For monodisperse polymers it is reasonable to assume

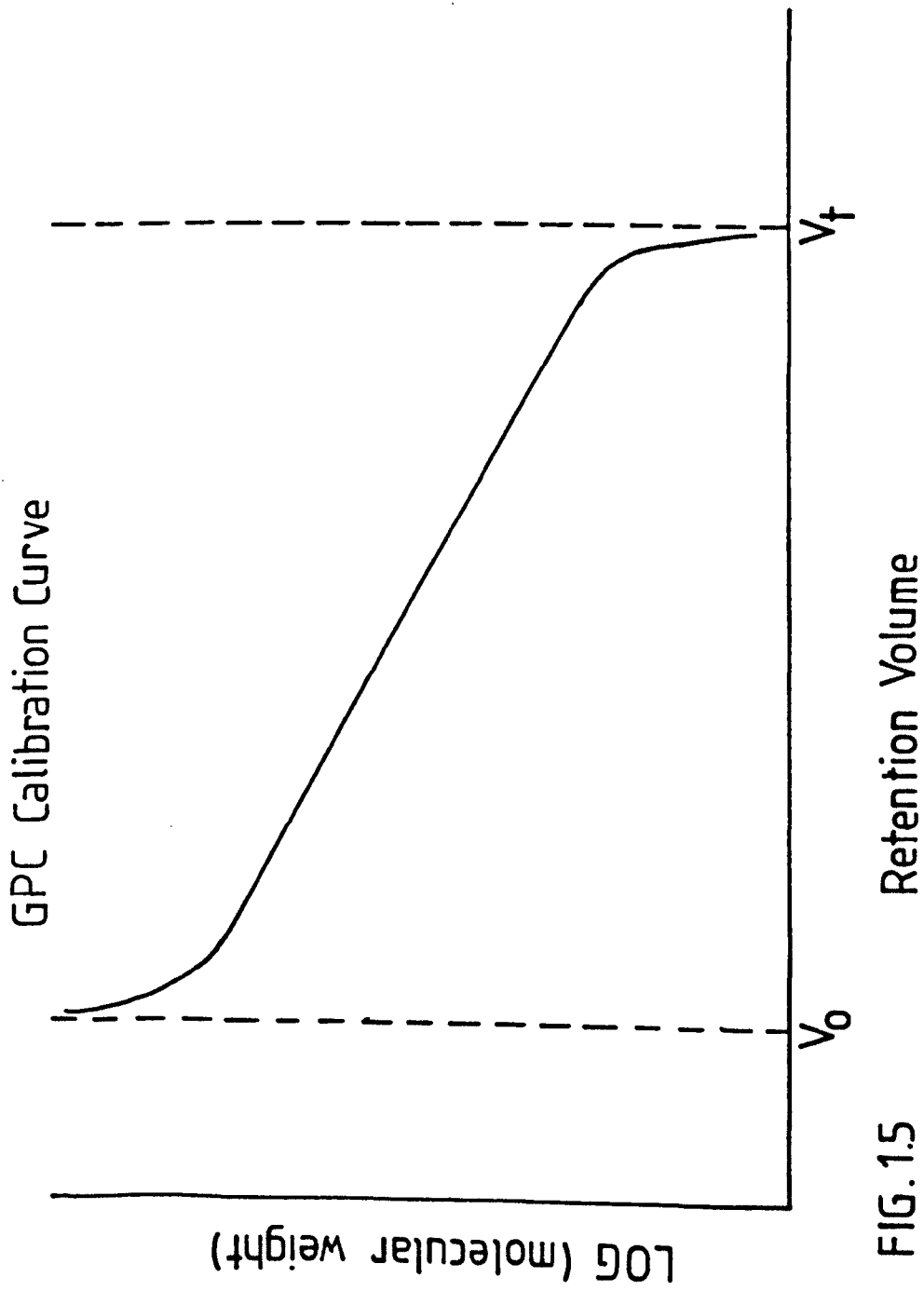


FIG. 1.5

that  $\bar{M}_n \approx \bar{M}_w \approx M_{\text{GPC}}$  ( $M_{\text{GPC}}$  is the GPC chromatogram peak molecular weight) and so the average molecular weight can simply be read off the calibration curve. For samples that have broad distributions, the average molecular weights  $\bar{M}_n$  and  $\bar{M}_w$  can be calculated from the following equations 1.48 and 1.49

$$\bar{M}_n = \frac{\sum h_i}{\sum (h_i/M_i)} \quad 1.48$$

$$\bar{M}_w = \frac{\sum (h_i M_i)}{\sum h_i} \quad 1.49$$

where  $h_i$  is the GPC chromatogram curve height at elution volume  $i$ ,  $h_i$  is taken at equally spaced intervals,  $M_i$  is the molecular weight at the elution volume  $i$ ,  $\sum$  denotes summation over a range of elution volumes in which the polymer elutes.

Detailed aspects of the procedures involved in the calculation of  $\bar{M}_n$  and  $\bar{M}_w$  by GPC are given in section 3.6

### 1.7.6 Applications

GPC has become a powerful tool of the polymer chemist and has applications other than determining <sup>n</sup> molecular weight and molecular weight distributions.

Its most simple application is in the detection of impurities particularly of low molecular weight in polymer



samples. Mixtures of polymers and polymer fractions can be separated providing there is a sufficient molecular weight difference between them. GPC may be useful in the analysis of branched chain polymers in relation to corresponding linear polymers. Recent work (56) has shown that GPC may be used to follow cross-linking reactions up to near the point of gelation.

GPC is extremely useful in the analysis of copolymers. Apart from the qualitative aspects of detecting homopolymer and impurities in the copolymer, GPC has been used in the compositional analysis of block copolymers (section 3.6).

### 1.8 Aims of Present Work

The primary aims of the work described in the following chapters is to extend earlier work of Eastmond and Woo (42), who used model compounds (bromine terminated polystyrene of  $2000\text{g mol}^{-1}$  molecular weight) in the anionic to free-radical transformation polymerization mechanism.

Here it is proposed to increase the range of B-components that can be incorporated into block copolymers, by using a series of acrylates and methacrylates, hitherto unused with this transformation process. Polystyrene blocks of higher molecular weight than those previously used, will be synthesised and used, as they will more likely undergo microphase separation.

The block copolymers once synthesised are subjected to

physical and mechanical testing, so as to provide information on properties and structure. By judicious use of acrylate monomers, it is hoped that the block copolymers produced may show potentially useful thermoplastic elastomeric properties.

## CHAPTER II

## COPOLYMER SYNTHESIS

In this chapter the techniques employed in the synthesis of block copolymers will be discussed. The overall method used to prepare block copolymers was the anion to free-radical transformation process (section 1.4.4). The basic series of events being;

- 1) the production of bromine terminated polystyrene,
- 2) the removal of the terminal bromine to form a radical; this was effected by photochemically reacting dimanganese decacarbonyl with the polymeric halide,
- 3) initiation, propagation and termination of the growing radicals in the presence of a suitable monomer.

Free-radical homopolymerizations were investigated for each of the vinyl monomers that were used in this study. The reason for investigating the homopolymerizations was to establish reaction conditions that would allow the polymerizations to obey simple kinetics. These conditions were then applied to the copolymerization processes, so that the free-radical stage of the copolymerization would also obey simple kinetics. The homopolymer once produced would also be used to aid the analysis of GPC data for the copolymers.

The copolymers produced were of the AB and ABA type,

where the A component in each copolymer was polystyrene that had been prepared anionically. The B component of the copolymers was one of the following acrylates or methacrylates; methylmethacrylate, n-butylmethacrylate, methyl acrylate, ethylacrylate and n-butylacrylate. Preliminary experiments were also carried out using chloroprene as the B component, but were not carried through to large scale copolymer preparations, due to purification problems with the necessary amounts of chloroprene required.

## 2.1 EXPERIMENTAL

### 2.1.1 Purification of materials

#### i) Monomers

All the monomers used during this work were commercially available, stabilised with low concentrations of inhibitor. Chloroprene was kindly supplied by DuPont. All the inhibitors present in the monomers were effectively removed before polymerizations were undertaken by the following method.

The monomers were passed through a column (approximately 40 cm in height) containing powdered aluminium oxide, using suction from a water pump. The unstabilised monomers were then distilled under vacuum, then flushed with nitrogen before being stored at  $-30^{\circ}$  C in a freezer until required. In all cases calcium hydride was added at this stage to

remove water that may be present. None of the purified monomers was stored for more than 14 days before use. Immediately before use the monomers were de-gassed using a freeze-pump-thaw method on a high vacuum line and then pre-polymerized by U.V. irradiation or heating in a water bath for various times, depending on the particular monomer, to remove any last traces of inhibitor. The pure monomer was distilled from the polymer on the vacuum line and then immediately used.

The aluminium oxide used in the column was supplied by B.D.H. (Brockmann Grade 1, active, neutral).

Distillation and pre-polymerization data for the monomers used is given below:-

| Monomer             | Source  | Temperature<br>/° C | Pressure<br>/mmHg | Pre-polymerization<br>time/minutes |
|---------------------|---------|---------------------|-------------------|------------------------------------|
| Styrene             | B.D.H.  | 45                  | 20                | 60                                 |
| Methylmethacrylate  | B.D.H.  | 42                  | 80                | 60                                 |
| n-Butylmethacrylate | B.D.H.  | 57                  | 12                | 90                                 |
| Methylacrylate      | B.D.H.  | 32                  | 140               | 15                                 |
| Ethylacrylate       | Aldrich | 35                  | 80                | 20                                 |
| n-Butylacrylate     | B.D.H.  | 48                  | 12                | 30                                 |
| Chloroprene         | DuPont  | 58                  | 760               | 60*                                |

\* U.V. radiation

Difficulties were encountered in the purification of n-Butylmethacrylate. A dilatometric technique was used

to study the free-radical polymerization kinetics of the individual monomers. Conversion-time curves generated in the n-butylmethacrylate case were characterized by an induction period, due to the presence of residual inhibitor. This residual impurity was removed by passing the monomer through the alumina column a second time.

### ii) Initiators

Dimanganese decacarbonyl (Alpha Chemicals Ltd) was purified by sublimation under vacuum and was stored in the dark at  $-10^{\circ}\text{C}$  in a refrigerator.

Azo-bis-isobutyronitrile (BDH) was purified by recrystallization from hot methanol and stored in a freezer.

N-butyl lithium (Aldrich, 2.7 M in hexane) was used without further purification.

### iii) Solvents

Benzene (BDH, AR grade) was dried by refluxing with sodium wire for two hours and was then distilled onto calcium hydride and stored under nitrogen.

Tetrahydrofuran (THF) was supplied by May and Baker and was distilled from sodium diphenyl ketone under nitrogen.

#### iv) Other materials

1-bromoethyl benzene (Eastman Kodak) was used without further purification.

$\alpha, \alpha'$  Dibromo-m-xylene (Fluka) was purified by recrystallization from petroleum spirit (57) and stored in a desiccator.

1,2 Dibromoethane, supplied by Fluka, was freshly distilled under atmospheric pressure, collecting the fraction at a temperature of  $130^{\circ}$  C before use. Calcium hydride was used as an anti-bumping and drying agent.

### 2.2 Preparation and Purification of brominated Polystyrenes

The bromine terminated polystyrenes (prepolymer) were prepared by methods devised by Richards and co-workers. In this study, prepolymers were made by both nitrogen and high vacuum anionic polymerization techniques. The prepolymers used in all cases were anionically prepared polystyrenes that had terminal bromines. These prepolymers were then used to initiate free-radical polymerizations of vinyl monomers. The methods used were adapted from methods described in section 1.4.1 and involved the use of a Grignard intermediate.

### i) Preparation of the Grignard Reagent

Magnesium turnings were washed in diethyl ether to remove the surface coating of oxides. An anhydrous solution of magnesium bromide in tetrahydrofuran was prepared "in situ" (Equation 2.1) by the gradual addition of 0.2 M (37 g) of 1,2 dibromoethane to 6 g of magnesium turnings in 350 ml of refluxing tetrahydrofuran.



Caution was used while adding the 1,2 dibromoethane dropwise, as the reaction was extremely exothermic and rapid stirring was necessary to prevent uncontrolled frothing. The reaction was carried out under a nitrogen atmosphere.

When the addition of 1,2 Dibromoethane had been completed, the mixture was refluxed for one hour. While the mixture was hot (58), it was transferred to a clean vessel via nitrogen pressure. This involves using a sintered glass bulb attached to the transfer tube, so as to stop unreacted magnesium from also being transferred with the Grignard solution into the clean vessel. (Figure 2.1).

### ii) Anionic Polymerization of Styrene

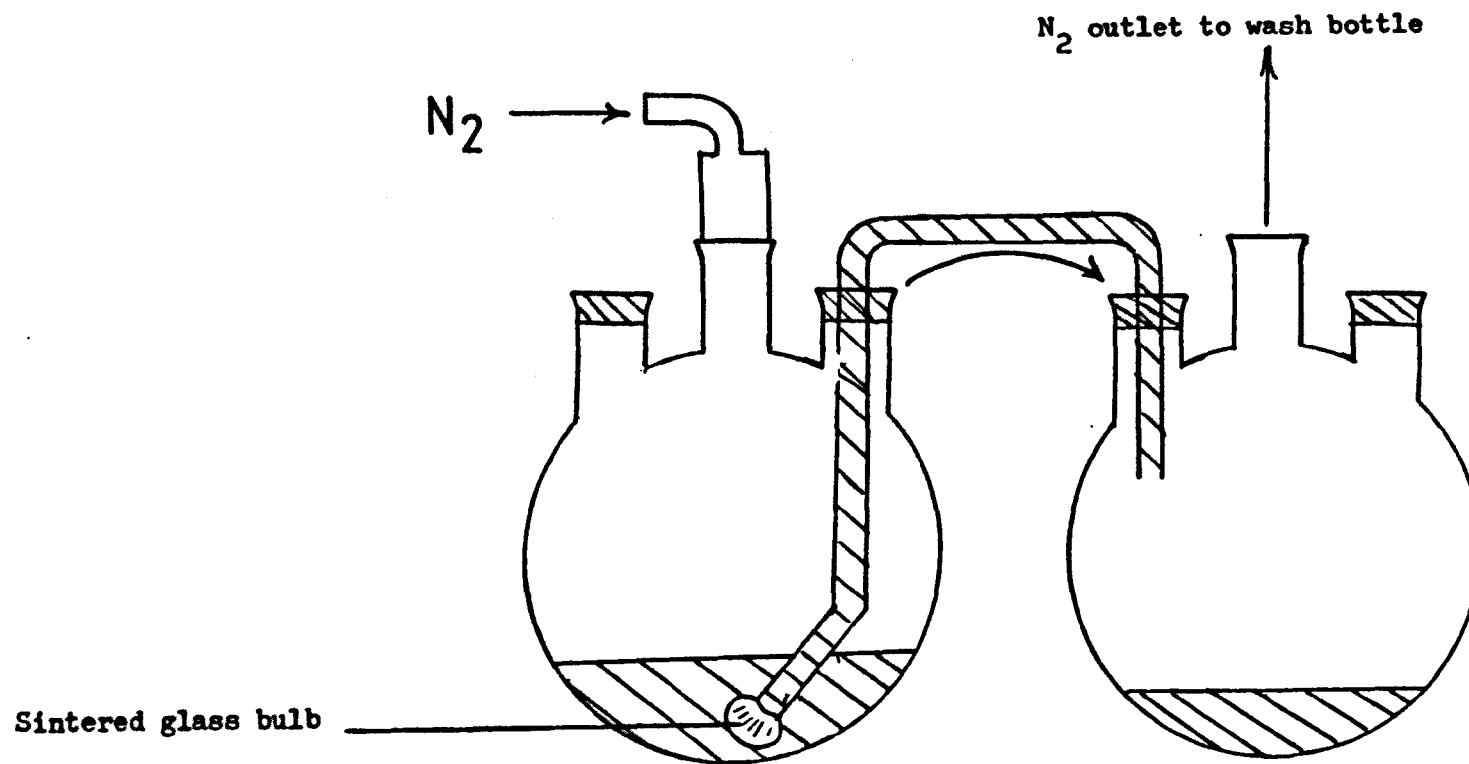
#### a) Nitrogen technique

A solution of purified styrene and benzene was de-gassed by bubbling nitrogen through it. The required amount of

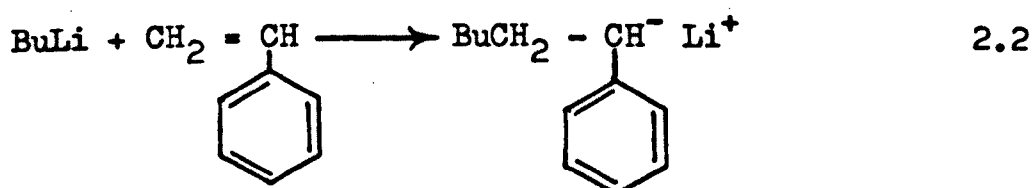


FIG.2.1

Solutions transferred by Nitrogen pressure



n-butyl lithium was then injected through a rubber septum, followed by a few drops of tetrahydrofuran. The resulting solution went red, indicating the formation of 'living' polymer, the red colouration was due to the presence of polystyryl ions (equation 2.2).



The reaction was left for two hours for the propagation process to proceed.

The 'living' polymer solution was then transferred using nitrogen pressure into the vessel containing the Grignard reagent, where the 'living' polymer was terminated by the Grignard as described in Chapter 1.4.1. On completing the termination, the Grignard intermediate was transferred again by nitrogen pressure, to a third vessel containing a degassed solution of  $\alpha, \alpha'$  dibromo-m-xylene in tetrahydrofuran. The ensuing reaction gives the prepolymer as shown in equation 1.30. The overall set up of equipment is given in figure 2.2.

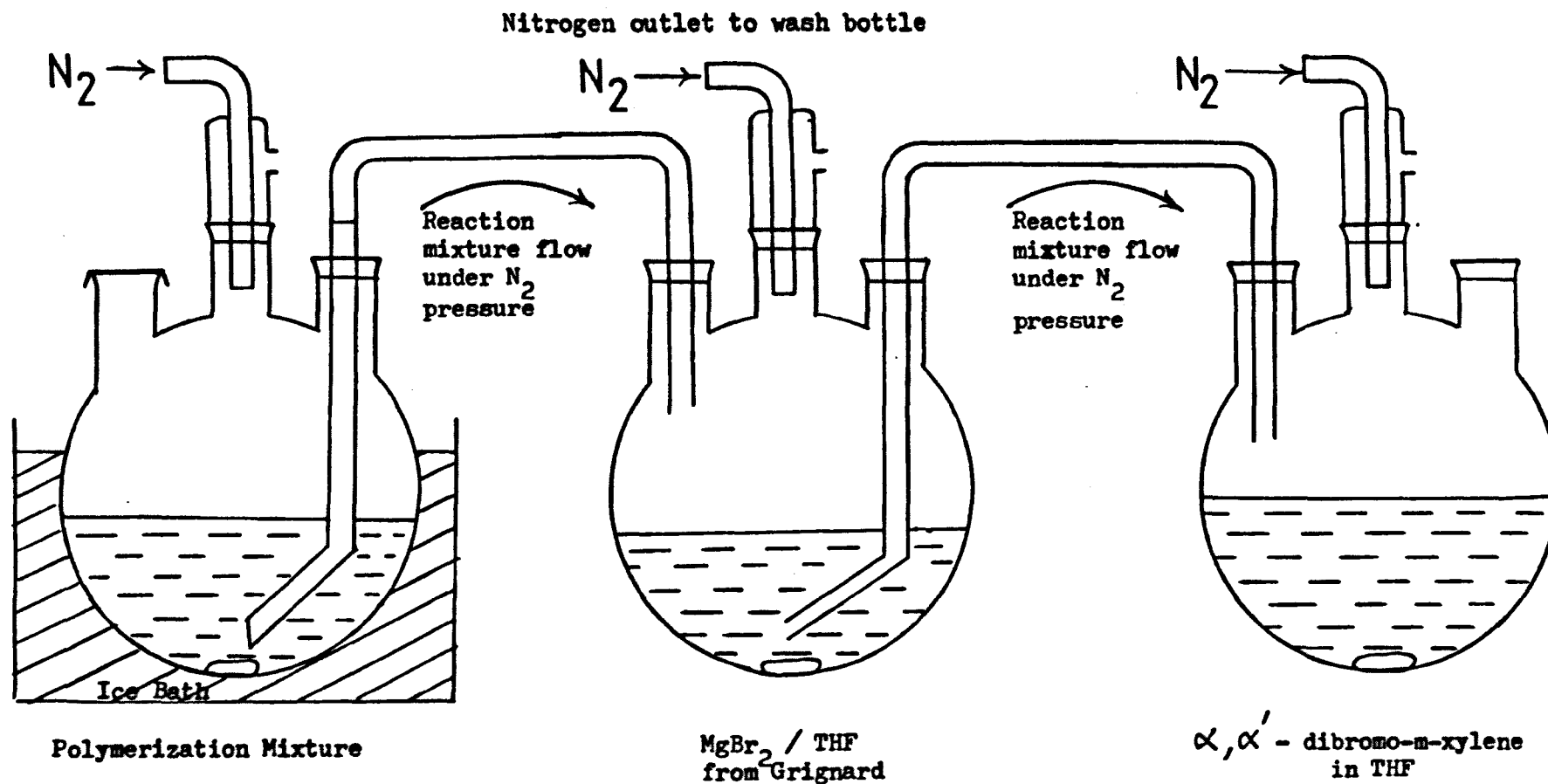
The prepolymer was extracted by precipitation into methanol, dried in a vacuum oven and then stored until required.

#### b) High vacuum technique

To produce polystyrene of high molecular weight with a

FIG. 2.2

Nitrogen Atmosphere Anionic Polymerization set up



narrow molecular weight distribution requires very high degrees of purity, because to get high molecular weights, only small quantities of initiator are used. The high vacuum technique affords the purity aspect of the polymerization by not having an atmosphere in which impurities are present, (oxygen in the atmosphere will terminate the anionic species) so providing the reagents have been purified sufficiently, there should be no termination of the propagating species by impurities. The overall order of events in this preparation is the same as for the nitrogen technique (initiation, propagation, termination with Grignard reagent and termination with  $\alpha, \alpha'$ -dibromo-*m*-xylene).

The two terminating agents were first prepared, purified and then placed in similar vessels denoted A, B as shown in figure 2.3. The Grignard reagent and the  $\alpha, \alpha'$ -dibromo-*m*-xylene were introduced into the vessels A, B in a nitrogen bag (Aldrich) that had been purged with nitrogen, the vessels A, B were then sealed using the greaseless taps. The vessels were placed on the vacuum line, where dry, degassed tetrahydrofuran was distilled onto the reagents to dissolve them and then the vessels A, B were sealed off at the constrictions denoted as X. These vessels were then glass-blown on to the polymerization vessel in figure 2.4. The styrene monomer and benzene were degassed by the freeze-thaw-pump method in the presence of calcium hydride (drying agent). The degassed liquids were then left on the line overnight and

FIG.2.3 Vessel A, B

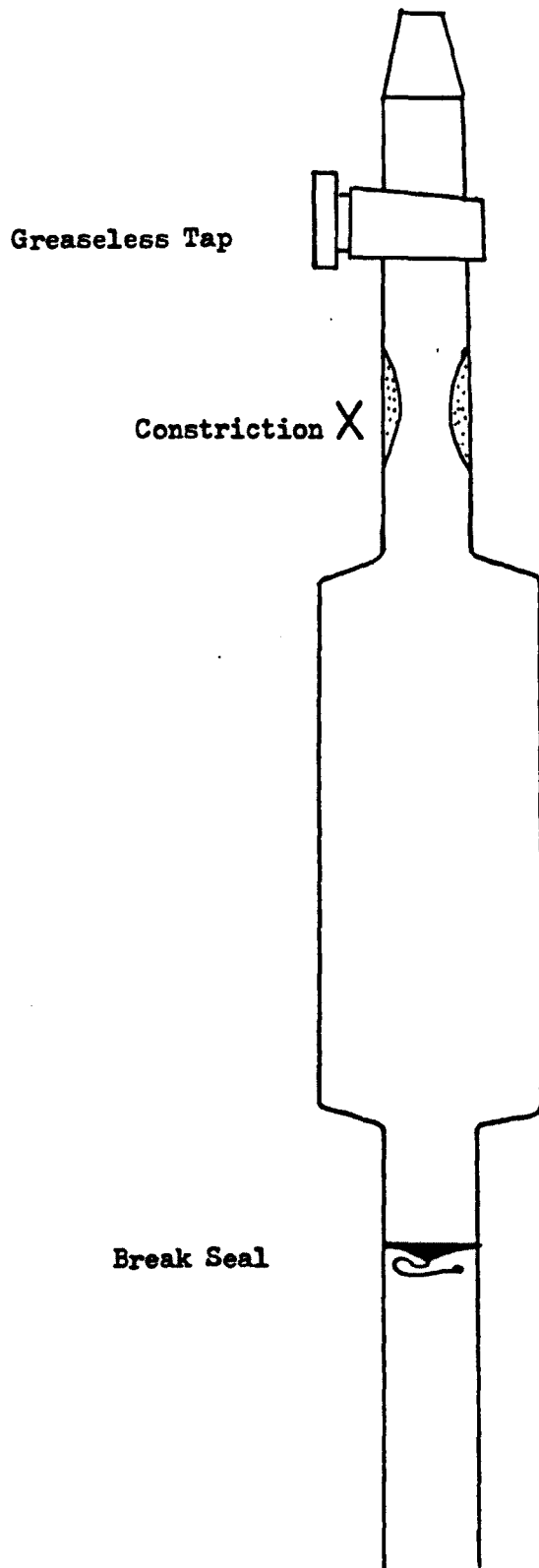
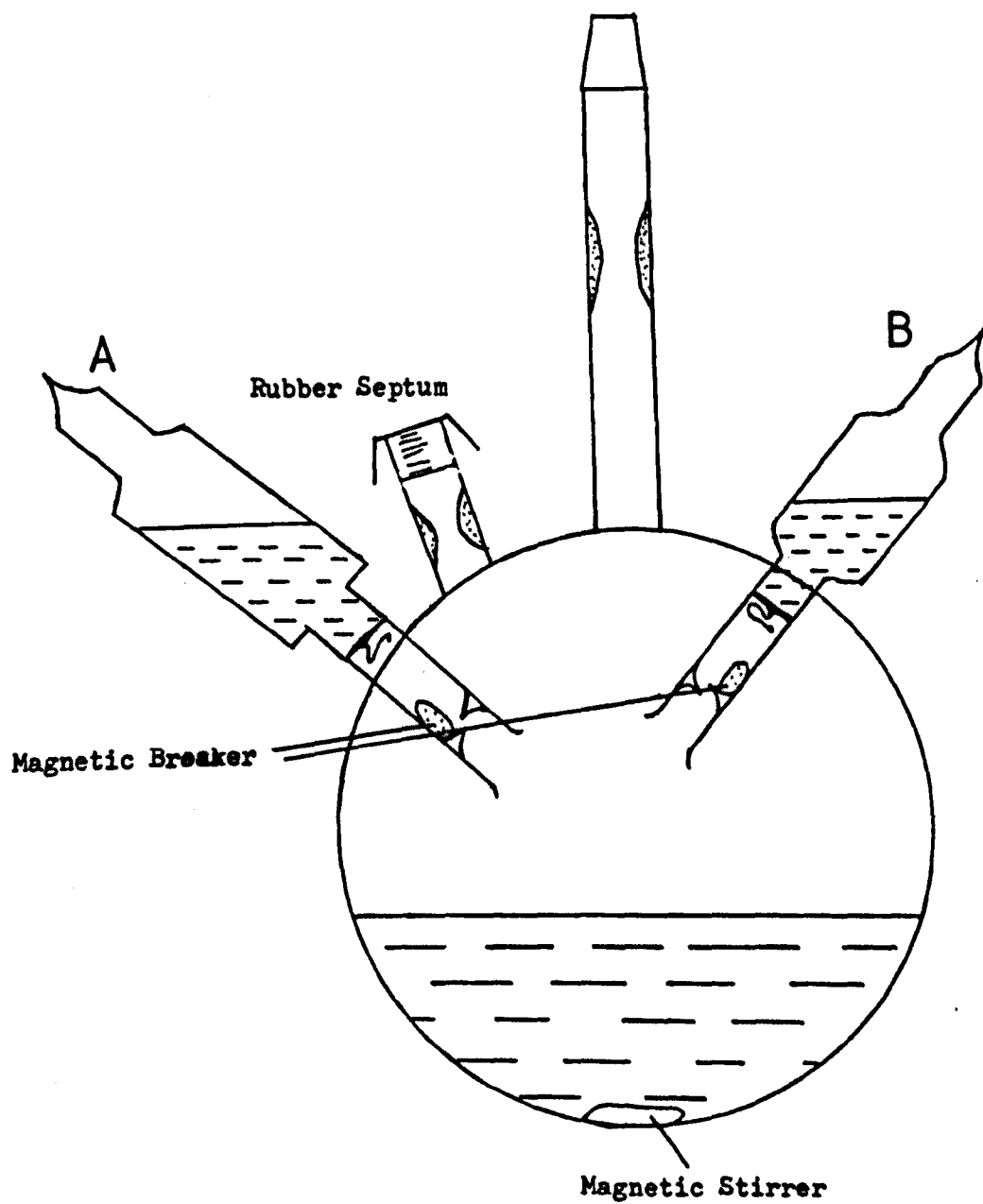


FIG. 2.4

High Vacuum Anionic Polymerization Vessel.



then distilled under vacuum into the polymerization vessel.

As an intermediate step, the styrene was first distilled into a vessel containing dibutyl magnesium (Phase Sep.). The dibutyl magnesium was obtained in solution with hexane, but for the purposes of this preparation the hexane had been previously distilled off on the vacuum line. The dibutyl magnesium acts as a scavenger, removing impurities that could affect the ionic polymerization of styrene, thus purifying the styrene. After 30 minutes pure styrene was distilled off into the polymerization vessel.

The actual polymerization was initiated by injecting the required amount of n-butyl lithium initiator into the polymerization vessel via a rubber septum, followed by a few drops of tetrahydrofuran. The tetrahydrofuran was added to catalyse the break up of the butyl lithium complex into individual molecules (equation 2.3).



After 3 hours the anionic polymerization was terminated as in the nitrogen technique, except that the terminating agents are added via break-seals on the vessel.

Again the resulting polymer was precipitated into methanol.

### 2.3 Free-radical Homopolymerizations

Bamford et al (45) in the mid 1960's showed that transition metal carbonyls could be used with organic halides to photoinitiate vinyl polymerizations; this general system was used throughout this work. The small molecule halide, bromoethyl benzene (bEb) was used with dimanganese decacarbonyl to prepare homopolymers, bEb being used because it is a model for the macroinitiators used in copolymerizations, and so will behave similarly to the macro-polystyryl radical that will later be used.

The kinetics of the homopolymerizations will be discussed in section 2.9, but polymerization conditions were adjusted, so as to obtain conditions under which homopolymerizations obeyed simple kinetics. The reactions were all carried out at 25° C in a thermostat tank. The concentrations of bEb used were between  $10^{-3}$  mol l<sup>-1</sup> and  $10^{-2}$  mol l<sup>-1</sup>, while dimanganese decacarbonyl concentrations were typically between 3.5 and  $4.2 \times 10^{-4}$  mol l<sup>-1</sup>.

The Norrish-Trömsdorff gel effect is observed in the free radical polymerization of bulk acrylates from virtually zero conversion. This effect occurs during a polymerization when high molecular weight chains are formed which increase the viscosity of the solution significantly; because termination is diffusion controlled, an increase in viscosity will decrease the rate of



termination and so even higher molecular weight chains are produced, so giving a highly concentrated solution with high viscosity that has the appearance of a gel. This "gel" effect is undesirable and must be removed. The effect can be reduced by polymerizing the monomer in solution. Dyson (59) has reported that the rate of polymerization obeys the simple kinetic equations up to 40% (V/V) methylacrylate in benzene. Polymerizations were undertaken for the three acrylate monomers being used (methylacrylate, MA; ethylacrylate, EA; n-Butylacrylate, NBA), from which it was found that a 20% (V/V) solution of acrylate monomer in benzene showed kinetic behaviour consistent with simple free-radical mechanisms, providing the conversions were kept low.

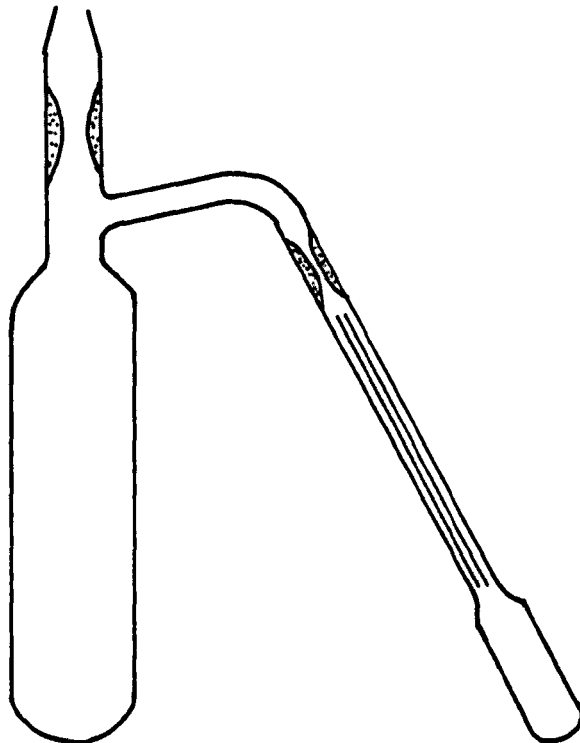
### 2.3.1 Small scale preparations

Irradiation of small samples (10 ml or less) and dilatometry were carried out by putting the samples in a thermostat tank full of water and irradiating them through a suitably positioned porthole. Figures 2.5 and 2.6 show the types of vessel employed in the small scale preparations and dilatometry respectively. Solutions were introduced to the vessels, de-gassed by the conventional freeze-pump-thaw technique on a high vacuum line ( $< 10^{-5}$  torr) and sealed off under vacuum at the constriction shown. For dilatometry, the vessel was then tipped up to allow a suitable amount of solution to pour into the dilatometer,

FIG. 2.5 Small Scale Vessel



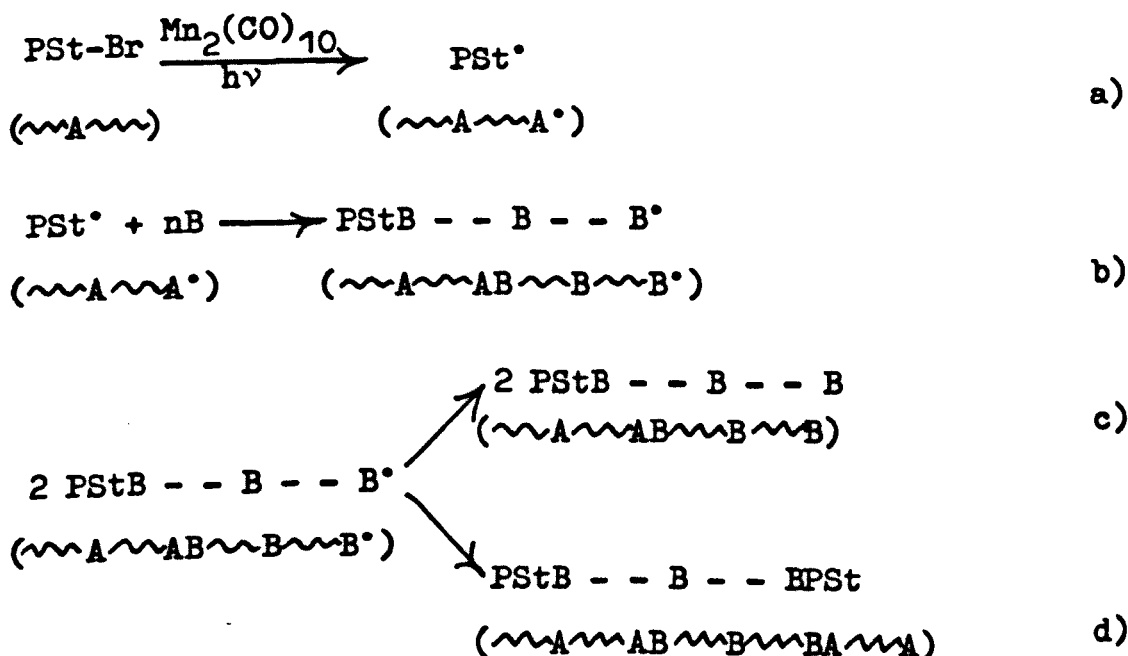
FIG. 2.6 Dilatometry Vessel



which was then sealed off at the second constriction. Dilatometer meniscus heights were measured by means of a cathatometer.

#### 2.4 Copolymerizations

The simplified overall reaction scheme which would describe the way a copolymer is formed from a preformed polymer (PSt-Br, A component, where PSt-Br denotes the bromine terminated polystyrene) and monomer B is as follows:



SCHEME 2.1

The structure of the block copolymers formed by the bimolecular termination process will depend on the actual termination process involved, either disproportionation or combination. Disproportionation termination leads to AB block copolymers by reaction 2.1 (c), while combination

leads to ABA block copolymers by reaction 2.1 (d). With the acrylate monomers used, it would be reasonable to assume that the structures produced would be of the ABA type, as it is known that acrylates almost exclusively terminate by combination (60). For methacrylate monomers the radicals generated undergo both modes of termination to produce a mixture of AB and ABA block copolymers; this is the case with n-butylmethacrylate which terminates approximately 25% by combination (60) with the remainder by disproportionation.

The synthesis of block copolymers requires the duplication of the reaction conditions found for the homopolymerizations of the various monomers, if it is hoped that the reaction will observe simple kinetic behaviour; the small molecule halide (bEb) being replaced by the preformed bromine terminated polystyrene. Woo (42) established the essential chemistry required and showed that if the molecular weight of the preformed polymer was low, the macroradicals produced obeyed simple kinetics and that the limiting halide concentration was similar to that of the small molecule halide.

Copolymerizations were carried out in small reaction vessels (10 ml or less), as described in 2.3.1. The products from these small scale vessels were isolated by precipitation into cold methanol and then dried in a vacuum oven to constant weight. From the weight of polymer isolated, the rate of polymerization of monomer B could be calculated.

Since all the primary radicals formed are macroradicals, the synthesis produces only small amounts of homopolymer B, which arises from transfer to monomer (the transfer constants gained from the literature (61) range from  $1.8 \times 10^{-5}$  for ethylacrylate to  $3.4 \times 10^{-6}$  for methylacrylate), so the reaction products should be a blend of copolymer and unreacted prepolymer (PSt-Br). Providing polymers A, B have sufficiently different properties, the texture of the reaction products can often indicate the presence of the second polymer B, and if the only initiating radicals are formed via the prepolymer, then the texture can sometimes indicate the presence of copolymer. Gel Permeation Chromatography (GPC) was also used to identify copolymer formation and this will be discussed in Chapter 3.

In order to produce sufficient material for mechanical testing it was necessary to use a different set of reaction vessels. The large scale apparatus was designed for the synthesis of copolymers and homopolymers, using up 100 ml of reaction solution.

#### 2.4.1 Large Scale Preparations

The large scale apparatus is illustrated in Figure 2.7. The reaction chamber consisted of a brass cylinder to which glass windows were clamped at both ends, sealed by rubber 'O' rings, to render the vessel airtight. Attached to the sides of the chamber were two inlet ports, which were used to evacuate the chamber and to introduce the polymerization

mixture. The chamber was placed in an optical system also shown in Figure 2.7. (A mirror, X, was used to ensure even irradiation throughout the sample). Reactions were carried out according to the following procedure.

The reaction mixture was put in a vessel of the type illustrated in Figure 2.8. The solution was de-gassed on a high vacuum line as previously described and then sealed by means of the greaseless tap E. The vessel was then attached to the reaction chamber as shown in Figure 2.7 and with taps A and B open, tap C connected to a manometer and tap D connected to a rotary pump, the system was evacuated. Following evacuation, nitrogen was introduced via tap D, the increase in pressure being monitored with the manometer. When atmosphere pressure was attained tap C was switched to the wash bottle, so that the excess nitrogen could escape. To evacuate the chamber again taps D and C were closed and then tap D was opened to the rotary pump and tap C to the manometer. This evacuation and nitrogen flushing procedure was repeated, at least eight times. After the final evacuation, tap A was closed and tap E opened, so that the solution could flow into the chamber, followed by the closure of tap B and the admission of nitrogen to the system by tap D, the excess nitrogen being released via tap C. The polymerizations were all then carried out under a nitrogen atmosphere.

The reaction chamber was always checked for leaks by means of a Pirani vacuum gauge attached to one of the inlet ports prior to use.

FIG. 2.7

Large Scale Preparations.

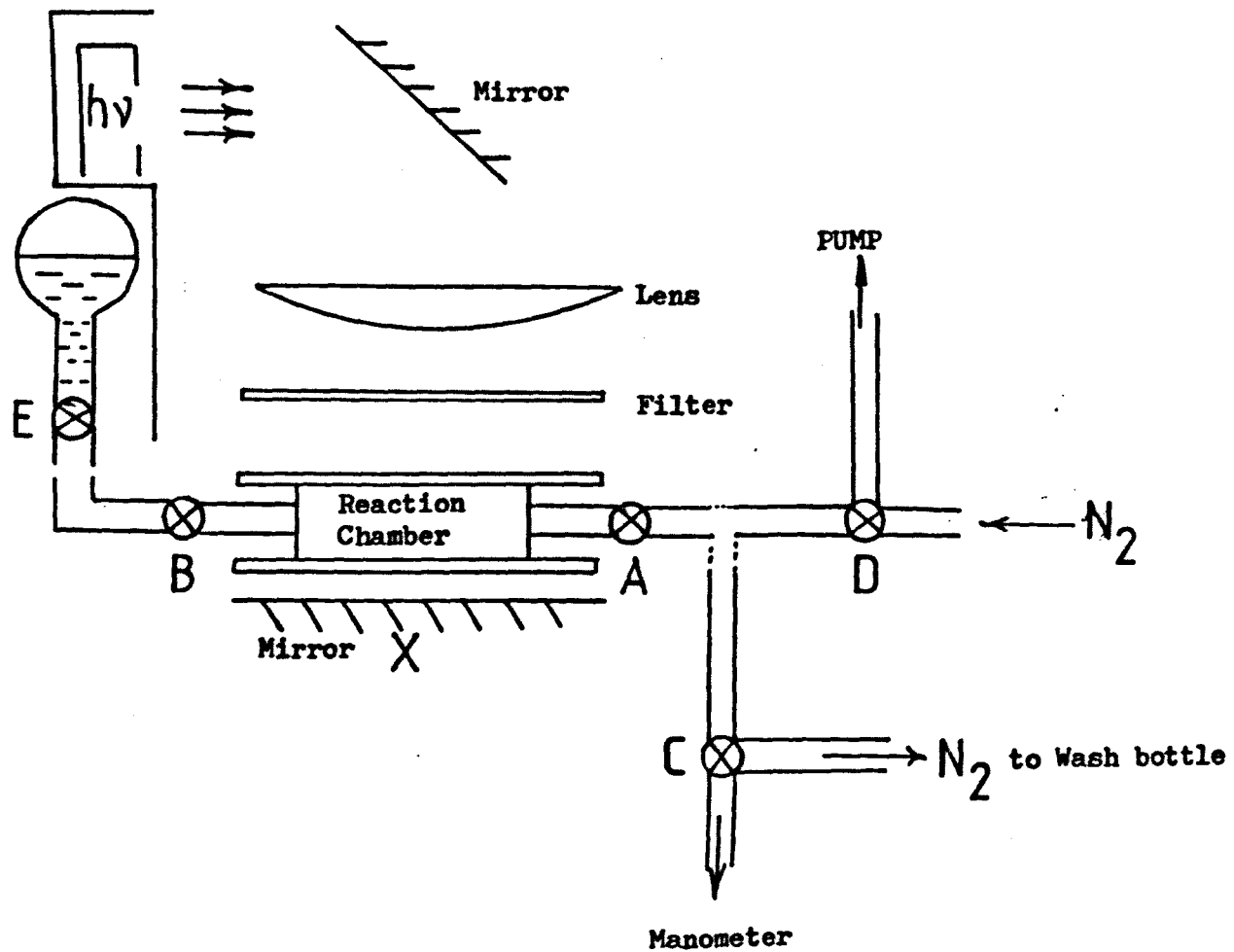
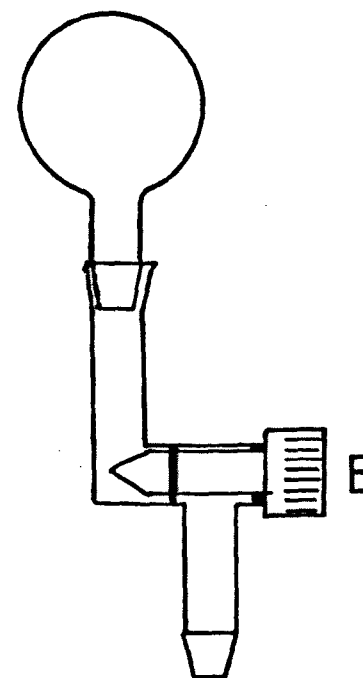


FIG. 2.8



## 2.5 Photoinitiation apparatus

One of two sets of apparatus was employed for the photoinitiation of mixtures depending on the volume of solution being irradiated. In both cases, light of wavelength,

$\lambda = 438.5 \text{ nm}$ , was obtained by using a 250 watt mercury lamp in series with two Kodak filters, type 2E and 98, and focussed into a parallel beam by means of a lens system. Polymerizations photoinitiated by azo-bis-isobutyronitrile employed a 365 nm filter. Light intensity was varied by means of neutral density filters (Kodak) which were calibrated at the requisite wavelengths by measuring the rates of polymerization for simple homopolymerization reactions. Rates were measured by means of a gravimetric method for identical samples, using the different intensity filters. The light intensity alters the rate of initiation which is directly related to the rate of polymerization and so the rate of polymerization can be related to the light intensity used. All polymerizations were conducted in a closed room illuminated by inactive sodium light.

## 2.6 The High Vacuum System

All polymerization reaction mixtures were de-gassed on a high vacuum line except for the anionic polymerizations done under nitrogen. The polymerizations involving the use of the small scale reaction vessels were also carried out under vacuum. The pumping system used consisted of a



mercury diffusion pump backed by a rotary pump; this system gave residual gas pressures of less than  $10^{-5}$  torr. Attached to the high vacuum end of the system was a manifold, which had a number of outlet taps connected to B14 quickfit sockets. Through these outlets all the various high vacuum operations were effected.

## 2.7 Concentration of dimanganese decacarbonyl used in reaction mixtures

Using the Beer-Lambert equation the intensity of light transmitted through a solution can be found (equation 2.4).

$$\ln\left(\frac{I}{I_0}\right) = - \epsilon c l \quad 2.4$$

where  $I$  and  $I_0$  are the transmitted light and incident light intensities respectively, while  $\epsilon$ ,  $c$  and  $l$  are the extinction coefficient, the concentration of the solute, and the path length respectively.

For essentially uniform light intensity and reaction rates throughout the reaction vessel, not more than 10% of the incident light must be absorbed. From equation 2.4, it can be seen that as the concentration of the carbonyl increases, more light is absorbed by the solution and so there is a limiting concentration at which the absorbed light becomes significant<sup>with</sup> respect to the transmitted light, resulting in non-uniform light absorption. The maximum value of carbonyl concentration used that would

mean no more than 10% of the incident light would be absorbed was  $4.4 \times 10^{-4} \text{ mol l}^{-1}$ , for a path length of 1 cm. The decadic molar extinction coefficient for dimanganese decacarbonyl was reported by Bamford et al (45) to be  $254 \text{ l mol}^{-1} \text{ cm}^2$ .

## 2.8 Measurement of Polymerization Rates

Using a gravimetric method the rate of polymerization could be calculated. This method involved weighting the polymer formed in a given irradiation period. Typically, this was done for small preparations (10 ml or less) accurately, but for the large scale preparations the experimental rates were very approximate, because it was virtually impossible to recover all the polymer from the vessels used.

After polymerization, the vessels were broken open and the contents slowly added to a ten-fold excess of cold methanol, in order to precipitate the polymer. After settling, the polymers were filtered off (using sintered glass crucibles), washed with methanol and then dried in a vacuum oven until a constant weight was reached. The average rate of polymerization,  $\omega$  ( $\text{mol l}^{-1} \text{s}^{-1}$ ) is given by

$$\omega = \frac{X \times 1000}{M \cdot V \cdot t}$$

where X is the weight of polymer formed (g), V, M and t are the volume of solution ( $\text{cm}^3$ ), the molecular weight of monomer ( $\text{g mol}^{-1}$ ), reaction time (s) respectively.

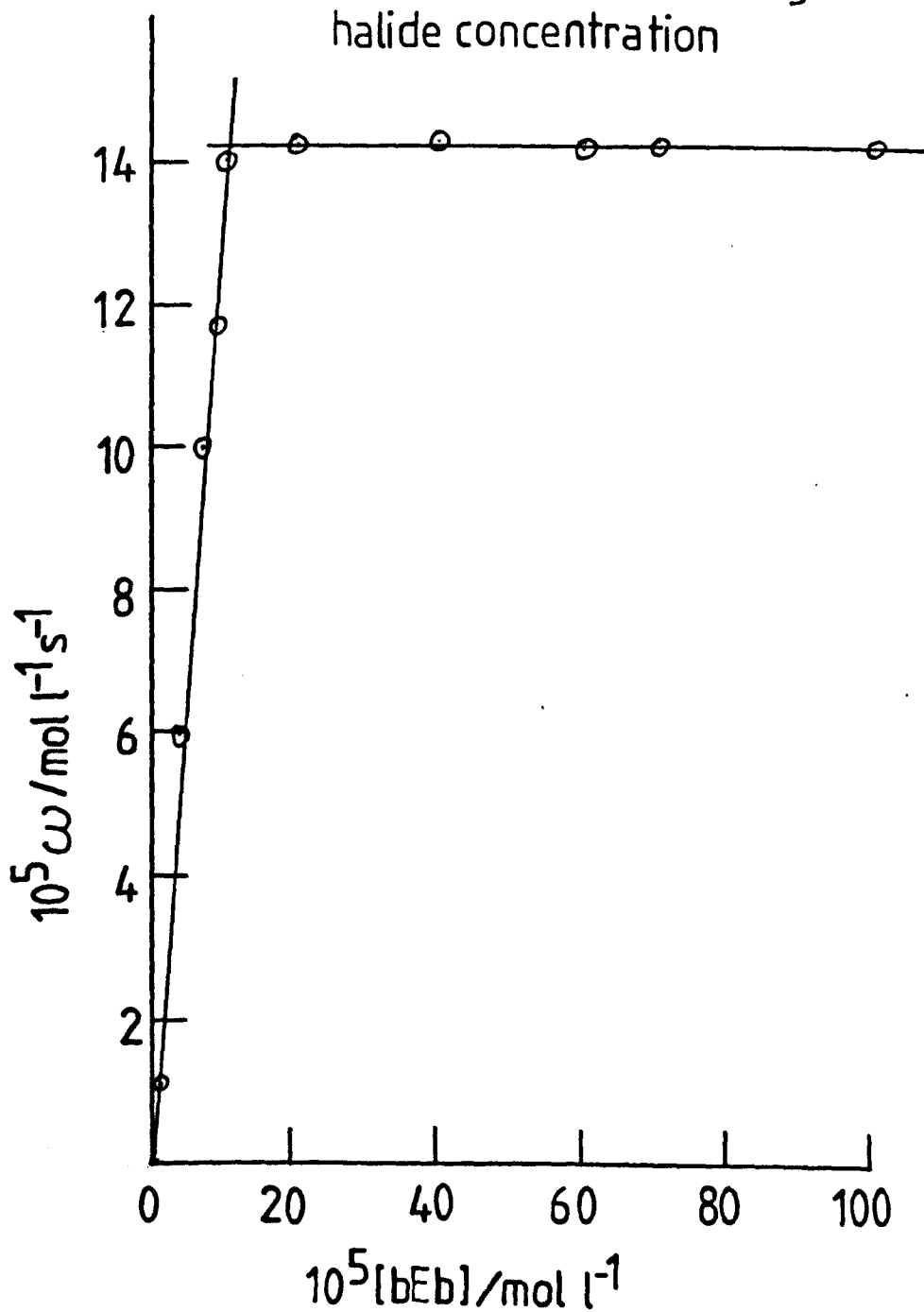
## 2.9 Kinetic Studies

### 2.9.1 Homopolymerizations

It was found during this study that there was a dependency of rate of polymerization on the halide concentration, and that above a limiting halide concentration the rate essentially became constant; these observations were in agreement with the findings of Bamford et al (45, 46). To maintain a constant rate during the reaction, the halide concentration must not fall below the value at which the rate becomes dependant on the halide concentration. For the polymerization of bulk methylmethacrylate, this limiting value of halide concentration was found to be approximately  $1 \times 10^{-4} \text{ mol l}^{-1}$  (see Figure 2.9), which is in agreement with Woo (42). Assuming that there are no interactions between the monomer and solvent that could affect initiation, the rate of initiation using the carbonyl/halide initiating system is independant of the monomer/solvent system under investigation (62). It would therefore be reasonable to assume the limiting halide concentration would approximate to a constant, providing the initiating system remains the same.

If the homopolymerizations of the different monomers

FIG. 2.9 Measurement of limiting halide concentration



Bulk Polymerization at  $25^\circ\text{C}$   
 $[\text{Mn}_2(\text{CO})_{10}] = 4.2 \times 10^{-4} \text{mol l}^{-1}$

obey simple kinetic theory, they would all comply with equation 1.15.

$$-\frac{d[M]}{dt} = \omega = \frac{k_p}{k_t^{1/2}} M I^{1/2} \quad 1.15$$

where  $\omega, I^{1/2}$  are the rate of polymerization and the square root of the rate of initiation respectively,  $k_p/k_t^{1/2}$  is a constant related to the monomer type and  $[M]$  is the monomer concentration. By judicious use of different light intensity filters on the optical system, the rate of initiation can be controlled, as the initiation is a photochemical process as described in Chapter I. It was found that when graphs were plotted of rate of polymerization,  $\omega$ , against the square root of the intensity (arbitrary units), straight line graphs were observed, which would agree with equation 1.15 and so simple kinetics. The figures 2.10-15 show these graphs; it must be pointed out that the graphs do not go through the origin because of slight thermal polymerization during the reaction (low rate of initiation).

It was also found that the rate,  $\omega$ , was constant over a time period longer than the normal irradiation time of 30 minutes.

For each set of results used in each homopolymer case, the Mayo Equation (equation 1.18) was used to calculate an "apparent" value of the characteristic parameter  $k_p.k_t^{-1/2}$  ( $k_p, k_t$  are respectively, the rate coefficients for

FIG. (2.10- 2.15)

All Polymerizations were undertaken at 25°C  
[bEb] =  $10^{-3}$  mol l<sup>-1</sup> in all cases

FIG. 2.10 Polymethylmethacrylate(bulk)

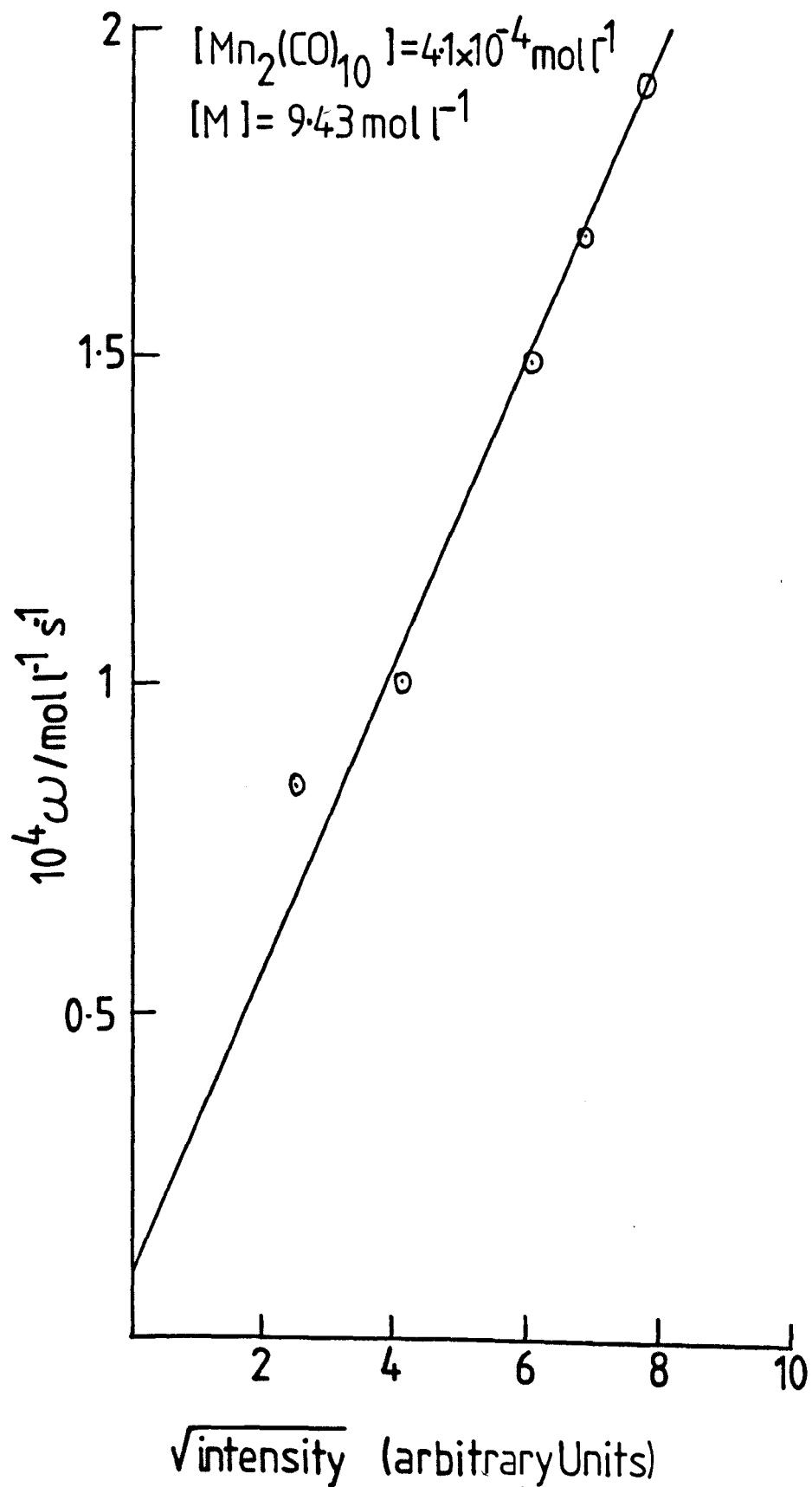


FIG. 2.11 Polyn-butylmethacrylate (bulk)

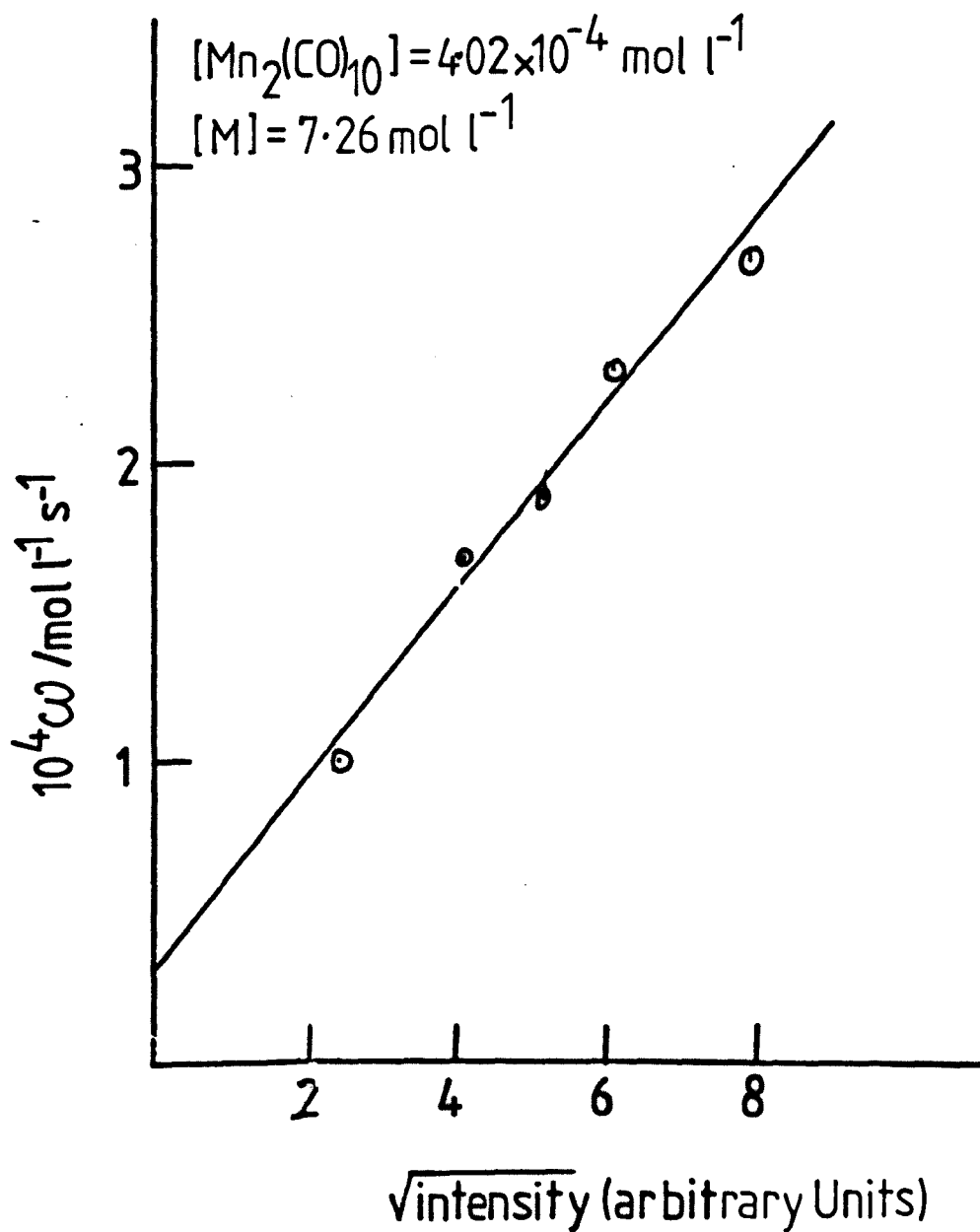




FIG. 2.12

Poly n-butylmethacrylate (50% solution)

$$[\text{carbonyl}] = 3.96 \times 10^{-4} \text{ mol l}^{-1}$$

$$[M] = 3.78 \text{ mol l}^{-1}$$

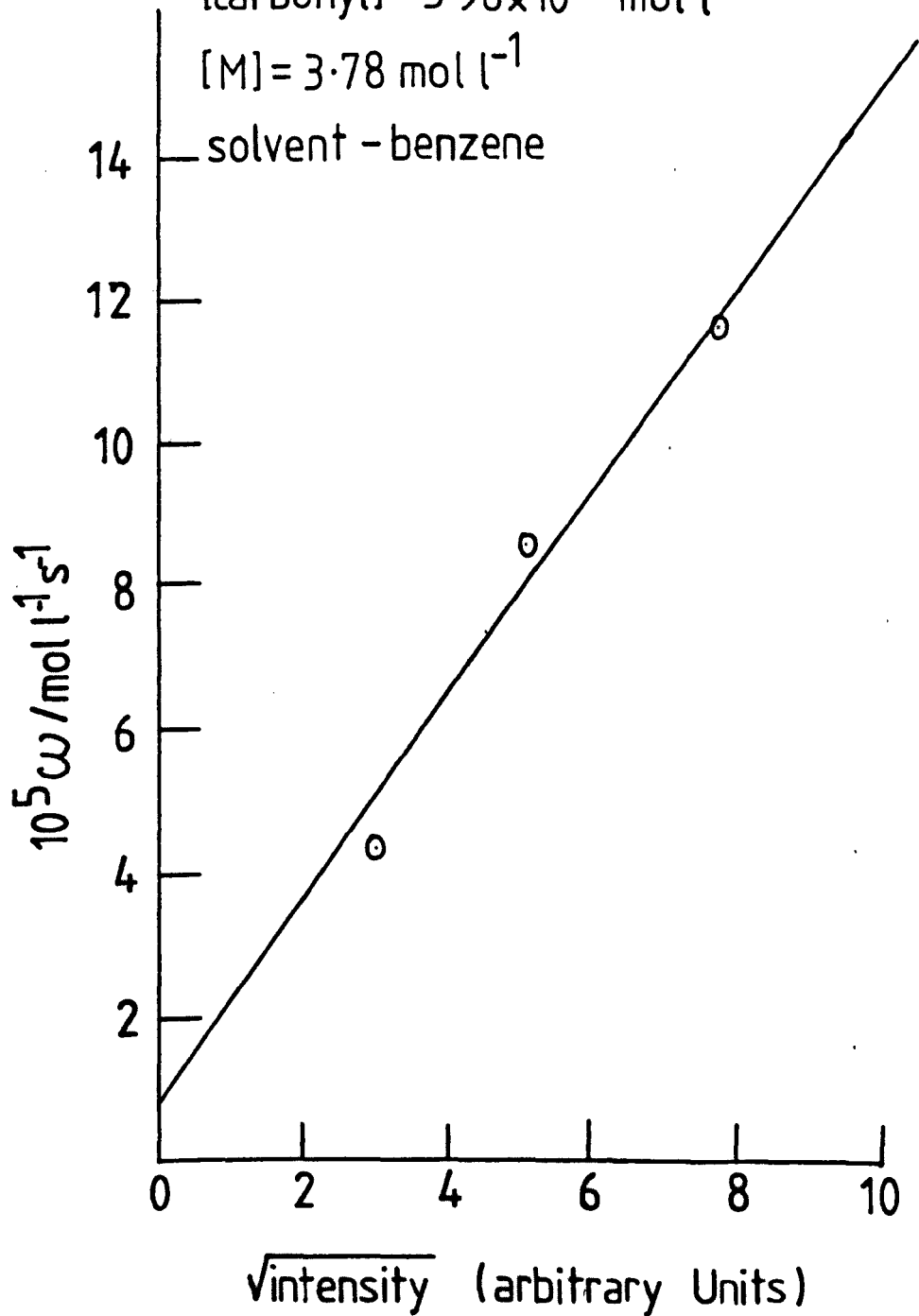


FIG. 2.13

Poly n-butylmethacrylate (30% solution)

[carbonyl] =  $4.02 \times 10^{-4} \text{ mol l}^{-1}$

[M] =  $2.27 \text{ mol l}^{-1}$

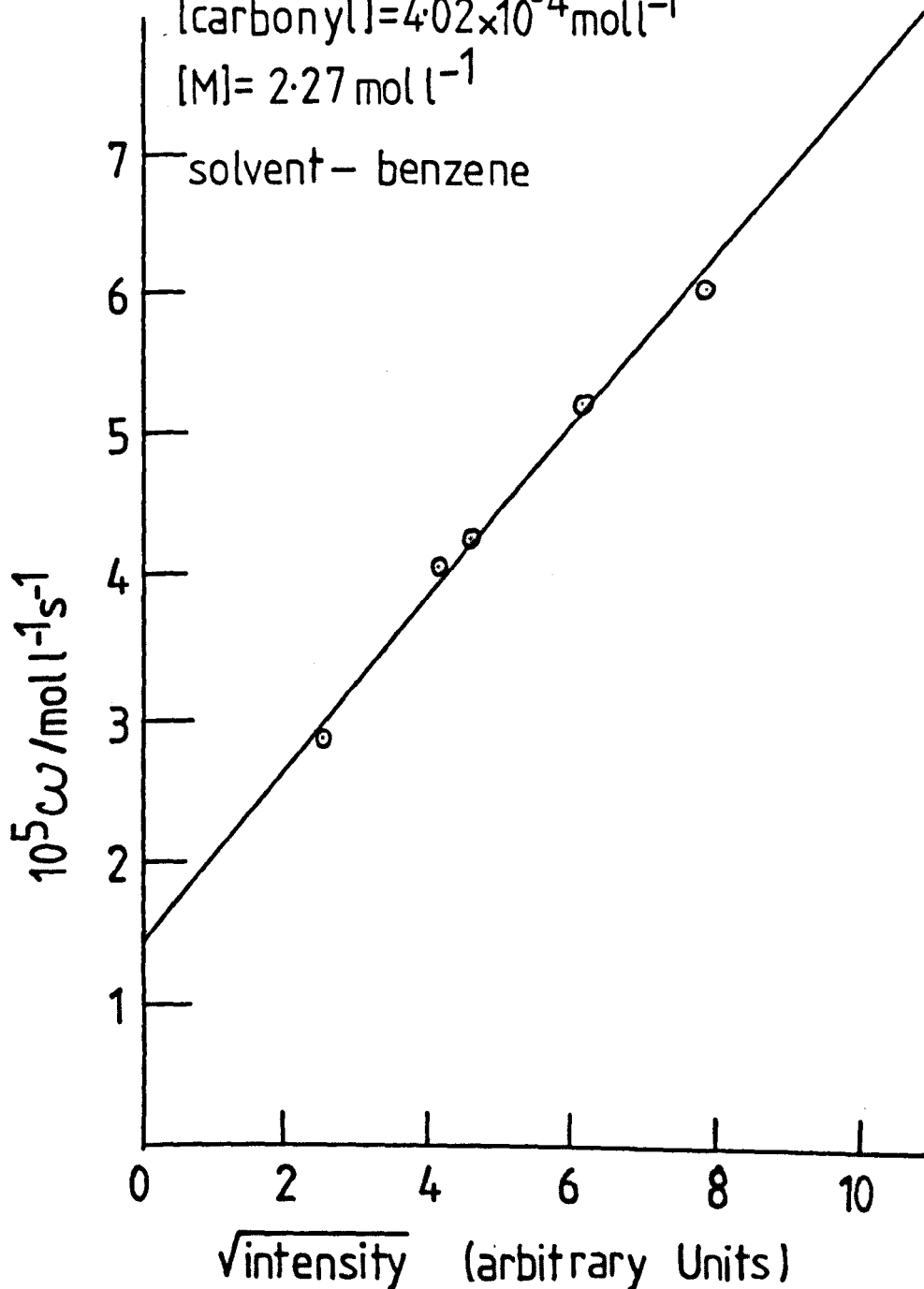


FIG. 2.14

Polymethylacrylate

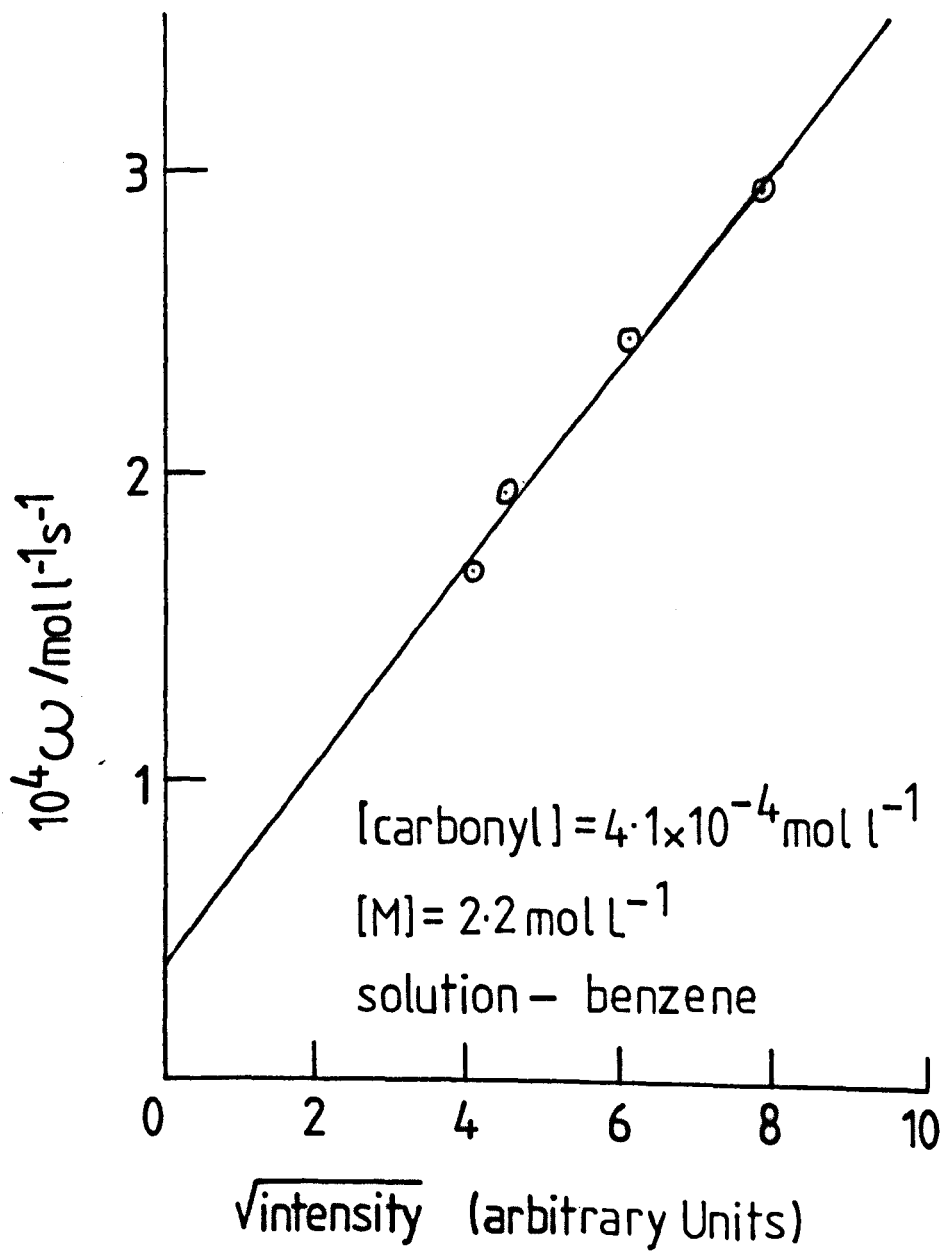
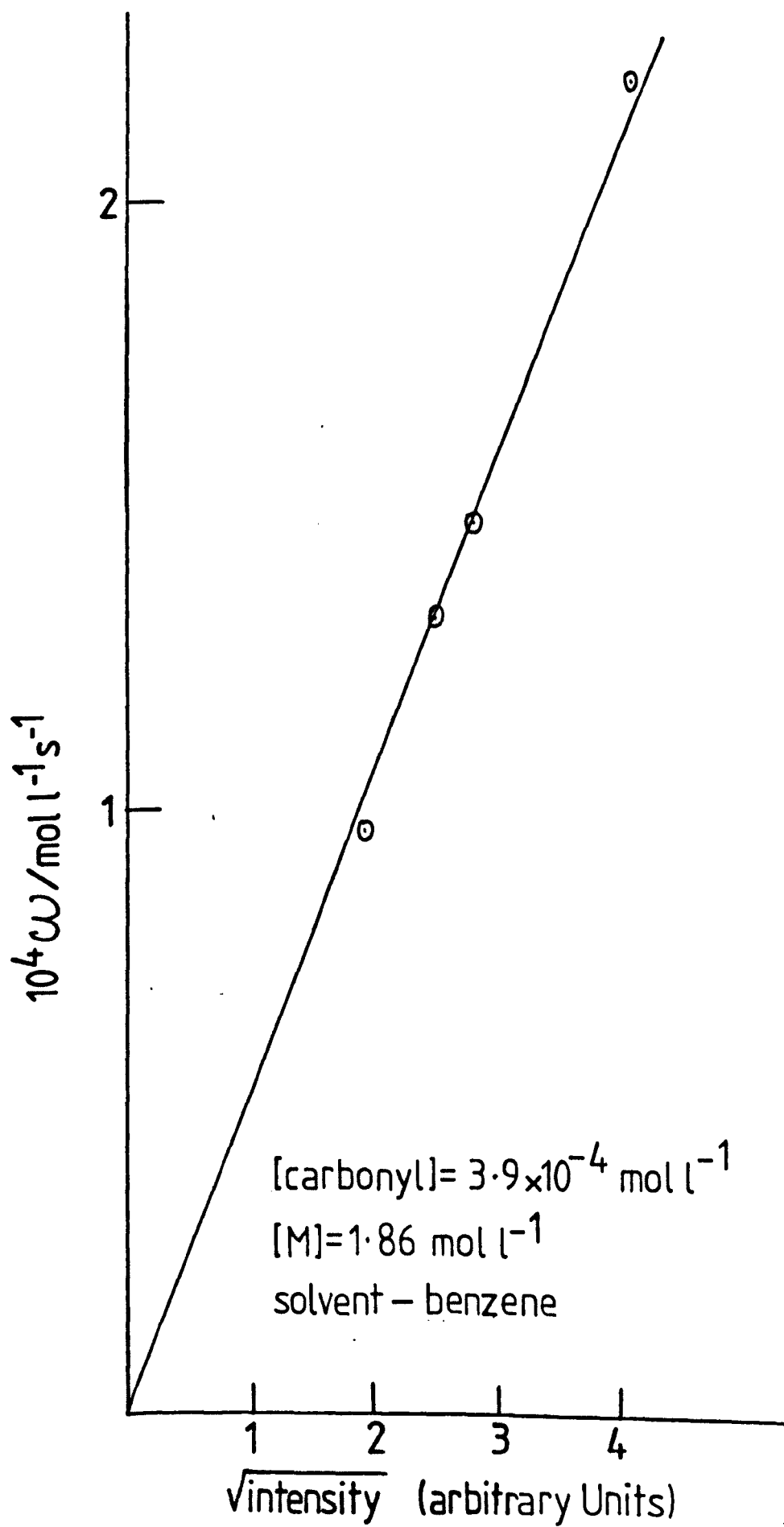


FIG. 2.15 Polyethylacrylate



propagation and termination of radical polymerization), these values being compared to literature values, see table 2.1

$$\frac{1}{\bar{P}_n} = \frac{1}{\bar{P}_{no}} + \frac{C_s [S]}{[M]} \quad 1.18$$

if there is no transfer  $C_s = 0$  ( $C_s$  is the transfer constant)

$$\frac{1}{\bar{P}_n} = \frac{1}{\bar{P}_{no}}$$

$$\text{where } \frac{1}{\bar{P}_n} = \frac{(k_{td} + k_{tc}/2)^{1/2}}{(k_{td} + k_{tc})^{1/2} k_p [M]} + \frac{k_{fm}}{k_p}$$

It can be shown that

$$\frac{1}{\bar{P}_n} = \frac{kt \left( \frac{1+x}{2} \right) \omega}{k_p^2 [M]^2} \quad 2.6$$

where  $x$  is the proportion of disproportionation termination in the reaction. From equation 2.6 it can be seen that if a graph of  $1/\bar{P}_n$  against  $\omega$  were drawn, the slope of the graph could be used to calculate the "apparent" value of  $k_p k_t^{-1/2}$  for that monomer. For the monomers used values of  $\bar{P}_n$  were determined using gel permeation chromatography, the standards used being methylmethacrylate. A conversion factor was applied to account for the lack of suitable standards for the different polymers (this factor being based on the 'Q-factor' method for calibration of Moore and Hendrickson (53)). This 'Q-factor' method for calibration makes use of the extended chain length as a calibration parameter, in that it is assumed that polymers with the same extended chain length will elute at the same retention volume, irrespective of chemical nature. The Q-factor is defined

TABLE 2.1

| Homopolymer         | % (v/v) of monomer in reaction mixture | $(k_p/k_t^{1/2})_{app}/l^{1/2}mol^{-1/2}s^{-1/2}$ |             | Ref.   |
|---------------------|----------------------------------------|---------------------------------------------------|-------------|--------|
|                     |                                        | Experimental                                      | Literature  |        |
| Methylmethacrylate  | 100                                    | 0.053                                             | 0.055       | 9      |
| n-Butylmethacrylate | 100                                    | 0.1098                                            | 0.099-0.11  | 59     |
| n-Butylmethacrylate | 50                                     | 0.093                                             | 0.099-0.11  | 59     |
| n-Butylmethacrylate | 30                                     | 0.089                                             | 0.099-0.11  | 59     |
| Methylacrylate      | 20                                     | 0.231                                             | 0.213-0.227 | 61     |
| Ethylacrylate       | 20                                     | 0.227                                             | 0.24        | 61     |
| n-Butylacrylate     | 20                                     | 0.247                                             | 0.13-0.72   | 59, 61 |

as the molecular weight per extended chain length unit. The conversion factor for the molecular weight of a polymer using a polymethylmethacrylate calibration involves the multiplication factor,  $Q(\text{polymer})/Q(\text{polymethylmethacrylate})$ . As a guide this factor is assumed to be the ratio of the monomer molecular weight to the molecular weight of methylmethacrylate monomer.

The graphs of  $1/\bar{P}_n$  against rate,  $\omega$  are given in figures 2.16-21. The value in table 2.1 for the homopolym-Butylacrylate is based on one point, as this homopolymer proved to be extremely difficult to handle, *owing* to its low glass transition temperature. As a result, the samples obtained often gave inconsistent results with respect to the rate; not all the polymer could be collected and so the rate,  $\omega$ , would often be artificially low.

The 'apparent' values of  $k_p/k_t^{1/2}$  are in good agreement with literature values and this again would seem to show that the homopolymerizations undertaken were proceeding in a manner obeying simple kinetics under the conditions used. These conditions were then transferred to the copolymerization experiments in the hope that the monomers would still behave as they did for the homopolymerizations.

### 2.9.2 Copolymerizations

The activity of samples of polystyrene (PSt) with terminal bromine atoms (PSt-Br) used in copolymer synthesis

FIG. (2.16-2.21)

Conditions as for FIGS. 2.10-2.15



FIG. 2.16 Polymethylmethacrylate

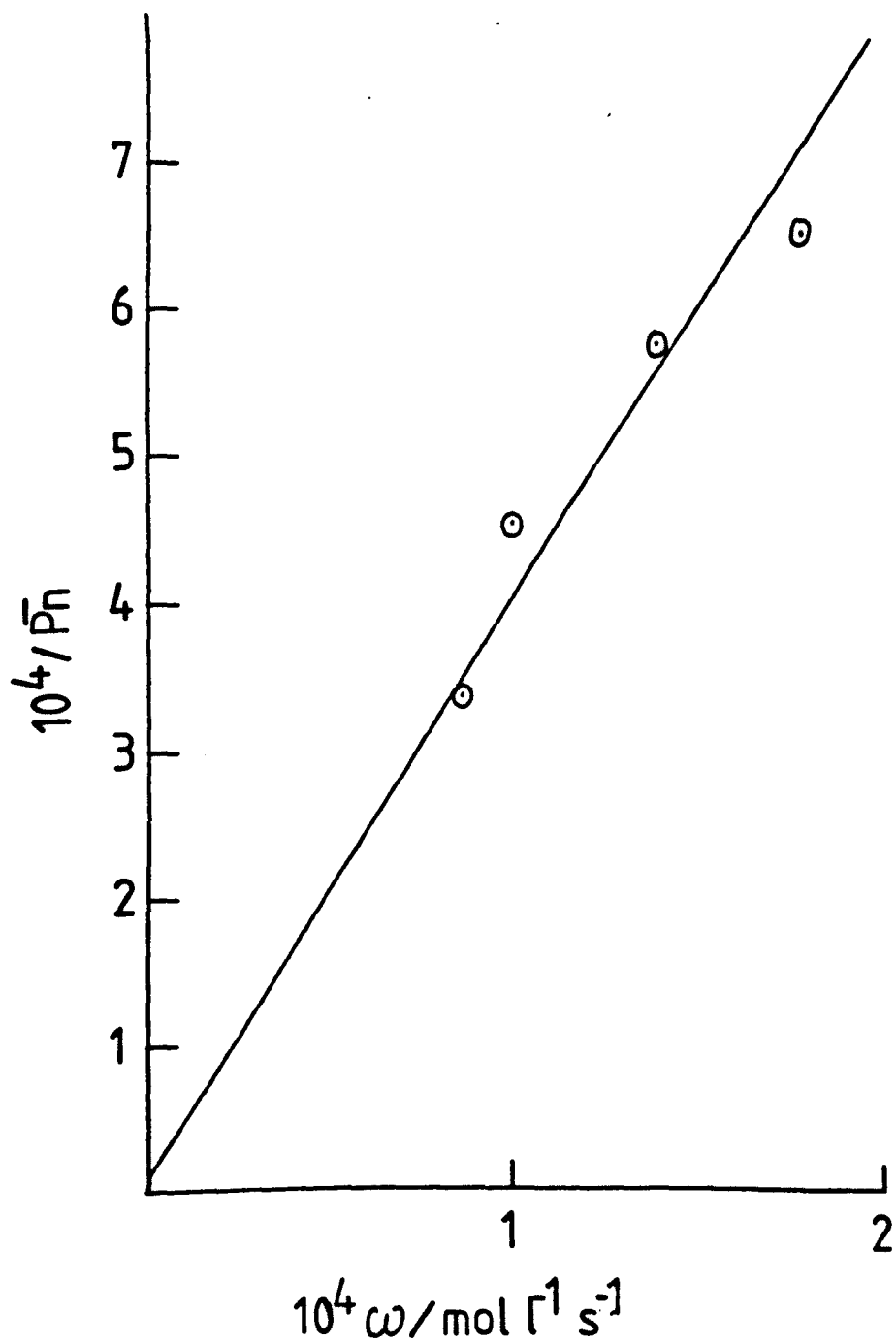


FIG. 2.17 Polymethylacrylate

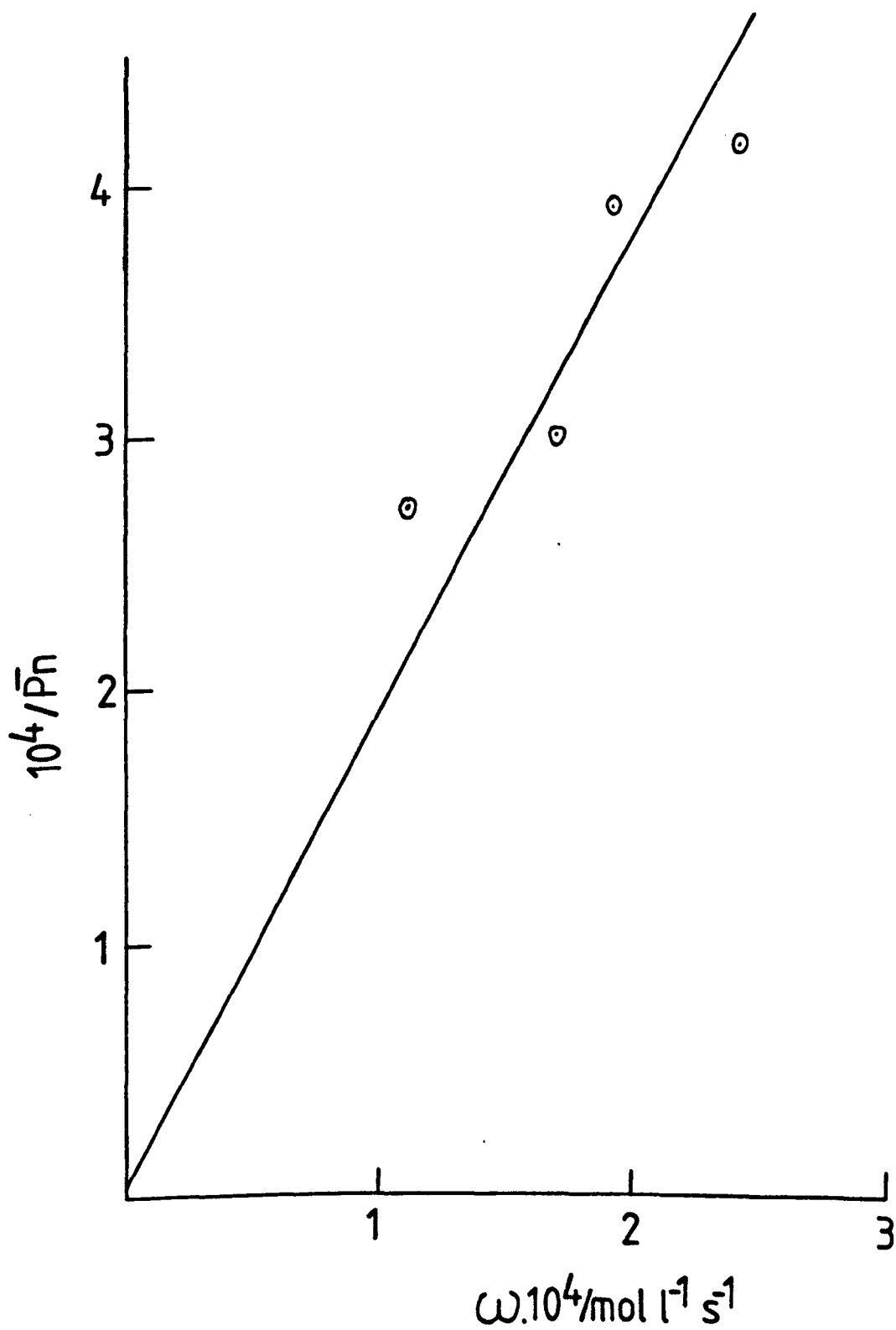


FIG. 2.18 Polyethylacrylate

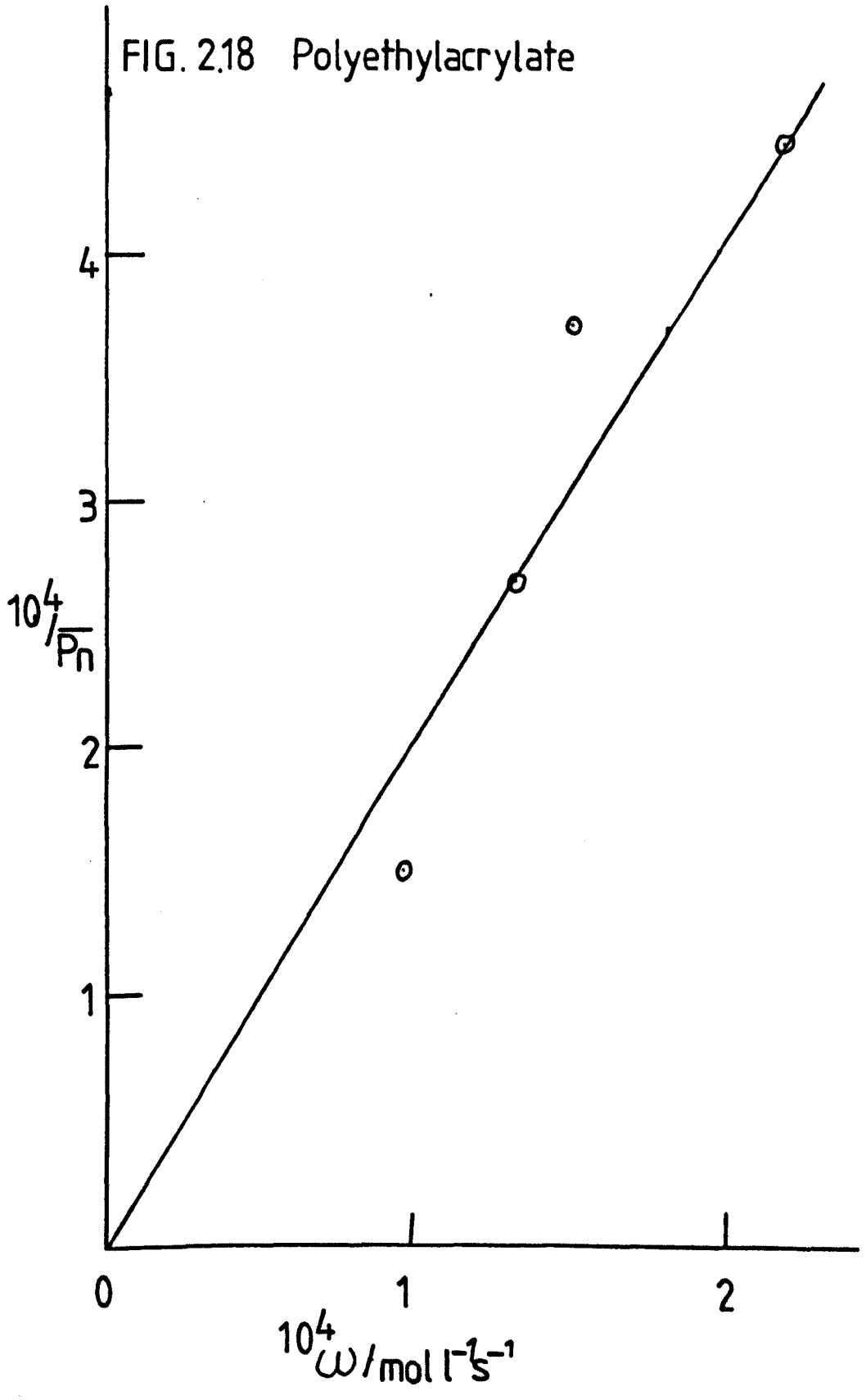


FIG. 2.19

Polyn-butylmethacrylate (bulk)

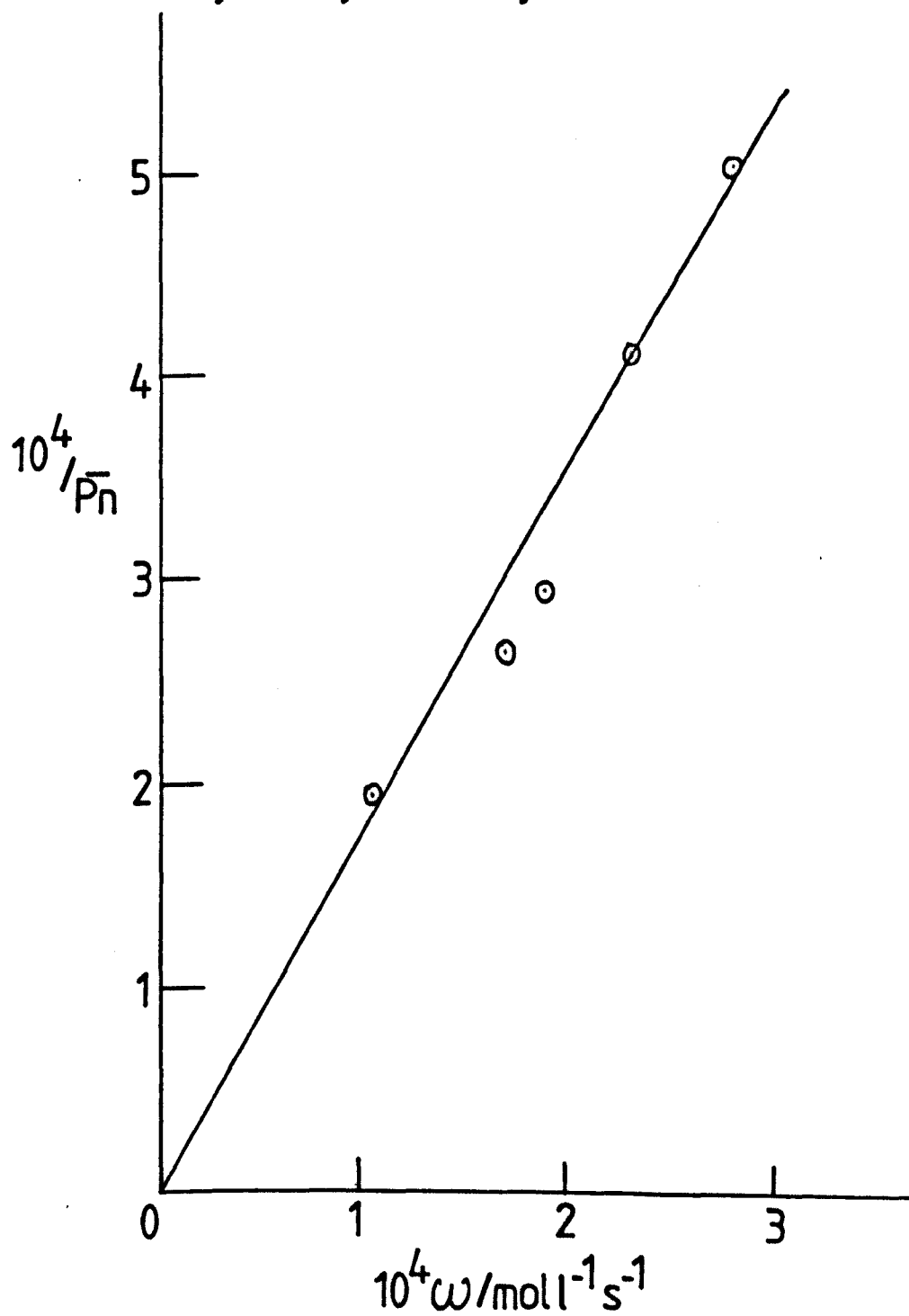


FIG. 2.20

Poly n-butylmethacrylate (50% solution)

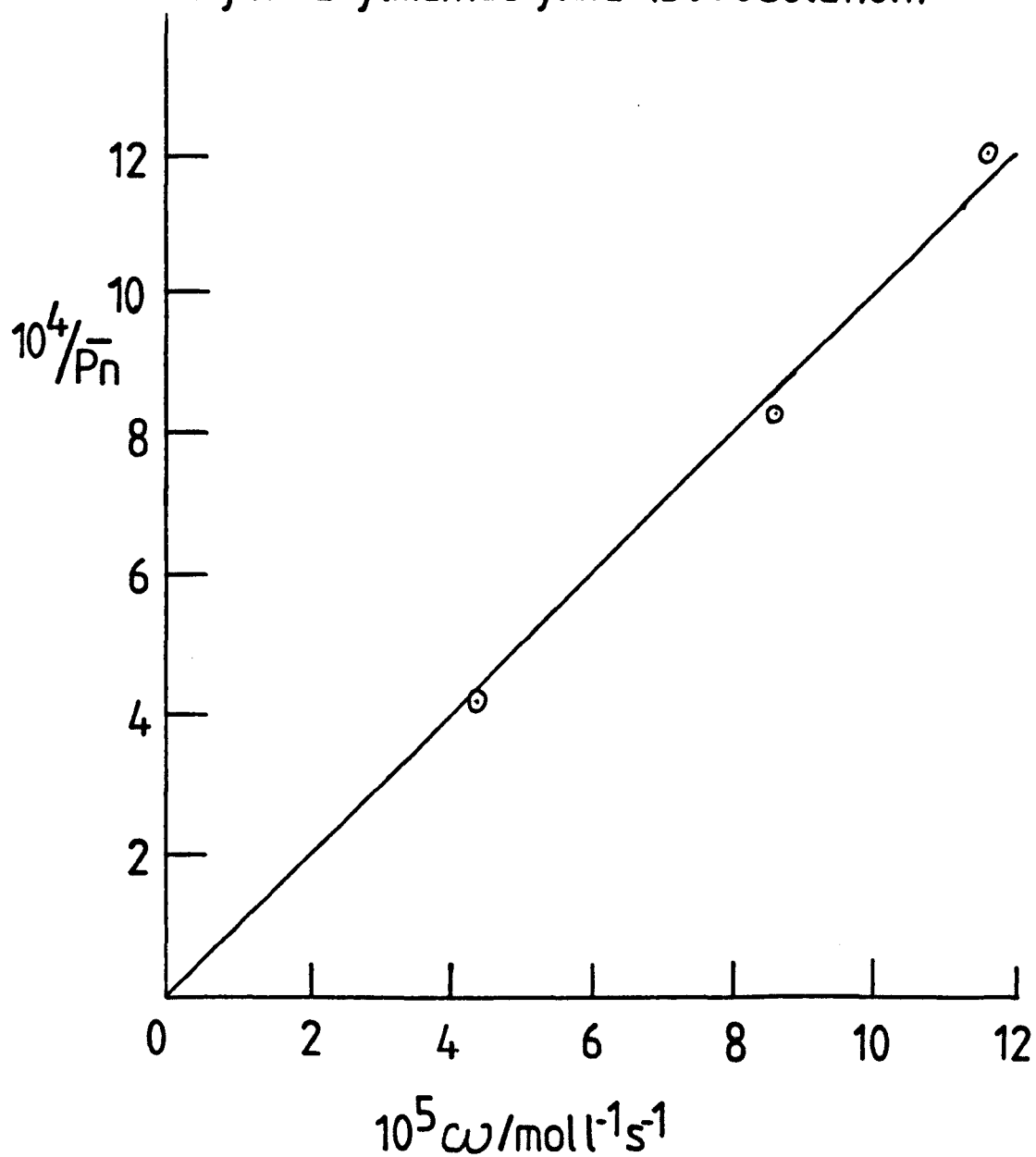
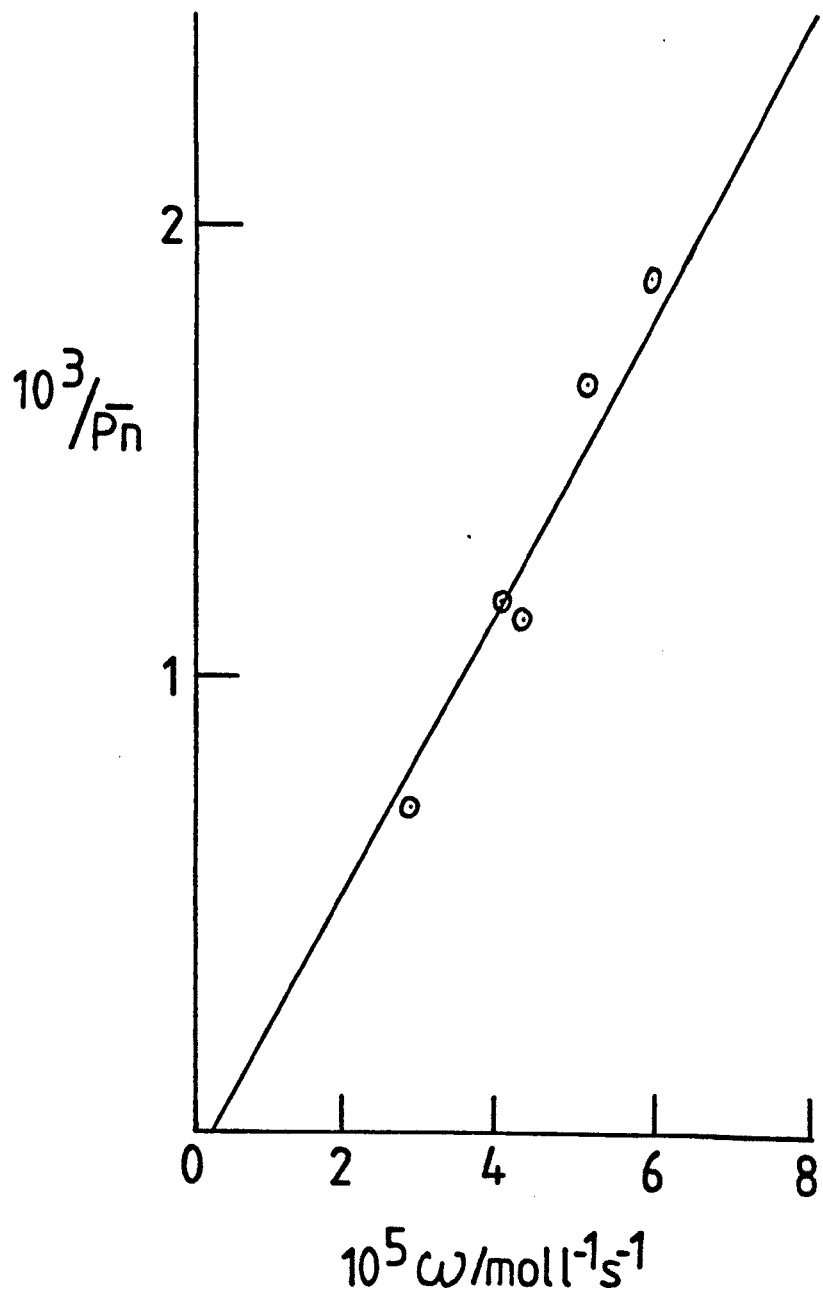


FIG. 2.21

Poly n-butylmethacrylate (30% solution)



were initially found to be variable; this being true for samples of PSt-Br prepared under a nitrogen atmosphere and under vacuum. Some samples of PSt-Br were almost as reactive in initiating radical polymerization as low molecular weight model halides, but most were much less reactive (lower rates of polymerization of second monomer) and some totally inactive. These variations in reactivity for the PSt-Br samples of intermediate reactivity, were due to such samples containing an impurity which acted as a retarder for free-radical polymerizations.

Evidence for the presence of a retarder in the system was shown in that the rates of polymerization of methyl methacrylate were reduced in the presence of PSt-Br, but also the molecular weights of the B-blocks were lower than those of the corresponding homopolymers prepared at the same rate of initiation. Table 2.2 shows the relevant data for the polymerization of methylmethacrylate. Rates of polymerization,  $\omega$ , are given for polymerizations initiated by the model halide bromoethyl benzene and samples of PSt-Br. To provide comparability, all polymerizations were performed at 25° C using the same halide concentration ( $10^{-3}$  mol l<sup>-1</sup>) and dimanganese decacarbonyl concentration ( $4.2 \times 10^{-4}$  mol l<sup>-1</sup>) and the same incident light intensity. Apparent values for the parameter  $k_p/k_t^{1/2}$  are also given, which have been derived from the product of the rates and degrees of polymerization.

TABLE 2.2 KINETICS OF FREE-RADICAL POLYMERIZATION OF METHYL METHACRYLATE

| HALIDE     | $\frac{10^4(-d[M]/dt)}{\text{mol l}^{-1}\text{s}^{-1}}$ | $\frac{(k_p/kt^{1/2})_{app}}{\text{l}^{1/2}\text{mol}^{-1/2}\text{s}^{-1/2}}$ | SOURCE OF PSt-Br                                          |
|------------|---------------------------------------------------------|-------------------------------------------------------------------------------|-----------------------------------------------------------|
| BEB*       | 2.36                                                    | 0.050                                                                         | -                                                         |
| PSt-Br(P)  | 1.79                                                    | 0.048                                                                         | PERME, prepared under high vacuum                         |
| PSt-Br(S4) | 1.48                                                    | 0.039                                                                         | Liverpool, prepared under nitrogen atmosphere             |
| PSt-Br(S4) | 1.79                                                    | 0.048                                                                         | As above but PSt-Br purified by multiple reprecipitations |

\* BEB = 1-bromoethyl benzene



The presence of a retarder has the effect of terminating the propagating B-chains prematurely, so giving a reduced molecular weight. This premature termination of the propagating species would have serious consequences when trying to synthesize elastomeric copolymers, as they require the formation of ABA triblock copolymers produced by combination termination of pairs of propagating B-radicals. Termination with a retarder means that AB, rather than ABA block copolymers are generated. If AB diblock copolymers were required the presence of the retarder would cause no problems providing the molecular weight of the B-blocks were not negligible, as the B-radicals would be required to terminate by disproportionation.

It was found that there was a strong correlation between the activity of the PSt-Br and its synthesis. Samples of PSt-Br prepared by anionic polymerization under a nitrogen atmosphere contained the undesirable impurity which was acting as a polymerization retarder; while the concentration of that impurity was found to be reduced in a sample of PSt-Br prepared under high vacuum. Extensive purification of PSt-Br prepared under nitrogen was necessary before it was useful for the synthesis of ABA copolymers. These samples of PSt-Br were dissolved in AR dichloromethane and then precipitate ~~into~~ methanol at least six times, each time being filtered using a millipore filter system with 0.2 $\mu$ m filters before the samples were used. The obvious

conclusion would seem to be that the PSt-Br samples prepared under high vacuum would be the best choice for the A-block of a copolymer, if ABA copolymers are to be produced with little or no contamination of the AB copolymer species.

Apparent values of  $k_p/k_t^{1/2}$  were calculated for the copolymers synthesized and are given in table 2.3. The values were calculated using equation 2.6.

The values for  $\bar{P}_n$  being again calculated from GPC chromatograms. The tail of the copolymer response often overlaps the residual homopolymer response; when this has happened the tail has been estimated, so leading to some degree of error in  $\bar{P}_n$ , hence  $k_p/k_t^{1/2}$ . Even so the values of  $k_p/k_t^{1/2}$  apparently gained are in reasonable agreement with the values gained from the homopolymerizations, so indicating the polymerization has obeyed simple kinetics.

TABLE 2.3 SYNTHESIS OF BLOCK COPOLYMERS WITH POLYSTYRENE AS THE A-COMPONENT

| B-Component                  | % (v/v) of B in<br>Reaction mixture | $\frac{(k_p/k_t^{1/2}) \text{ app}}{l^{1/2} \text{ mol}^{-1/2} s^{-1/2}}$ | % (W/W) of B<br>in copolymer |
|------------------------------|-------------------------------------|---------------------------------------------------------------------------|------------------------------|
| Methylacrylate (Pst-<br>MA1) | 50                                  | 0.23                                                                      | 80                           |
| Ethylacrylate (CL1)          | 20                                  | 0.235                                                                     | 62                           |
| n-Butylacrylate (CL2)        | 20                                  | 0.224                                                                     | 65                           |
| n-Butylmethacrylate<br>(CL3) | 100                                 | 0.085                                                                     | 58                           |
| Ethylacrylate (CL4)          | 20                                  | 0.193                                                                     | 63                           |
| n-Butylmethacrylate<br>(CL6) | 50                                  | 0.099                                                                     | 54                           |

## CHAPTER III

IDENTIFICATION AND CHARACTERIZATION OF BLOCK COPOLYMERS  
BY GEL PERMEATION CHROMATOGRAPHY

In general, the use of a single detector in the analysis of mixtures of different homopolymers or copolymers will not provide much useful information. Even though the synthetic procedures used in this work have been chosen to help simplify polymer identification, actual characterization is still difficult. To determine the composition and molecular weight distribution of a block copolymer by Gel Permeation Chromatography (GPC) requires the use of dual detection procedures. In principle to determine the composition of a copolymer comprising of  $n$  different repeat units requires  $n$  detectors. The multiple detector procedure is however limited to copolymers in which the different repeat units have different relative responses for the different detectors.

Runyon et al (63) and Richards et al (31) have reported the use of GPC equipment fitted with refractive index (ri) and ultraviolet (uv) detectors in series to determine the composition distribution of binary block copolymers. The ri detector being sensitive to the concentration of any solute in the eluant, while the uv detector requires the presence of suitable chromophores.

### 3.1 The GPC Instrument

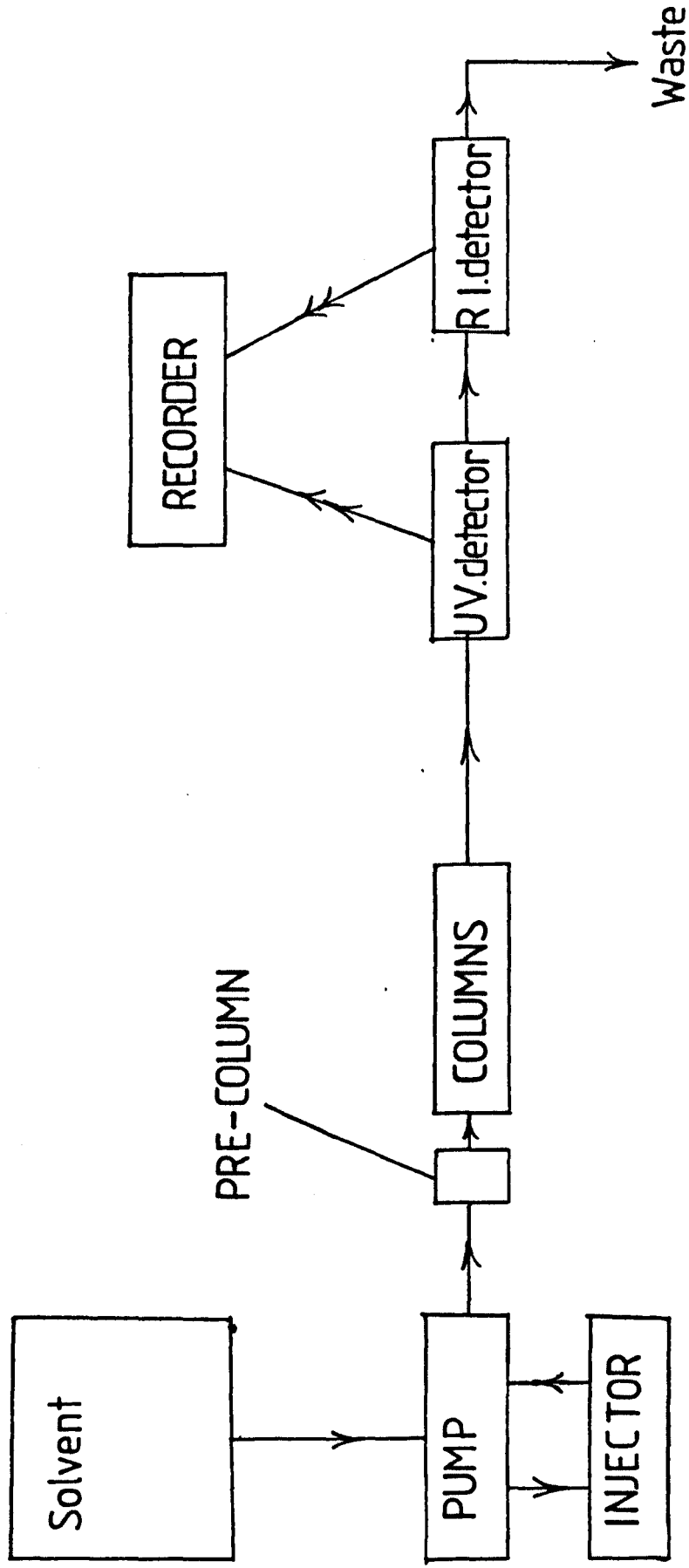
GPC was carried out using the system shown schematically in figure 3.1. The solvent, hplc grade tetrahydrofuran (unstabilised) or AR grade ethyl acetate, was pumped continuously through the system, using a DuPont 870 chromatographic pump to maintain a constant flow rate of 1 ml per minute. Samples were injected into the system using a syringe loading sample injector valve (Valco instruments, Rheodyne Model 7120) in conjunction with a 50  $\mu$ l sample loop. The samples then pass through a Water Associates LC pre-filter and to effect separation, through a porous silanised microsphere (PSM) bimodal column kit (DuPont), that was housed in a DuPont 860 heated column chromatography compartment, which was set at 50<sup>o</sup> C. Eluant was monitored by two detectors in series, an ultraviolet spectrophotometer (Kratos-Schoeff),  $\lambda$  = 260 nm, and a differential refractometer (Waters Associates R401). The chart recorder used to give a visual display of the detector outputs was a Rikadenki quartz R-02 recorder.

### 3.2 Sample Preparation

Polymers were normally injected into the GPC instrument as a 50  $\mu$ l sample of a 0.2% (w/w) solution. Owing to the gradual build up of peroxides in unstabilised THF, solutions for analysis were injected and run as soon as possible after allowing the polymer samples to dissolve. Prior to injection,

FIG. 3.1

GPC. SYSTEM



the polymer solutions were filtered through a  $0.2\mu\text{m}$  filter (Millipore), using a 2 ml Luer Lock syringe with a Swinney filter holder, into samples bottles which had previously been rinsed with filtered solvent and dried.

### 3.3 Calibration

GPC, being a secondary method for determining molecular weight, requires calibration for a given polymer/solvent system. The GPC was calibrated with respect to molecular weight by the peak position method, ie, by relating the peak retention volume to molecular weight for a series of narrow molecular weight distribution standards. Peak retentions were measured in terms of the elution volume. Because the flow rate is constant, the elution volume can be related (directly proportional to) to the distance of the chart recorder trace, measured in cm. The elution volume of a narrow molecular weight distribution standard was taken to be the distance in cm of the recorder trace that corresponded to the distance between the point of injection and the maximum height of the polymer peak.

Polystyrene standards were supplied by Waters Associates. A limited number of poly(methylmethacrylate) standards were supplied by Polysciences and these were supplemented with samples specially prepared as potential standards by Röhm GmbH.

Calibration data were obtained from several chromatograms

of each standard by measuring the retention times (volumes) for each peak position and then averaging the results for each individual standard. These sets of data were regularly checked by obtaining chromatograms for several standards before and after the day's samples were analysed by GPC. The data produced were plotted on a graph of  $\log_{10}$  (molecular weight) against elution volume, the calibration curve was approximately linear apart from the two extreme limits of the elution volume, ie, very high and very low molecular weights. Using linear regression analysis it was established that the calibration data could be accurately represented by a straight line. The slope and intercept of the calibration curves were noted. (See figure 3.2 for the Polystyrene curve).

No suitable standards were available to calibrate the instrument for the polyacrylates and poly(n-butyl methacrylate) used during this work.

### 3.4 Detector Response

In order to determine the concentration of polymers in eluants, response factors for each polymer in each detector were determined.

Detector responses were determined from the peak areas of the chromatograms obtained by injecting accurately

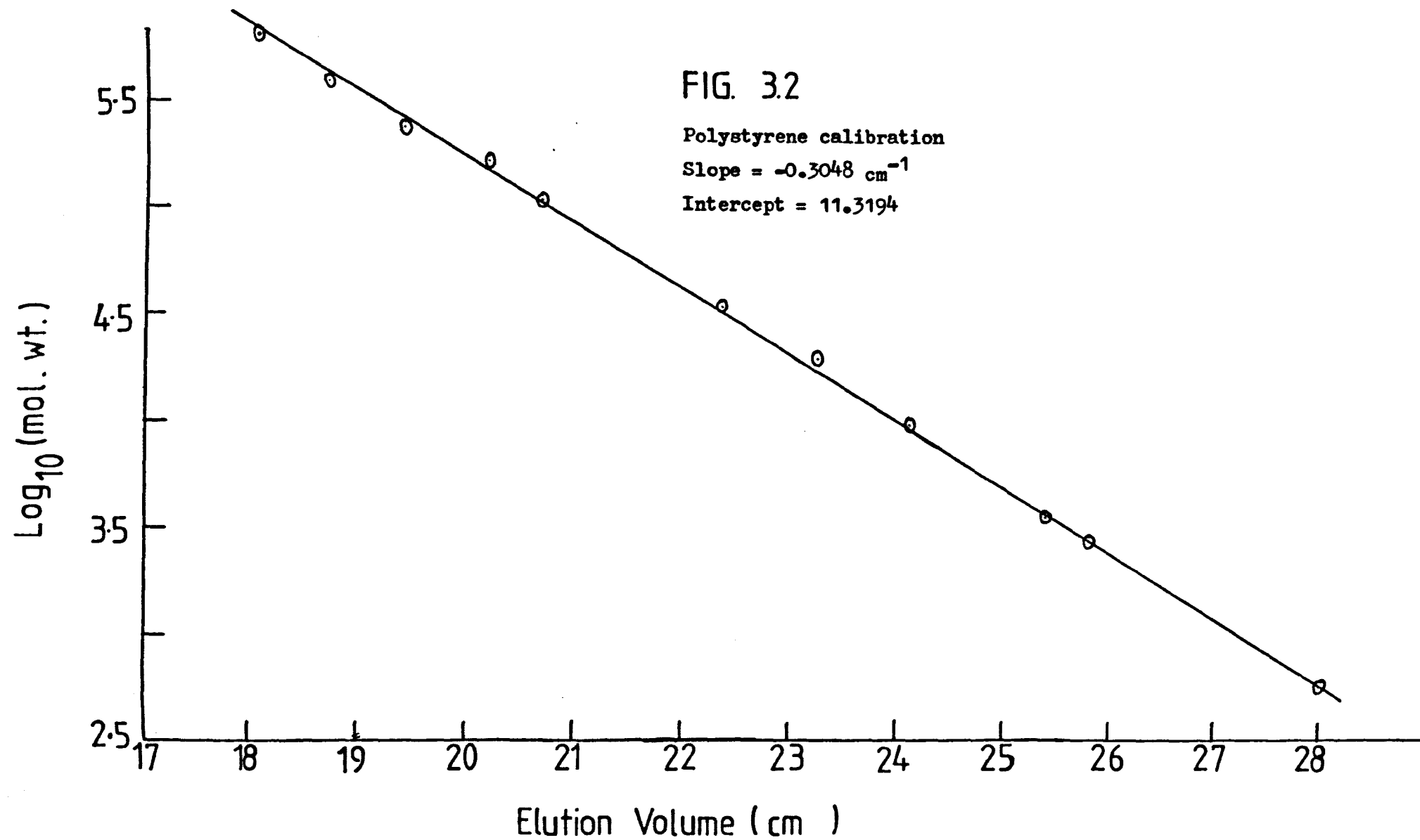


FIG. 3.2

Polystyrene calibration

Slope =  $-0.3048 \text{ cm}^{-1}$

Intercept = 11.3194



known values of solutions of homopolymers of known concentration. The response factors thus determined were only applicable to a specific detector sensitivity setting and chart recorder speed. The chart speed used was 3 cm per minute. The response factors for the homopolymers were determined by the use of the following equation.

$$\text{Detector Response Factor} = \frac{\text{Area (cm}^2\text{) under chromatogram}}{\text{concentration of polymer sample (g/100 ml)}} \quad 3.1$$

Response factors thus calculated were then used for the different polymer/solvent systems are given in table 3.1.

### 3.5 Copolymer Identification

Since all primary radicals formed by the reaction between the brominated polystyrene and the photolysis products of dimanganese decacarbonyl are macroradicals, the synthesis should produce only minimal amounts of homopolymer of the second monomer and so the reaction products should be a blend of copolymer and unreacted prepolymer (PSt-Br). By examination of the chromatograms, it is possible to differentiate between the copolymer and the prepolymer.

In comparison with polystyrene, other polymers used as B-component monomers in the copolymer were virtually transparent at a wavelength of 260 nm, as can be seen from the data in table 3.1. *Owing* to this lack of absorption at  $\lambda = 260$  nm, the ultraviolet detector response in these

TABLE 3.1 - DETECTOR RESPONSE FACTORS

| Solvent         | Polymer                   | Detector Response Factors |       | Comments                                                                                                                                                                                                                                              |
|-----------------|---------------------------|---------------------------|-------|-------------------------------------------------------------------------------------------------------------------------------------------------------------------------------------------------------------------------------------------------------|
|                 |                           | RI                        | UV    |                                                                                                                                                                                                                                                       |
| Tetrahydrofuran | Polystyrene               | 42.37                     | 36.2  | The units for detector Response Factors are $\text{cm}^2 \text{g}^{-1} \cdot 100 \text{ ml}$<br><br>All Response Factors measured at detector setting of 2 for the ri and 0.2 for the uv.<br><br>The uv response was taken at a wavelength of 260 nm. |
| Tetrahydrofuran | Poly(methylmethacrylate)  | 18.4                      | 0     |                                                                                                                                                                                                                                                       |
| Tetrahydrofuran | Poly(n-Butylmethacrylate) | 38.6                      | 0     |                                                                                                                                                                                                                                                       |
| Tetrahydrofuran | Poly(methylacrylate)      | 97.28                     | 0     |                                                                                                                                                                                                                                                       |
| Tetrahydrofuran | Poly(ethylacrylate)       | 103.5                     | 0     |                                                                                                                                                                                                                                                       |
| Tetrahydrofuran | Poly(n-Butylacrylate)     | 95.12                     | 0.9   |                                                                                                                                                                                                                                                       |
| Ethyl Acetate   | Polystyrene               | 43.95                     | 32.62 |                                                                                                                                                                                                                                                       |
| Ethyl Acetate   | Poly(methylmethacrylate)  | 25.46                     | 0.15  |                                                                                                                                                                                                                                                       |

studies is almost entirely due to polystyrene (64). The refractive index (ri) detector on the other hand responds to all the polymers used but, because the reaction products consist largely of the second polymer B, typically 50%-80% (w/w), the response at high molecular weight, ie, not residual homopolymer A, is primarily from the B component of the copolymer.

Figures 3.3-3.5 show chromatograms for the different preformed polystyrenes used in the synthesis of copolymers during the course of this work. All three figures show both uv and ri chromatograms with the relevant gain settings used. In all cases the molecular weight distributions are seen to be narrow and so the molecular weight corresponding to the elution volume of the major peak was taken to be the molecular weight of the prepolymer.

The chromatograms all show a second minor peak at a molecular weight approximately equal to twice that of the major peak. This minor peak corresponds to polystyrene, formed by the coupling of chains during the termination of the anionic polymerization used in the preparation of the prepolymer (see section 1.4.1, equation 1.27). This product by virtue of its mechanism of formation is unreactive and does not take part in copolymerizations, so giving an internal marker on the chromatograms, because the resulting peak should appear at the same elution volume in a copolymer blend as in a homopolymer blend.

FIG. 3.3  
POLYSTYRENE

UV (setting 0.2) →

R.I. (setting 2) →

100K 10K 2K  
MOL. WT.

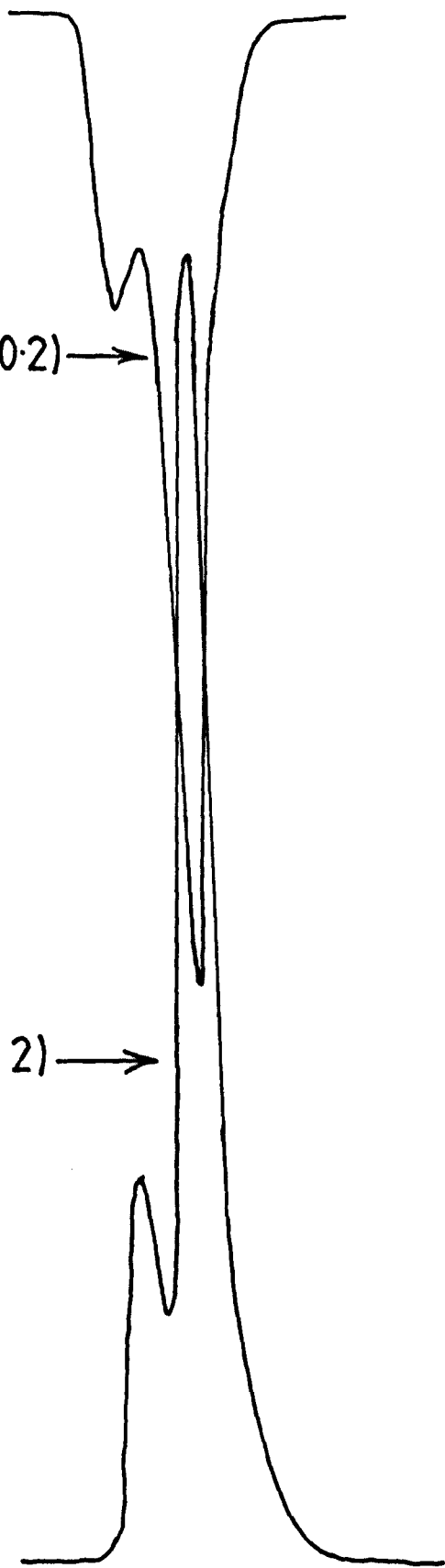
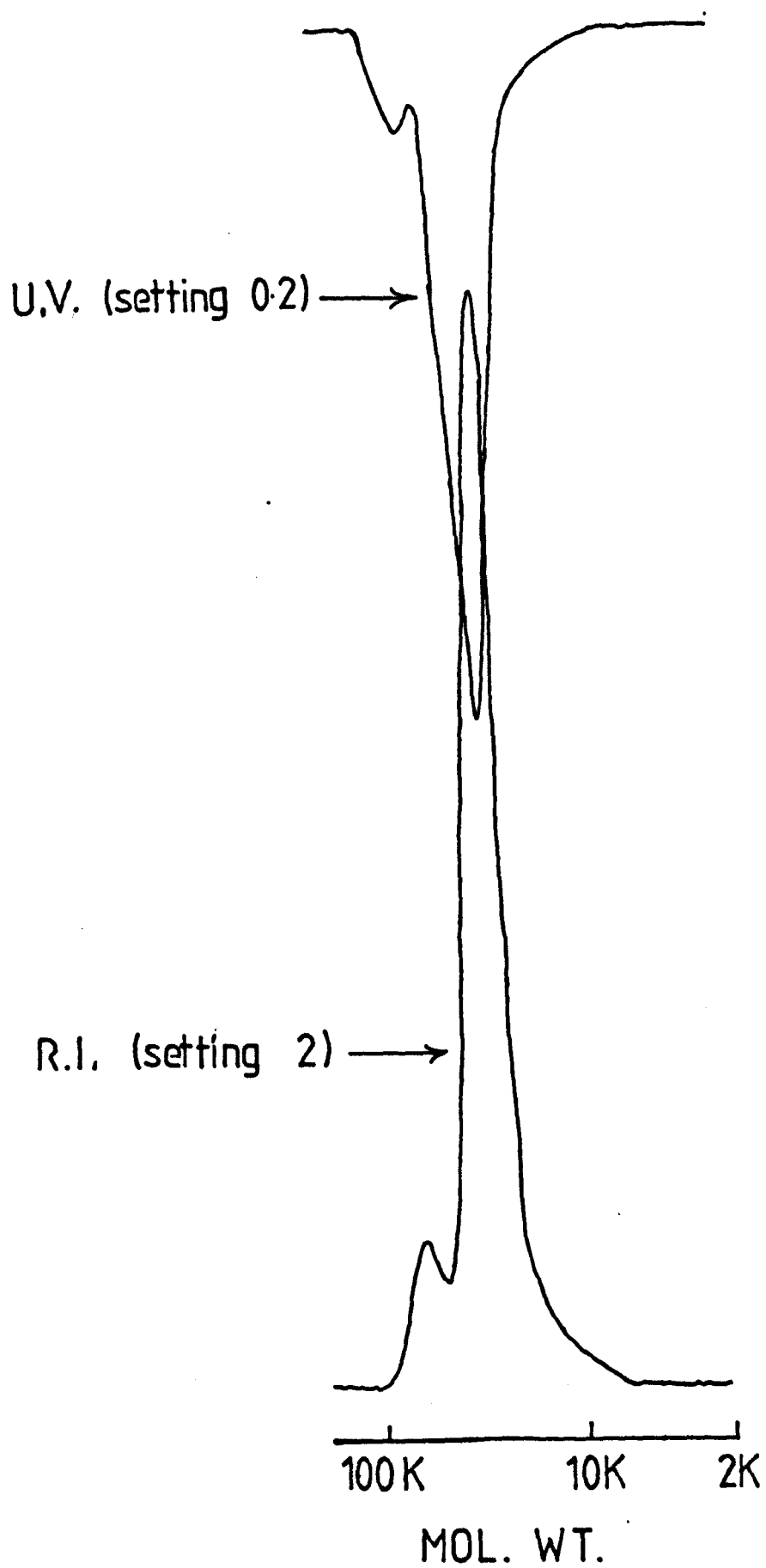


FIG. 3.4  
POLYSTYRENE (S4)



FIG. 3.5

POLYSTYRENE (S6)



Figures 3.6-3.13 show chromatograms of the total polymeric products isolated from reaction mixtures after irradiation. In each case, the chromatograms show products that lie in three distinct regions. The first and second regions at low molecular weight correspond to the unreacted prepolymer and the unreactive homopolystyrene at approximately twice the molecular weight of the prepolymer respectively. Changes in the relative intensities of the prepolymer peak and the unreactive polystyrene peak with respect to before copolymerization, are due to the consumption of the reactive prepolymer during copolymerization.

The third region includes the peaks at high molecular weight, which are due to reaction products produced on irradiation of the reaction mixture. The uv absorption at high molecular weight must be due to polystyrene which started in the first region at low molecular weight and has been moved to higher molecular weight, because of its incorporation in the copolymer. The large  $r_i$  peak must be partly due to polystyrene (as in the uv peak), but also B-component. At any elution volume in the higher molecular weight region, the relative intensities are not consistent with polystyrene or the B-component individually, but a ratio  $h_{ri}/h_{uv}$  intermediate, that is consistent with a mixture of polymers or copolymers. The uv peak shifts relative to the  $r_i$  and is consistent with copolymer in which the polystyrene content increases as the copolymer molecular



weight decreases (Polystyrene blocks have a uniform molecular weight).

By using the general concepts above, the polymeric materials produced during this study were identified as being blends of homopolymer and copolymer.

The poly(styrene-methylmethacrylate) copolymer in figure 3.6 shows a chromatogram that is consistent with copolymer formation. Methylmethacrylate terminates by approximately 30% combination, giving copolymers predominantly of the AB type especially at low molecular weight; at higher molecular weight the molecules will tend to be of the ABA type. The  $k_{pct}^{-1/2}$  value of  $0.055 \text{ l mol}^{-1} \text{ s}^{-1}$  means that the calculated  $\bar{M}_n$  and  $\bar{M}_w$  values would be of the order of a few hundred thousand depending on the conditions. Transfer can occur between the propagating species and the monomer or solvent. Transfer produces chains with the same shaped distribution as disproportionation termination and has the effect of shifting the whole distribution to lower molecular weight, ie, chains produced by transfer cannot be distinguished from others, except by end group analysis. In this case, any propagating chains produced by transfer would not have a polystyrene end group and still would not have if terminated by disproportionation, but would if terminated by combination, thus leading to some homopolymer being formed of sufficient molecular weight to be occluded by the residual prepolymer in the chromatogram.

FIG.(3·6–3·13)

[M] as for homopolymerizations

FIG. 3.6

PSt-PMMA Copolymer

[carbonyl] =  $4.162 \times 10^{-4} \text{ mol l}^{-1}$  [PSt.] =  $10^{-3} \text{ mol l}^{-1}$



Figure 3.7 shows a copolymer consisting of polystyrene and polymethylacrylate. Here the chromatogram shows a narrower, but higher molecular weight distribution peak than in figure 3.6. This peak would be due to the copolymer, where the acrylate component has terminated by a combination mechanism and has a higher value of  $k_{pct}^{-1}$  than the methacrylate component in figure 3.6. Transfer to monomer or solvent would move and change the molecular weight distribution, because it would produce an amount of AB copolymer instead of ABA copolymer. The slight tail in the copolymer distribution in ri chromatogram may be due to a small amount of transfer giving lower molecular weight AB copolymer, instead of the higher molecular weight ABA copolymer. Figures 3.8-3.9 show similar features to figure 3.7.

Figure 3.10 shows chromatograms of poly(styrene-n-butylmethacrylate), where the n-butylmethacrylate component shows that the termination step is a mixture of combination and disproportionation, similar to the methylmethacrylate case. At high molecular weight there is a greater probability that the copolymer was produced by combination termination giving ABA type copolymer, while at lower molecular weight the AB type is more probable, owing to disproportionation termination.

Figure 3.11 shows a chromatogram of poly(styrene-ethylacrylate), but unlike figure 3.8 has the copolymer peak at lower molecular weight than expected. This movement of the copolymer peak to lower molecular weight would

FIG.(3.7- 3.13)

room temp. ;[PSt.] =  $10^{-3}$  mol l<sup>-1</sup> in all cases  
using 0.1(61.6%) intensity filter " "

FIG. 3.7

PSt.-PMA Copolymer

$[\text{carbonyl}] = 4.1 \times 10^{-4} \text{ mol l}^{-1}$

U.V. (setting 0.2) →

R.I. (setting 2) ↓

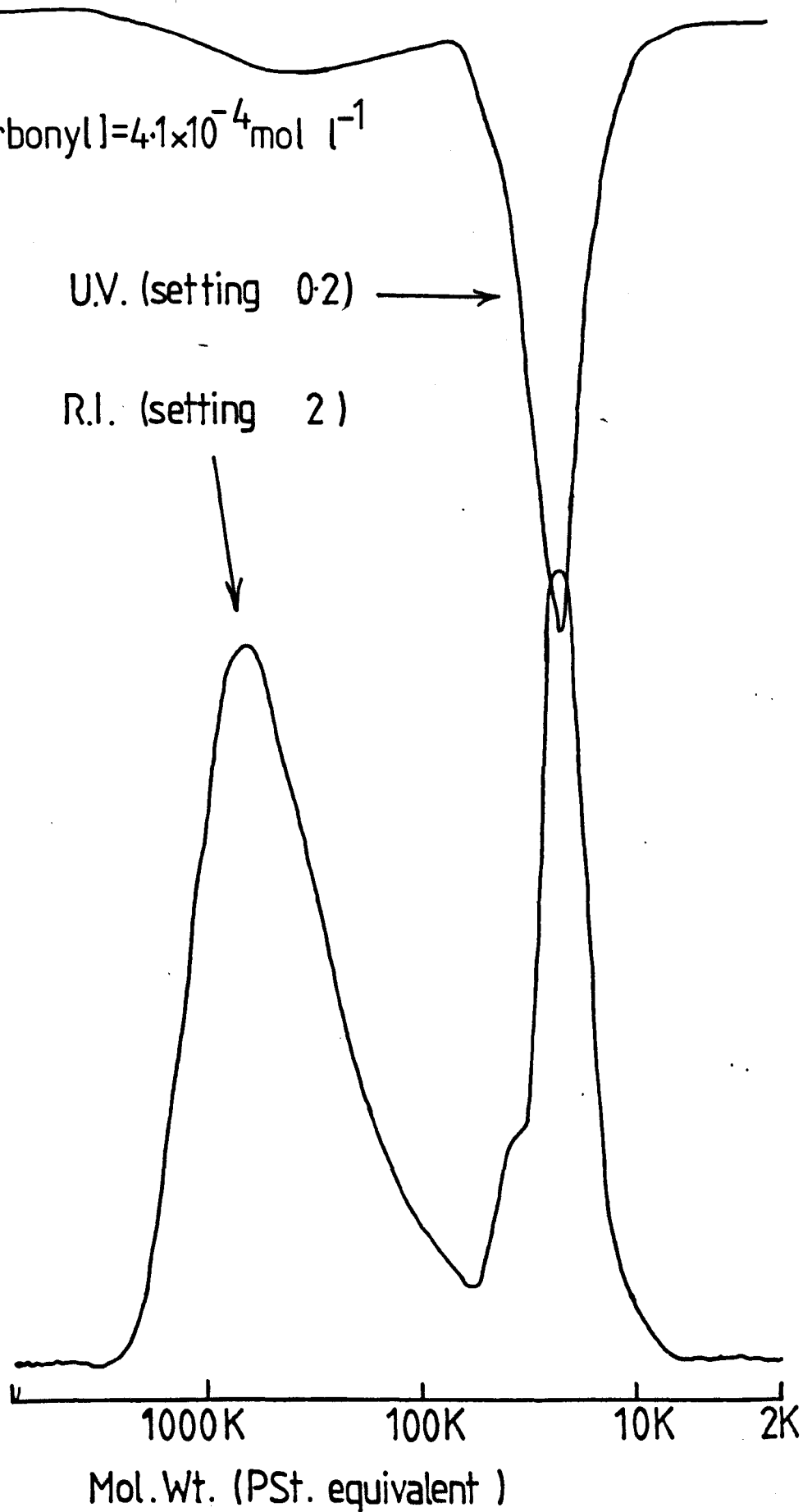


FIG. 38

PSt.-PEA. Copolymer (CL1)

[carbonyl] =  $3.94 \times 10^{-4} \text{ mol l}^{-1}$

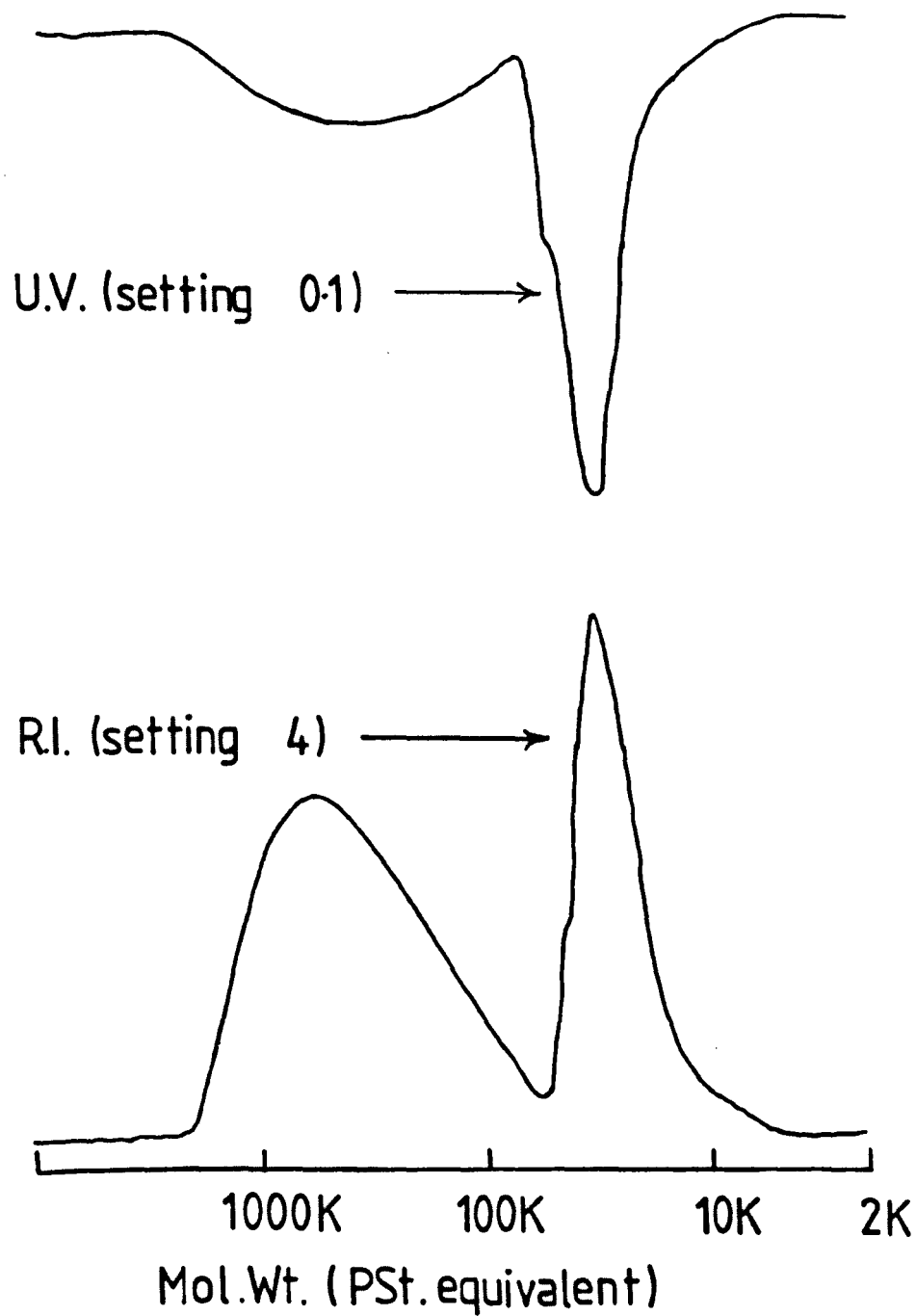


FIG. 3.9

PSt.-PnBA. Copolymer(CL2)

[carbonyl] =  $3.97 \times 10^{-4} \text{ mol l}^{-1}$

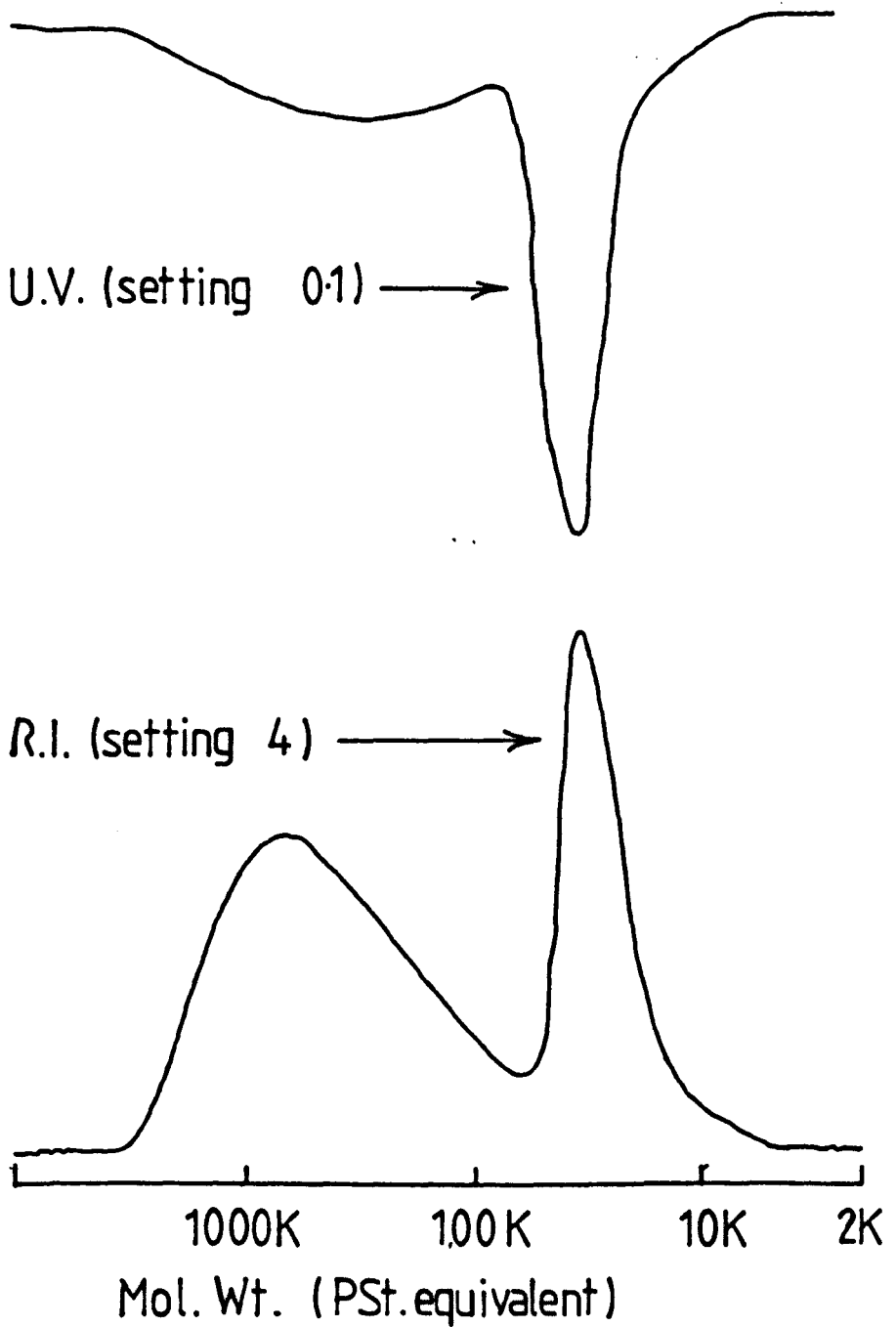




FIG. 3.10

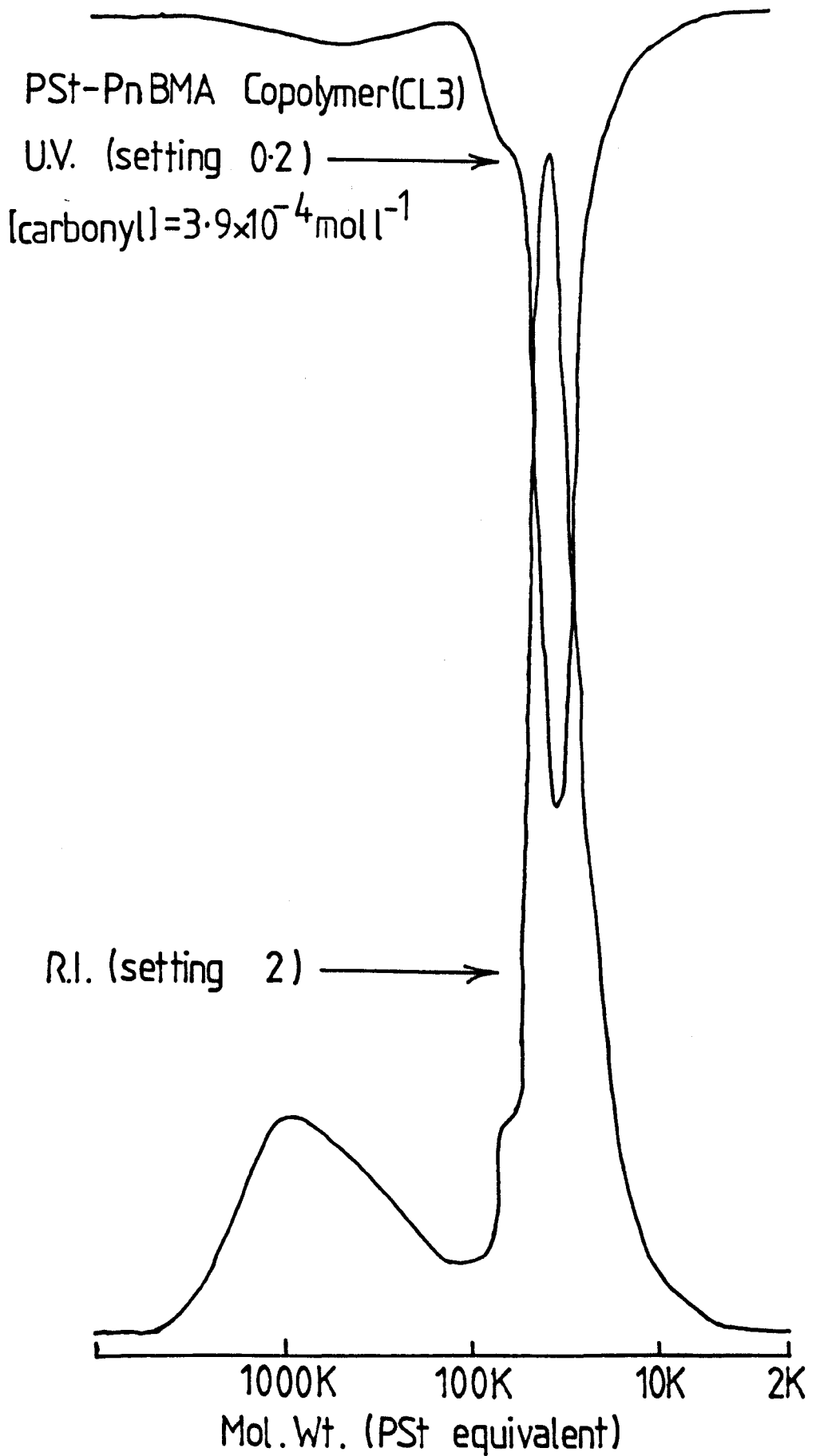


FIG. 3.11

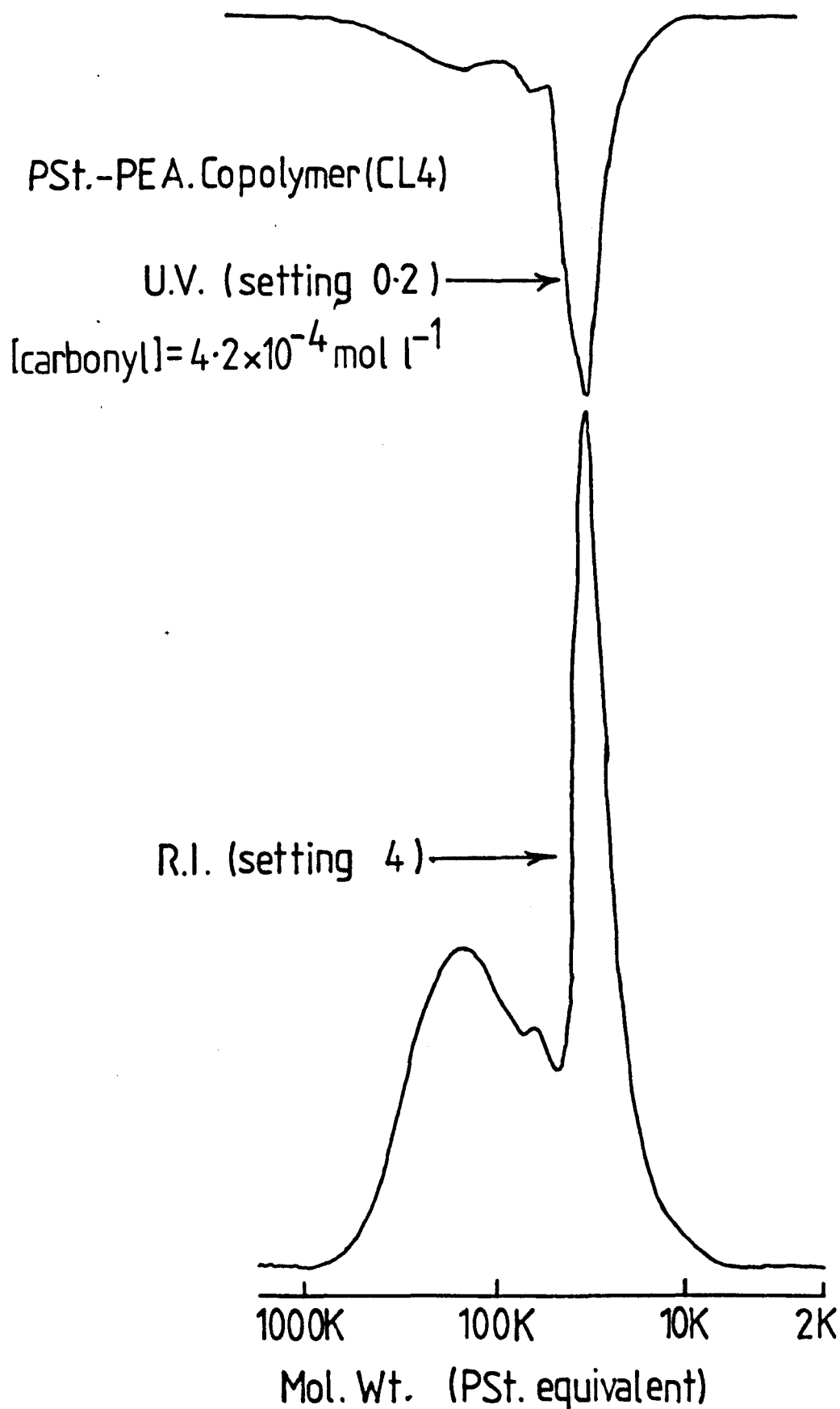


FIG. 3.12

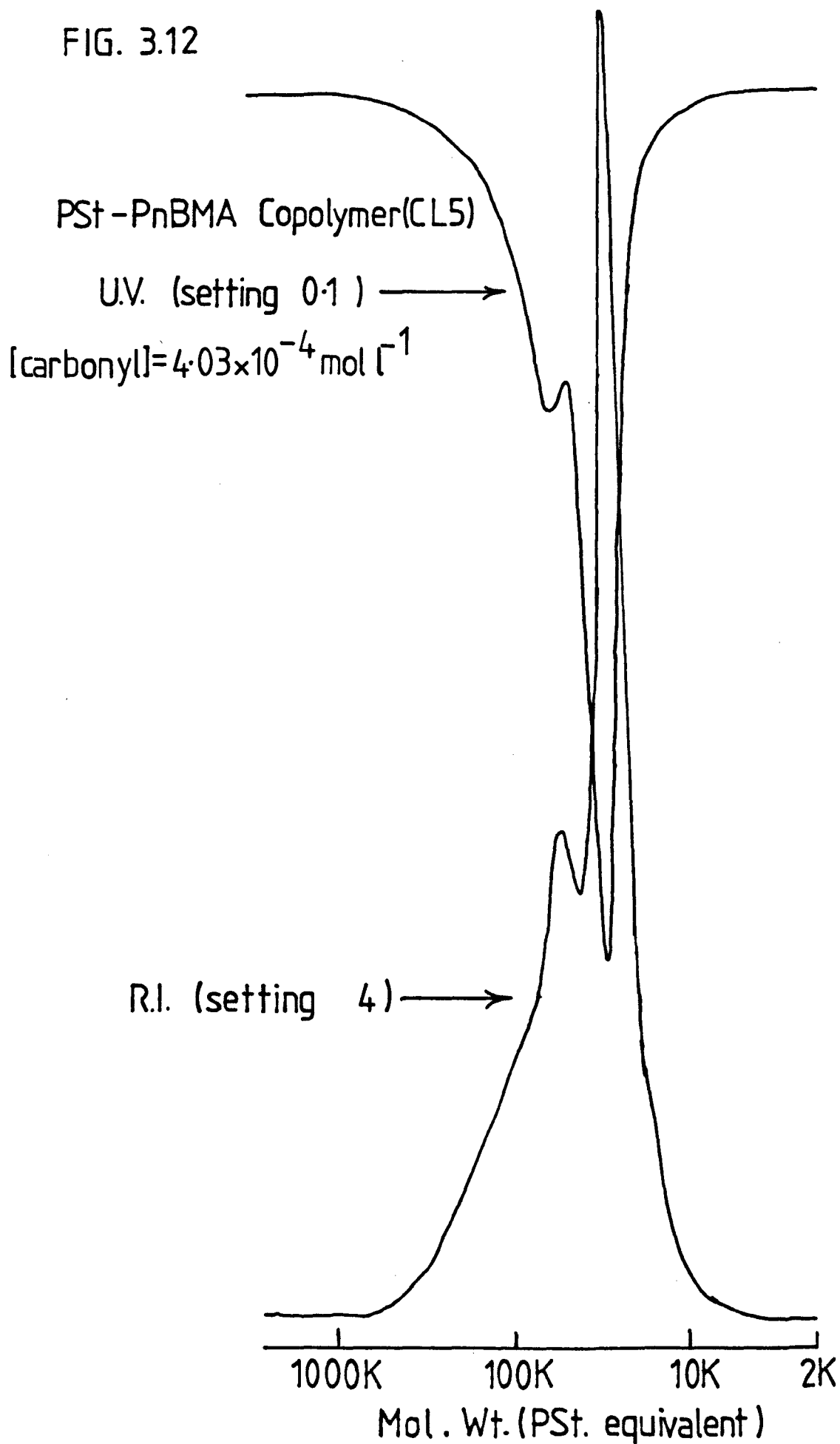
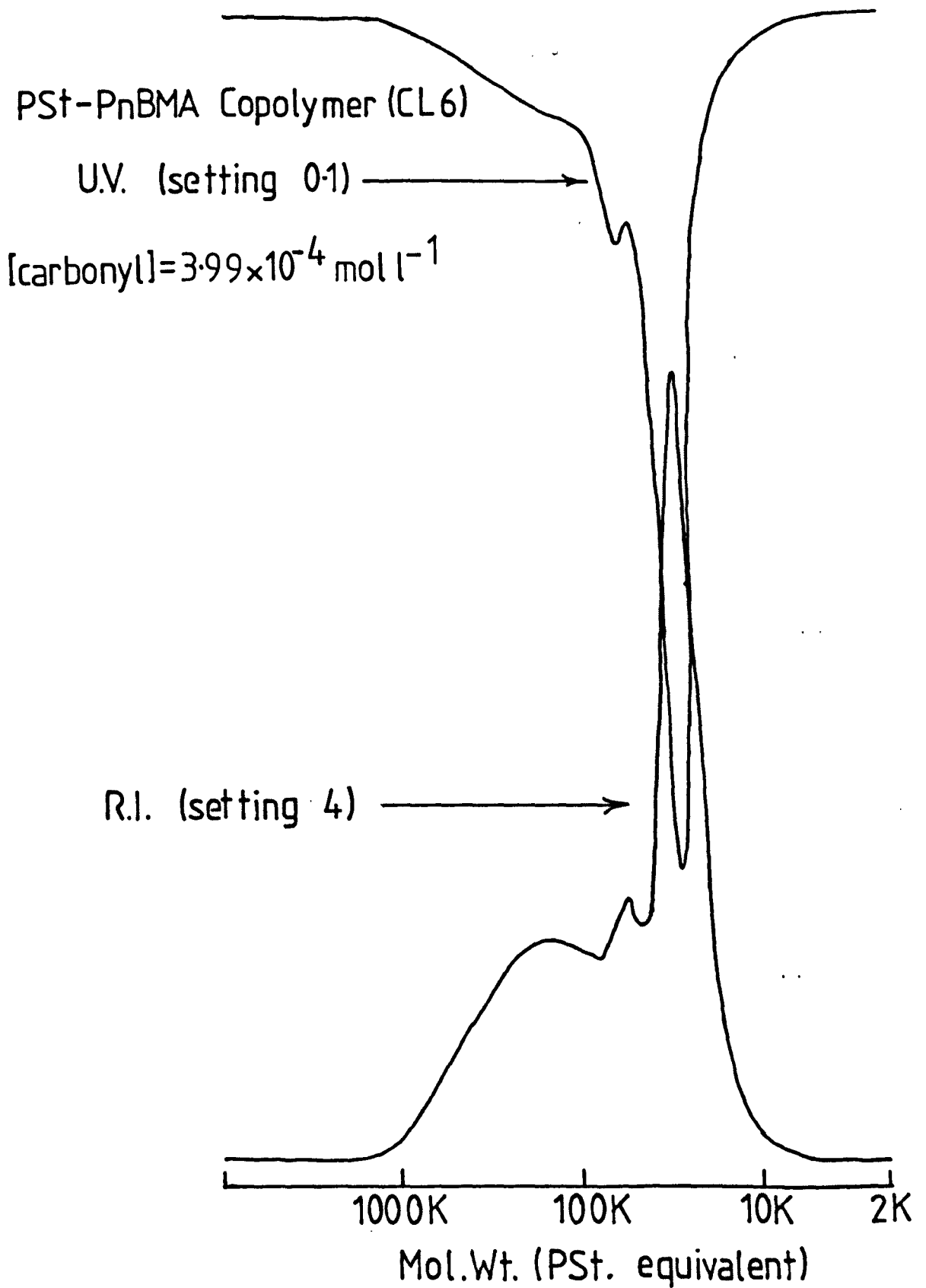


FIG. 3.13



probably be due to significant amounts of AB copolymer being present; the AB copolymer being due to possible transfer with an impurity in the reaction mixture.

Figures 3.12-3.13 show copolymer chromatograms whose component polymers are polystyrene and n-butylmethacrylate. The differences between the chromatograms are due to the conditions of polymerization, ie, different monomer concentration. The monomer concentrations were  $2.27 \text{ mol l}^{-1}$  in figure 3.12 and  $3.78 \text{ mol l}^{-1}$  in figure 3.13, which give rise to distributions that have different molecular weight values. With figure 3.12, the distribution is obscured to a large extent by the residual homopolymer.

### 3.6 Chromatogram Analysis

GPC analysis of copolymer samples produce two chromatograms for each sample studied, an ri trace and a uv trace. From these chromatograms the composition distribution and concentration of B chains can be obtained by the following method.

- 1 A suitable baseline is constructed by joining the portions of the chromatogram occurring prior to the sample peak and after the impurity peaks have eluted.
- 2 The heights of the traces are measured to  $\pm 0.25 \text{ mm}$  with a set of dividers at equally spaced intervals of elution volume in cm, the interval usually being  $0.25 \text{ cm}$ .
- 3 The weight fraction of the B-component could then be calculated at each elution volume.

Steps 1 and 2 were carried out manually, while all calculations were done using the computer program GPCGF1.BAS (Appendix A) on a Research Machines 380Z microcomputer.

### 3.6.1 Characterization

#### 3.6.1.1 Copolymer Composition

The copolymer composition at each elution volume, expressed as weight fractions of the component blocks, was calculated from the data provided by the ri and uv traces of the chromatogram. The equation used to calculate the weight fraction of polymer B in the copolymer,  $W_B$ , as a function of elution volume,  $V$ , is given in equation 3.2.

$$W_B(V) = \frac{R_H h_{A2} - h_{A1}}{h_{B1} - h_{A1} - R_H(h_{B2} - h_{A2})} \quad 3.2$$

where  $R_H$  is the ratio of the heights of the uv trace to the ri trace at an elution volume,  $V$ ,  $h_{B1}$  and  $h_{B2}$  are the response factors for the B-component for the uv and ri detectors respectively, while  $h_{A1}$  and  $h_{A2}$  are the response factors for the A-component for the uv and ri detector respectively. The derivation of the equation 3.2 can be found elsewhere (31).

#### 3.6.1.2 Molecular Weight Calibration

GPC has been developed into a most convenient technique for the determination of molecular weight distributions

of polymers. For homopolymers the interpretation of raw data now has standard procedures, even though accurate molecular weights are difficult to assign, owing to the lack of standards for various polymers. With block copolymers the data interpretation is complicated by the presence of a composition distribution along with molecular weight distribution.

The GPC calibration plot of hydrodynamic volume as a function of retention introduced by Benoit et al (54) (the so-called "universal calibration") was an early approach to address the problems incurred in the characterization of block copolymers. Benoit et al showed that this calibration plot was equally applicable to homopolymers as copolymers. Runyon et al (63) proposed a method for calibration, based on the assumption that the size of a copolymer molecule is the sum of the sizes of the various components of the molecule, as though each were a homopolymer. Tung (65) has shown that Runyon's method provides a very good estimate of molecular weight of block copolymers, when AB interactions (interactions of unlike segments of the copolymer) do not significantly affect the molecular dimensions. Chang (66) suggested a procedure for estimating linear block copolymer molecular weights based on the linear relationship between the log (molecular weight) and retention volume for the homopolymers of the constituent repeat units. Chang's procedure also requires a knowledge of the copolymer composition distribution and involves defining the B block molecular weight of an 'equivalent A-block' molecular

weight using the relevant homopolymer calibration constants.

In this work, a new approach to block copolymer characterisation recently proposed by Eastmond and Woo (42, 67) is used. This approach assumes that whatever parameter is deemed to control the elution volume of a polymer<sup>it</sup> is additive, that is, the parameters of the components are additive and the sum of the parameters will control the elution volume of the copolymer. If the hydrodynamic volume of a polymer were the relevant parameter, copolymers with equal hydrodynamic volumes would have equal elution volumes and the constituent blocks would have hydrodynamic volumes equal to those of the free homopolymers.

The analysis was simplified by the use of A blocks that have narrow molecular weight distributions and have known molecular weights. Relationships were developed which permitted the calculation of the molecular weight of the B-block ( $M_B$ ) at any elution volume ( $V_C$ ), if the slopes ( $S_A$ ,  $S_B$ ) and intercepts ( $I_A$ ,  $I_B$ ) of the calibration curves for the homopolymers A, B in the same solvent are known and if the molecular weight of the A-block ( $M_A$ ) is known. Equation 3.3 gives values for  $\log M_B$  when the block copolymer is of the AB or ABA type,  $n$  = number of A-blocks, ie,  $n = 2$  when ABA.

$$\log M_B = \frac{S_A}{S_B} \left\{ \log \left[ 10^{(S_A V_C - I_A)} - n M_A \right] - I_A \right\} + I_B \quad 3.3$$



This equation permits the construction of theoretical curves of weight fractions of B-block as functions of elution volume for AB and ABA block copolymers separately (figure 3.14).

Experimentally determined variations in weight fraction of B with elution volume, assuming a mixture of AB and ABA type copolymer should, in principle, fall between the two theoretical curves and along a curve consistent with the proportions of AB and ABA copolymer in the sample, which are determined by the termination mechanism and possible effects of transfer.

### 3.6.1.3 Results and Discussion

A computer program GPCGF1 was written for the data analysis and figures 3.17-3.21 were generated by this program. The program was used to compare theoretical curves to experimental data and had the facility to change the calibration data and response factors as required. During the application of the model, the solvents used were tetrahydrofuran and ethyl acetate.

Calibration data are given in figures 3.15-16 for polystyrene and poly methylmethacrylate.

Examination of figures 3.17-3.19 shows that the model is obeyed qualitatively over part of the elution volume range for some copolymers; this range includes the bulk of the copolymer. Using the program GPCGF1 it was possible

FIG. 3.14 Calculated Wt. Frac. of B Unit for AB and ABA Copolymers at  $V_{rj}$

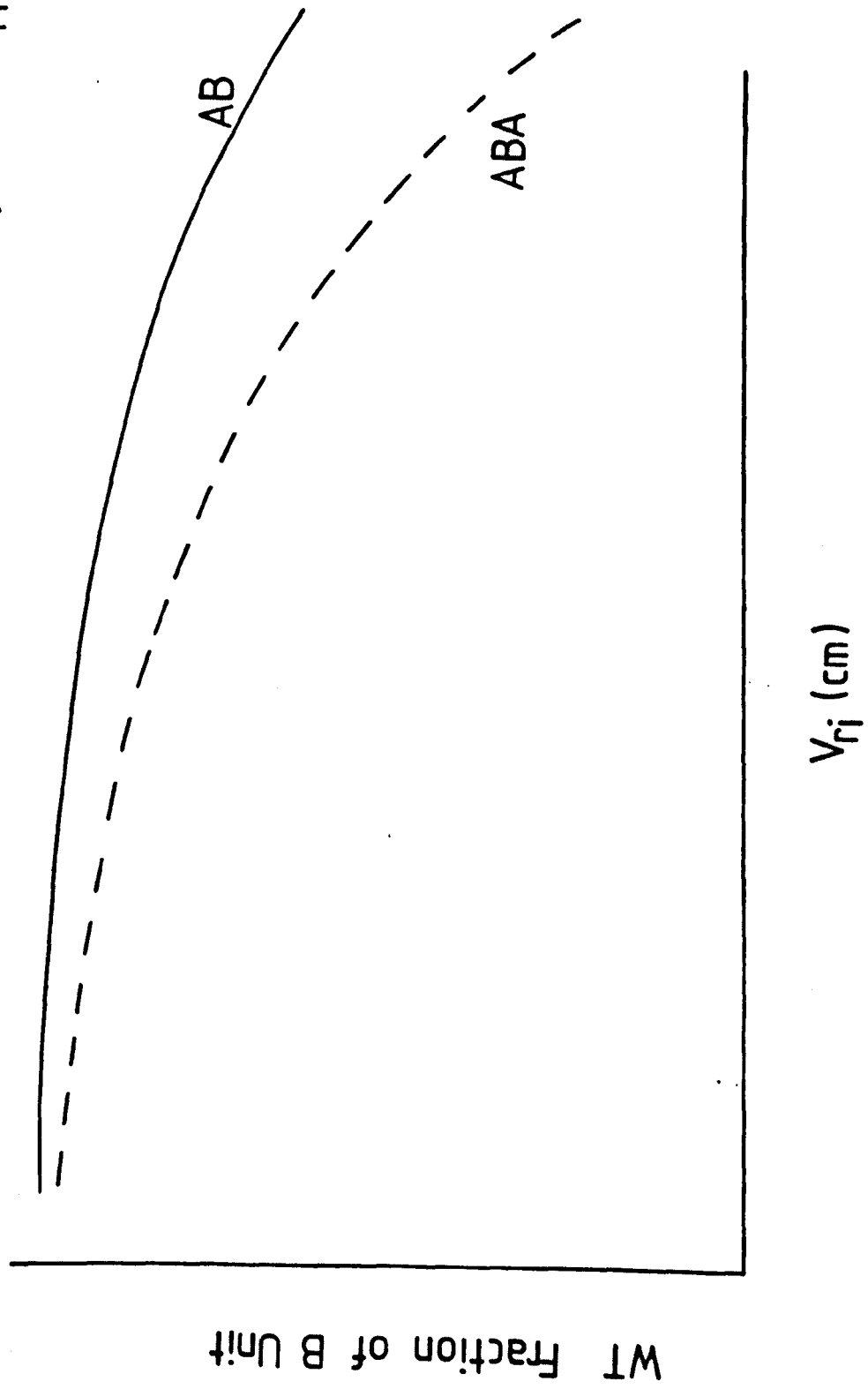


FIG. 3.15

Calibration for methylmethacrylate and styrene copolymers

⊙ Polystyrene standards in THF

slope = -0.3022 , intercept = 11.8051

△ Polymethylmethacrylate standards in THF (Röhm)

◻ Polymethylmethacrylate standards in THF (Polysciences)

slope = -0.2553 , intercept = 10.882

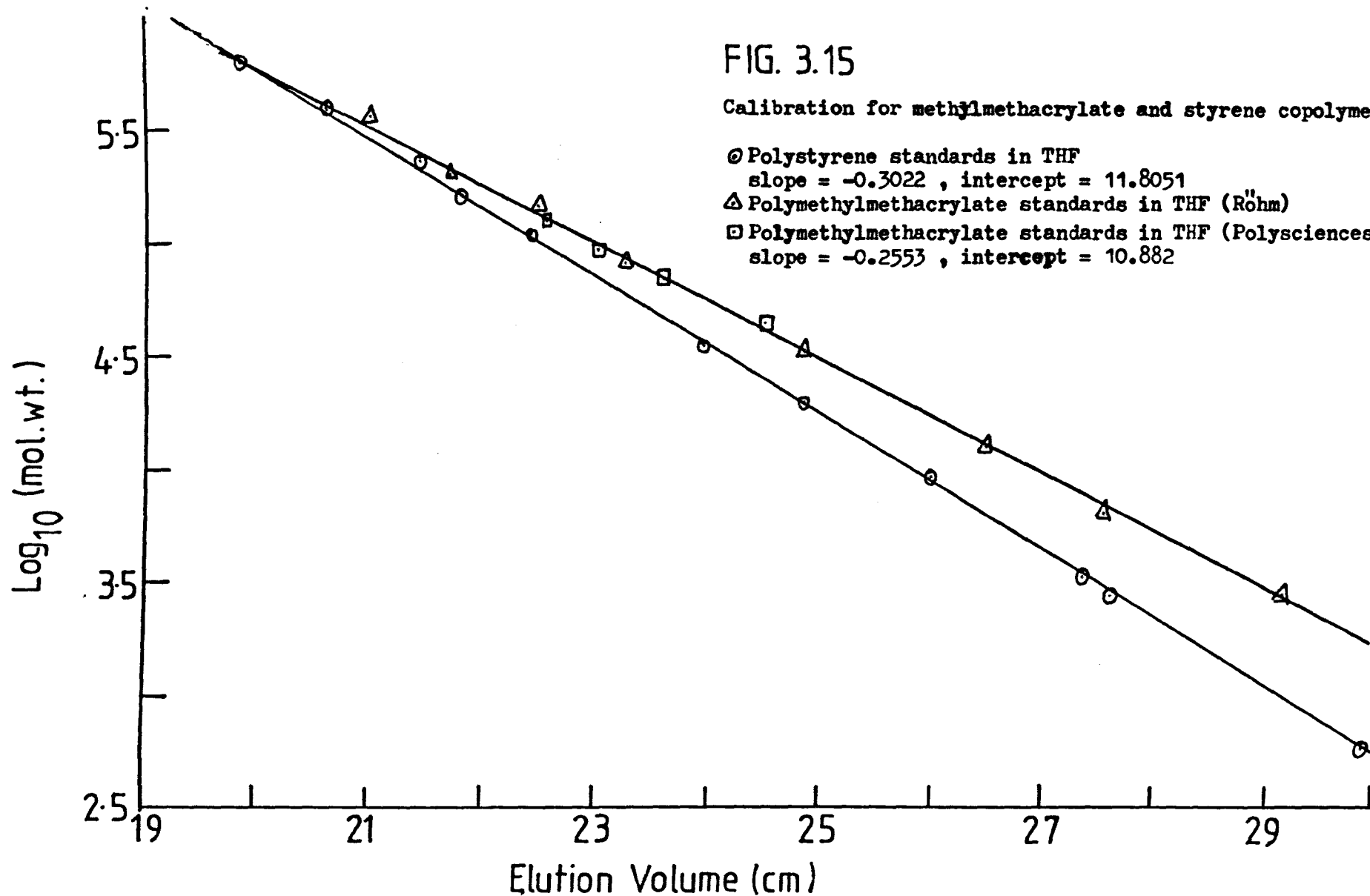
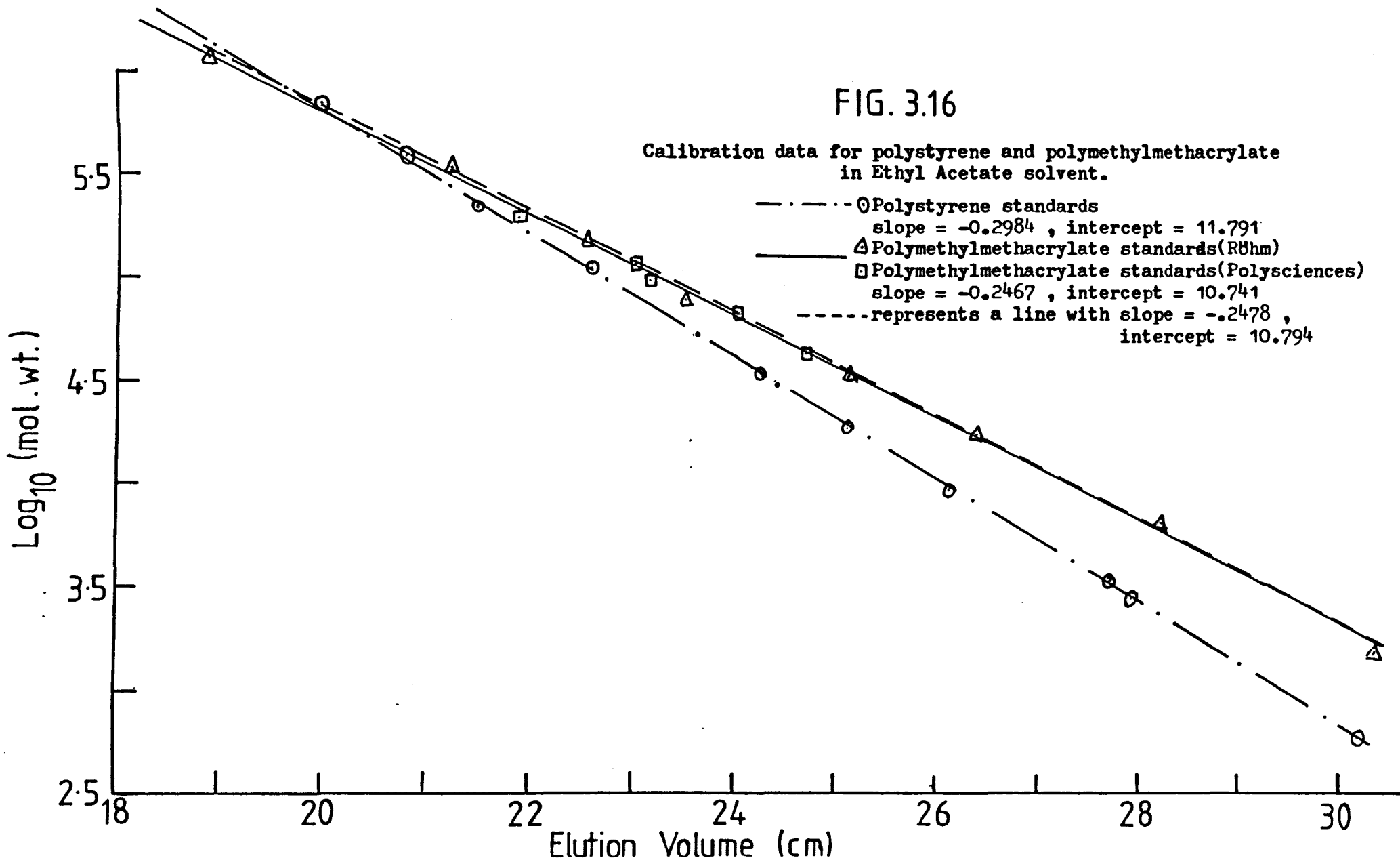


FIG. 3.16

Calibration data for polystyrene and polymethylmethacrylate  
in Ethyl Acetate solvent.



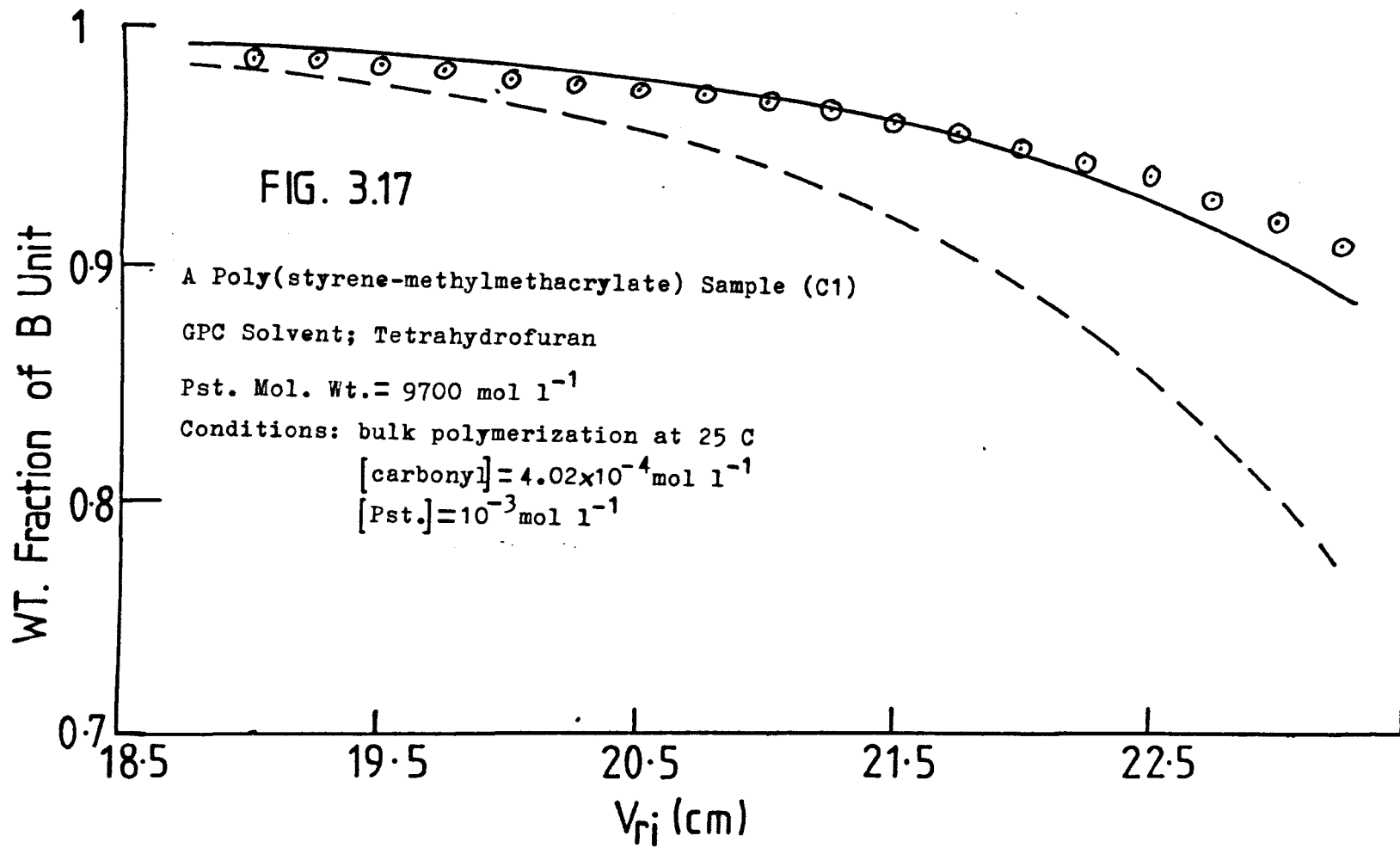
Figures 3.17 to 3.21

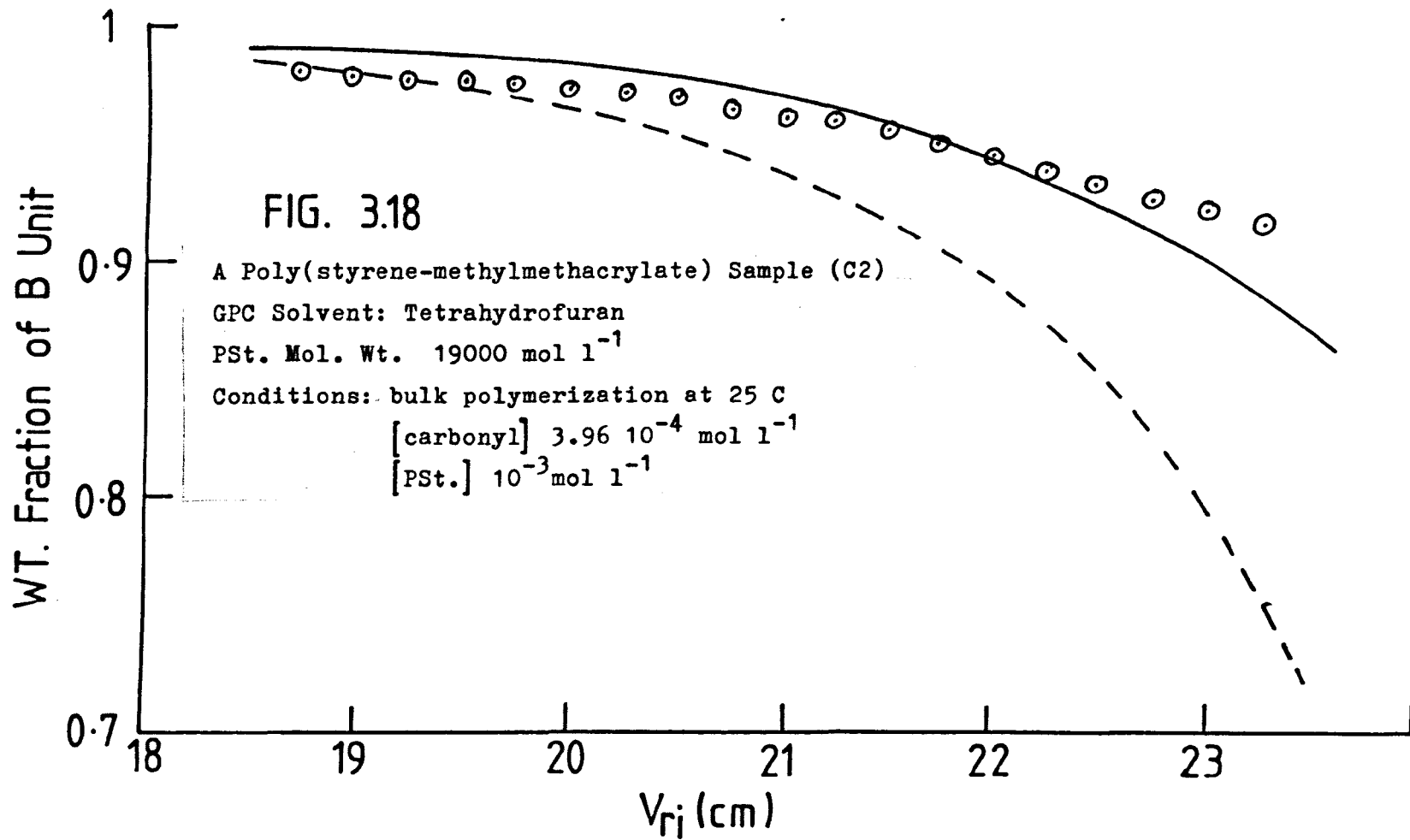
———— AB type block copolymers

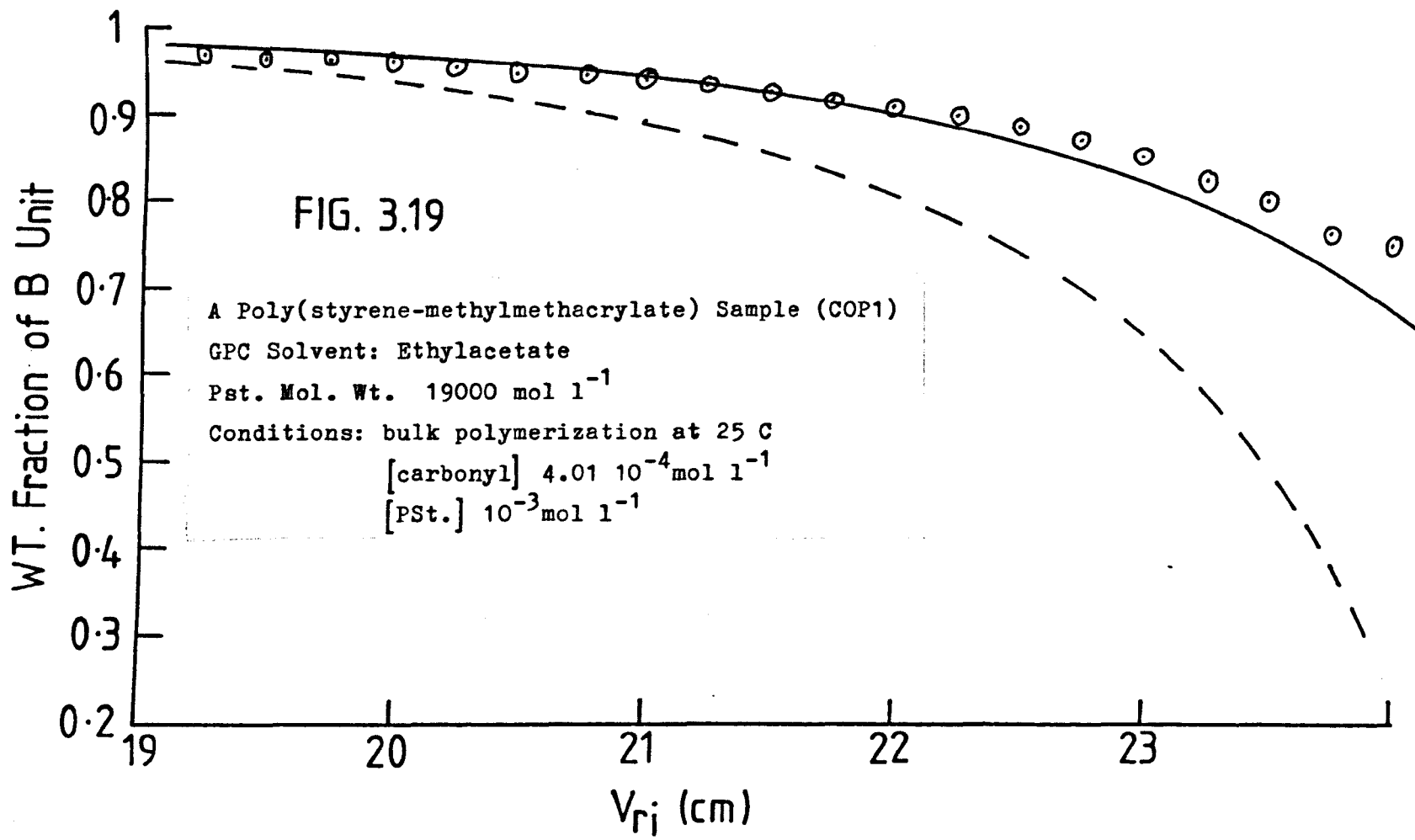
----- ABA type block copolymers

Experimental and Theoretical values for the Wt.

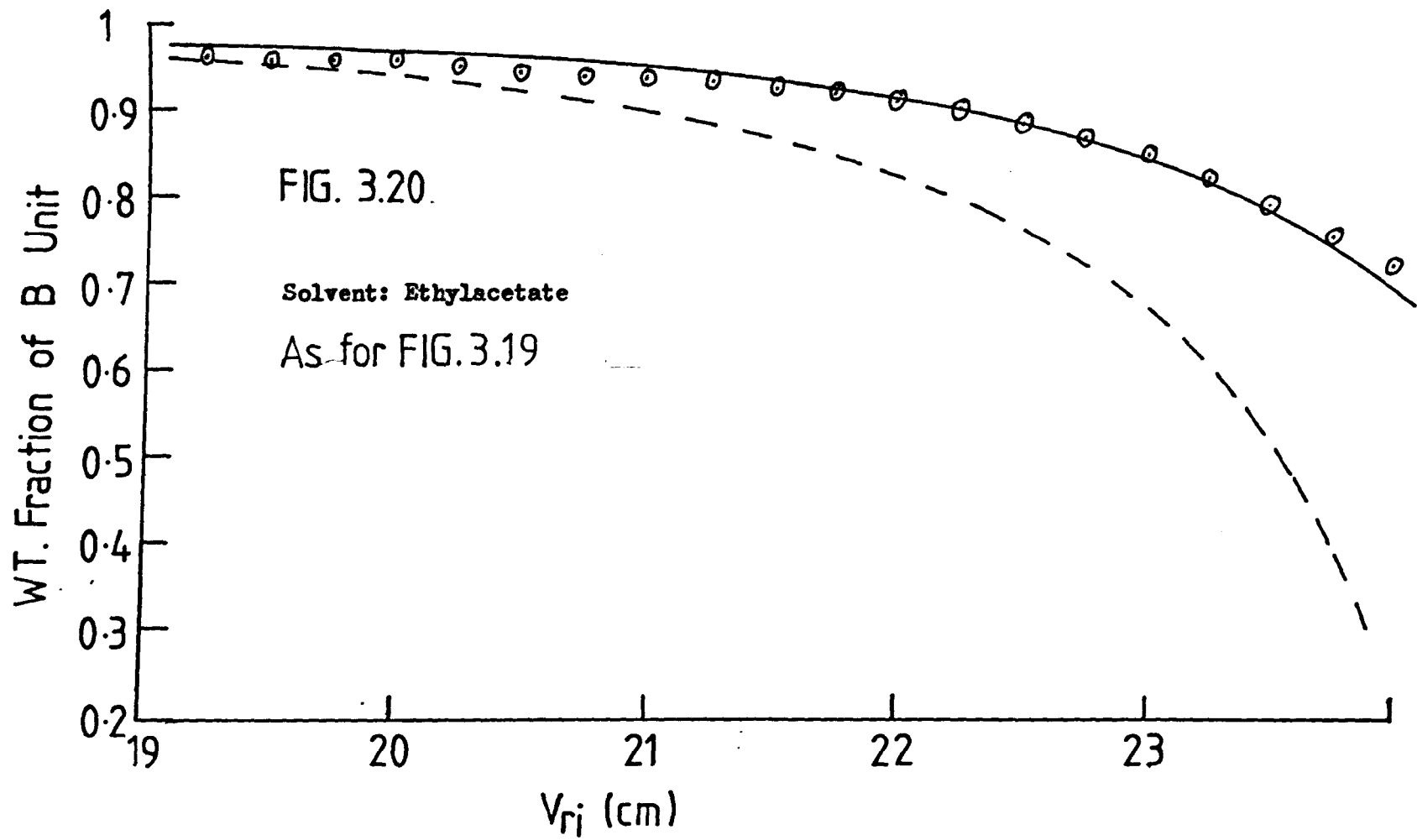
Fractions of AB and ABA Copolymers at  $V_{ri}$











to examine the sensitivity to the calibration data. In this work, only the calibration data for the free-radically prepared component of the copolymer was altered, even though manipulation of the calibration data for the anionic component was possible. It was found that the calibration parameters (slope and intercept) were very important and that a small change in these values could increase or decrease the agreement between the experimental and the theoretical curves for the samples considered under the model. Figure 3.19 shows the analysis of a poly(styrene-methylmethacrylate) sample using the standard GPC calibration parameters, while figure 3.20 shows the analysis for the same copolymer, but using parameters that have been altered by 0.5% from the originals. Comparison shows that the agreement especially at higher elution volumes is better for the altered parameter curve, which would indicate that the analysis is very sensitive to calibration data. Figure 3.16 shows the relevant calibration data, including the resulting calibration curve for the altered parameters. It can be seen that the altered calibration curve is a reasonable fit to the data points, so highlighting the problem of accurate calibration that occurs with the model. Because of the sensitivity of the calculated curves to errors in calibration data and a shortage of accurate standards for some components, it will remain unclear whether the deviations are a result of calibration errors or limitations on the application of the model, until more accurate standards become available.

Differences in figure 3.19 and figure 3.21 for the same copolymer sample when using different solvents indicates that the model may not be an accurate representation of copolymers in solution. They further indicate that the copolymers tend to have smaller hydrodynamic volumes in solution than those based on the simple additivity model. If this deduction is true, the general model may be the basis of a good characterization procedure, if the shrinkage factors for selecting 'ideal' copolymers could be determined and lead to a possible method of studying hydrodynamic volumes of copolymers in solution.

If the basis of the model in the absence of interactions between the different polymer segments is valid, the deviations from the theoretical could, in principle, be used to examine such interactions, as well as offering a means of determining shrinkage factors and solute behaviour. If interactions are present, they may be the root cause of the shrinkage factors for the copolymers in solution. Repulsive interactions between segments for instance, may in solution cause the unlike components to segregate and so allow the components to act as two smaller but linked molecules. The segregated component situation would probably cause a reduction in hydrodynamic volume, thus moving the copolymer response to higher elution volumes and so give results that would show more polymer at lower weight fractions than the theoretical curves of Equation 3.3. Attractive interactions between segments would possibly cause an increase in hydrodynamic volume, because although a single molecule would

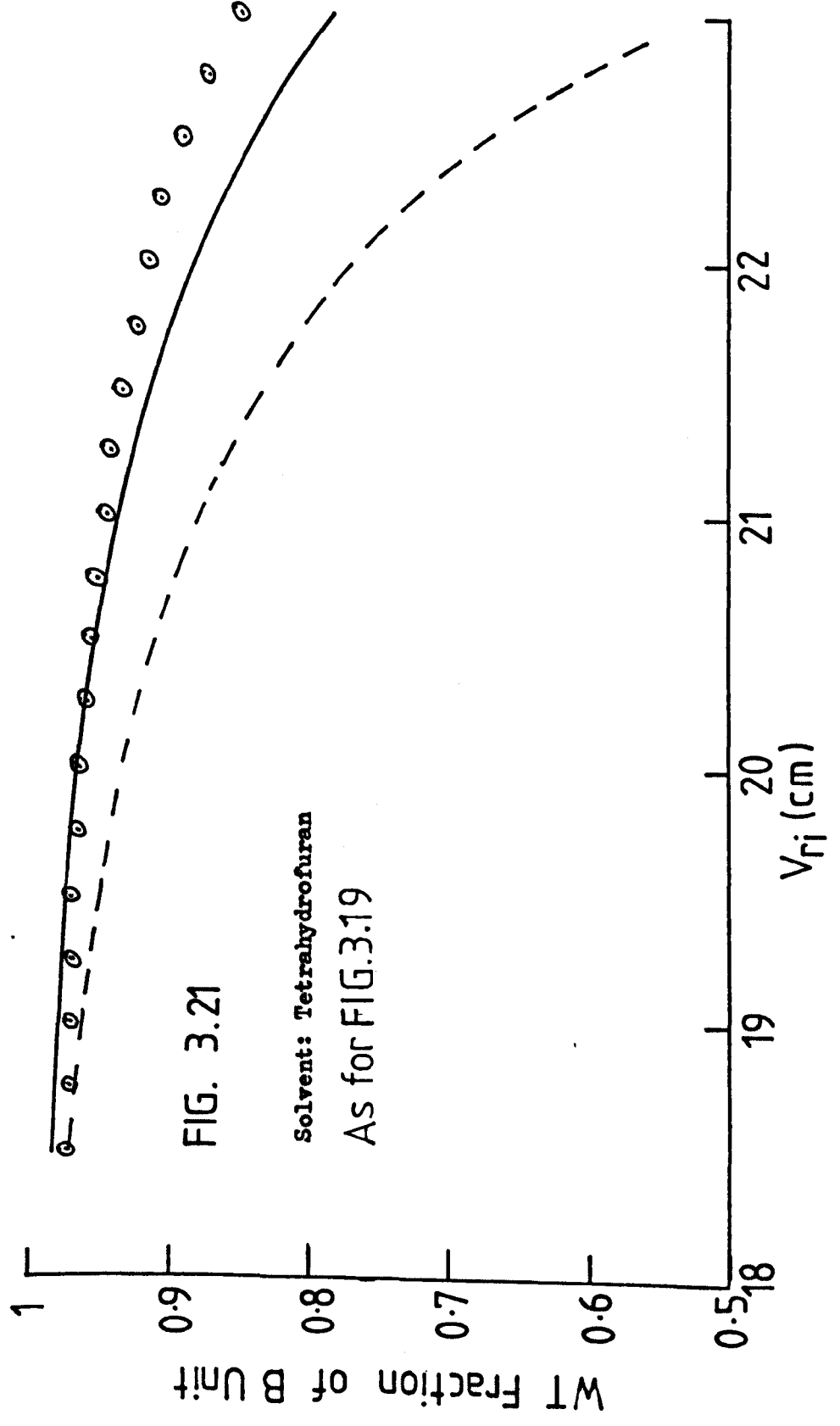


FIG. 3.21

Solvent: Tetrahydrofuran  
As for FIG.3.19

shrink, the attraction of segments may occur between other molecule segments, so forming close groups of molecules that may behave as larger molecules during the GPC separation process (have a combined larger hydrodynamic volume than individual components).

Shrinkage may also occur if the A-component units represent a poor solvent for the B component, then the presence of A in the vicinity of B could reduce the local overall solvent quality and so cause shrinkage.

All the deviations of the experimental from theory, would seem to indicate a lot of B-component at large elution volumes and this could be caused by some homopolymer produced by transfer. These deviations may also indicate the the free-radical polymerization component of the copolymer synthesis may not be as straightforward as first thought, in that there may be reactions which have not been considered or are unknown.

Copolymers containing polymethylmethacrylate were the only ones analysed using the model proposed by Eastmond, because of the lack of accurate calibration standards for the other polymers used as components in the copolymer synthesised. It is interesting to note that if the model is applicable to block copolymers, assuming interactions and shrinkage effects are negligible, then it may offer a method of determining calibration data for homopolymers that hitherto have required complicated calibration methods.

Exploratory work was undertaken to evaluate the possibility of determining calibration data for polymethylacrylate from copolymers synthesised by an anionic to free-radical transformation mechanism. As discussed earlier in section 3.6, the chromatograms of the copolymer poly(styrene-methylacrylate) indicated that there had been little or no transfer during the copolymerization and that only a small quantity of copolymer was hidden under the prepolymer peak (almost all the copolymer could be observed). From the copolymer chromatograms the weight fraction of polymer B in the copolymer could be determined at different elution volumes by the use of equation 3.2.

It is known that in the free-radical polymerization of methylacrylate the termination mechanism is almost exclusively by combination (62, 68), therefore it is valid to assume that the copolymer formed would be of the ABA type. In this case the A block being of known molecular weight (polystyrene,  $19000 \text{ g mol}^{-1}$ ) means that in conjunction with the weight fraction of polymer B data, it is possible to determine the molecular weight of polymer B at a given elution volume. A calibration graph of  $\log(\text{molecular weight})$  against elution volume can be drawn for polymethylacrylate as in figure 3.22.

The polymethylacrylate calibration thus determined, was used to determine the molecular weight distributions of two samples of polymethylacrylate homopolymer, which

were then compared to theoretical distributions using the computer program GR7. As can be seen in figures 3.23-3.24 the experimental and theoretical distribution curves agree very well apart from the lower molecular weight end (below 150000 mol. wt.). This discrepancy at lower molecular weight would be due to the calibration data not applying exactly at those molecular weights. This is a valid explanation as the calibration curve (figure 3.22) does not show a linear relationship at high elution volumes that would correspond to molecular weights below  $150000 \text{ g mol}^{-1}$ , this discrepancy could be due to the difficulty in measuring the chromatogram near the point where the residual prepolymer begins to elute, so overlapping the tail of the copolymer chromatogram.

The analysis described above is of a very exploratory nature, but would seem to indicate that the general concepts used by Eastmond are valid and that with refinement may offer a way of gaining calibration data from copolymer systems. It must be noted that this approach requires (1) that the model is applicable in these cases, (2) accurate knowledge of the copolymer structure, in that, in relevant cases, the mechanism of termination with associated side reactions and the extent of transfer must be known.

FIG. 3.22 From CL1

Polymethylacrylate Calibration Curve.

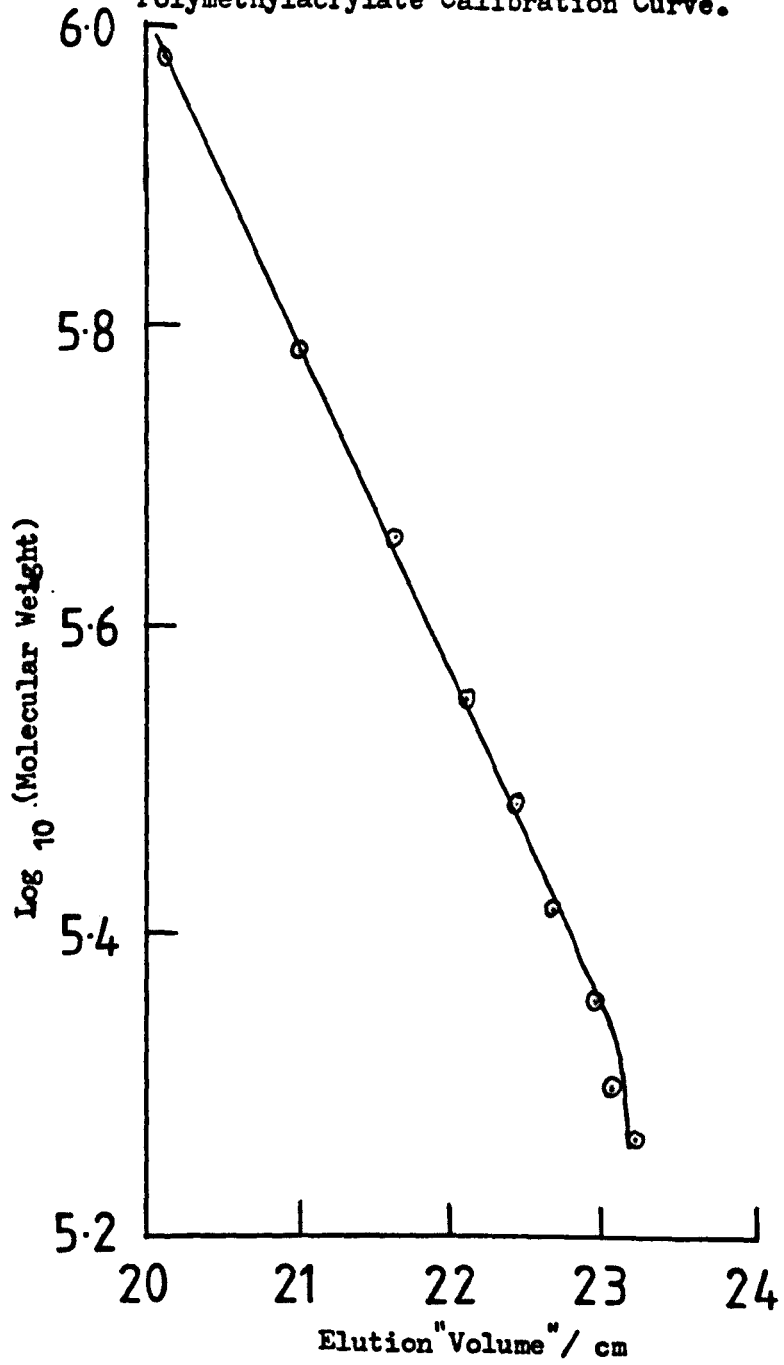




FIG. 3.23–3.24 Conditions as in FIG. 2.14

FIG. 3.23

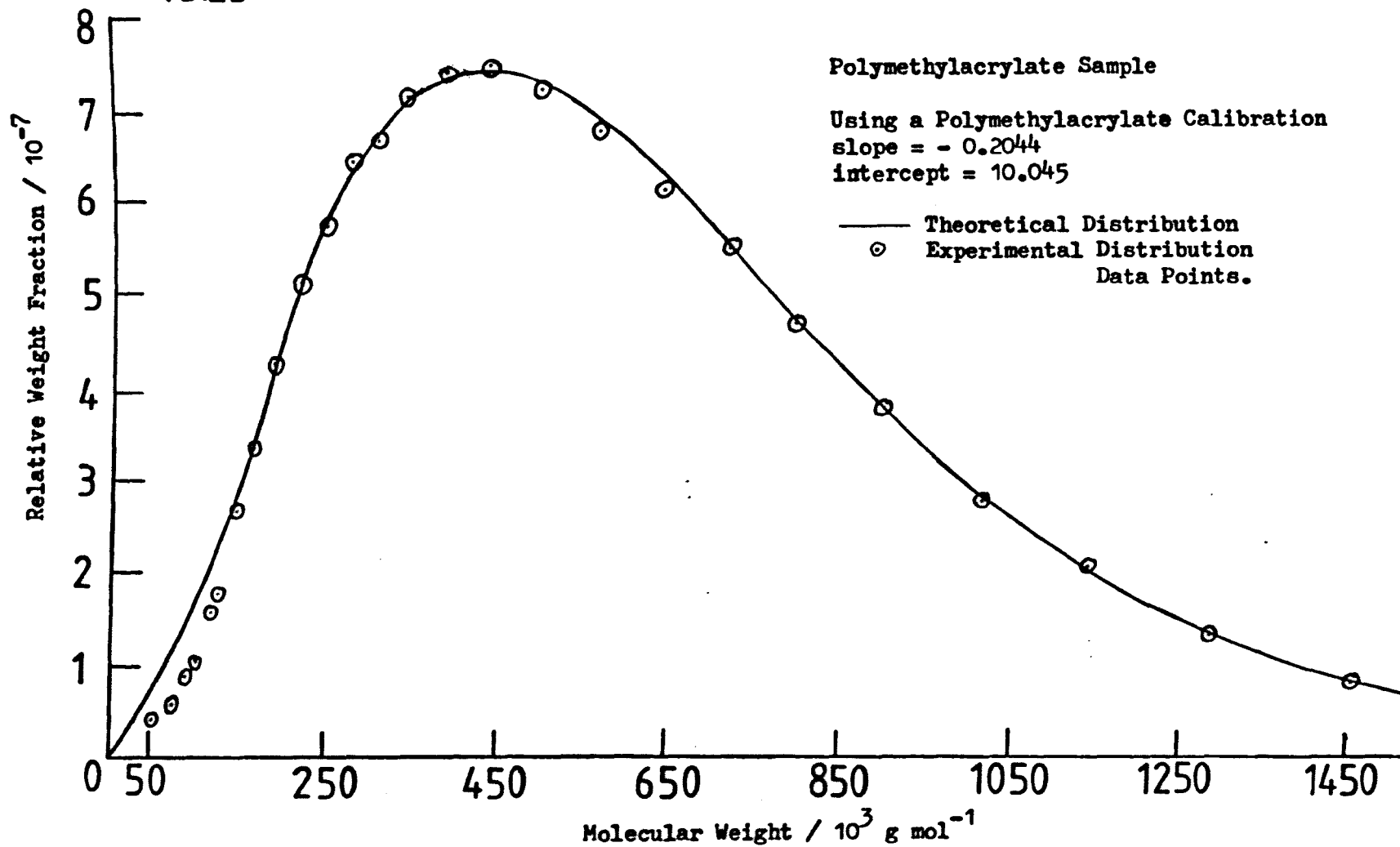
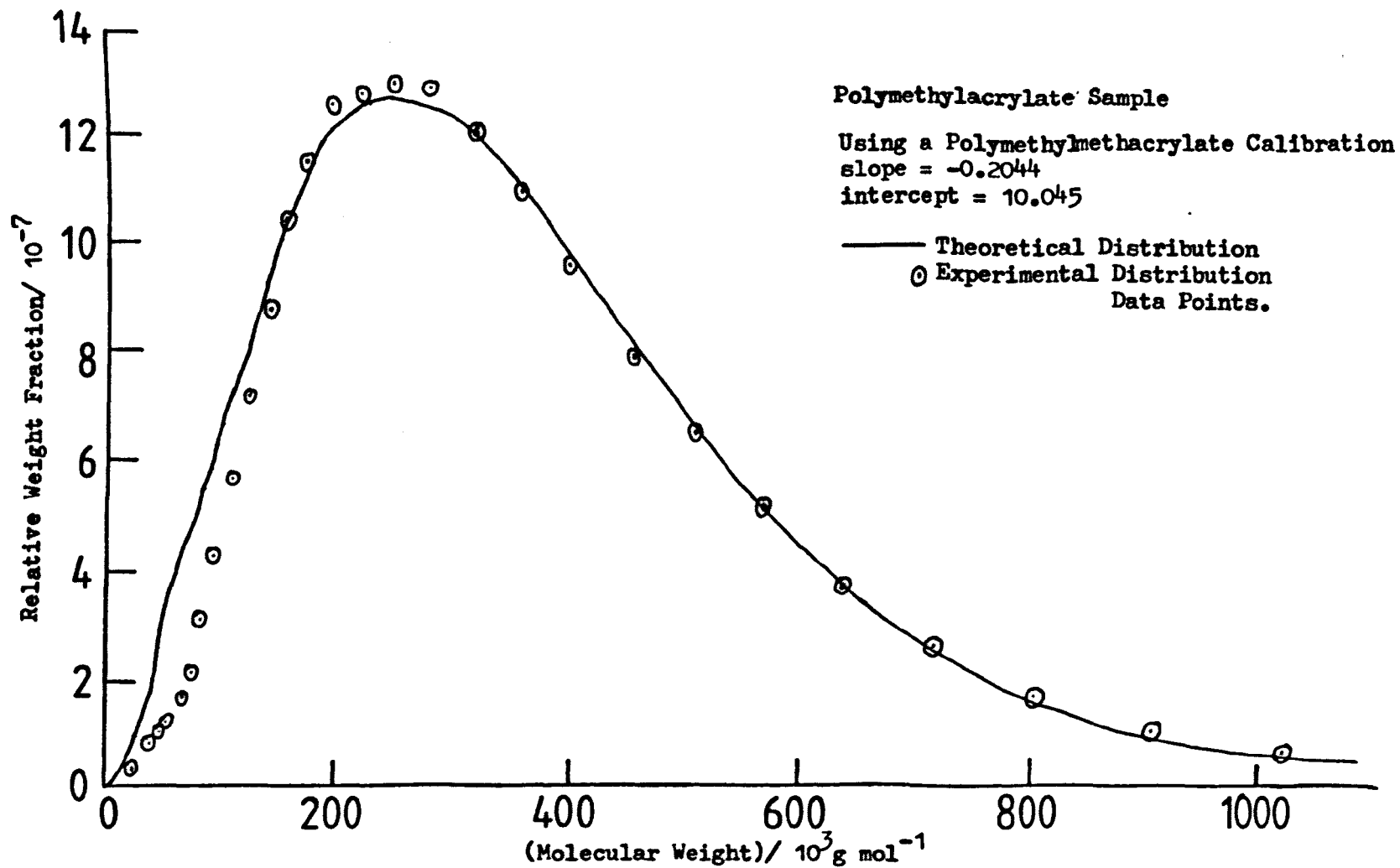


FIG. 3.24



## CHAPTER IV

## PHYSICAL TECHNIQUES, RESULTS AND DISCUSSION

Here the techniques employed to investigate the physical characteristics of the block copolymers synthesized are described. The methods used for data analysis are given, followed by a discussion of the results obtained. The techniques employed required quantities of block copolymer in several-gram quantities and so the copolymer blends studied were produced using the large scale preparation method described in Section 2.4.1. The compositions of the blends studied are given in Table 4.1.

Table 4.1

| Copolymer                         | Notation | % of B component |
|-----------------------------------|----------|------------------|
| Poly(styrene-methylacrylate)      | PST-MA1  | 70.3             |
| Poly(styrene-ethylacrylate)       | CL1      | 65.1             |
| Poly(styrene-n-Butylacrylate)     | CL2      | 59.75            |
| Poly(styrene-n-Butylmethacrylate) | CL3      | 48               |
| Poly(styrene-ethylacrylate)       | CL4      | 62.6             |
| Poly(styrene-n-Butylmethacrylate) | CL5      | 18               |
| Poly(styrene-n-Butylmethacrylate) | CL6      | 27               |

#### 4.1 Viscoelasticity

The two extreme cases of mechanical behaviour are elastic behaviour and viscous flow behaviour, which can be represented very well by mechanical models. A compressed Hookean spring can serve as a model for an elastic body under load (figure 4.1a); the compressed or elongated spring immediately returning to its original position on removal of the load, so giving back all the energy stored on deformation. The relationship between stress,  $\sigma$ , the modulus,  $E$ , and the strain,  $\epsilon$ , is given by Hooke's Law (equation 4.1)

$$\sigma = E \cdot \epsilon \quad 4.1$$

At the other extreme is the case of viscous flow; the model being a dash pot consisting of a piston in a viscous Newtonian liquid (figure 4.1b); here the relationship is given by equation 4.2, where  $\eta$  is the viscosity of the Newtonian liquid,  $t$  is the time for which the stress was applied.

$$\epsilon = \frac{t\sigma}{\eta} \quad 4.2$$

Polymers are examples of viscoelastic materials, in that they exhibit both elastic and viscous flow properties. The viscoelastic behaviour of polymeric materials can be reproduced by using combinations of the elastic and viscous flow mechanical models. Maxwell bodies are obtained if Hookean and Newtonian bodies are connected in series

FIG. 4.1a

Hooke

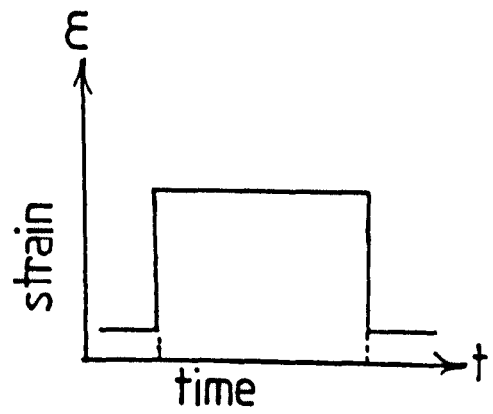


FIG. 4.1b

Newton

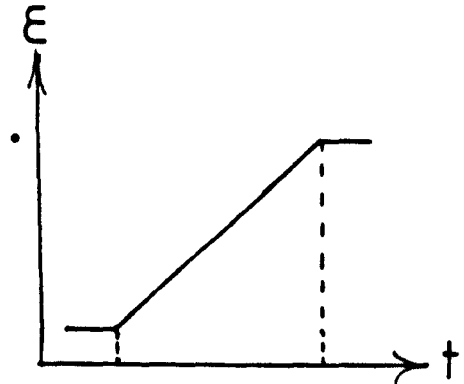
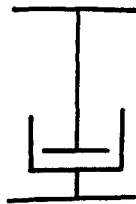


FIG. 4.1c

Voigt, Kelvin

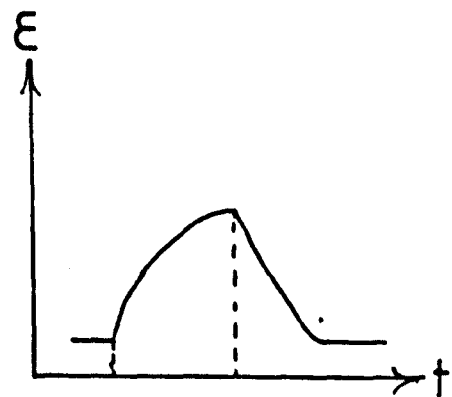
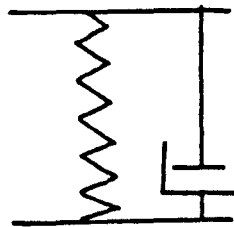
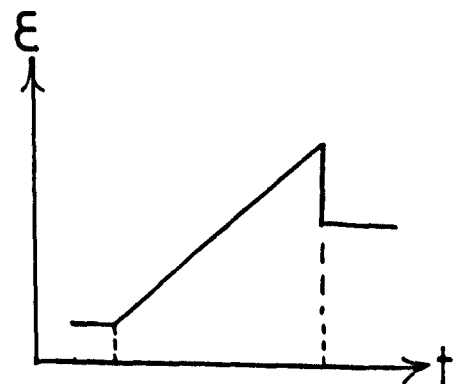


FIG. 4.1d

Maxwell



(figure 4.1c). The Kelvin or Voigt model, on the other hand contains Hookean and Newtonian bodies in a parallel arrangement (figure 4.1d). The Maxwell and Kelvin models describe the phenomena of stress relaxation and retardation (Creep) respectively, that are characteristics of visco-elastic materials.

#### 4.1.1 Stress Relaxation

A relaxation is defined in mechanics as the decrease in stress while maintaining a body under constant deformation. The origin of this relaxation phenomenon can be explained as follows:- a stress is applied during the deformation of a viscoelastic medium, when the deformation ceases, the stress will gradually fall off (relax) as the molecules or molecular segments return to their equilibrium positions.

A spring (ideally) will respond instantaneously to an applied stress, while a viscous liquid responds gradually as it is unable to respond instantaneously to an applied stress. If the deformation (strain) is kept constant, the piston of the viscous liquid dash pot has time to respond to the strain applied (moves slowly through the viscous liquid); this response results in the relaxation of the spring to its equilibrium stress position. If the stress is suddenly removed, the spring contracts immediately, but the piston remains in the elongated state. The rates of deformation  $d\epsilon/dt$  are additive in these processes. By

combining the expressions for the rates of deformation according to Hooke's Law and according to Newton's Law, we obtain the following for the total rate of deformation:

$$\frac{d\epsilon}{dt} = \frac{d\epsilon_e}{dt} + \frac{d\epsilon_n}{dt} = \frac{1}{E} \frac{d\sigma}{dt} + \frac{\sigma}{\eta} \quad 4.3$$

where  $e$  and  $n$  represent Hooke's Law and Newton's Law respectively. When the deformation is constant,  $d\epsilon/dt = 0$ , equation 4.3 becomes

$$\frac{1}{E} \frac{d\sigma}{dt} = -\frac{\sigma}{\eta} \quad 4.4$$

or, when integrated

$$\sigma = \sigma_0 \exp\left(\frac{-Et}{\eta}\right) = \sigma_0 \exp\left(\frac{-t}{\tau}\right) \quad 4.5$$

where  $\sigma_0$  is the initial stress and  $\tau = \eta/E$  is the relaxation time;  $\tau$  indicates the time interval required for the stress to fall to a value  $1/e$  times the original value.

With real polymers, however, there exists a whole spectrum of relaxation times. This spectrum can be shown through the use of a model with a number of Maxwell bodies in a parallel arrangement.

#### 4.1.2 Retardation (Creep) Processes

Retardation can be defined as the increase in deformation



with time under constant stress. This phenomenon occurs when a constant stress is applied to a sample and the resulting deformation increases gradually. The process can be described by equation 4.6,

$$\sigma = \sigma_H + \sigma_n = E\epsilon + \eta \frac{d\epsilon}{dt} \quad 4.6$$

from integration of equation 4.6

$$\epsilon = \frac{\sigma}{E} \left[ 1 - \exp\left(-\frac{t}{\tau_i}\right) \right] \quad 4.7$$

$\tau_i$  is the retardation time. As a rule there are usually a whole spectrum of retardation times in the retardation processes.

Retardation and relaxation time distributions are similar, but they are not identical since they pertain to different models of the deformation behaviour.

#### 4.2 Dynamic Measurements

Dynamic mechanical relaxation measurements are often used to examine the properties of viscoelastic materials, including polymers. These measurements usually make use of the concept of sinusoidal excitation and response, where the applied load and the resulting deformation both vary sinusoidally with time, the rate of oscillation is specified by the frequency ( $f$ ) in Hertz (Hz) or  $\omega = 2\pi f$  in radians/second. For linear viscoelastic behaviour, the strain

alternates sinusoidally but is out of phase with the stress, as seen in figure 4.2. This phase lag results from the time necessary for molecular rearrangements to occur and is associated with relaxation phenomena (69). The stress  $\sigma$  and strain  $\epsilon$  can be expressed as follows:-

$$\text{stress, } \sigma = \sigma_0 \sin(\omega t + \delta) \quad 4.8$$

$$\text{strain, } \epsilon = \epsilon_0 \sin(\omega t) \quad 4.9$$

where  $\omega$  is the angular frequency, and  $\delta$  is the phase angle.

Then,

$$\sigma = \sigma_0 \sin \omega t \cos \delta + \sigma_0 \cos \omega t \sin \delta \quad 4.10$$

The stress can be considered to consist of two components, one in phase with the strain ( $\sigma_0 \cos \delta$ ) and the other  $90^\circ$  out of phase ( $\sigma_0 \sin \delta$ ). When these are divided by the strain, we can separate the modulus into an in-phase (real) and out of phase (imaginary) component. These relationships are

$$\sigma = \epsilon_0 E' \sin \omega t + \epsilon_0 E'' \cos \omega t \quad 4.11$$

$$E' = \frac{\sigma_0 \cos \delta}{\epsilon_0} \text{ and } E'' = \frac{\sigma_0 \sin \delta}{\epsilon_0} \quad 4.12$$

where  $E'$  is the real part of the modulus, and  $E''$  the imaginary part. The complex representation for the modulus as shown in figure 4.3 can be expressed as

$$\epsilon = \epsilon_0 \exp i \omega t \quad 4.13$$

FIG. 4.2

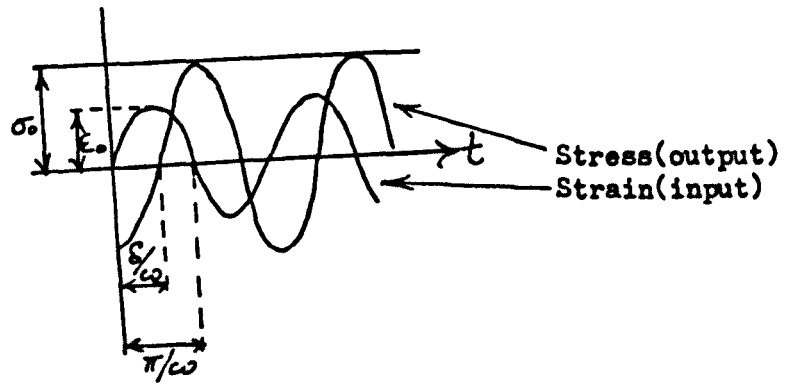
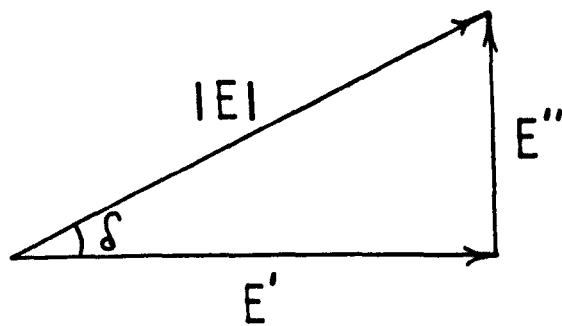


FIG. 4.3



Relations between various parameters used to express the results of a dynamic mechanical measurement.

$$\sigma = \sigma_0 \exp i (\omega t + \delta) \quad 4.14$$

Then

$$\frac{\sigma}{\epsilon} = E^* = \frac{\sigma_0}{\epsilon_0} e^{i\delta} = \frac{\sigma_0}{\epsilon_0} (\cos \delta + i \sin \delta)$$

$$= E' + iE'' \quad 4.15$$

and similarly for the other deformation types.

The real part of the modulus,  $E'$ , the storage modulus, is related to the storage of energy as potential energy and its release in the periodic deformation. The imaginary part of the modulus,  $E''$ , the loss modulus, is associated with the dissipation of energy as heat when materials are deformed. The phase angle  $\delta$  is given by

$$\tan \delta = \frac{E''}{E'} \quad 4.16$$

where  $\tan \delta$  is called the loss tangent and is the ratio of energy dissipated per cycle to the maximum potential energy stored during a cycle.

The same arguments can be used for deformations as for stress deformations, when dielectric measurements are undertaken. With dielectric measurements the material responds to a perturbation caused by an external electric field.

Under the influence of small electric fields, electrons can move quite freely through conductors but not insulators

(dielectrics). These fields displace the electrons only slightly from their positions, thus causing a separation of charges to give dipoles. This overall process is called polarization. In polymeric materials the polarization is normally due to electronic or atomic polarization. Polymer molecules with polar groups also exhibit permanent dipoles, which in presence of an electric field can produce orientation polarization.

As a result of the imposed polarization, the polymeric material will respond by a re-orientation of the dipoles, as to align the polarization with the direction of the electric field. This re-orientation is limited by opposition from the structure and thermal motions of the polymeric material.

When a sinusoidal field is applied to a polymeric material, the dipoles attempt to align themselves in the direction of the field. The more rapidly the direction of the field changes, the less easily they are able to align themselves to the applied field. At frequencies where the dipoles can align, the polarization contributes to the permittivity, ie,  $C/C_0$  where  $C_0$  is the capacitance of a vacuum filled capacitor and  $C$  is the capacitance with the material present.

$$\text{For a voltage } V = V_0 \sin(\omega t) \quad 4.17$$

$$\text{charge } Q = CV = \epsilon C_0 V_0 \sin(\omega t) \quad 4.18$$

$$\text{current } i = dQ/dt = \omega \epsilon C_0 V_0 \cos(\omega t) \quad 4.19$$

At high frequencies the polarization can no longer re-orientate fast enough to keep up with the alternating field and so lags behind. This delay between response and stimulus, results in an out of phase current  $\omega \epsilon C_0 V_0 \cos \delta$  and an in-phase current  $\omega \epsilon C_0 V_0 \sin \delta$ , where  $\delta$  is the phase (lag) angle. The out of phase component is called the storage or charge current and the in-phase component is called the loss current because it gives rise to the dissipation of energy as heat.

With respect to the permittivity it has two components; these are termed relative permittivity  $\epsilon'$  and loss permittivity  $\epsilon''$ .

As can be seen dielectric deformations are similar to mechanical deformations, when the deformation is applied sinusoidally.

#### 4.3 Time, Temperature and Frequency

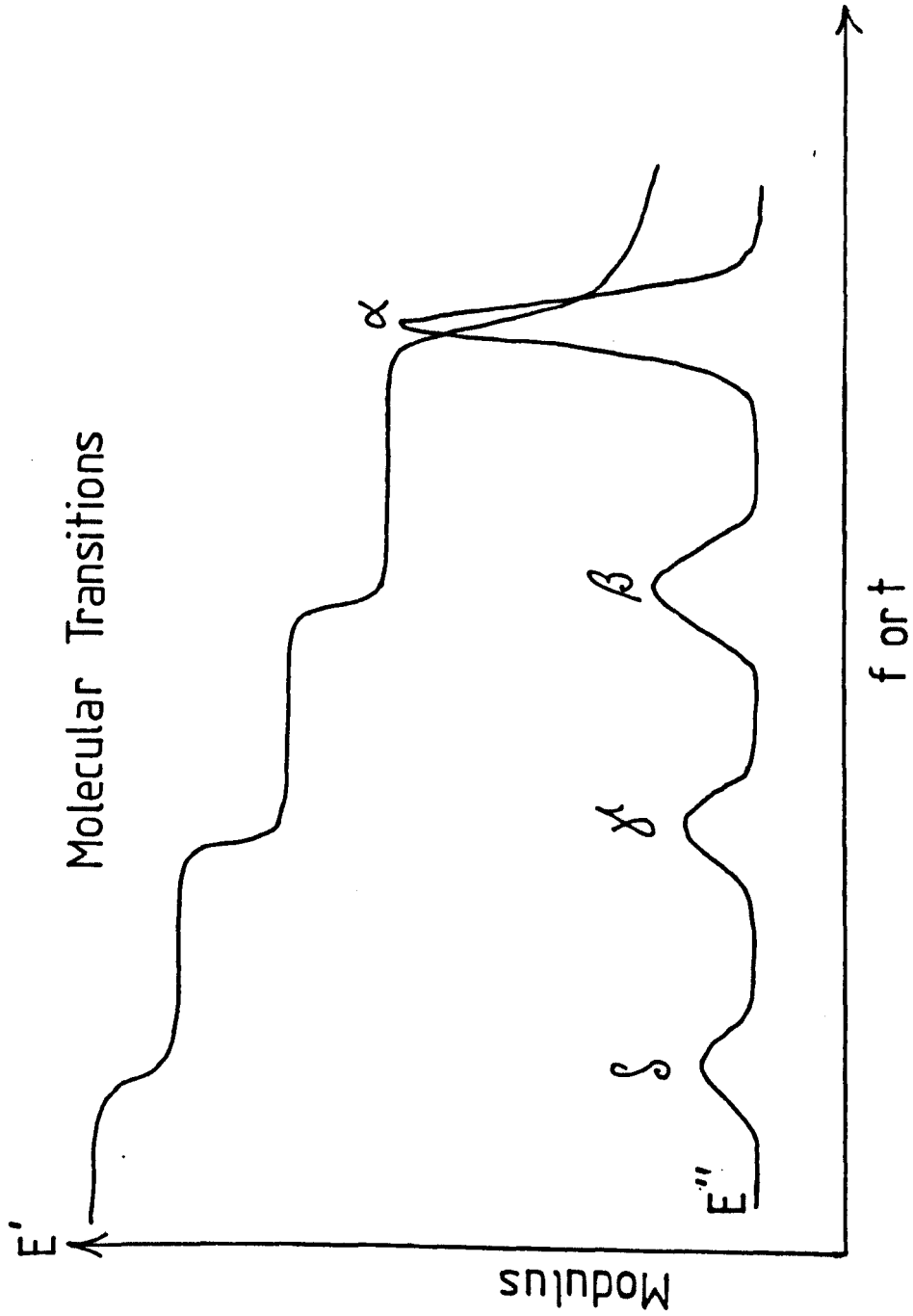
Polymer properties are temperature dependant, ie, rubbers are elastic and soft at room temperature, but become harder at low temperatures. This hardness is reflected in the storage modulus,  $E'$  for mechanical

deformations, where  $E'$  is high for hard (glass) materials and low for soft (rubbery) materials. Therefore it can be seen that the moduli of polymers are temperature dependent.

Rates of application of stress or strain to materials are important variables in the determination of mechanical properties, eg, stress-strain curves, stress relaxation and creep. Modulus measurements over short time periods result in high values of modulus, whereas measurements over longer periods result in low values of modulus. A dynamic mechanical analysis at frequency  $\omega = 2\pi f$  is qualitatively equivalent to a transient experiment over a time  $t = 1/\omega$ .

When moduli are measured as a function of temperature,  $t$  (fixed frequency) or of frequency,  $f$  (fixed temperature) a series of transitions or relaxations are observed. These transitions are labelled  $\alpha$ ,  $\beta$ ,  $\gamma$ ,  $\delta$  etc. in order of decreasing temperature (figure 4.4). The  $\alpha$ -relaxation is the major transition which corresponds to the glass transition temperature,  $T_g$ , for an amorphous polymer. Many mechanical properties change in the neighbourhood of  $T_g$ ; the storage modulus commonly decreases by about three orders of magnitude at  $T_g$ , while the loss modulus and  $\tan \delta$  exhibit maxima.

FIG. 4.4





Activation energies for the processes of molecular and segmental motion, that give rise to the Tg of a polymeric system, can be gained from the analysis of data generated by dynamic experiments. The instruments used here to supply data were the Rheovibron (see section 4.4) and the dielectric measurement cell (see section 4.5).

Activation energies for the segmental motions responsible for the Tg process were calculated by the use of an Arrhenius plot, which is derived from the equation for the relaxation time of deformation (equation 4.20) (69)

$$\tau = \tau_0 \exp \frac{E_a}{RT} \quad 4.20$$

where  $\tau$  is the relaxation time, which is equal to the reciprocal of the angular frequency,  $\omega$ , of molecular motion and is related to the probability of segmental motion,  $E_a$  is the activation energy,  $R$  is the gas constant,  $T$  is absolute temperature and  $\tau_0$  is a constant that is related to the frequency of the vibration of the segments and the entropy of the system.

$$\tau = \frac{1}{\omega} \text{ where } \omega = 2 \pi f$$

$$\text{Therefore } \tau = \frac{1}{2 \pi f} \quad 4.21$$

where  $f$  is the frequency of segmental motion in hertz.

$$(2 \pi f)^{-1} = \tau_0 \exp \frac{E_a}{RT} \quad 4.22$$

$$f = (2 \pi \tau_0)^{-1} \exp - \frac{E_a}{RT} \quad 4.23$$

$$\ln f = \text{Constant} - \frac{E_a}{RT}$$

4.24

The equation 4.24 can be used for both the Rheovibron data and the dielectric data. From equation 4.24 it can be seen that if a plot of  $\ln f$  against  $(T)^{-1}$  is drawn and it is a straight line, the slope of the plot will be equal to  $-E_a/R$ , from this  $E_a$  can be calculated.

For the lower temperature transitions ( $\beta$ ,  $\gamma$  relaxations) that can be seen, it is more difficult to define their origins and calculate their activation energies without additional evidence, but it is thought that they are due to motion of pendant groups on the polymer backbones.

#### 4.4 Dynamic Viscoelastic Testing: The Rheovibron

The Rheovibron is an extremely useful instrument for the examination of the mechanical properties of polymer samples and provides data which allows the calculation of the real, loss and complex modulus ( $E'$ ,  $E''$  and  $E^*$  respectively) and  $\tan \delta$  as a function of temperature and or frequency for the sample. This instrument was originally developed by Takayanagi and a detailed discussion of the operation of the instrument is given in a review by Murayama (70).

The Rheovibron makes use of the method of sinusoidal excitation and response, as described in section 4.2 and is usually run at a fixed frequency with temperature as

the variable. The fixed frequency can be changed to 0.01 to 1 Hz, 3.5 Hz, 11 Hz, 35 Hz and 110 Hz according to the requirements of the experiment.

During the course of this work the instrument used was the Direct Reading Rheovibron Viscoelastometer - DDV-II-C which had been interfaced with a Research Machines 380Z microcomputer. The microcomputer was used to read switch and gauge positions on the instrument to calculate  $E'$ ,  $E''$  and  $\tan \delta$  and to give a graphic print out. The overall operation of the instrument was manual, even though it would be possible to automate the instrument. The computer program used for the operation and analysis of data was RHEO 251; built into the program there was a graphics routine which would plot  $E'$ ,  $E''$ , and  $\tan \delta$  against temperature.

The Rheovibron operates by having a sample placed in the jaws of the instrument, (typical sample dimensions  $2.5 \times 0.03 \times 0.3$  cm) figure 4.5a, a small static strain is then applied manually by means of a fine screw control on the instrument stage. The instrument then applies a sinusoidal strain to the sample via a driver motor; the sinusoidal strain being of an amplitude smaller than the manually applied strain, as shown in figure 45b. The sinusoidal strain is monitored by a strain gauge and the resulting stress is measured by a stress gauge at the opposite end of the sample. It is important that the initial manual straining of the sample is greater than the maximum amplitude

FIG. 4.5a

Sample in the Rheovibron Jaws.

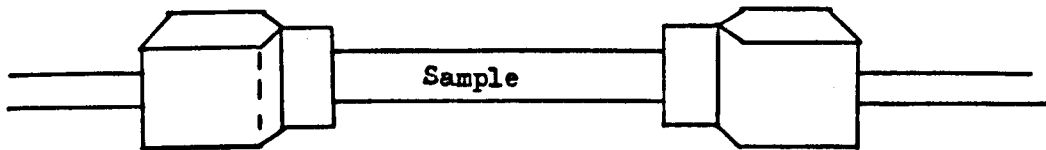
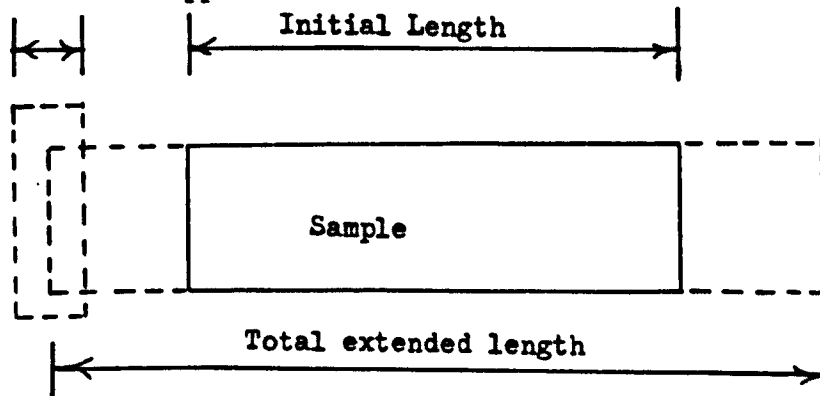


FIG. 4.5b

Sinusoidal strain applied



of the sinusoidal strain applied by the instrument, as otherwise errors are introduced owing to the sample buckling during the compression period of the strain cycle.

The heating rate was controlled manually, by using a variac to control the current to the heating element in the instrument. The rate of heating being typically  $2^{\circ}$  C/min. This was achieved by calibrating the variac. The sample was heated in a nitrogen atmosphere.

#### 4.4.1 Sample Preparation (Cast films)

Prior to casting all samples were dissolved in dichloromethane and the solutions were filtered through a prefilter and  $0.4\mu\text{m}$  'millipore' filtration system in a Buckner flask arrangement. The casting took place from a 4% homogeneous solution in all cases.

Following filtration, the copolymer samples were placed in a flat-bottomed petri dish on a level surface and covered. The rate of solvent removal of the samples was approximately  $0.75\text{ cm}^3/\text{hour}$  overall. After casting, the samples were dried under vacuum at ambient temperature for 24 hours, after which they were heated under vacuum at  $110^{\circ}$  C for a further 24 hours.

When using the acrylate copolymers it was found necessary to use a release agent to remove the cast film from the

petri dish surface without damaging the film. The release agent used was dimethylchlorosilane solution ( $\sim 2\%$  in 1, 1, 1-trichloroethane) supplied by BDH and was used according to the manufacturer's instructions.

Using this method of solvent casting, films of copolymers in the range of 0.2-0.4 mm thick were produced. The samples were cut using a straight edge and a razor blade.

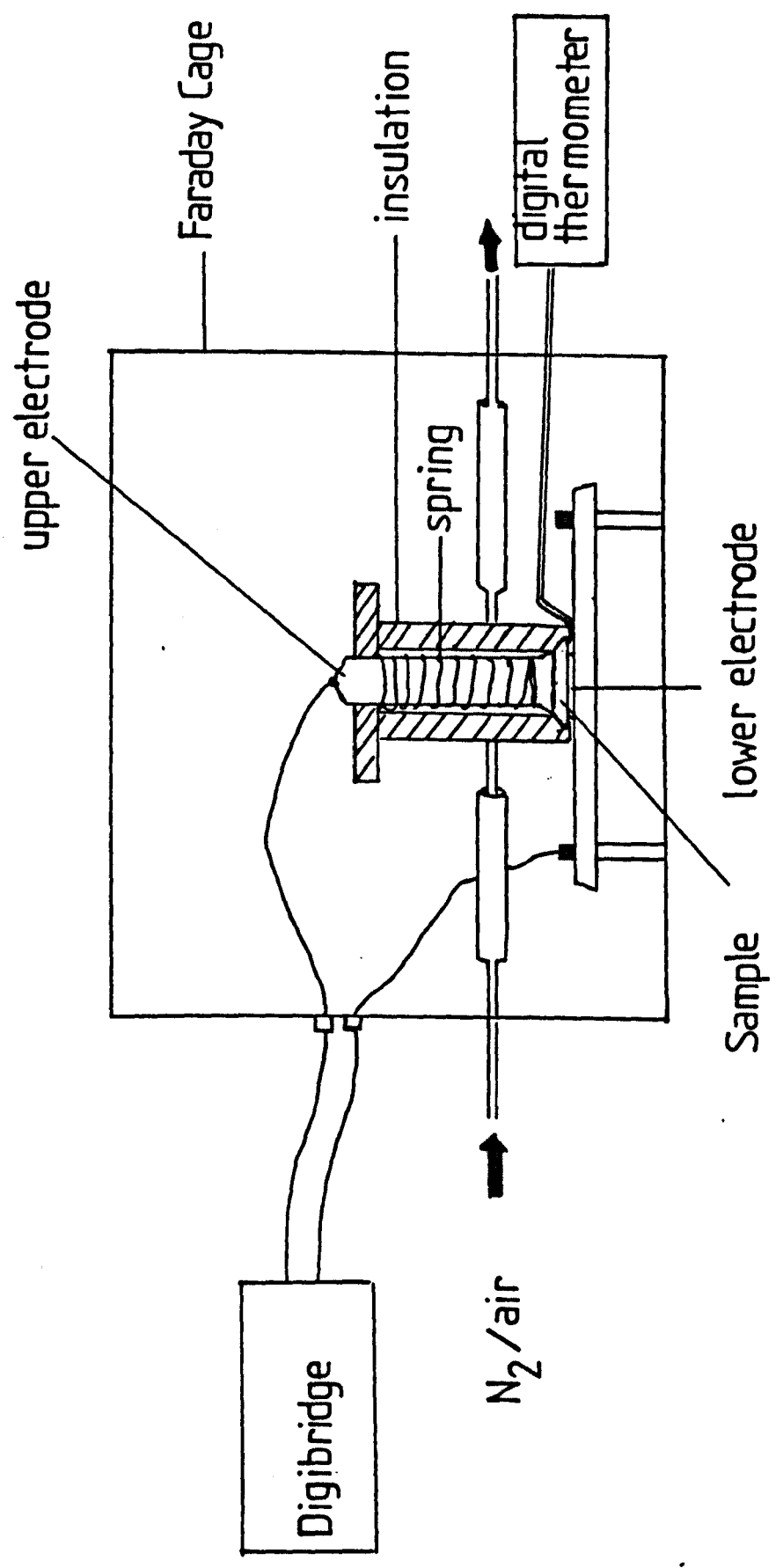
#### 4.5 Dielectric Measurements

The dielectric cell used during this study was a two terminal cell as shown in figure 4.6. The two electrodes were made from highly polished brass, the upper electrode was spring-loaded so as to produce a good contact between the electrode surface and sample. For temperatures above ambient a heated air stream was used, supplied from a red-rod heater and the compressed air supply. For temperatures below ambient a liquid nitrogen boiler was used to supply coolant; the cell was flushed with nitrogen before use, to stop water droplets from condensing in the cell.

Sample preparation was as follows: 50 mg of sample was weighed out and placed inside a teflon 'O' ring which fitted on the lower electrode. The 'O' ring was cut from a teflon sheet using 7 mm and 15 mm diameter cork borers. The cell was then assembled and heated to approximately  $150^{\circ}$  C for 1 hour, ie, above  $T_g$ 's of the

# DIELECTRIC CELL

FIG. 4.6



components, and then allowed to cool. This procedure forms a coherent film between the two electrodes. The dielectric bridge was then calibrated and trimmed according to the instructions given in the manual (71). The cell and bridge were then ready to be used.

The instrument used during the whole of this work was a Gen Rad 1689 RLC Digibridge which was interfaced with an Apple Europlus microcomputer, allowing total automation of the instrument functions, except for the changing of the temperature of the cell between individual runs. Each run generated information at 35 different frequencies; at each frequency chosen, 5 to 10 measurements of conductance and capacitance were made and the results averaged. The temperature was normally increased by approximately 5 degrees centigrade between runs and a run would take in the region of 15 minutes to complete.

#### 4.6 Differential Scanning Calorimetry (DSC)

This is a very important technique for the polymer chemist and can be used for a variety of purposes.

The instrument works by measuring the difference in power supplied to two independent heating systems, when they are heated simultaneously at the same rate. One heating system will contain the sample to be investigated, while the other will contain a reference sample or is empty.



The power required to heat the systems at a constant rate will depend on the specific heat of any material in the heating system. As long as there are no thermal transitions or reactions, the power differential between systems would be approximately constant, but during a thermal transition or reaction, the specific heat of the sample under investigation would change and so the power differential would change. A signal proportional to differential power is transmitted to a recording system, giving a curve of differential power versus time or temperature, thus thermal transitions can be found.

A recent review that gives more information on DSC techniques and other thermal analysis techniques is given by Turi (72).

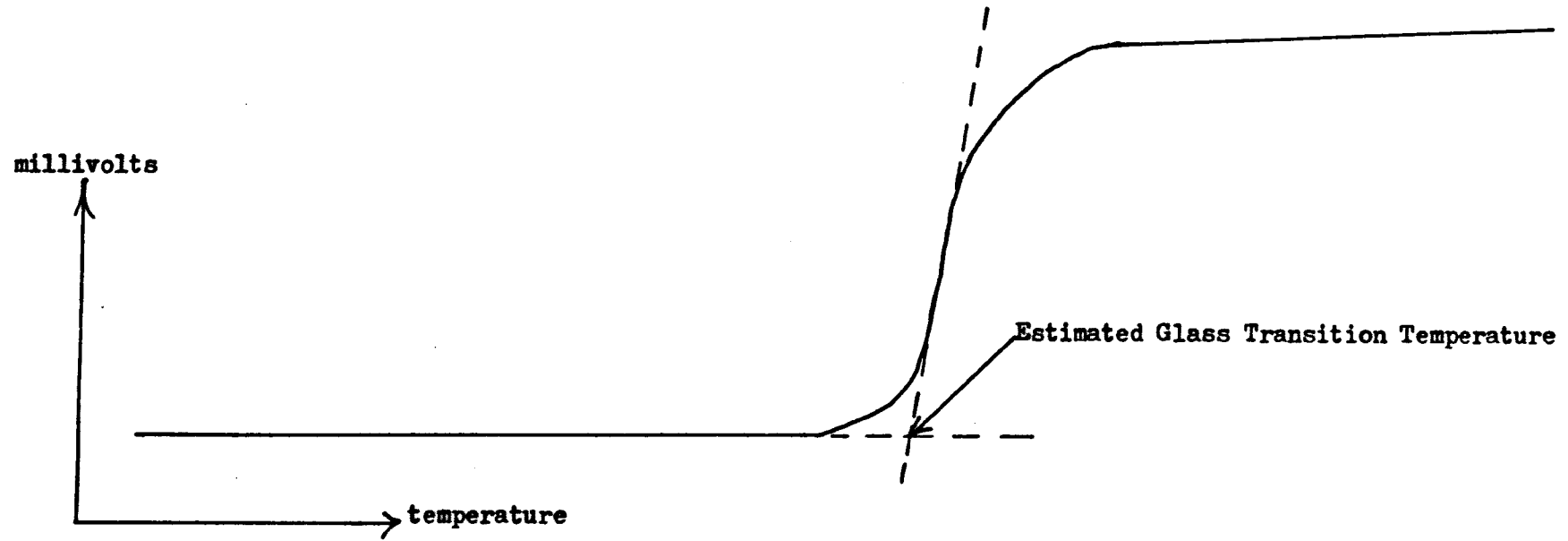
During this work, the instrument used was a Perkin-Elmer DSC-2C which was linked to a Bryan X-7 recorder, this system being used to collect information that would allow the determination of glass transition temperatures.

The samples used were of the order of 10 mg in weight and were encapsulated in an aluminium sample container by methods described in the manual (73).

A typical trace from a DSC run is given in figure 4.7. The  $T_g$  was determined by extending the initial base line and then drawing a line to the base line that corresponded to the maximum slope of the trace at the

FIG.4.7

A Typical DSC. Trace

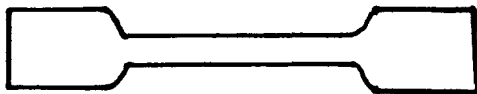


transition. The intersection of the lines was denoted as the glass transition temperature.

#### 4.7 Stress/Strain Relations

Stress/strain measurements were made with an Instron Tensile Tester (model TM-SM). Standard dumb-bell shaped samples for stress/strain measurements were stamped from a cast film. The sample itself (figure 48) was considered to have the dimensions, length 30 mm, breadth 4 mm; these were the dimensions of the central section of the dumb-bell shaped sample. The thickness of each sample investigated was measured using a micrometer.

Figure 4.8



The samples were individually clamped between a fixed load cell and a crosshead which could be lowered at a constant rate, so applying strain to the sample being investigated. Changes in stress in the sample during extension at a constant rate or with time at a fixed extension are detected by the load cell and recorded. In the former case all the features of a stress/strain test including initial modulus, yield stress, ultimate tensile stress and elongation at break could be observed.

For the hard, brittle polymers (CL3 and CL6) the crosshead speed was 0.5 cm/min and the chart speed was 20 cm/min. For the soft, rubbery polymers (CL1, CL2 and CL4) the crosshead speed was 5 cm/min and the chart speed was 2 cm/min, but the chart speed was changed for the stress relaxation and initial modulus experiments to 100 cm/min.

The copolymer denoted CL5 could not be investigated, because it was too brittle to stamp a sample cut from a cast film.

#### 4.8 Results and Discussion

##### 4.8.1 Macroscopic Observations

All the copolymers produced were opaque and depending on the Tg's of the components, the copolymers had a tacky, rubbery texture. All three acrylate copolymers had this tacky texture; this being most prevalent in the n-Butylacrylate copolymer, CL2, then the ethylacrylate copolymer, CL1, and finally the methylacrylate copolymer, PST-MA1.

The n-Butyl methacrylate copolymers (CL3, CL5, CL6) were hard, brittle and showed no signs of a rubbery texture. It was noted that on warming the samples between one's fingers, the samples would soften a little.

When in cast form all the copolymers were semi-opaque and this appeared to be due to macroscopic phase separation of the homopolymer and copolymer in the samples.

The acrylate copolymers showed a change in texture in the cast film, between the upper and lower surfaces of the film. The upper surface being smooth to the touch, while the lower surface was very tacky, again this seemed to indicate macroscopic phase separation and that during casting the unreacted homopolymer (polystyrene - hard, brittle) partially phase separated from the copolymer, forming a layer on the top of the film.

The n-Butylmethacrylate copolymer films were brittle and in some cases the films were difficult to handle, as they would shatter on cutting samples for the Rheovibron and Instron equipment. Phase separation was again evident and in these samples, spheres and lamellar type structures could be seen with the naked eye, where phase separation between homopolymer and copolymer had occurred. A number of the samples cast into films showed on closer examination a domain type structure on the surface of the film, this being a visual manifestation of the Bérnard effect (74).

#### 4.8.1.1 Bérnard Effect

The Bérnard effect arises during the evaporation of

shallow layers of solvent. Cooling of the surface due to evaporation or possibly a concentration gradient within the layer, initiate the formation of large cells containing ordered convection currents within the layer. This effect is not recent and was described by Bérnard and studied by Lord Rayleigh (75) at the beginning of the twentieth century.

#### 4.8.2 Phase Separation

It would seem from the texture, 'feel' and optical nature of the copolymer blends synthesised by methods described earlier, that there is evidence of gross phase separation of the homopolymer residue from the copolymer. Information from infrared spectroscopy and the Rheovibron would be of use with respect to phase separation during casting, this being especially evident with the acrylate copolymers.

As already described, the acrylate films were opaque and showed phase separation between the components of the blend by the difference in the upper and lower surfaces of the cast film. These differences in composition of the components at the surfaces were established by internal reflection infrared spectroscopy (76).

##### 4.8.2.1 Internal Reflection Infrared Spectroscopy

When a beam of radiation enters a prism it can be reflected internally with all the energy being reflected.

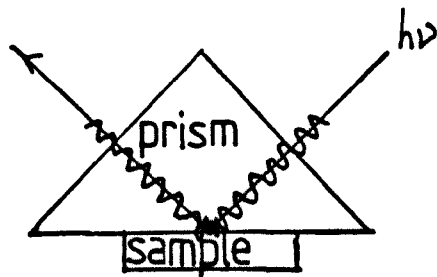
However, the beam appears to penetrate slightly beyond the reflecting surface and then return, as shown in figure 4.9a.

When a material which selectively absorbs radiation, is placed in contact with the reflecting surface, the beam will lose energy because the material will absorb energy at specific wavelengths. By using a spectrophotometer, it becomes possible to get an absorption spectrum for the material.

The depth to which the radiation penetrates is a function of (1) wavelength, (2) the refractive index of both reflector and sample and (3) the angle of incident radiation. To obtain a spectrum of sufficient quality for analysis the incident beam must be internally reflected a number of times. To do this, the beam is passed through a special crystal with sample placed on both sides of the crystal (see figure 4.9b). This spectroscopic technique was used to look at the surface composition of polymer films, as the films can be placed on both sides of the crystal easily.

During the course of this work the spectrometer used was a Perkin-Elmer 257 Grating Infrared Spectrometer with a Beckmann TR-25 internal reflective optical system (see figure 4.10). The crystal used was a type KRS-5 crystal, a Thallium bromide-iodide composite.

FIG. 4.9a



Internal Reflection Effect

FIG. 4.9b

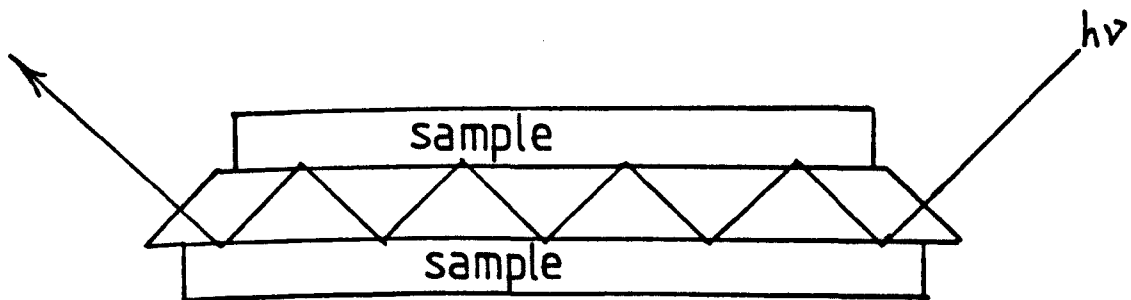
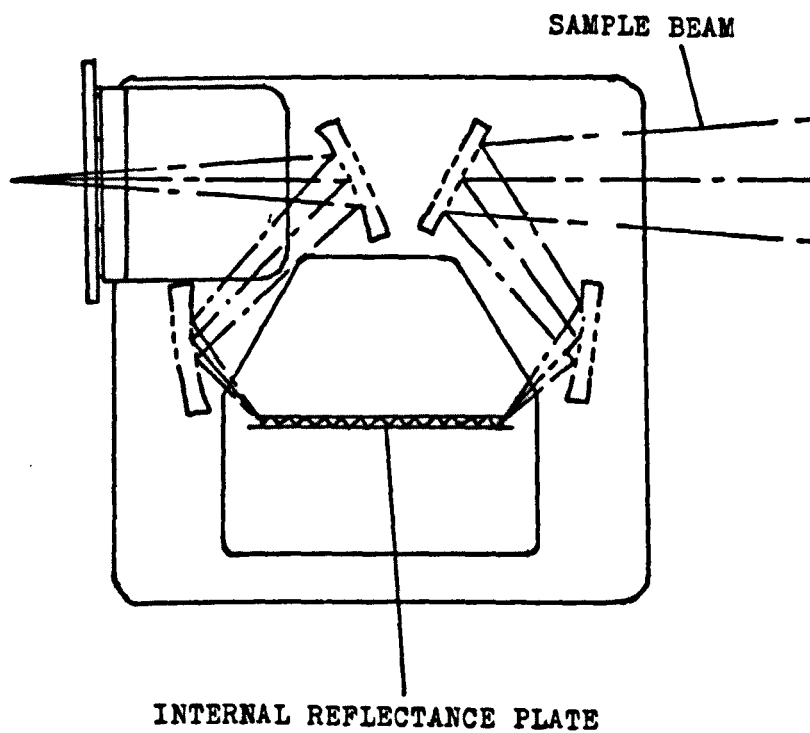
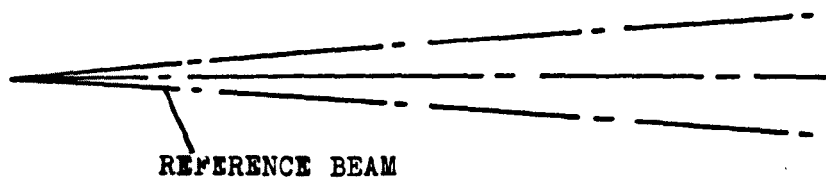




FIG. 4.10



The copolymer CL1 consisting of polystyrene and poly (ethylacrylate) was subjected to this physical technique of analysis. By careful cutting and placing, the film side being analysed would be known, ie, top or bottom surface of the cast film. Figures 4-11 a, b, c show the infrared spectra for polystyrene, the top of the cast film and the bottom of the cast film, respectively. It can be seen from figures 4.11 b, c that the compositions of the top and bottom surfaces of the film are not the same, showing that the film did not have a uniform composition. Figure 4.11 a shows polystyrene with C-H bond stretch responses between 2840-2960 wave numbers ( $\text{cm}^{-1}$ ); the responses at 3010 and 3060  $\text{cm}^{-1}$  correspond to the C-H stretch modes from the aromatic ring of the styrene. The medium response at 1480  $\text{cm}^{-1}$  will be due to the  $-\text{CH}_2-$  group, while the response at 1600  $\text{cm}^{-1}$  corresponds to the  $-\text{C}=\text{C}-$  group stretching frequency of the aromatic ring. In figures 4.11 b, c there are new peaks in the spectra relating to the acrylate component of the copolymer, the most noticeable additions being the strong absorption at 1730  $\text{cm}^{-1}$  which is characteristic of the  $\text{C}=\text{O}$  group stretch and the medium absorptions at 1450 and 1380  $\text{cm}^{-1}$ , corresponding to  $-\text{CH}_3$  bend. The absorption characteristics for the  $-\text{C}-\text{O}-$  ester stretch occurs in the region 1300-1000  $\text{cm}^{-1}$ .

By comparing spectra, figures 4.11 b, c with figure 4.11 a, which is for homopolystyrene it can be seen that figure 4.11 b resembles the polystyrene spectrum more closely, which shows that there is more polystyrene at the

FIG. 4.11a

Polystyrene Sample

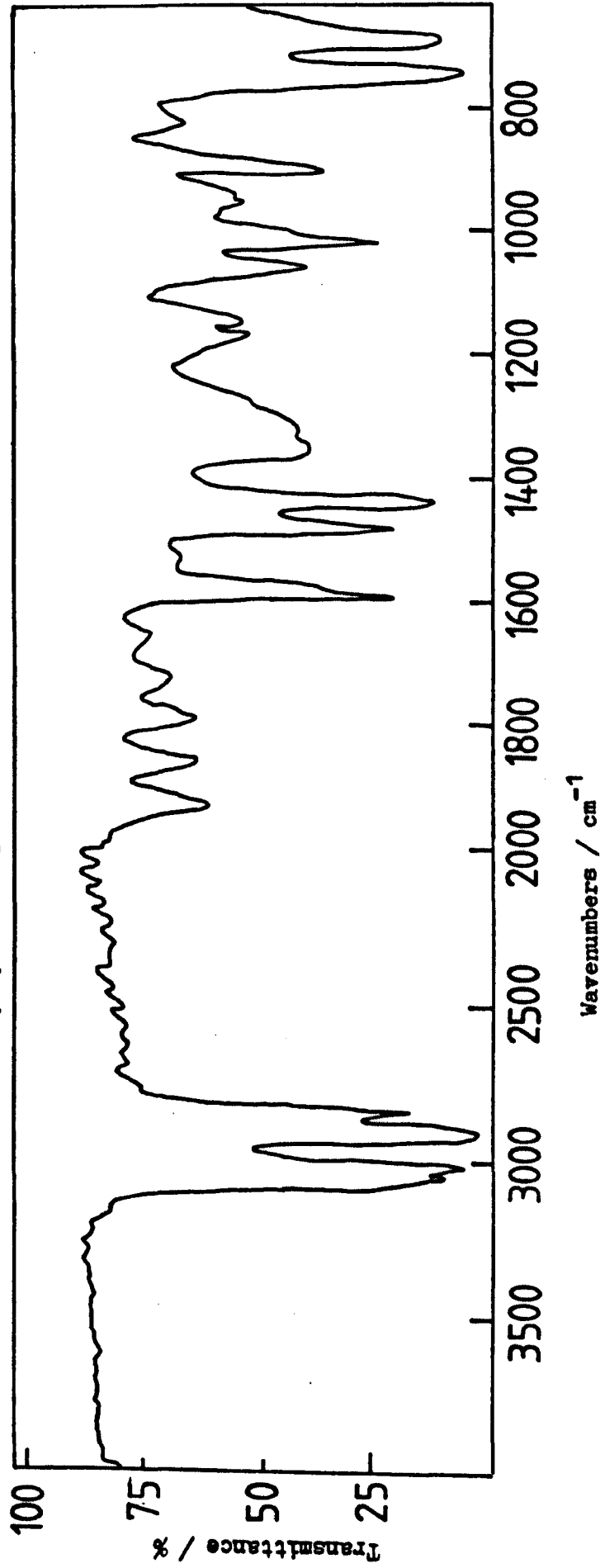


FIG.4.11b

Poly(Styrene-Ethylacrylate)(CL1):- top surface

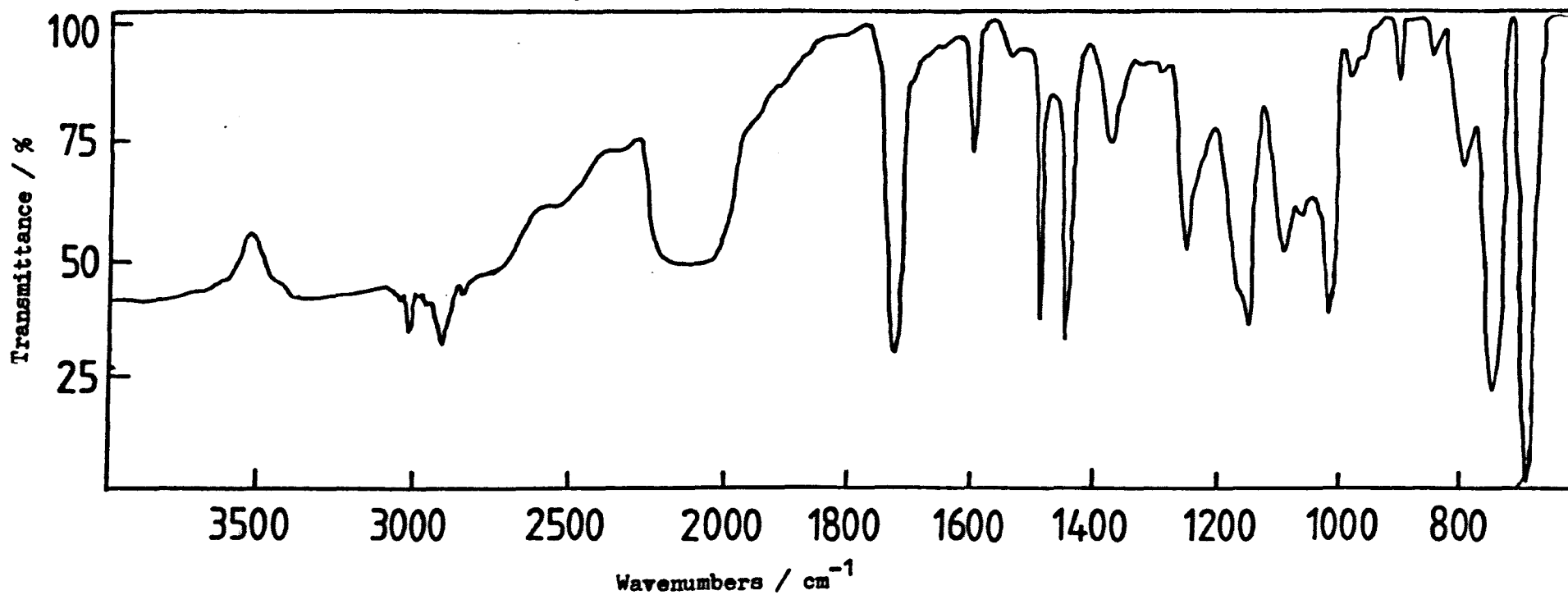
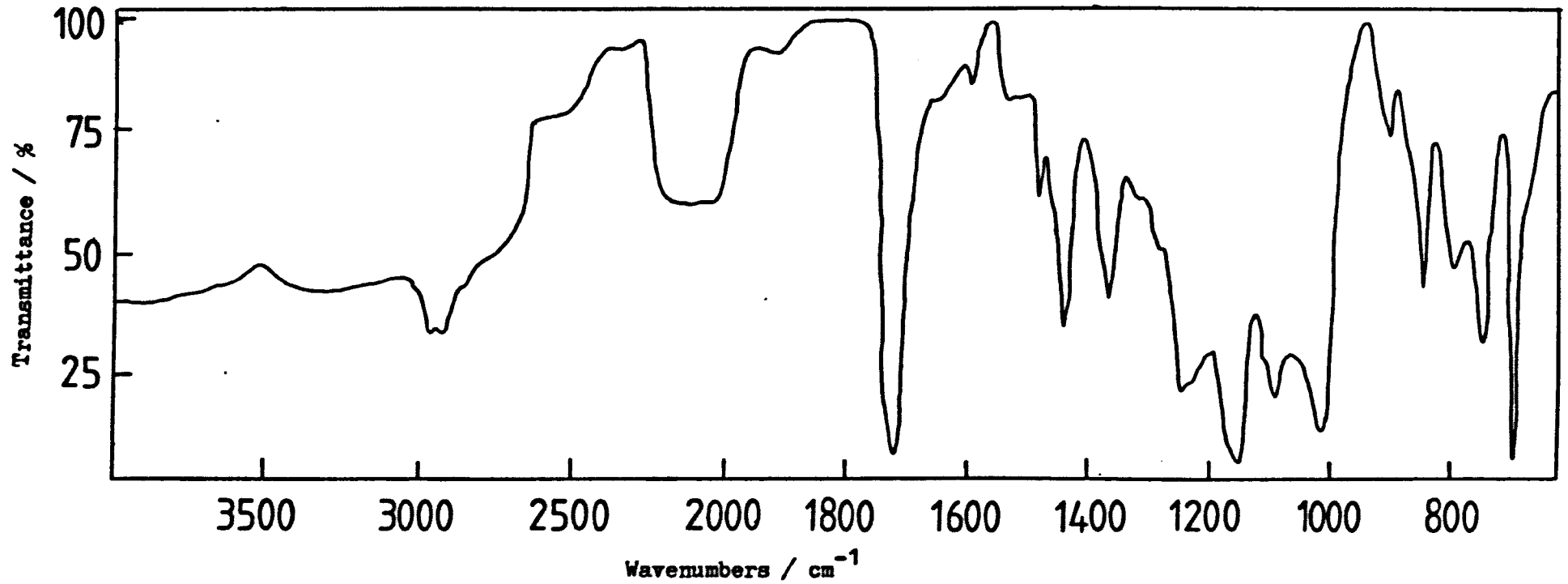


FIG. 4.11c

Poly(Styrene-Ethylacrylate)(CL1):- bottom surface



top surface than the bottom surface, ie, we have a copolymer rich bottom surface with a polystyrene rich top surface.

#### 4.8.2.2 Rheovibron Data

On examination of the Rheovibron data for the acrylate copolymer films (figures 4.12, 4.15-4.22), it can be seen that the  $E''$  plot shows signs of a double maxima, as opposed to a maximum for a normal  $T_g$ . The lower temperature maximum showed shifts on the temperature axis, when different samples were tested and were subjected to re-examination, while the second higher-temperature maximum remained constant throughout the testing of all samples (figure 4.12). We attribute the occurrence of the double maxima to the formation of a film sample that has a laminate structure as in figure 4.13a. The lower-temperature maximum being due to a thin layer of homopolystyrene, that has phase separated from the copolymer during casting; while the second higher-temperature maximum is due to the acrylate component of the copolymer. The thin homopolystyrene layer would be transparent and so not be observed visually.

An observation supporting the laminate structure in the cast film, was that samples denoted CL1, CL2 and CL4 all showed crazing on the upper surface after they had undergone Rheovibron experiments (see figure 4.13b); the direction of the crazing being perpendicular to the direction of applied stress.

FIG. 4.12

E'' responses for CL1

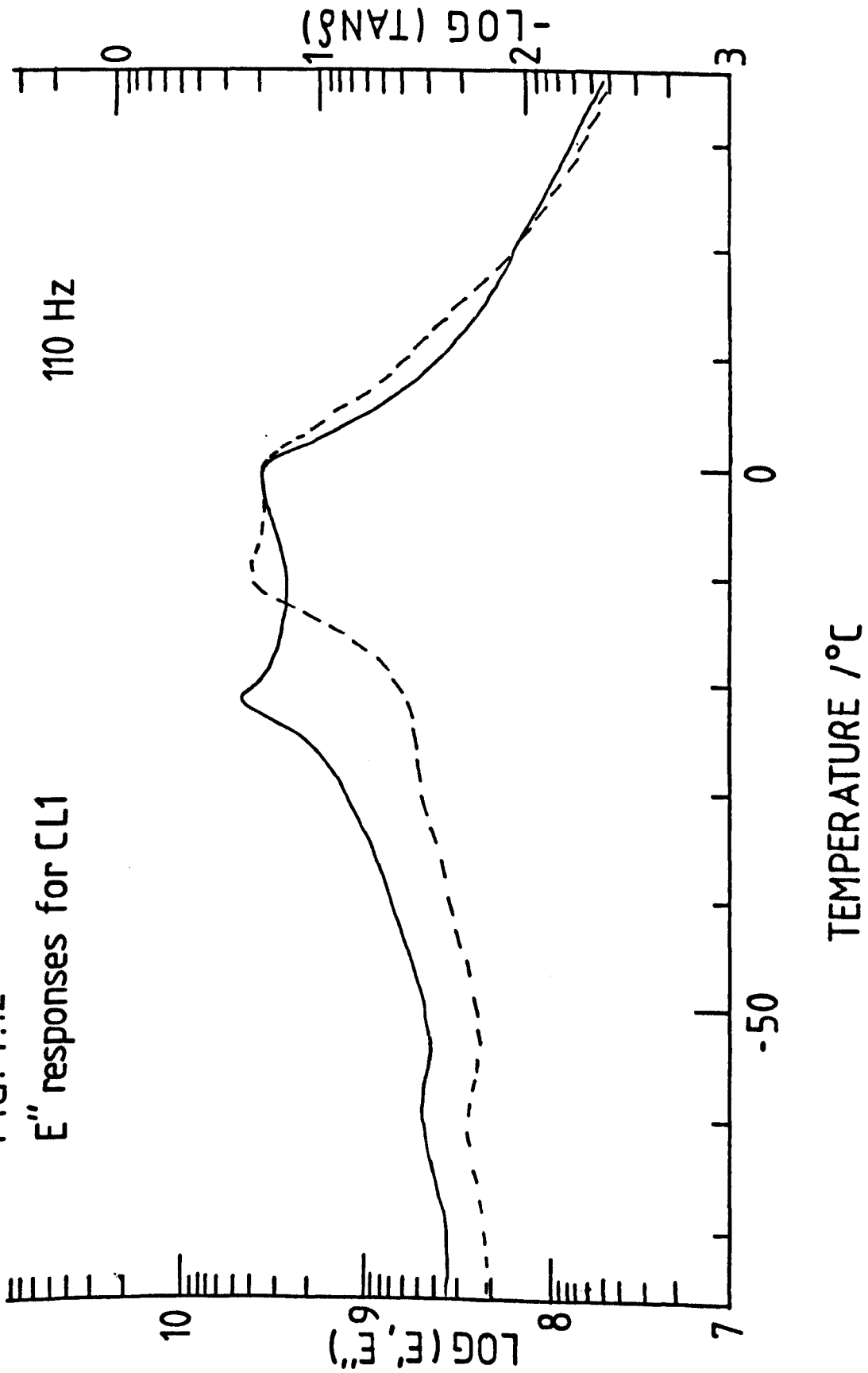
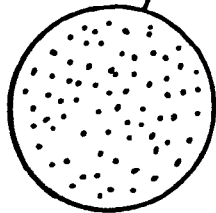
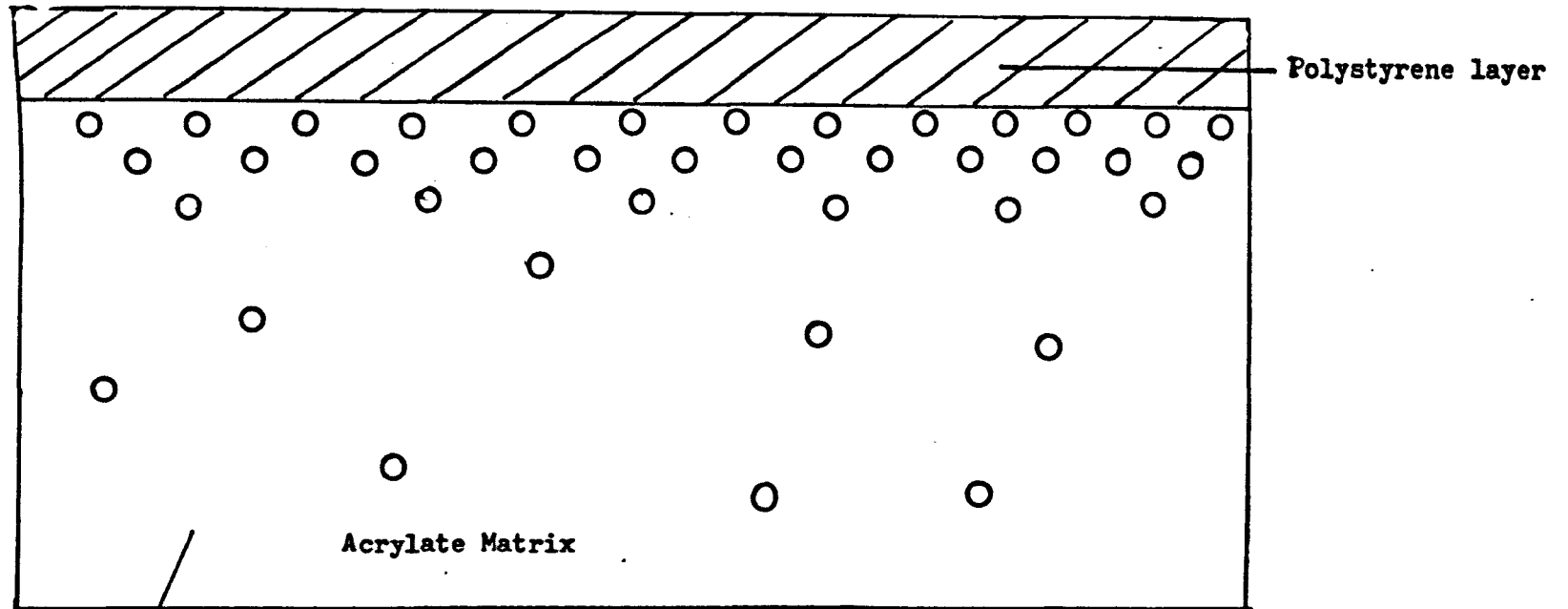


FIG.4.13a

INTERNAL STRUCTURE OF THE LAMINATE FILM



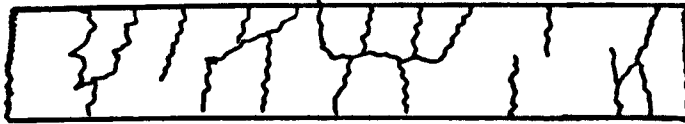
Microphase separation of polystyrene from the poly(acrylate)



Droplets of homopolystyrene that have phase separated from the copolymer



Figure 4.13b



The crazing of the top polystyrene layer showing up in the Rheovibron experiments as the first lower-temperature maximum in the  $E''$  plot. The crazing would occur in the homopolystyrene layer, as the sample temperature approaches the  $T_g$  of the copolymer's acrylate component, because the softened copolymer would no longer support the thin homopolystyrene layer, thus cracking when stress is applied. On subsequent re-test of samples or tests on new samples, the crazing would occur at slightly different temperatures, due to local variance in layer thickness and so the first maxima in  $E''$  spectra would move as observed.

#### 4.8.2.3 Discussion

It is appropriate at this point to discuss the phase separation of homopolymers and copolymers in relation to the findings of this study and the recent findings of other workers. In a block copolymer-homopolymer system, homopolymer may be soluble in the domains of the like component of the block copolymer. Several groups have presented experimental data concerning the solubilization of homopolymers by block copolymers (2, 4, 77-84). All agree that the quantity of homopolymer that can be solubilized by a block copolymer is dependant on the ratio  $M_H/M_A$ , the molecular weight of the homopolymer  $M_H$  to that of the

similar block of the block copolymer  $M_A$ . If appreciable quantities of homopolymer are to be solubilized,  $M_H/M_A$  must be less than one. The amount of homopolymer solubilized decreases rapidly as the value of the ratio  $M_H/M_A$  increases above 1. Meier (77) put forward a theory for the solubilization of homopolymer in the block copolymer that did not agree with experimental data available at that time, but did provide a reasonable explanation for the discrepancies between theory and experimental.

Meier's calculations related specifically to block copolymers plus homopolymer chemically identical with one of the blocks. He concluded that the solubility of homopolymer in copolymer is often limited and is dependent on the ratio  $M_H/M_A$ . If the homopolymer molecular weight is equal to or less than that of the block, equal volume fractions of homopolymer may be miscible with like blocks in the copolymer. For equal molecular weights as little as 5 per cent (V/V) of homopolymer would be miscible in the copolymer. Meier's theoretical calculations for the amount of miscibility of homopolymer in copolymer were found to be lower than those calculated experimentally. Meier concluded that the systems experimentally studied had not reached equilibrium when measurements were taken.

Experimentally Riess et al (78) and Jiang (79) found that homopolymer chains could be solubilized into block domains of the same type providing that the molecular weight of the former was the same as or less than the latter.

Jiang (80) also found that block copolymers with the same composition and sequence structure but with different molecular weight were incompatible and concluded that this was due to entropy effects. He also suggested that the sequence structure may play a part in determining whether a homopolymer will be miscible in a copolymer. Roe et al (81) also found a similar trend and suggested that the main driving force involved in de-mixing was the loss of entropy.

Eastmond et al (82), while studying multicomponent polymers of the AB crosslinked type found unusual features, characterized by the presence of discrete macroscopic domains with internal structures different from the matrix and were always present in slowly cast films. From studies on these polymers, Eastmond concluded that the homopolymers could not be solubilized in domains of the corresponding blocks, even when they have the same molecular weight. This conclusion found support from Meier's theoretical results.

Recently Eastmond and Muccianiello (83) presented a phenomenological approach to the miscibility of homopolymer in copolymer, in an attempt to provide an insight to the problem at a molecular level. In this approach they considered the entropy changes that occur when free homopolymer is mixed with bound polymer (in their work, the polymer was bound to glass beads). Where the number of attached chains per unit area at the interface is high,

the situation is comparable to that in block copolymer domains. They concluded that the highest overall entropy is achieved when the bound and free chains are immiscible with each other at equilibrium and that the immiscibility is entropy driven.

Recently, de Gennes (84) undertook some theoretical calculations that considered the influence of density of graft sites on the stretching of grafts and the volume fractions of grafts close to an impenetrable surface on the solubility of homopolymer with grafts. He concluded that under various conditions, particularly when the number of attached chains per unit area of the interface is high, bound polymer chains are immiscible with free homopolymer chains.

From the observations noted during the course of this present study and from the theoretical and phenomenological arguments put forward by others, it would seem that the copolymer blends studied have shown phase separation of homopolymer and copolymer, so justifying Eastmond's conceptual ideas. This phase separation would possibly give rise to ways of purifying the copolymer (separating the homopolymer from copolymer), by using the fact that they form two phases. To purify the copolymer in this way, it is envisaged that it would require the use of a good solvent for all the components and controlled evaporation of solvent to give phase separation at a critical concentration of component, this slow evaporation would probably take

a considerable amount of time.

#### 4.8.3 Copolymer Purification

The purification of the copolymers was attempted by the use of the phase separation of homopolymer and copolymer as described in the previous section. Dichloromethane was used as the solvent. These attempts proved unsuccessful in the time allowed, because it was difficult to impart a slow rate of evaporation, but it was evident from these early tests that the separations would require a considerable amount of time to be effective, probably weeks or even months.

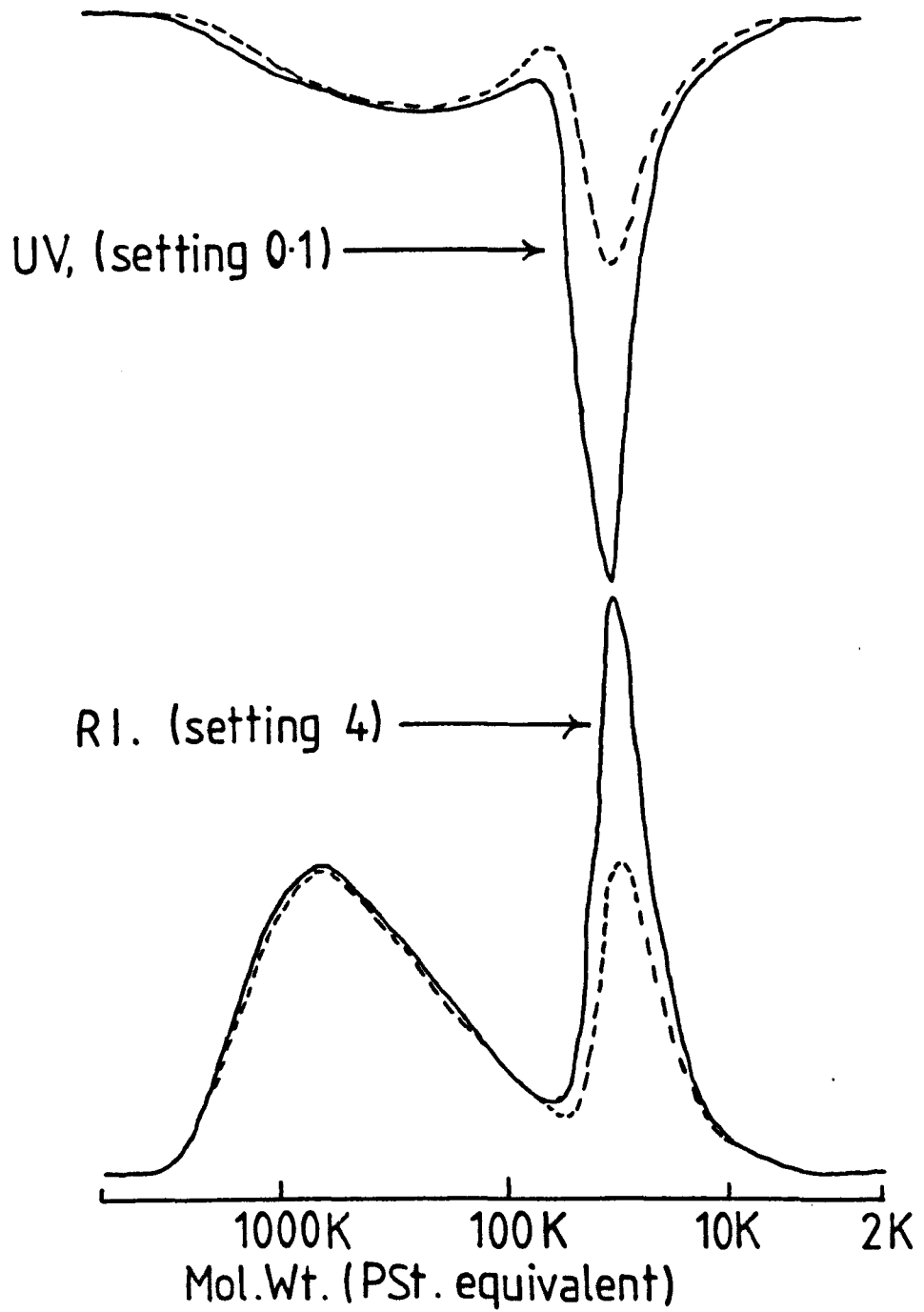
Attempts were made to remove the homopolymer by adding high molecular weight polystyrene and then extracting the polystyrene with acetone, the hope being that the homopolymer would be 'dragged' out of solution with the higher molecular weight polystyrene. This method did not work very well.

Attempts were made using selective solvents to purify the copolymers. Here the problem was that with the polymers involved, the components had similar solvents and non-solvents, except for acetone, which is a non-solvent for high molecular weight polystyrene, but a good solvent for the acrylate component of the copolymer.

The copolymer blends were dissolved in acetone and then centrifuged at 6000 rpm for approximately 10 minutes, to allow the homopolymer residue to separate out for the dissolved copolymer. Centrifuging was required because the homopolystyrene forms a very fine dispersion in the acetone and cannot be filtered off using conventional filters. Verification of the removal of homopolymer can be gained from comparing the ri and uv chromatograms (GPC) (figure 4.14) of the products before and after the purification procedure. The first solid line chromatogram corresponds to the unpurified copolymer blend, while the second broken line chromatogram represents the copolymer blend after purification. As can be seen the second chromatogram has less of the low molecular weight homopolystyrene. When cooled to Cardice temperatures ( $-78^{\circ}\text{C}$ ), the acetone solution became cloudy showing that at ambient temperatures acetone was only acting as a partial non-solvent. It was not possible to centrifuge at low temperatures and so this method for purification was not totally successful.

Any homopolystyrene contaminant remaining must have evaded separation by being either soluble in the solvent or miscible with the like components of the copolymer. Use of the uv chromatograms in figure 4.14 would allow an estimate of the upper limit of the miscibility of the homopolystyrene in the copolymer. The uv chromatograms only show the polystyrene content of the sample at the detector settings used ( $\lambda = 260\text{ nm}$ ), so the proportion of homopolystyrene to the polystyrene component of the

FIG. 4.14  
Copolymer CL2



copolymer can be found. By using the areas under the peaks, it was possible to deduce that the upper limit of miscibility of homopolymer in the copolymer when the polystyrene chains have identical molecular weight is 66% (V/V). This value can only be an estimate as it is known that some of the homopolystyrene was present in the sample, because of some solubility in the acetone. It is also likely that the system had not reached equilibrium during the purification process and so would more likely give higher miscibility values than those calculated by Meier.

#### 4.8.4 Glass Transition Temperatures (T<sub>g</sub>)

Glass transition temperatures were determined using the Rheovibron, the D.S.C., and the dielectric equipment. Each method involved in determining T<sub>g</sub> measures a different physical property, so it is not unexpected that the values gained for T<sub>g</sub> differ slightly between experimental techniques.

All the polymers studied with the Rheovibron were investigated at three frequencies, viz 110 Hz and 11 Hz and 3.5 Hz. The data from each polymer sample run was compiled by the computer, and displayed visually as a plot of E', E'' and  $\tan \delta$  against temperature. Figures 4.15-4.22 show the graphs for the copolymers studied; on each, E', E'' and  $\tan \delta$  curves are marked.



Figures 4.15-4.18 show the results from the copolymers denoted CL1, CL2, CL4 and PST-MA1 respectively, and show a double maxima in the  $E''$  trace near the  $T_g$  in each case, the significance of this being discussed earlier. This double maxima occurred in all Rheovibron studies of the acrylate copolymers, but at low frequencies of oscillation (3.5 Hz) these phenomena were less prominent, as shown in figure 4.19. These figures also show that the double maxima in  $E''$ , is to some extent also observed in  $\tan \delta$ . The modulus denoted by  $E'$  shows little variance in mechanical strength up to the region of the  $T_g$ , where it falls sharply as the polymer softens and enters the plastic region. At approximately  $-58^\circ\text{C}$  and  $-18^\circ\text{C}$  in the figures 4.15 and 4.18 respectively, there are possible signs of weak transitions that can just be observed in the  $E''$  and  $\tan \delta$  plots.

Figures 4.20-4.22 show the graphs for three different copolymers that have n-Butylmethacrylate as the B component. These graphs show only one broad transition in both the  $E''$  and  $\tan \delta$  plots. The  $E'$  trace in both cases did not show a sharp decrease in modulus; a reduction in modulus of 100 fold took approximately 50 degrees to occur. These broad transitions would indicate that these copolymers do not have total phase separation or that large amounts of homopolymer are solubilised in the copolymers, giving broader and shifted transitions, which are detected by the Rheovibron.

Measurements for the determination of  $T_g$  were taken from the loss modulus,  $E''$  maxima and the  $\tan \delta$  maxima. These values are given in table 4.2. It would be expected that the copolymers would have two  $T_g$ 's, one from each component of the copolymers studied. Only one  $T_g$  could be determined for the copolymers, because the samples became flexible and rubbery above the first  $T_g$ . At temperatures approaching the expected second higher  $T_g$ , the samples were found to be so flexible as to go beyond the measuring limits of the Rheovibron, because the sample would relax too quickly when strain was applied for the Rheovibron to make a measurement. Attempts were made to prepare samples with a glass fibre support by methods described by Cowie (85), so as to give enough strength to the sample for the second  $T_g$  to be determined from the  $\tan \delta$  curve, but these supported samples proved unsuccessful.

D.S.C. measurements were made for each of the copolymers synthesized and for the different homopolymers and prepolymers used. The copolymer CL2, poly(styrene-*n*-Butylacrylate) and the homopolymer *n*-Butylacrylate have not been investigated at low temperatures for their respective  $T_g$ 's, as the cooling system used in conjunction with the D.S.C. instrument could not attain the required temperature to make the relevant measurements. In table 4.3 values determined for the  $T_g$ 's are given.

The results from the dielectric experiments were first collated in the form of a graph of normalised conductance

FIG. 4.15 CL1 Poly(styrene-ethylacrylate)

110 Hz

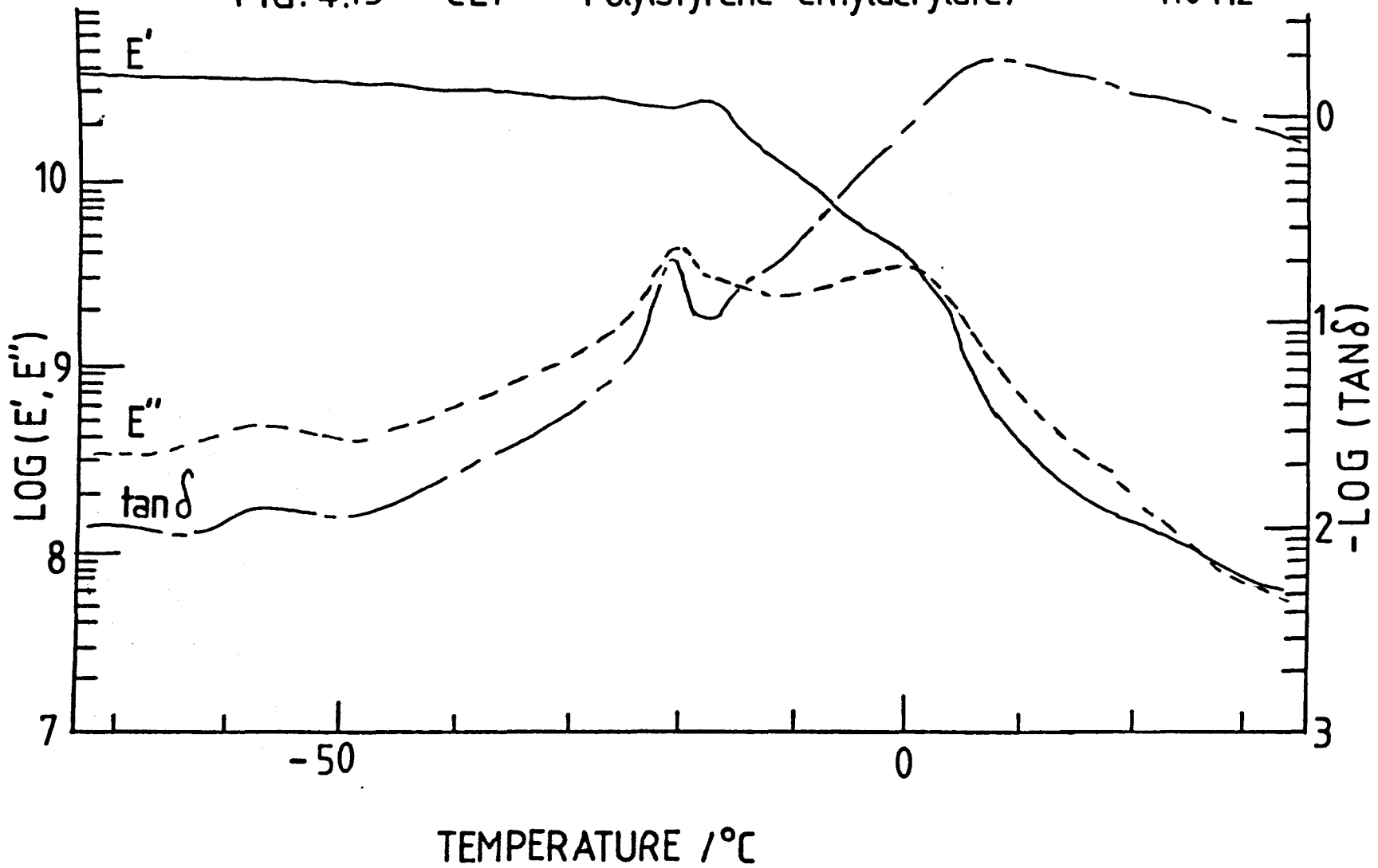


FIG. 4.16

CL2

Poly(styrene-n-butylacrylate)

110 Hz

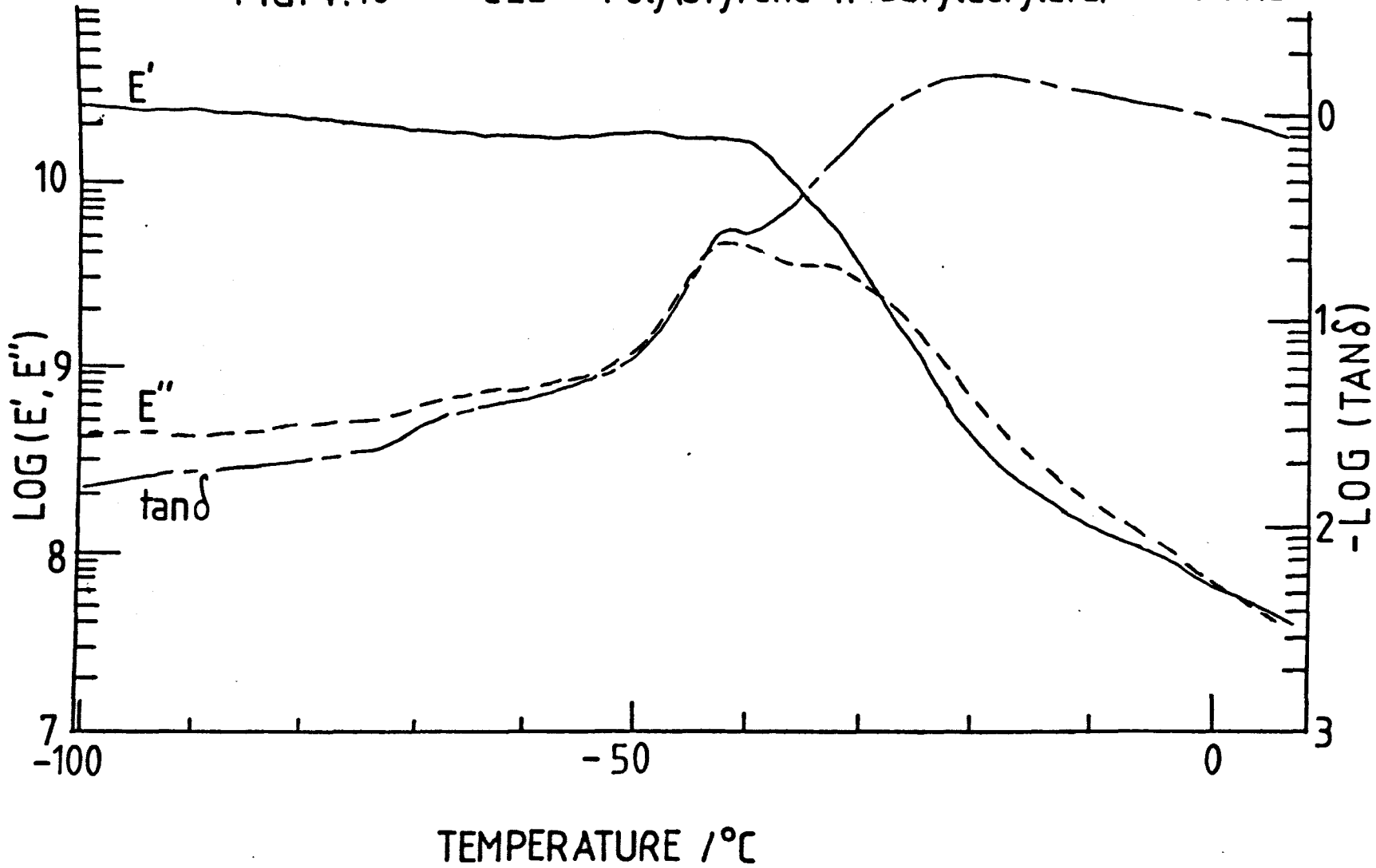


FIG. 4.17 CL4 Poly(styrene-ethylacrylate) 110Hz

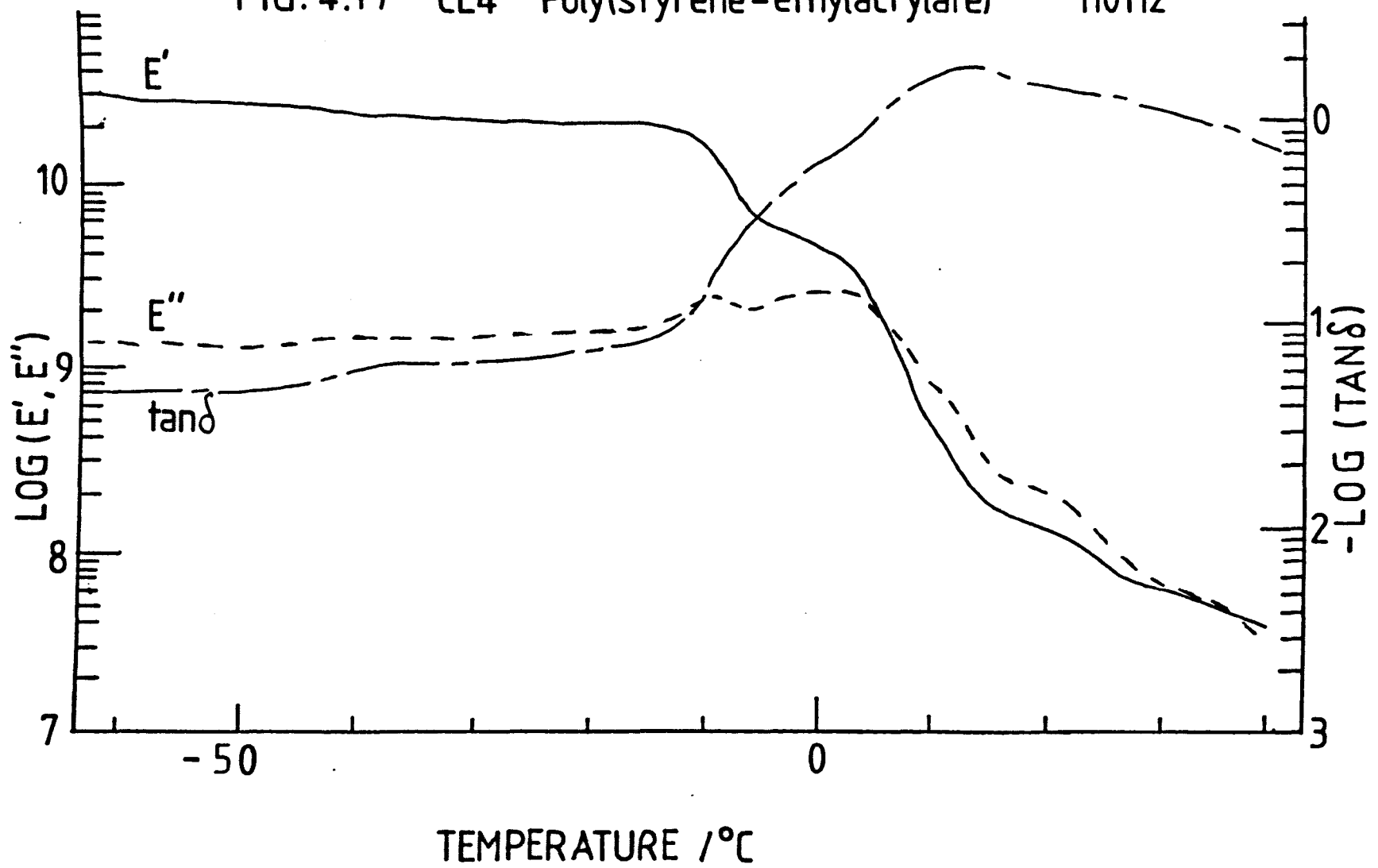


FIG. 4.18 PST-MA1 Poly(styrene-methylacrylate)

110 Hz

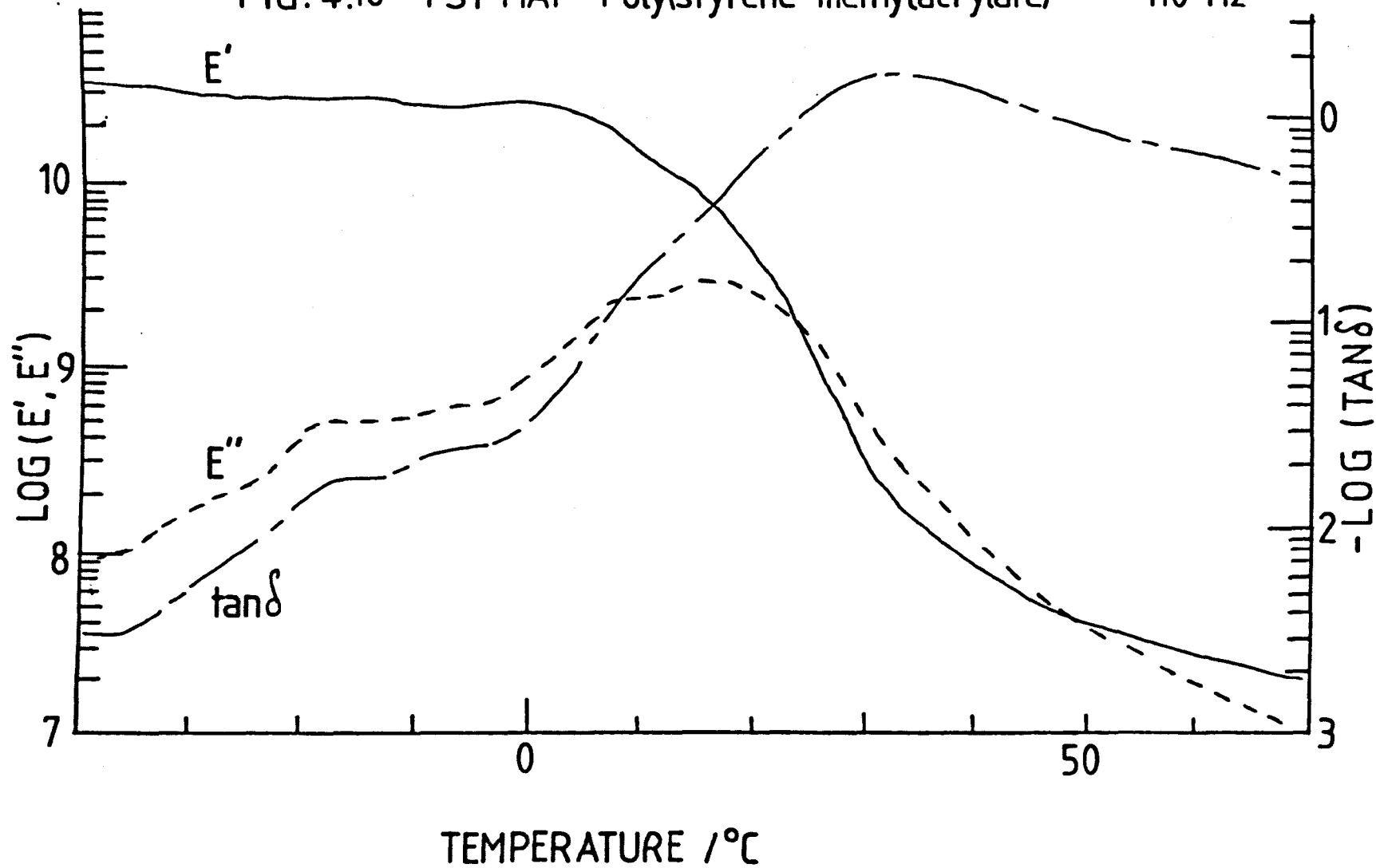


FIG. 4.19 CL1 Poly(styrene-ethylacrylate)

3.5 Hz

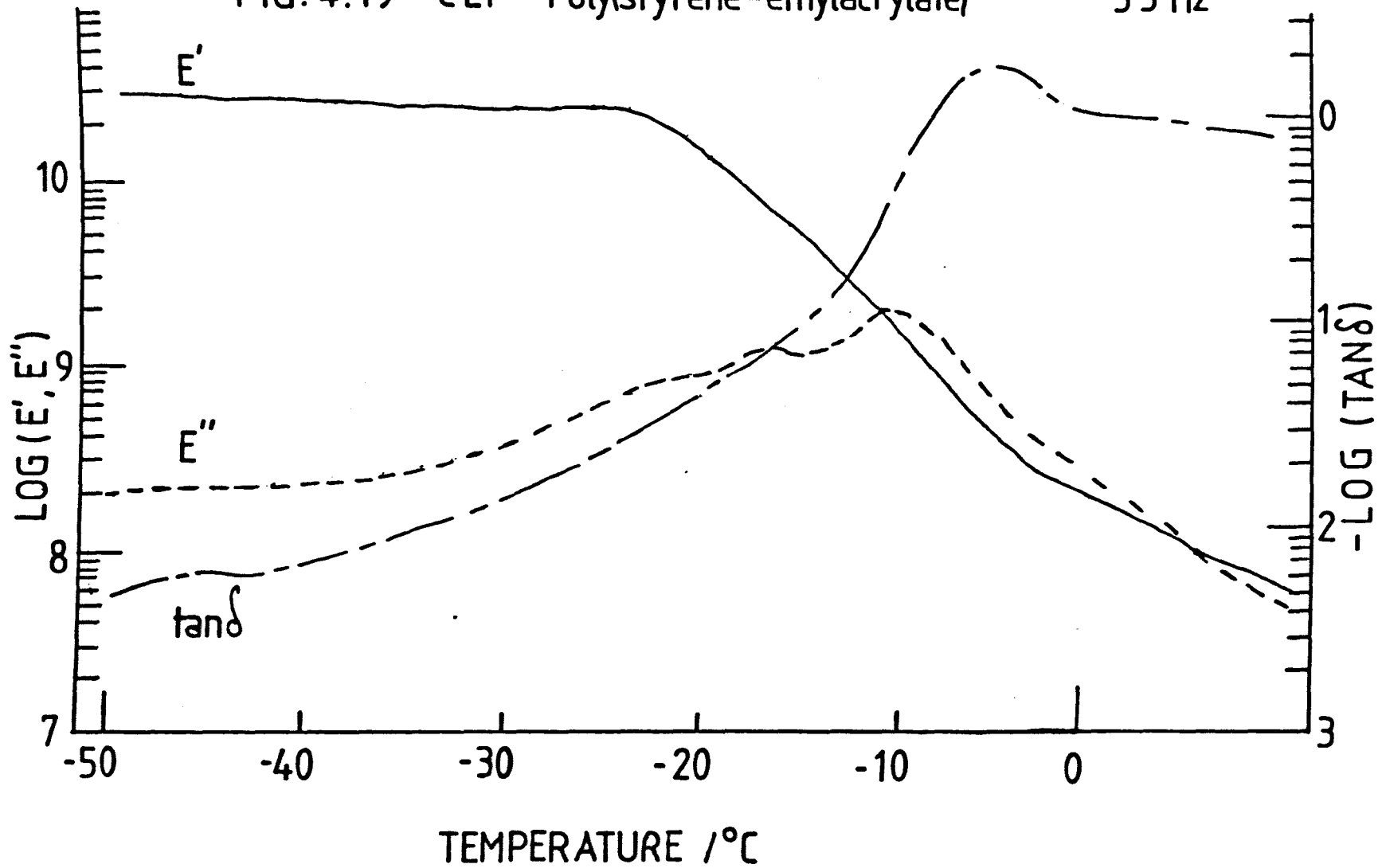


FIG. 4.20 CL3 Poly(styrene-n-butylmethacrylate) 11 Hz

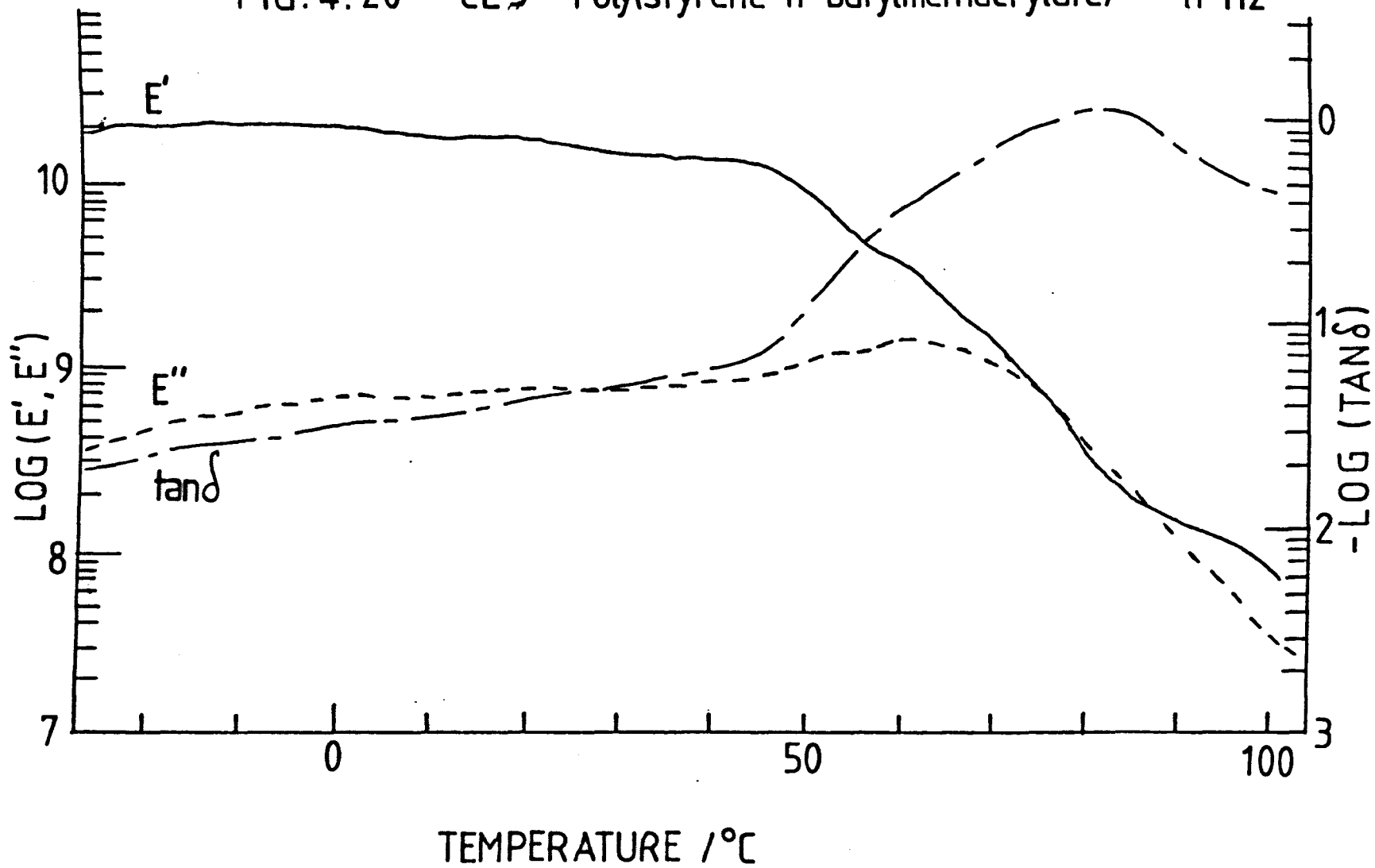




FIG. 4.21 CL5 Poly(styrene-n-butylmethacrylate) 110 Hz

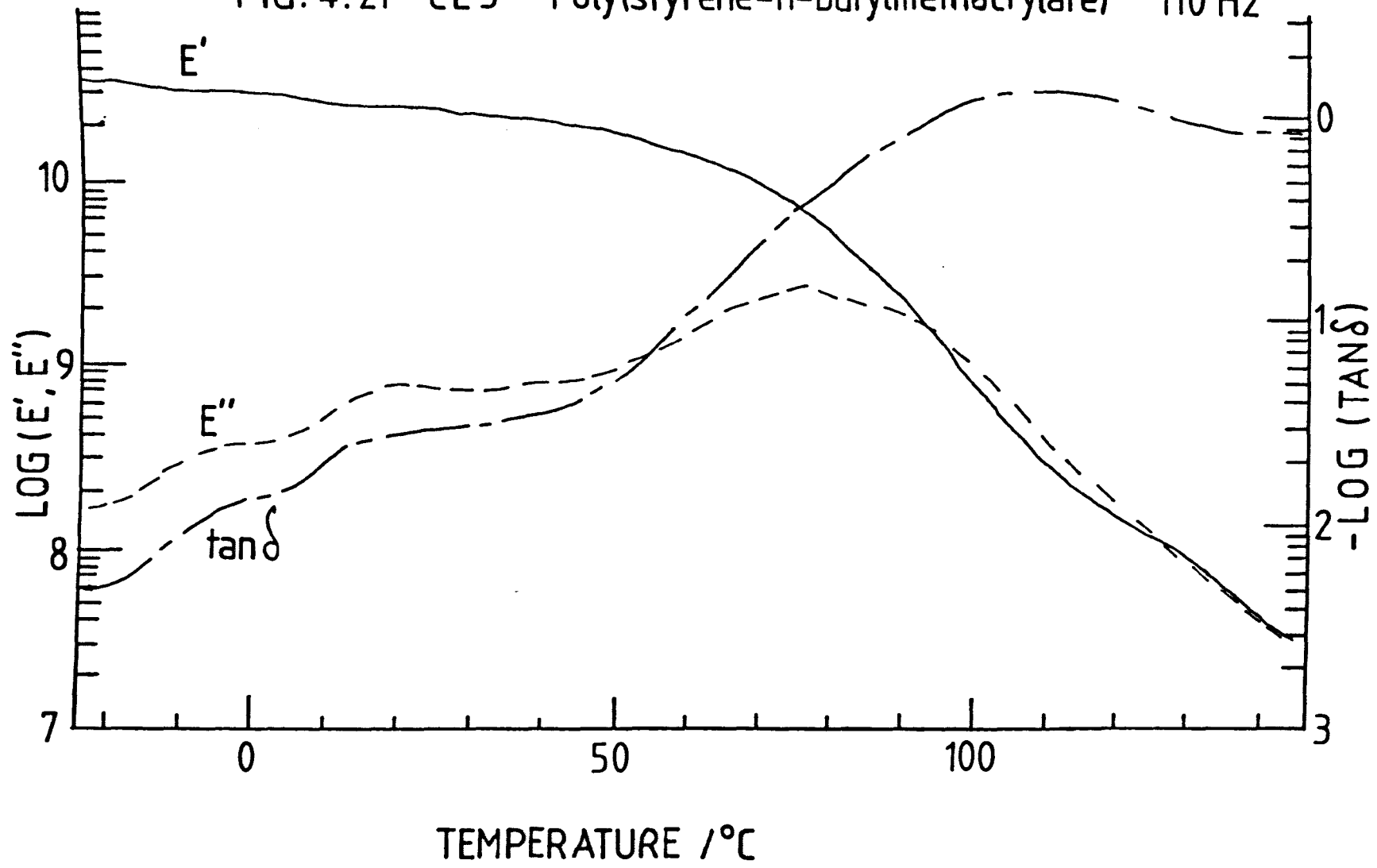


FIG. 4.22 CL6 Poly(styrene-n-butylmethacrylate) 11Hz

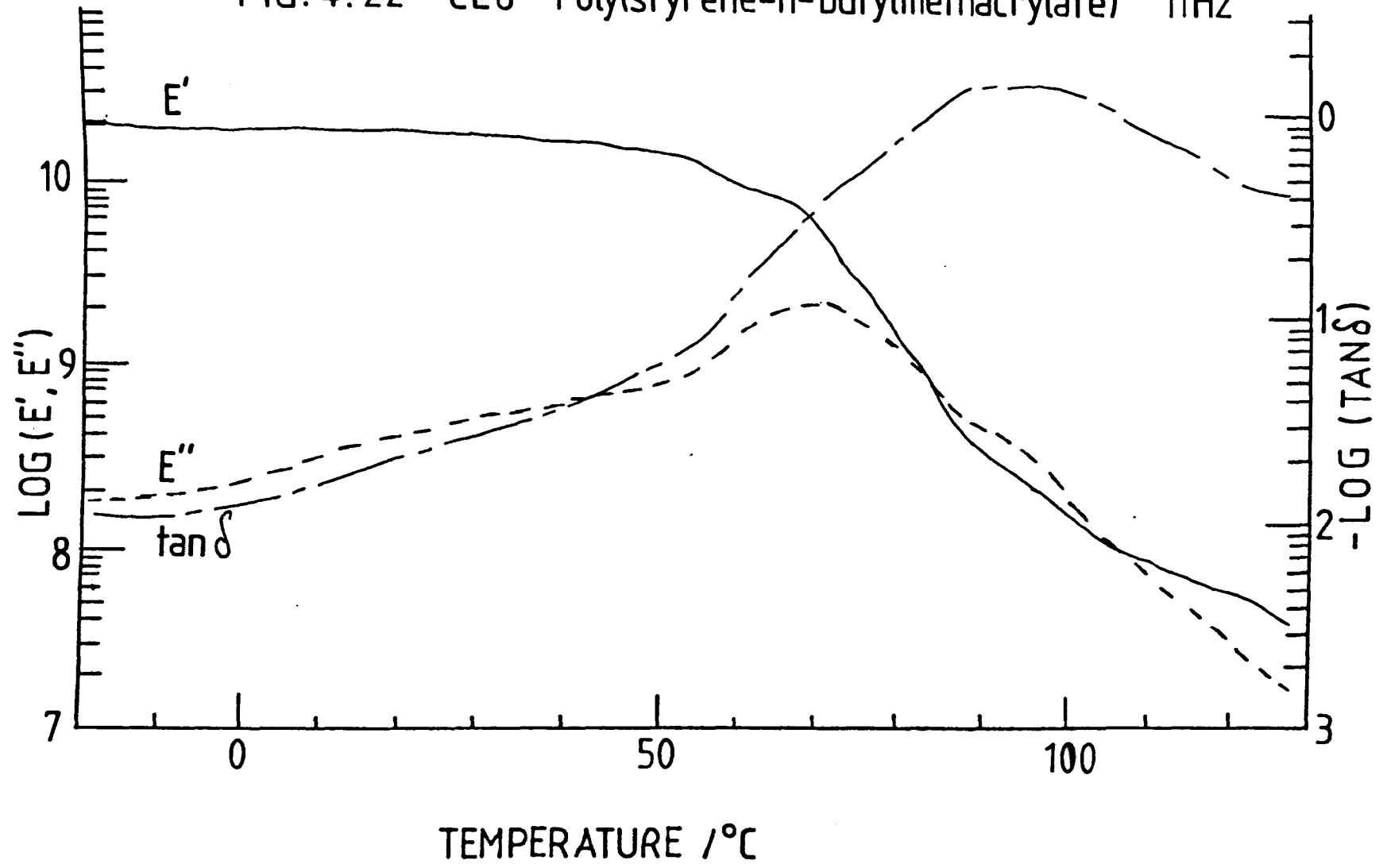


TABLE 4.2

| Sample                                | Frequency/Hz | T <sub>g</sub> /° C from E'' curve | T <sub>g</sub> /° C from tan δ curve |
|---------------------------------------|--------------|------------------------------------|--------------------------------------|
| Poly(styrene-methylacrylate) PST-MA1  | 110          | 13                                 | 34                                   |
|                                       | 11           | 8                                  | 26                                   |
|                                       | 3.5          | 5                                  | 24                                   |
| Poly(styrene-ethylacrylate) CL1       | 110          | 0                                  | 12                                   |
|                                       | 11           | - 5                                | 8                                    |
|                                       | 3.5          | - 10                               | 1                                    |
| Poly(styrene-n-Butylacrylate) CL2     | 110          | - 36                               | - 23                                 |
|                                       | 11           | - 44                               | - 31                                 |
|                                       | 3.5          | - 46                               | - 33                                 |
| Poly(styrene-n-Butylmethacrylate) CL3 | 110          | 68                                 | 105                                  |
|                                       | 11           | 60                                 | 84                                   |
|                                       | 3.5          | 57                                 | 80                                   |
| Poly(styrene-ethylacrylate) CL4       | 110          | 10                                 | 27                                   |
|                                       | 11           | 2                                  | 18                                   |
|                                       | 3.5          | - 2                                | 14                                   |
| Poly(styrene-n-Butylmethacrylate) CL6 | 110          | 74                                 | 126                                  |
|                                       | 11           | 66                                 | 99                                   |
|                                       | 3.5          | 64                                 | 93                                   |

TABLE 4.3

| Sample                         | High Tg |       | Low Tg |        | Literature Values        | Comments                                                                          |
|--------------------------------|---------|-------|--------|--------|--------------------------|-----------------------------------------------------------------------------------|
|                                | in K    | in °C | in K   | in °C  |                          |                                                                                   |
| Polystyrene prepolymer (PERME) | 373.7   | 100.7 | -      | -      | All approximately 100° C | All samples were run on range 0.1 m cal/sec, and at a heating rate of 20 deg/min. |
| Polystyrene prepolymer (S4)    | 375.3   | 102.3 | -      | -      |                          |                                                                                   |
| Polystyrene prepolymer (S6)    | 376     | 103   | -      | -      |                          |                                                                                   |
| Polymethylacrylate             | 279     | 6     | -      | -      | 6                        | The polystyrene prepolymer used in each copolymer is given in brackets.           |
| Polyethylacrylate              | 252.3   | -20.3 | -      | -      | -22                      |                                                                                   |
| Poly n-Butylmethacrylate       | 321     | 48    | -      | -      | 24                       |                                                                                   |
| CL1 (S4)                       | 372.7   | 99.7  | 257.3  | - 15.7 |                          | Copolymer CL2 does not show a lower Tg, because of instrument limitations.        |
| CL2 (S4)                       | 375     | 102   | -      | -      |                          |                                                                                   |
| CL3 (S4)                       | 369.3   | 96.3  | 318    | 45     |                          |                                                                                   |
| CL4 (S6)                       | 374.4   | 101.4 | 254    | - 19   |                          |                                                                                   |
| CL5 (S6)                       | 369.3   | 96.3  | 318    | 45     |                          |                                                                                   |
| CL6 (S6)                       | 371.3   | 98.3  | 317.5  | 44.5   |                          |                                                                                   |
| PST-MA1 (PERME)                | 372.5   | 99.5  | 280    | 7      |                          |                                                                                   |

against frequency at a constant temperature as in figure 4.23(a). The glass transition was determined as the frequency at which the conductance passes through a maximum. When runs for a series of temperatures had been collated, the information was converted to a normalised conductance against temperature at constant frequency graph (figure 4.23(b)). The Tg was subsequently determined as the temperature at which the conductance was a maximum. All the above data handling was done on the Apple micro-computer using the programs 'digifast' and 'maketemp'.

Due to the presence of two components in the copolymer, it would be expected that two Tg's would be observed, but it was not possible to get reliable information on the polystyrene component, as again the samples became soft at high temperatures. The problem here being that the sample would not support the top spring-loaded electrode when soft, causing a thinning of the sample and so giving irreproducible results at high temperatures. Note: This phenomenon is very similar to that found when using the Rheovibron at high temperatures, so the dielectric data only gives values for the acrylate or methacrylate components of the copolymer. Table 4.4 shows the values of Tg for each sample at different frequencies.

The activation energies for the process that manifests itself as the glass transition can be calculated using equation 4.21 and are calculated from the variations of

FIG. 4.23a

Fixed Temperature

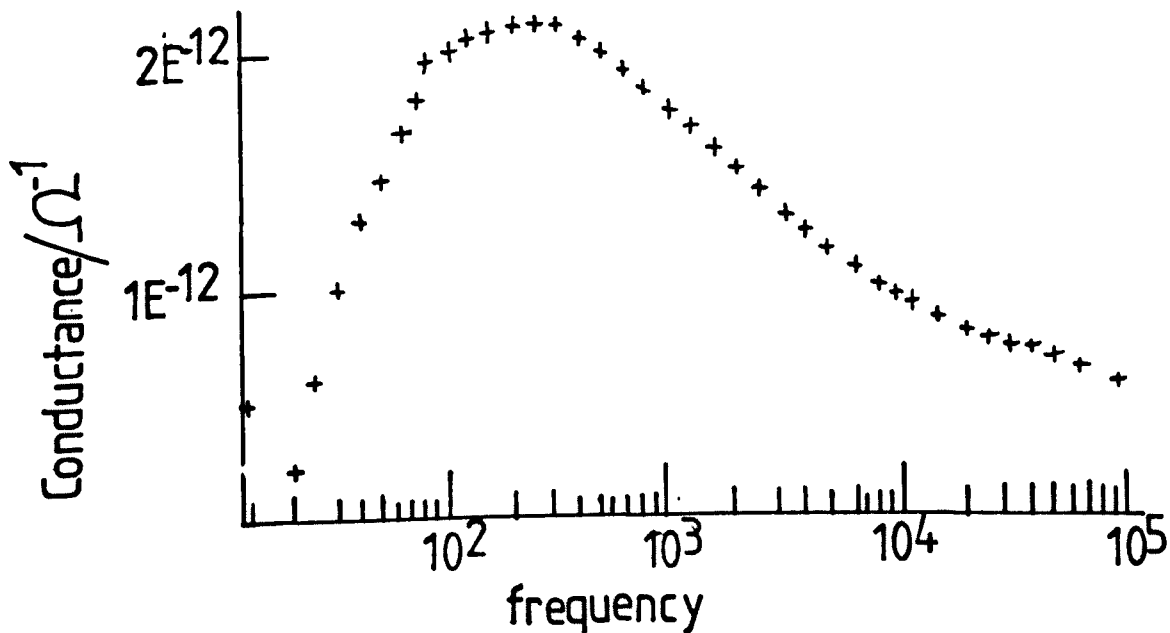


FIG. 4.23b

Fixed Frequency

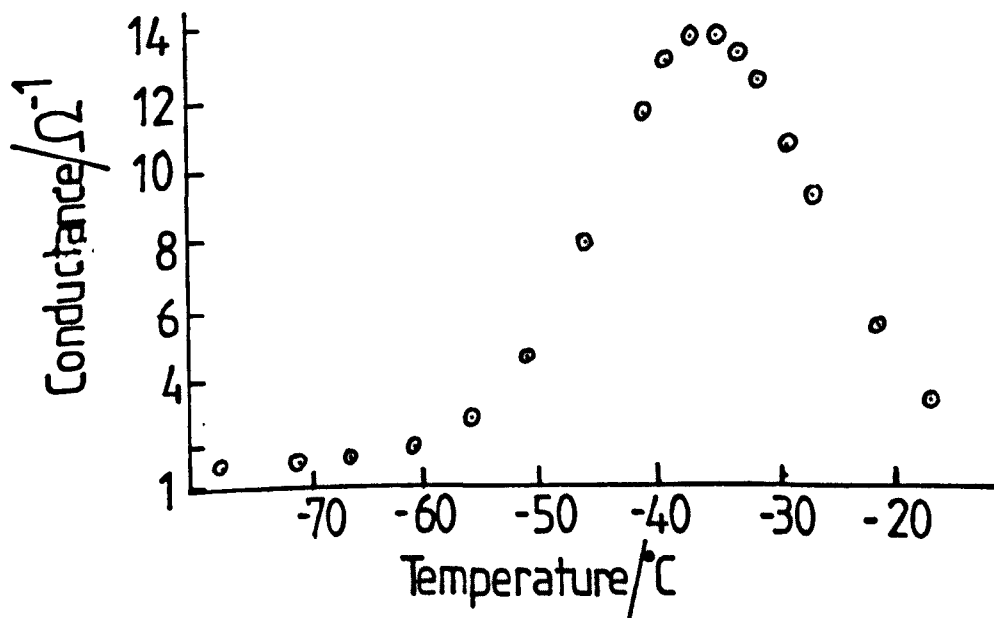


TABLE 4.4

|                                                   |         | Frequency/Hz |       |       |       |       |      |       |       |       |        |
|---------------------------------------------------|---------|--------------|-------|-------|-------|-------|------|-------|-------|-------|--------|
|                                                   |         | 100          | 200   | 500   | 1000  | 2000  | 5000 | 10000 | 20000 | 50000 | 100000 |
| Glass Transition Temperature (T <sub>g</sub> )/°C | CL1     | -4.5         | -2.25 | 1     | 3.25  | 5.5   | 8    | 11    | 13.75 | 17.5  | -      |
|                                                   | CL2     | -35          | -33   | -30   | -27   | -25.3 | -20  | -18.5 | -17   | -     | -      |
|                                                   | CL3     | 51           | 55    | 57    | 61    | 66.5  | 73.5 | 78    | 83    | 89.5  | 98     |
|                                                   | CL4     | -2.5         | -1    | 2.5   | 4.25  | 5     | 8    | 12    | 15.75 | 18    | -      |
|                                                   | CL5     | -            | 58    | 60    | 64    | 70.5  | 78.5 | 82    | 88    | 94    | 102    |
|                                                   | CL6     | 49.5         | 54    | 60    | 64    | 67    | 75   | 78.5  | 85.75 | 92    | 98.5   |
|                                                   | PST-MA1 | 25.5         | 26.5  | 28.25 | 31.25 | 32.5  | 36   | 38    | 41.5  | 45.5  | 48     |

$\ln$  (frequency) with  $T^{-1}$ .

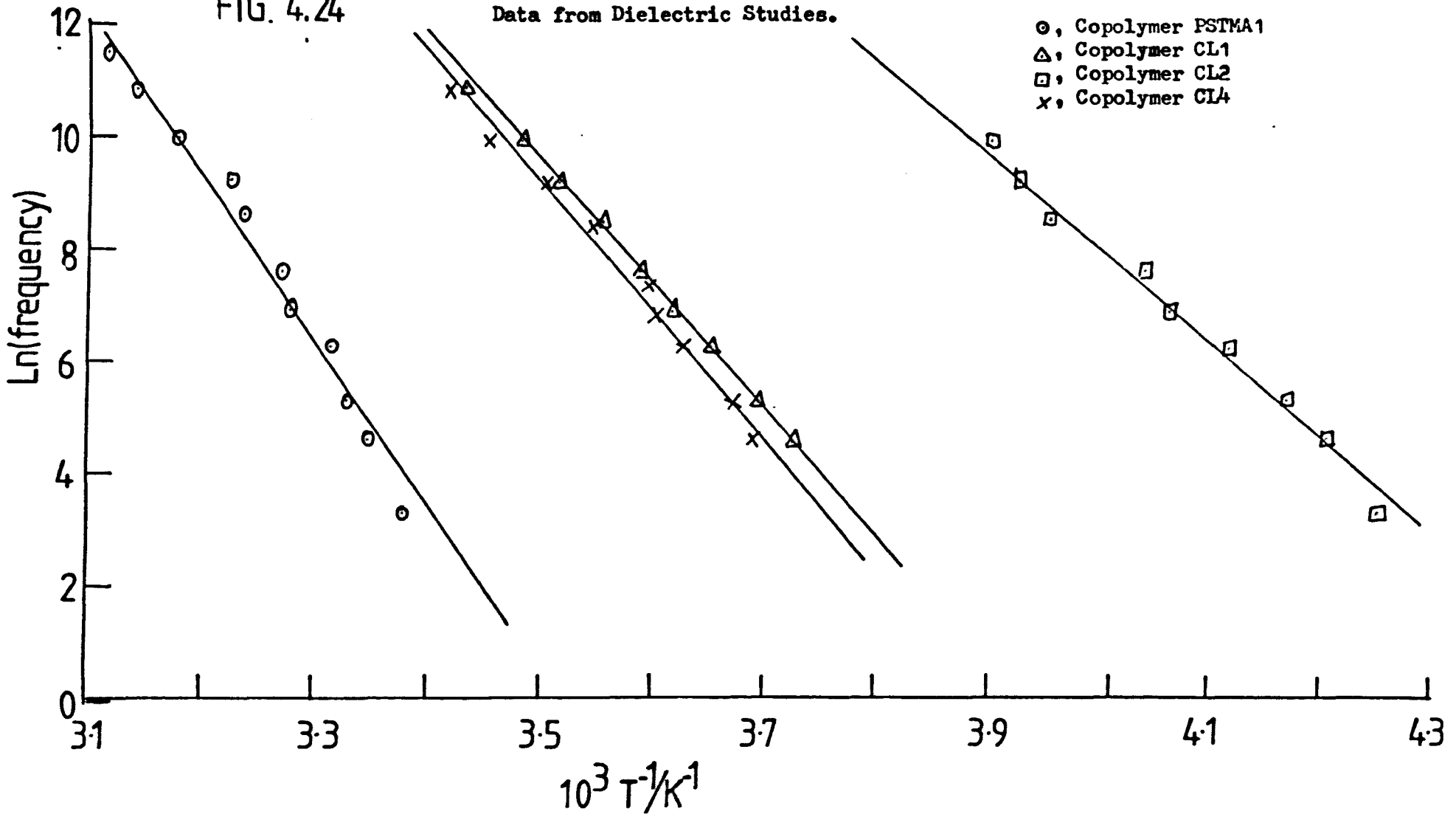
Figures 4.24-4.27 show these graphs for each copolymer, including data from both dielectric and Rheovibron experiments. From the Rheovibron data, activation energies were gained from both the  $E''$  and  $\tan \delta$  curves, the results are summarised in table 4.5. In most cases, the calculated activation energies from the  $E''$  and  $\tan \delta$  curves, were close together for a given copolymer (with  $7 \text{ KJ mol}^{-1}$ ;  $< 10\%$ ), thus showing that either curve may be used to gain the activation energy of the transition, ie, shows that the different techniques are looking at the same process.

The samples denoted CL3, CL5 and CL6, all show similar values for activation energy when considering the values gained from the conductance data, thus showing that the n-Butylmethacrylate component of the copolymer in each case was in a similar environment.

The conductance measurements are probably more accurate, as typically 9 or more points were used to calculate the activation energy, whereas with the Rheovibron data, only three points were used. The values gained for the activation energies of the homopolymer acrylates and methacrylates by other workers, are all slightly lower than the conductance values gained here, which would indicate that the components are not acting totally



FIG. 4.24



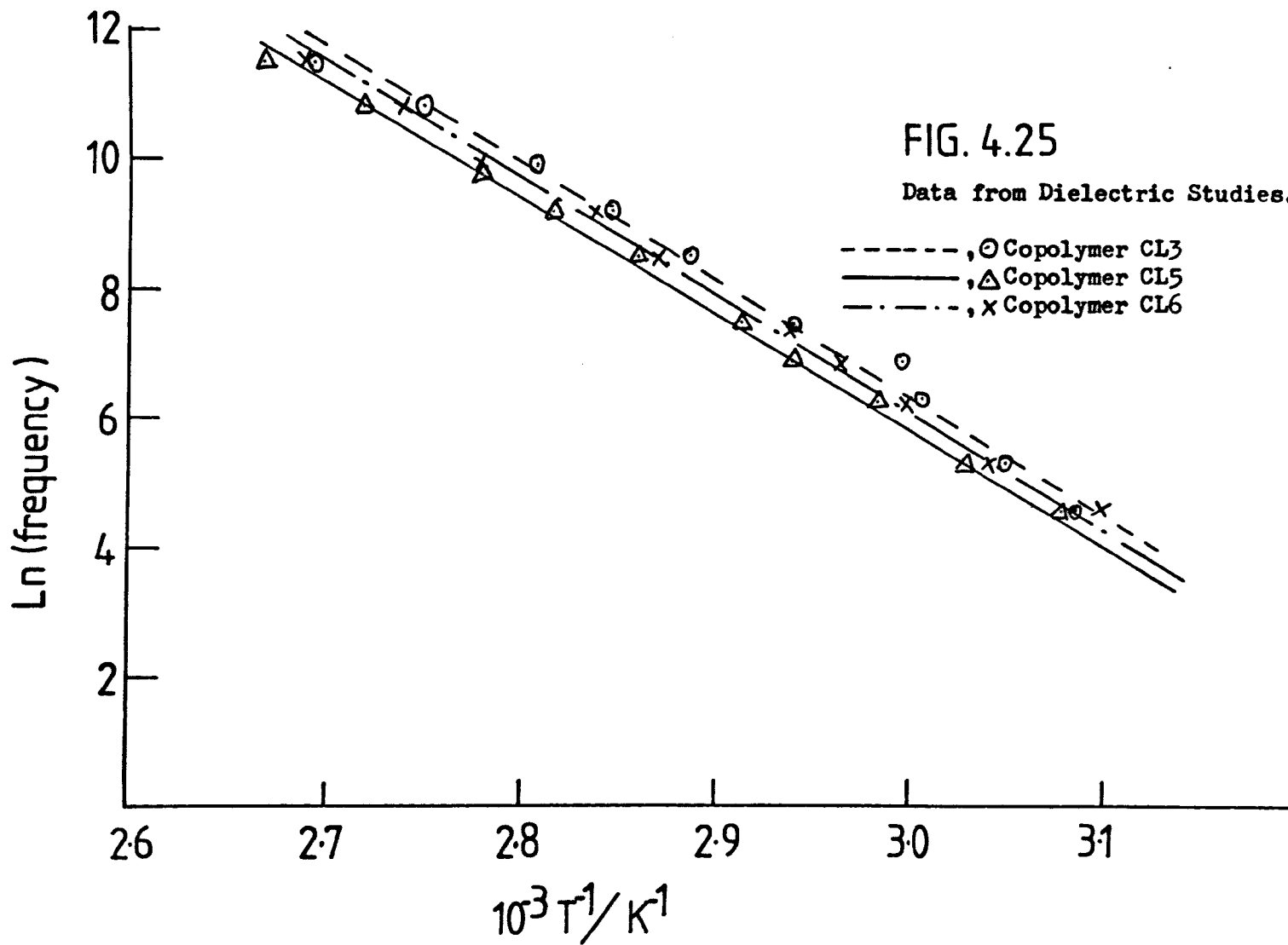


FIG. 4.26

Data from Rheovibron Studies ( $\tan \delta$  response).

△ Copolymer CL1

X Copolymer CL2

○ Copolymer CL3

△ Copolymer CL4

○ Copolymer CL6

□ Copolymer PSTMA1

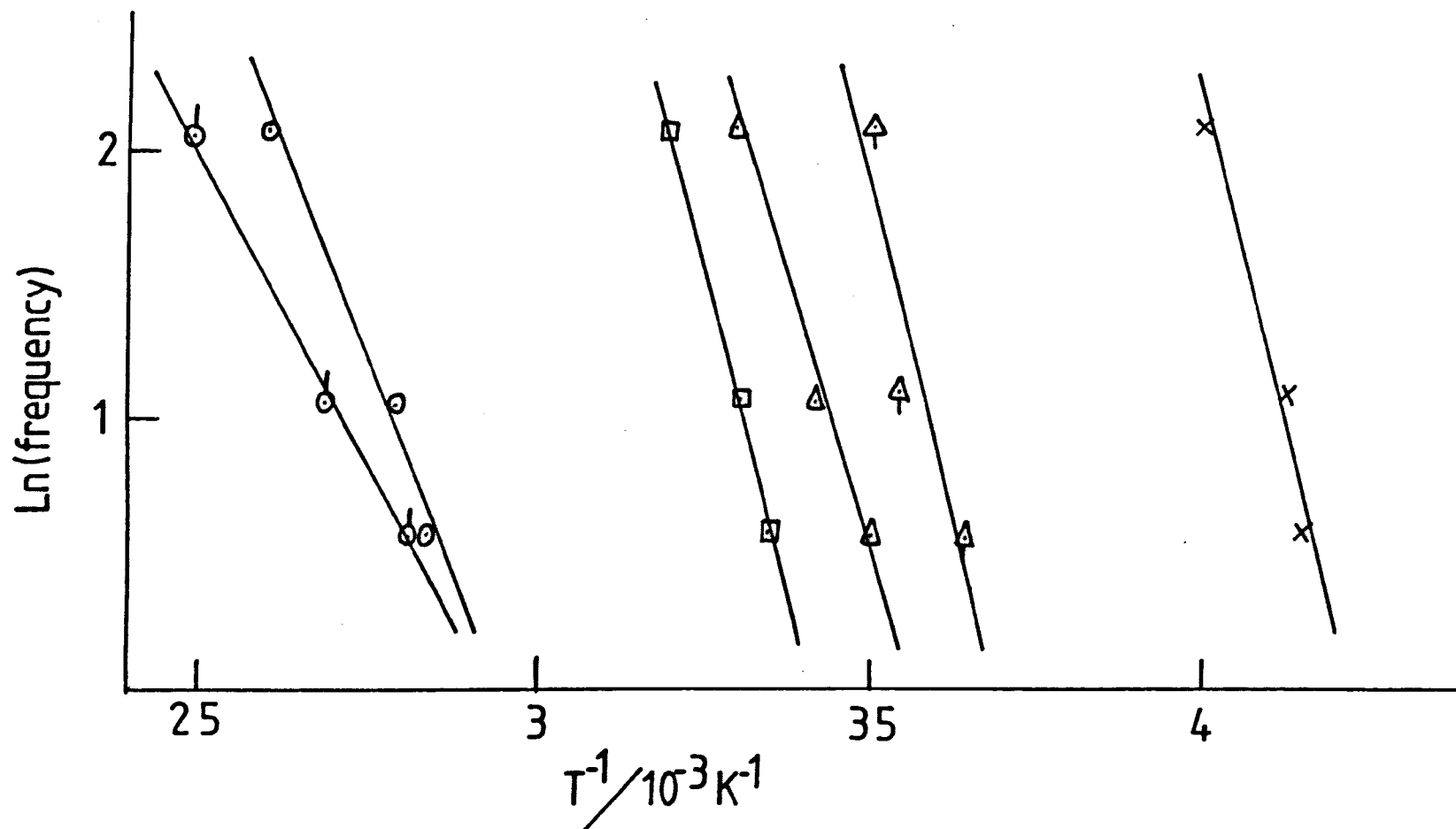


FIG. 4.27

Data from Rheovibron Studies (  $E''$  response).

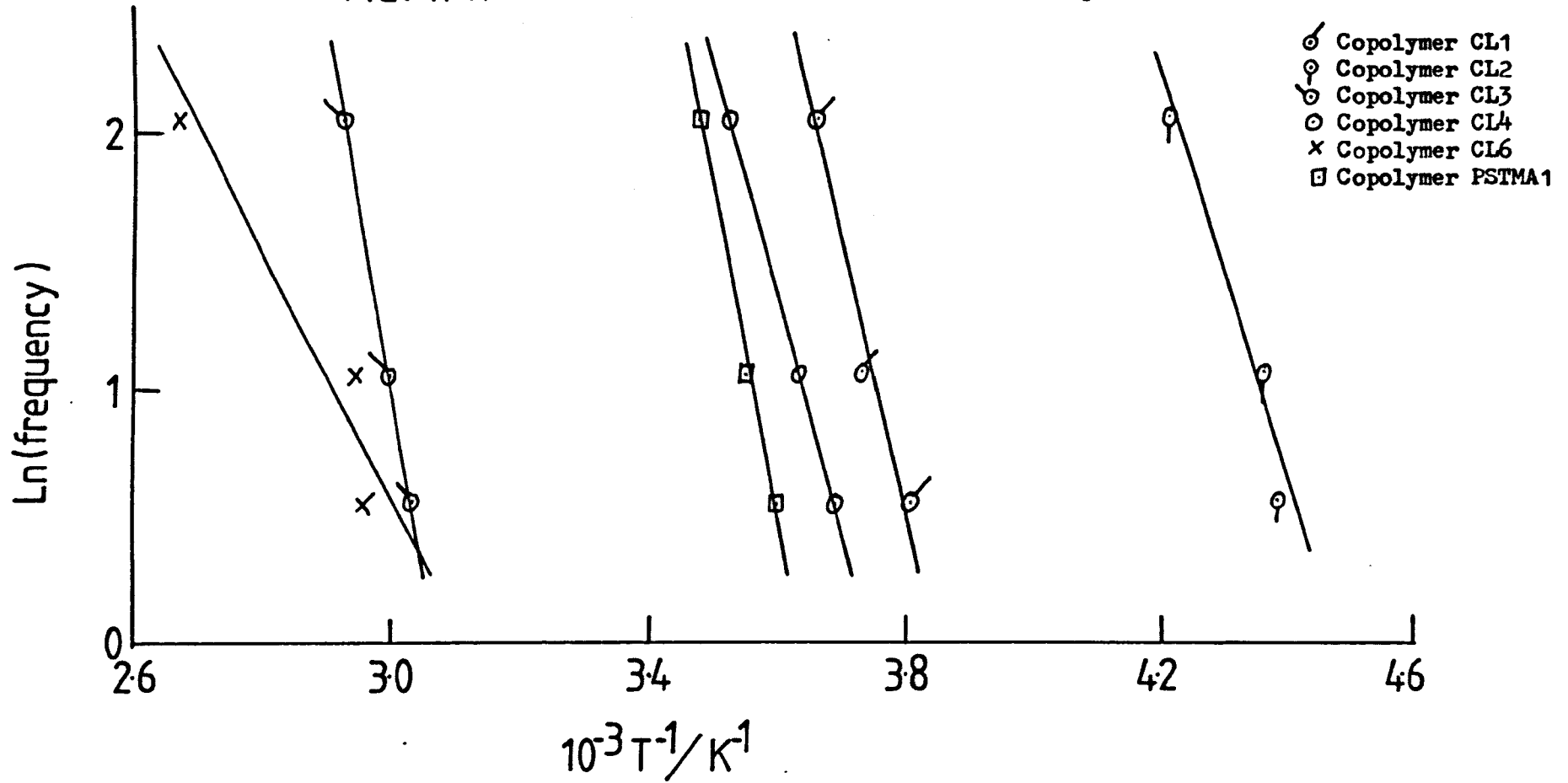


TABLE 4.5

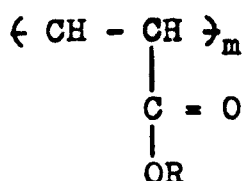
ACTIVATION ENERGIES DETERMINED USING THE RHEOVIBRON AND THE DIELECTRIC INSTRUMENTS

| Copolymer sample | Activation Energies for Tg                 |                                              |                                                       | Literature values |
|------------------|--------------------------------------------|----------------------------------------------|-------------------------------------------------------|-------------------|
|                  | From E'' response<br>/KJ mol <sup>-1</sup> | From tan δ response<br>/KJ mol <sup>-1</sup> | From conductance<br>measurements/KJ mol <sup>-1</sup> |                   |
| PST-MA1          | 251                                        | 249.5                                        | 246.2                                                 | 241.1             |
| CL1 PST-EA       | 192                                        | 200.6                                        | 188.6                                                 | 181.2             |
| CL2 PST-nBA      | 163.2                                      | 168.7                                        | 145.7                                                 | 140.5             |
| CL3 PST-nBMA     | 294                                        | 144                                          | 157                                                   | 126               |
| CL4 PST-EA       | 183                                        | 189                                          | 193                                                   | 181.2             |
| CL5 PST-nBMA     | -                                          | -                                            | 153                                                   | 126               |
| CL6 PST-nBMA     | 318                                        | 311                                          | 156                                                   | 126               |

NB All literature values gained from ref. 69

independently (not total phase separation) or there is homopolymer contamination. Homopolymer contamination could occur during synthesis if there is some transfer to solvent or monomer, leading to solubilization of the homopolymer into the copolymer, so giving data that is not true to the copolymer component. The gross phase separation of the polystyrene homopolymer may also distort the data, especially if quantities of homopolymer have distorted the copolymer domain boundary. Microphase separation of the copolymer components would give well defined relaxations, but if some of the homopolymers had been solubilized into the relevant domains, distortion would occur. The variation in activation energies between the Rheovibron and the literature values, may in part be due to the laminate structure of the samples described earlier affecting the raw data, which would then be carried through to the activation energy calculations.

Using the conductance data, a trend in activation energies for the acrylate copolymers can be observed; that as the substituent R on the acrylate group (equation 4.25) changes, the activation energy is either decreased or increased by a factor of approximately  $50 \text{ KJ mol}^{-1}$ .



4.25

In this study R is either  $\text{CH}_3$ ;  $\text{C}_2\text{H}_5$ ;  $\text{C}_3\text{H}_7$ , the order of decreasing activation energies was found to be  $\text{CH}_3 > \text{C}_2\text{H}_5 > \text{C}_3\text{H}_7$ . This trend was also borne out by the literature values, which indicate that the activation process giving rise to a relaxation for the B-component of the copolymer is not seriously affected by the A-component, ie, the copolymer has undergone microphase separation and that each component's relaxations are acting independently.

#### 4.8.5 Stress-Strain Data

The numerical results of elongation, ultimate tensile strength (UTS) and initial modulus for each of the polymers studied are given in table 4.6. All the experiments were done at  $19^\circ\text{C}$  and gave results consistent with those expected for the polymers at that temperature. Polymers CL3 and CL6 showed high values of initial moduli and UTS, while the elongations to break were low, which is typical of polymers below their glass transition temperature ( $T_g$ ). The other polymers CL1, CL2 and CL4, all showed low values of initial moduli and UTS, consistent with behaviour of polymers above their  $T_g$ 's and in the rubbery state. The elongations to break for the polymers CL1, CL2 and CL4, were very high, with the CL4 sample being extended to more than 1100% of the sample's original length prior to break; this large extension to break did not give a reversible deformation.

TABLE 4.6

| Sample | Extension to break | Number of experiments | Ultimate Tensile Strength/ $\text{Nm}^{-2}$ | Initial Modulus/ $\text{Nm}^{-2}$ |
|--------|--------------------|-----------------------|---------------------------------------------|-----------------------------------|
| CL1    | $990 \pm 50$       | 6                     | $(5.6 \pm 0.24) \times 10^5$                | $(4.1 \pm 0.2) \times 10^6$       |
| CL2    | $550 \pm 25$       | 6                     | $(6.21 \pm 0.27) \times 10^5$               | $(3.26 \pm 0.15) \times 10^6$     |
| CL3    | $2.12 \pm 0.06$    | 4                     | $(1.52 \pm 0.06) \times 10^7$               | $(9.9 \pm 0.25) \times 10^8$      |
| CL4    | $1150 \pm 100$     | 6                     | $(4.1 \pm 0.33) \times 10^5$                | $(5.78 \pm 0.46) \times 10^6$     |
| CL6    | $1.52 \pm 0.02$    | 3                     | $(9.68 \pm 0.12) \times 10^6$               | $(7.6 \pm 0.1) \times 10^8$       |

NB The sample CL5 was not studied using the Instron tensile tester because it was too brittle to stamp a sample from the cast film.



The shape of a stress-strain curve for a sample depends on the sample's chemical structure (composition, configuration, molecular weight, molecular weight distribution), on the physical structure (crystallinity, orientation), and on the form of the sample, as well as the deformation conditions (strain rate, temperature).

Figure 4.28 shows the variation in stress with applied strain for an experiment using the copolymer CL2. The section of the graph between strains of 0.8 and 2.4, shows some indication of strain hardening before the stress increases to a level where the polymer sample begins to flow. This phenomenon of strain hardening was only observed in samples of CL2.

It was observed that 'necking' occurs in the copolymers CL1, CL2 and CL4 and was a very prominent feature of CL1 and CL4 (see figures 4.29-4.30). Necking in many polymers is associated with the reorientation of molecules and increasing modulus, which manifests itself as an increasing extension, with a decreasing stress. Visually a constriction begins to form and with continued extension, increases in length at the expense of adjacent parts of the sample. The temperature can rise locally in the region of the neck, which causes a decrease in the viscosity, which in turn leads to increased flow. The actual 'neck' observed gradually extended to the whole length of the

FIG.4.28 Copolymer CL 2

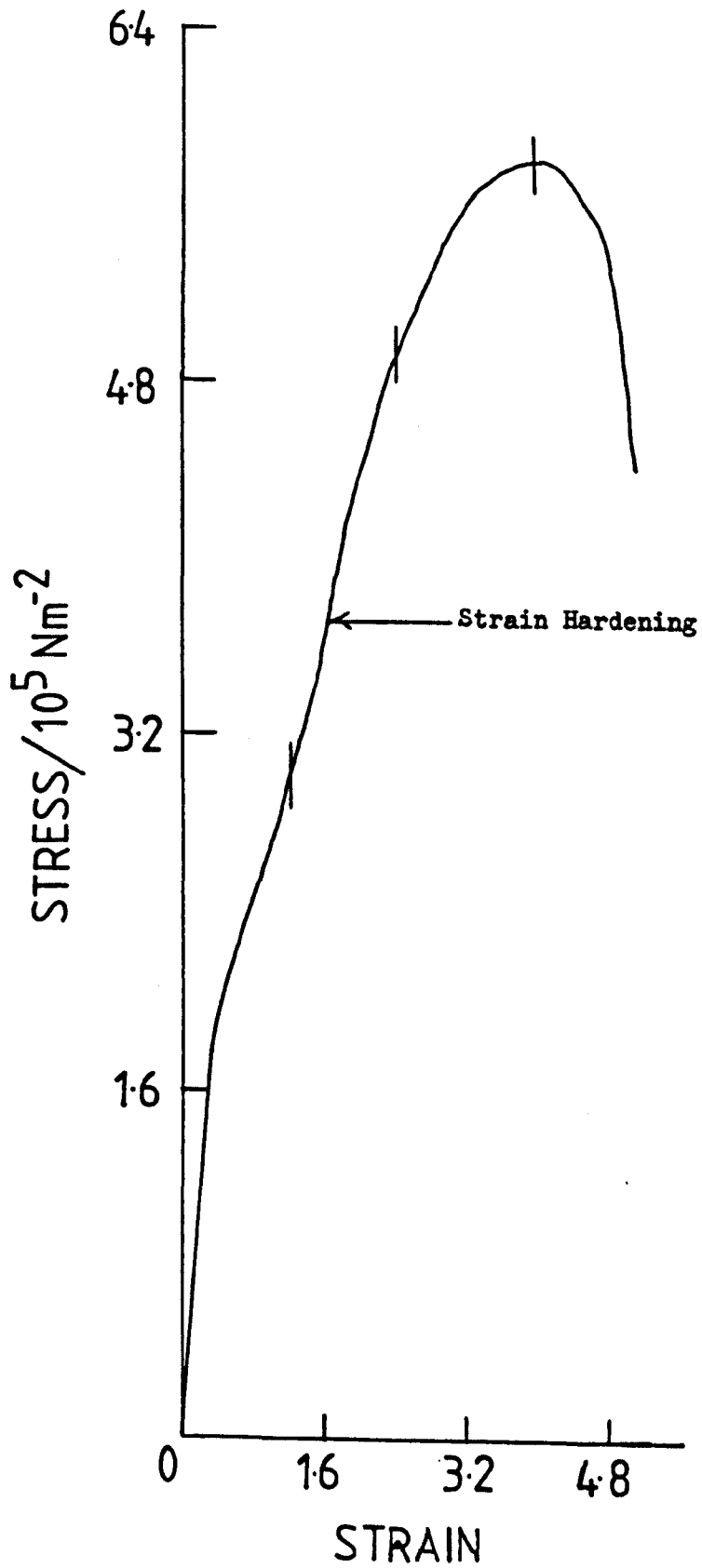


FIG. 4.29 Copolymer CL1

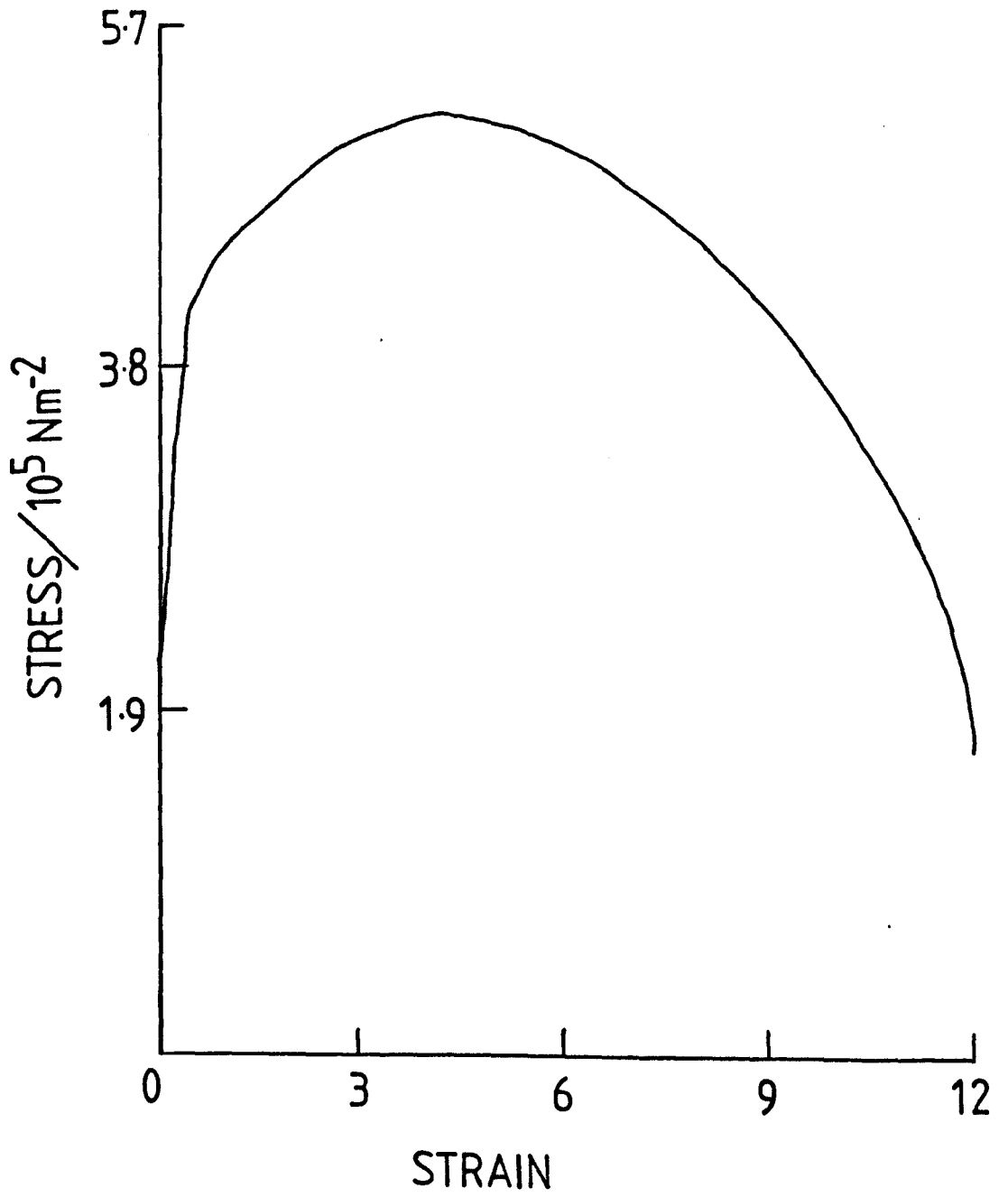
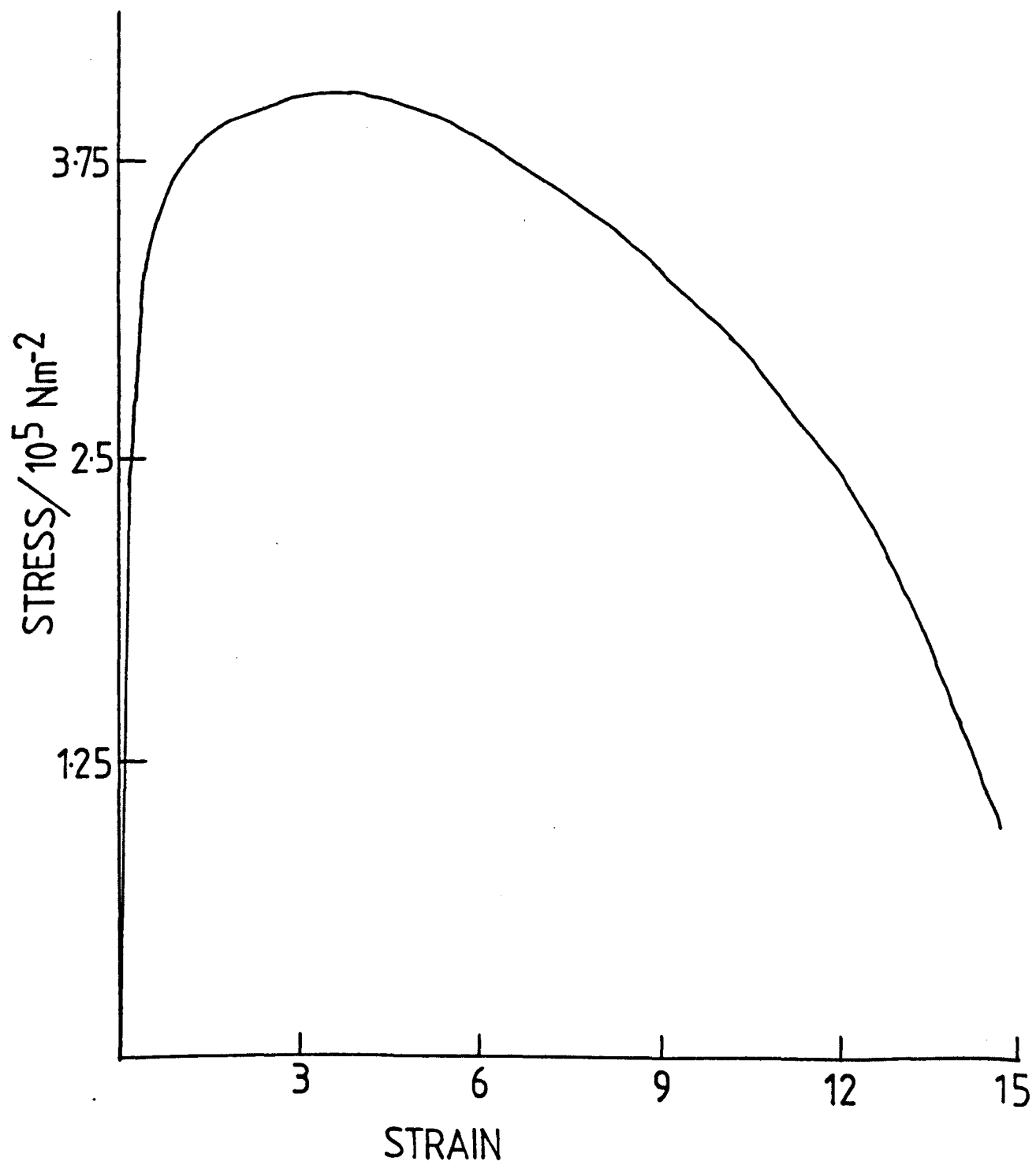


FIG. 4.30 Copolymer CL4



sample, as strain was applied. This region of the sample showed extensive flow, as shown in the stress-strain curve by a continued reduction in stress (no strain hardening), and at large extensions just before break, the sample appeared to be fibrous. Microscopic differences in cross-sectional area could affect the formation of a 'neck' when the sample is under stress and this may be a probable reason for the extended necking.

After break the samples were allowed time (30 minutes) to recover from the large extensions applied. The ethylacrylate component copolymers CL1, CL4, both recovered to approximately 3 times their original length before elongation (approximately 70% recovery). The n-Butylacrylate component copolymer CL2 behaved as a better elastomer than CL1 or CL4 and showed recovery of approximately 90%.

Short extension and stress relaxation experiments were also undertaken for copolymers CL1, CL2 and CL4. These experiments were carried out as follows:

- 1) samples were subjected to small strains in a cyclic manner (or hysteresis experiment). When a sample had returned to zero extension, it was left for a period of time to regain its original shape and dimensions, before re-running the experiment, ie, the experiment was looking for reversible deformations. Both the speeds of extension and return were 5 cm/min.

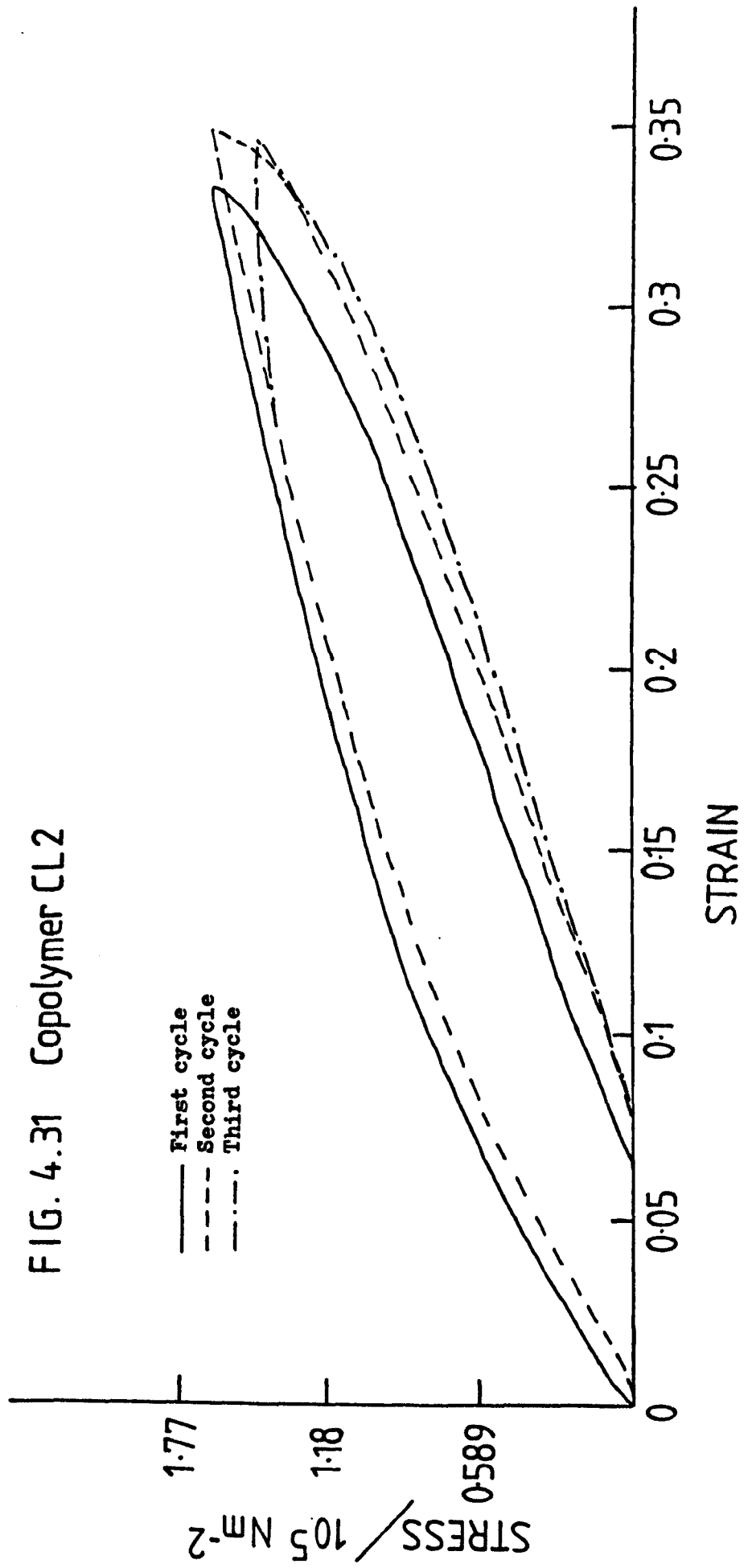
- 2) extending a sample to a given strain and then noting

the stress as a function of time.

Figure 4.31 shows the variation in stress with strain for three cycles of a sample of CL2; the total strain applied being 0.35 on each cycle. These cycling experiments showed that the sample behaved as an elastomer after the first extension cycle. The difference between the first and subsequent cycles, would seem to indicate that on the first extension a small permanent deformation occurs, that remains in the sample, but does not affect subsequent cycles. All the samples studied showed similar elastomeric properties after their first extension. The time required for the samples to regain their original shapes after the second and third cycles was approximately five minutes, indicating that they are slow elastomers at small deformations.

The fact that the samples studied show elastomeric properties, even if slow, indicates that microphase separation of the copolymer components has occurred and that the copolymer has a molecular arrangement similar to that in figure 1.4. The acrylate copolymers as described earlier will have the ABA type structure, where the A-component (polystyrene) will form discrete spherical domains in a matrix of B-component (polyacrylate); the B-component chains acting as effective cross links between the spherical domains. The B-component being above its  $T_g$  means that on the application of stress the B-chains (cross links) deform, but on removal of the deformation the B-chains

FIG. 4.31 Copolymer CL2



return to their equilibrium positions, ie, act as conventional thermoplastic elastomers. The small permanent deformation on the first extension could be due to the phase separated homopolystyrene in the sample undergoing permanent deformation as in the Rheovibron experiments. The samples did show, slow elastomeric properties, which could be attributed to the fact that the B-components were not significantly above their respective Tg's, for the B-chains revert to their equilibrium positions quickly after the deformation had been removed.

At moderate extensions the elasticity was lost, so indicating that the polymers are not really behaving as true thermoplastic elastomers. This loss of elasticity could be due to significant amounts of homopolymer (polystyrene and polyacrylates) or AB block copolymer being present. The homopolystyrene present is the minor component of the samples under test and should not significantly affect the elastomeric properties, unless large quantities of the homopolymer present are solubilized in the like component of the copolymer.

If there is transfer during the synthesis of the copolymers, homopolymer acrylate and AB block copolymer will be formed. Due to the dominant termination process being combination, the most likely product of transfer will be AB block copolymer, which could adversely affect the mechanical properties of the ABA block copolymer. The



AB block copolymer does not form effective cross links between the A-component rich spherical domains when the copolymer has undergone microphase separation and so will tend to flow under stress.

GPC data for the copolymer blends studied (figures 3.7-3.13) showed that for at least CL4 there could be a significant amount of transfer to monomer during synthesis, so giving AB copolymer that could be attributed to the lack of elastomeric behaviour at moderate extensions for the samples. Under stress, the samples would yield considerably before breaking, as the ABA cross links effectively stretch and the AB copolymer flows. The psuedo 'necking' behaviour described earlier would be a physical manifestation of flow, so indicating that the sample may contain AB copolymer as a contaminant.

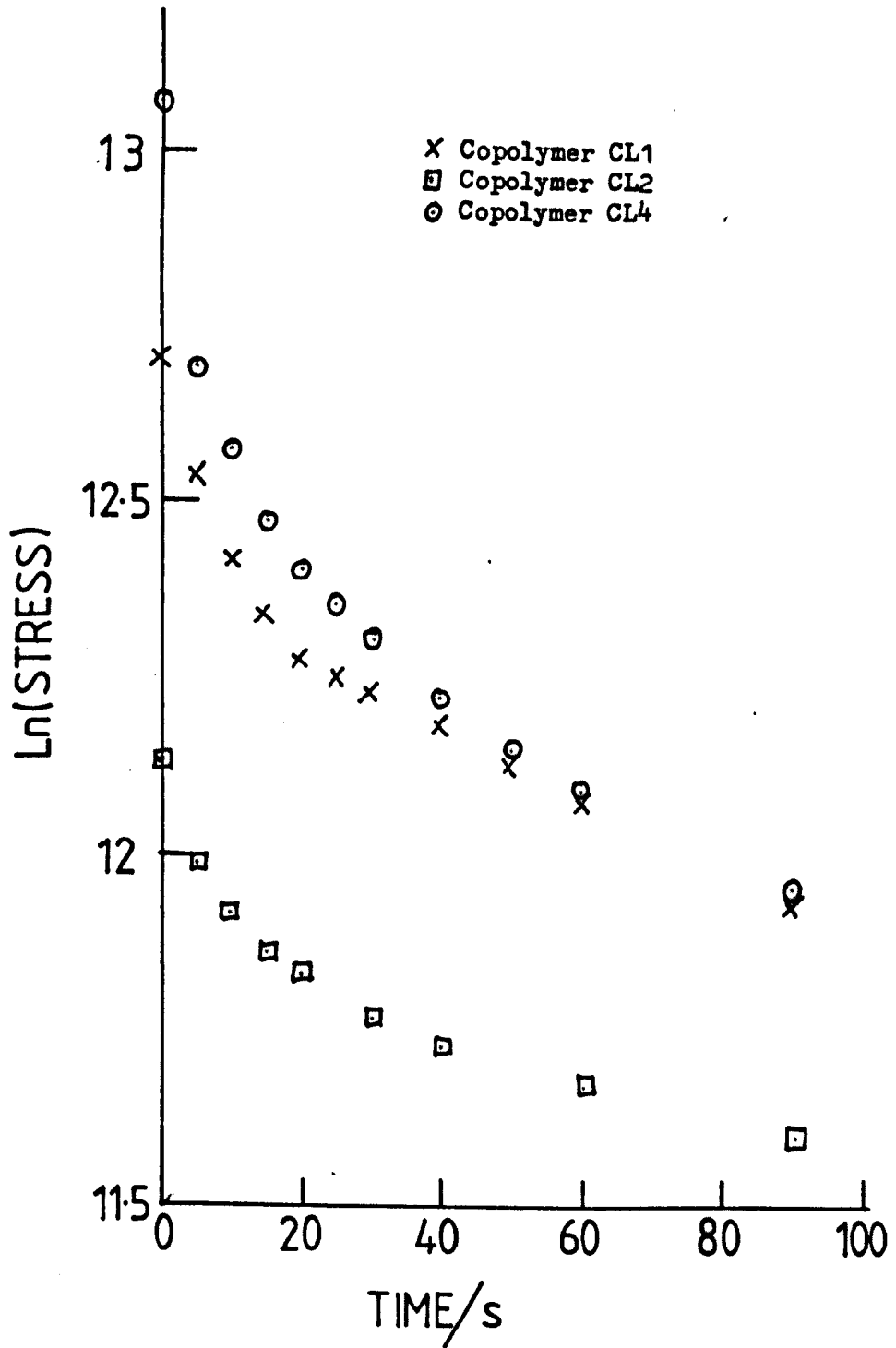
Several mathematical expressions exist for the description of stress relaxation phenomena in polymers at a given temperature (86). By the use of equation 4.5 it is possible to determine the stress relaxation time,  $\gamma$ , from stress relaxation experiments.

$$\sigma = \sigma_0 \exp\left(\frac{-t}{\gamma}\right)$$

4.5

A graph of  $\ln \sigma$  against  $t$  should give a straight line, whose slope is  $-1/\gamma$ . As can be seen in figure 4.32 the data for CL1, CL2 and CL4 do not lie on a straight line, which would indicate that the relaxation

FIG. 4.32



process involved was not simple; it does not obey the classical equation.

Karas (87) reported a relationship (equation 4.26) that described the decay of stress with time, in terms of the maximum stress developed and the time after the straining phase was completed.

$$(D_t/S_0) = n \log t + I \text{ where } D_t = S_0 - S_t \quad 4.26$$

where  $S_0$  = the stress developed at the end of the straining phase,

$S_t$  = the stress at any time  $t$  after the elongation has ceased,

$t$  = time after the elongation phase was completed,

$n$  = the slope of the plot of  $D_t/S_0$  against  $\ln t$ ; this is equivalent to a rate of stress relaxation.

$I$  = the intercept on the value of  $D_t/S_0$  when  $\ln t = 0$

Using the relationship of Karas, the polymers CL1, CL2, and CL4 all gave straight lines for a graph of  $D_t$  against  $\ln t$  (figure 4.33); the rate of stress relaxation,  $n$ , for each case was calculated and these are given below:-

for CL1,  $n = 1.025$

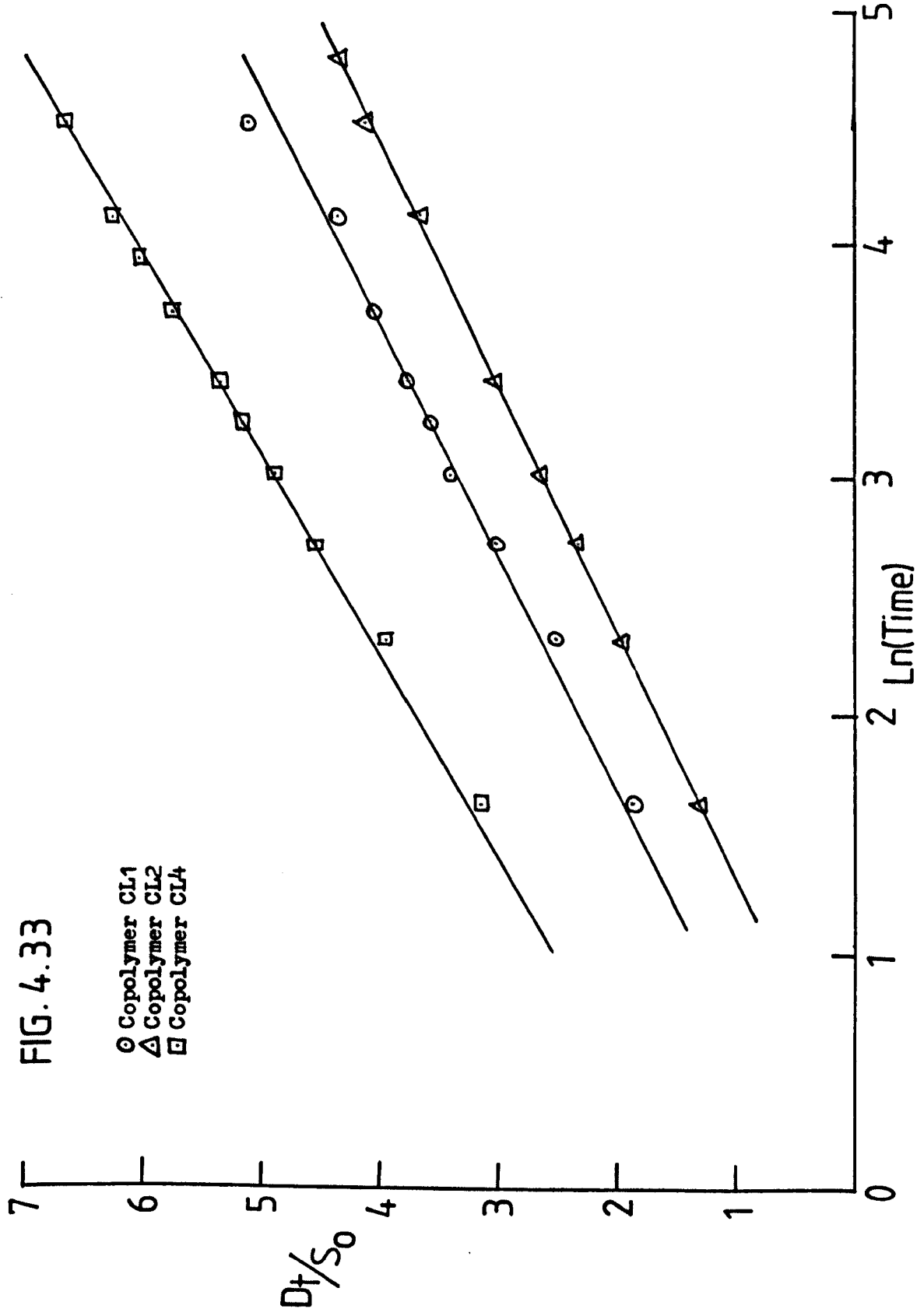
for CL2,  $n = 0.979$

for CL4,  $n = 1.175$

The fact that the rates of stress relaxation for the

FIG. 4.33

○ Copolymer CL1  
△ Copolymer CL2  
□ Copolymer CL4



copolymers studied, would indicate that similar relaxation phenomena were being measured in each case. Even though the relationship of Karas seems applicable to the copolymers studied, the findings are contradictory to those of classical theory. These differences may occur because the Karas relationship may be effectively ignoring the fact that the relaxation is complex owing to either AB or homopolymer contaminants.

At low elongations the copolymers showed slow elastomeric behaviour, which indicates an ABA type structure that had undergone microphase separation, with an elastomeric component B that was not well above its  $T_g$ . The morphology of the copolymer system would consist of spheres of A-component in a matrix of B-component. The segregation of the homopolystyrene and copolymer may account for the small permanent deformations observed, which result from small structural changes in the sample.

At long extensions the flowing fibrous nature of the sample indicate the presence of some AB type copolymer of lower molecular weight than the ABA copolymer. The incorporation of the AB copolymer into the domain structure would effectively reduce the number of B-chains acting as physical cross links in the overall ABA system, thus causing a reduction in the elastomeric properties. The reduced molecular weight of molecules would also contribute to bad tensile properties, leading to flow under stress.

The overall tensile properties of the copolymers studied showed that the copolymers were not behaving as ideal thermoplastic elastomers.

#### 4.8.6 Closing Remarks

The general kinetics of the free-radical process for the various monomers used, was found to be simple under controlled conditions and agreed with the findings of Bamford et al (9) and Woo (42). It was observed that the initial activity of the anionically prepared prepolymer greatly depended on the actual method of synthesis (either under a nitrogen atmosphere or under high-vacuum conditions). With purification the activity of the prepolymers increased and calculation of the parameter  $k_p/k_t^{1/2}$  gave similar values for copolymerizations, as for homopolymerizations of the various monomers.

It is proposed that a new series of transformation processes may be defined, using the recent development of group transfer polymerization (GTP) (88, 89); the GTP to free-radical polymerization process has recently been shown to be feasible during work at Liverpool (90). This new series of possible transformation processes involving GTP, could offer a whole range of novel polymers with interesting properties, based on the ability of GTP to give near monodisperse acrylates and methacrylates.

The GPC approach developed by Eastmond and Woo (42, 67) was used to analyse various copolymers during this work. It was observed that solvent changes and calibration had a considerable effect on the comparison of experimental and theoretical data generated. A common feature being the reduction in the hydrodynamic volumes of copolymers, giving higher quantities of AB copolymer than predicted by theory, even so, the general model was obeyed quantitatively over the major area of analysis, that includes the bulk of the copolymer. These unexpected changes in hydrodynamic volume may not be real, if there is a lack of understanding of the polymerization mechanism for these copolymers. It was concluded that if these discrepancies are real and the experimental data were compared to a theoretical 'ideal', then it may be possible to study the shrinkage of copolymer chains in solution by Eastmond's model.

A method for determining GPC calibration data for homopolymers was devised, that showed encouraging results for methylacrylate, based on Eastmond's model. It was concluded that the general concepts used by Eastmond for the construction of the model were valid, assuming polymer interactions and shrinkage effects are negligible. This model could be tested more fully, if suitable GPC standards for the various polymers used could be prepared. GTP may offer a method to acrylate and methacrylate standards, so allowing the model to be rigorously tested.

Cast films of the copolymer blends produced during this work, were semi-opaque and had a laminate structure, which consisted of a polystyrene rich layer over a copolymer rich layer. Infrared studies showed compositional variations between the upper and lower surfaces of the cast film, which backed up the concept of the laminate film. The dynamic mechanical data for  $E''$  showed a double maxima, of which, one maximum would move on subsequent retest; this phenomena being attributed to the breakdown of the laminate structure. Visually the samples used were observed to craze on one surface only during experiments. It was concluded that the prepolymer, polystyrene, had undergone macroscopic phase separation from the copolymer in the sample, so giving the laminate structure, which was suggested to be the cause of the visual and dynamic observations. This phase separation was in general agreement with Meier's theoretical considerations and vindicated Eastmond's recent conceptual arguments about the phase separation of homopolymer from copolymers.

Purification of the copolymer was found to be difficult, but by using preparative GPC, it would be possible to separate most of the copolymer from the homopolymer. With the pure copolymer it would be possible to study the macroscopic phase separation of the blended system by controlled doping. All the dynamic and tensile experiments undertaken would also give more accurate information on the copolymers, as the samples would not be contaminated.



Rheovibron, dielectric and DSC studies all gave values for  $T_g$  that were in reasonable agreement with literature values. Activation energies for the glass transition process were calculated and showed similar trends to literature values, even if a little high, which may be due to the presence of the prepolymer. The activation energies from  $E''$ ,  $\tan \delta$  and dielectric data were similar, thus showing that each experiment was measuring the same process.

Tensile experiments showed pseudo necking phenomena and non classical relaxations, which showed that the copolymers were not behaving as true thermoplastic elastomers. At short extensions, the copolymers were found to act as slow elastomers. These observations could be due to the presence of prepolymer or AB copolymer. The AB copolymer could be present because of some transfer or through processes occurring during the free-radical polymerization that are not yet understood. The use of pure copolymer would help resolve these tensile problems and offer scope for further work, to improve the physical properties of these copolymers.

REFERENCES

1. Meier  
J. Poly. Sci. C, 26, 81, (1969)
2. Meier  
ACS. Polym. Prepr., 11, 400, (1970)
3. Krause  
Macromolecules, 3, 84, (1970)
4. Inoue, Soen, Hashimoto and Kawai  
Macromolecules, 3, 37, (1970)
5. Eastmond and Smith  
Polymer, 17, 367, (1976)
6. Eastmond and Phillips  
Polymer, 20, 1501, (1979)
7. Kato  
J. Electron Micros, 14, 219, (1965)
8. Bamford and Jenkins  
Proc. Roy. Soc, A216, 515, (1953)
9. Bamford, Jenkins and Wayne  
Trans. Faraday Soc, 56, 932, (1960)
10. Smets and Woodward  
J. Poly. Sci, 14, 126, (1954)
11. Woodward and Smets  
J. Poly. Sci, 17, 51, (1955)
12. Bamford and White  
Trans. Faraday Soc., 52, 716, (1956)
13. Bamford and White  
Trans. Faraday Soc., 54, 268, (1958)

14. Arfaei, Haszeldine and Smith  
JCS. Chem. Comm., 260, (1976)
15. Kataoka and Ando  
Polymer, 25, 507, (1984)
16. Szwarc  
Nature, 178, 1168, (1956)
17. Szwarc, Levyand and Milkovitch  
J. Am. Chem. Soc., 78, 2656, (1956)
18. Dreyfuss and Dreyfuss  
Adv. Chem. Ser., 91, 335, (1969)
19. Bollarde and Melville  
Proceedings of 1st Rubber Technol., London, 239, (1938)
20. Bamford, Jenkins and Johnson<sup>t</sup><sub>λ</sub>  
Proc. Roy. Soc. Serv. A, 239, 214, (1957)
21. Schlick and Levy  
J. Phys. Chem., 64, 883, (1960)
22. Fetters  
J. Poly. Sci. part C, 26, 1, (1969)
23. Morton  
"Anionic Polymerization: Principles and Practice",  
Publ. Academic Press, (1983)
24. Morton  
Macromolecular Reviews, 2, 71, (1967)
25. Young, Quirk, and Fetters  
"Anionic Polymerization of non-polar monomers involving  
lithium", Advances in Polymer Science, 56, 1, (1984)
26. Berger, Levy, and Vofsi  
Polymer Letters, 4, 183, (1966)

27. Richards, Kingston and Souel  
Polymer, 19, 68, (1978)
28. Burgess, Cunliffe, MacCallum, Sherrington and Richards  
Polymer Letters, 14, 471, (1976)
29. Burgess, Cunliffe, MacCallum and Richards  
Polymer, 18, 719, (1977)
30. Burgess, Cunliffe, MacCallum and Richards  
Polymer, 18, 726, (1977)
31. Burgess, Cunliffe, Dawkins and Richards  
Polymer, 18, 733, (1977)
32. Abadie, Hartley, Schue, Souel and Richards  
Polymer, 23, 445, (1982)
33. Abadie, Hartley, Schue, Souel and Richards  
Polymer, 23, 1105, (1982)
34. Abadie, Burgess, Cunliffe and Richards  
Polymer Letters, 14, 477, (1976)
35. Cunliffe, Hayes and Richards  
Polymer Letters, 14, 483, (1976)
36. Abadie, Schue, Souel and Richards  
Polymer, 18, 1292, (1977)
37. Abadie, Schue, Souel and Richards  
Polymer, 22, 1076, (1981)
38. Abadie, Cohen, Schue and Richards  
Polymer, 22, 1316, (1981)
39. Burgess and Richards  
Polymer, 17, 1020, (1976)
40. Brossas, Catala, Clouet, and Gallot  
Compt. Rend. Acad. Sci, C278, 1031, (1974)

41. Richards  
Brit. Poly. J, 12, 89, (1980)
42. Woo  
Ph.D. Thesis, Liverpool, (1985)
43. Bamford and Finch  
Proc. Roy. Soc. Ser A, 268, 553, (1962)
44. Bamford  
"Reactivity, Mechanisms and Structure in  
Polymer Chemistry,"  
Eds. Jenkins and Ledwith, Publs. Wiley, NY., (1974)
45. Bamford, Crowe and Wayne  
Proc. Roy. Chem. Soc. Ser A, 284, 455, (1965)
46. Bamford, Crowe and Wayne  
Proc. Roy. Chem. Soc. Ser A, 292, 153, (1966)
47. Eastmond and Harvey  
Unpublished results
48. Bamford, Dyson, Eastmond and Whittle  
Polymer, 10, 759, (1969)
49. Bamford and Mullik  
Polymer 17, 94, (1976)
50. Yağci  
Polymer Comm., 26, 7, (1985)
52. Bamford, Barb, Jenkins and Onyon  
"The Kinetics of Vinyl Polymerization by Radical  
Mechanisms",  
Butterworths, London, (1958)
52. Yau, Kirkland and Bly  
"Modern Size Exclusion Liquid Chromatography"  
Publs. Wiley, (1979)
53. Moore and Hendrickson  
J. Polym. Sci, C8, 233, (1965)

54. Grubisic, Rempp and Benoit  
J. Polym. Sci, B6, 753, (1967)
55. Grubisic, Picot, Gramain and Benoit  
J. Appl. Polym. Sci., 16, 2931, (1972)
56. Seymour and Eastmond  
unpublished results
57. Wenner  
JOC., 17, 523, (1952)
58. Burgess  
MSc. Thesis MOD (1977)
59. Dyson  
PhD. Thesis, Liverpool, (1968)
60. Eastmond  
"Free Radical Polymerization", Vol. 14A of  
Comprehensive Chemical Kinetics, (Eds. Tipper  
and Bamford), Elsevier, (1976), Chapter 1
61. Polymer Handbook  
Eds. Brandrup and Immergut, Interscience, (1967)
62. Bamford, Eastmond and Dyson  
Polymer, 10, 885, (1969)
63. Runyon, Barnes, Ruso and Tung  
J. Appl. Polym. Sci, 13, 2359, (1969)
64. Bamford, Eastmond, Woo and Richards  
Polymer 23, 643, (1982)
65. Tung  
J. Appl. Polym. Sci, 24, 953, (1979)
66. Chang  
J. Chromatography, 55, 67, (1971)

67. Eastmond  
Polymer Surfaces and Interfaces (Eds: Feast and  
Monroe)  
J. Wiley (1986) in press
68. Ayney, Humphrey and Poller  
Polymer, 18, 840, (1977)
69. Mcrum, Read and Williams  
"Anelastic and Dielectric Effects in Polymeric  
Solids",  
Publs. Wiley, (1967)
70. Murayama  
Material Science Monographs, 1, (1978), Publ. Elsevier
71. Digibridge Manual  
GENRAD, USA, (1983)
72. Turi  
"Thermal Characterization of Polymeric Materials",  
Publ. Academic Press, (1981)
73. Perkin-Elmer Model DSC-2 Manual  
Perkin-Elmer Corporation, USA, (1982)
74. Bénard  
Rev. gén Sci, Pure Appl., 11, 1261, (1900)
75. Rayleigh  
Scientific Papers, 6, 432, (1920)
76. Miller and Stace  
"Laboratory Methods in Infrared Spectroscopy" 2nd Ed.,  
Heyden (London), (1972)
77. Meier  
ACS. Polymer Preprints, 18, 340, (1977)

78. Riess  
Macromolecular Sci-Phys B., 17, 335, (1980)
79. Jiang, Huang and Yu  
Polymer, 24, 1259, (1983)
80. Jiang, Huang and Yu  
Polymer, 26, 1689, (1985)
81. Roe and Zin  
Macromolecules, 17, 189, (1984)
82. Eastmond and Phillips  
Polymer 20, 1591, (1979)
83. Eastmond and Maccianiello  
Brit. Poly. J. 16, 63, (1984)
84. de Gennes  
Macromolecules 13, 1069, (1980)
85. Cowie  
Poly. Eng. Sci., Mid-August, 19(10), 709, (1979)
86. Alfrey  
"Mechanical Behaviour of High Polymers"  
Publ. Interscience, NY, (1948)
87. Karas  
British Plastics, September, (1961)
88. Webster, Farnham and Sogah  
European Patent No. O 068 887 A1
89. Webster, Hertler, Sogah and Farnham  
J. Am. Chem. Soc. 105, 5706, (1983)
90. Eastmond and Grigor  
Unpublished results



**APPENDIX A**

```

10 PRINT "      GPC COPOLYMER ANALYSIS  "
20 PRINT:PRINT
25 CLEAR2000
30 REM GEOP'S MODEL FOR COPOLYMERS
35 GOSUB6500
40 GOSUB 2500
160 FOR J=1TON
180 INPUT"ENTER ELUTION VOL.INcm";K(1,J)
200 INPUT"HEIGHT OF RI AT EL.VOL.INmm";K(2,J)
220 INPUT"HEIGHT OF UV AT EL.VOL.INmm";K(3,J)
240 GOSUB6000
260 NEXT J
760 PRINT"ENTER UPPER&LOWER LIMITS OF X-AXIS(ELUTION VOL.)
770 PRINT
780 INPUT"LOWER LIMIT";F1:INPUT"UPPER LIMIT";F2
790 PRINT"LIMITS FOR Y-AXIS":INPUT"LOWER LIMIT";F5:INPUT"UPPER LIMIT";F6
800 PRINT
810 PUT12
820 CALL"CLEAR"
830 GRAPH1
840 CALL"RESOLUTION",0,2
845 CALL"COLOUR",0,0,0,1
847 CALL"COLOUR",2,7,7,0
850 CALL"PLOT",319,31,3:CALL"LINE",39,31,3
860 CALL"LINE",39,191
870 LET F3=(F2-F1)/10
880 LET F4=1/F3
890 LET F7=1/(F6-F5)
900 FOR G1=F1TOF2
910 CALL"PLOT", (28*F4*(G1-F1)+39),31,3
920 CALL"LINE", (28*F4*(G1-F1)+39),36
930 LET G1%=STR$(G1)
940 CALL"STPLOT", (28*F4*(G1-F1)+22),22,VARADR(G1%),3
950 NEXT G1
960 LET D1%="Vri/cm"
970 CALL"STPLOT",130,10,VARADR(D1%),3
980 FOR G2=F5TOF6 STEP0.1
990 CALL"PLOT",39,(160*F7*(G2-F5)+31),3
1000 CALL"LINE",45,(160*F7*(G2-F5)+31)
1010 LET G2%=STR$(G2)
1020 CALL"STPLOT",15,(160*F7*(G2-F5)+27),VARADR(G2%),3
1030 NEXT G2
1040 LET D2%="WT.FRAC.OF B UNIT"
1050 CALL"STPLOT",8,36,VARADR(D2%),3,1
1205 PRINT"NB. STEP IS THE INTERVAL BETWEEN POINTS"
1207 PRINT
1210 INPUT"ENTER CURVE STEP FOR THEORETICAL CURVES";X1
1220 FORC=K(1,1)TOX(1,N)STEPX1
1230 GOSUB4000
1240 CALL"PLOT", (28*F4*(C-F1)+39),(160*F7*(W5-F5)+31),2
1260 CALL"PLOT", (28*F4*(C-F1)+39),(160*F7*(W6-F5)+31),2
1280 NEXTC
1285 GOSUB 5000
1290 INPUT"DO YOU WANT THE GRAPH PRINTED TYPE(Y/N)";D$
1293 IF D$="Y" THEN4200 ELSE 1300
1300 END

```

```

1480 RETURN
2000 PRINT"DO YOU WANT PRINTER OUTPUT"
2010 INPUT"TYPE(Y/N)";B$
2020 IF B$="Y" THEN2030 ELSE 2090
2030 PRINTER3
2035 LPRINT CHR$(18)
2040 LPRINT TAB(45);"GPC COPOLYMER ANALYSIS":LPRINT:LPRINT
2042 LPRINT;E1$:LPRINT TAB(50);"FILE NAME";D1$:LPRINT:LPRINT
2043 LPRINT"THE A BLOCK UNIT IS ";C2$:LPRINTTAB(50);"SOLVENT ";E2$
2044 LPRINT"THE B BLOCK UNIT IS ";A$:LPRINT:LPRINT
2045 LPRINT"THE RESPONSE FACTORS FOR ";C2%;" ARE"
2046 LPRINT TAB(10);"UV=";U1;TAB(40);"RI=";R1:LPRINT
2047 LPRINT "THE RESPONSE FACTORS FOR ";A%;" ARE"
2048 LPRINT TAB(10);"UV=";U2;TAB(40);"RI=";R2:LPRINT
2049 LPRINT TAB(25);"MOL.WT. OF ";C2%;" BLOCK IS";M1:LPRINT
2050 LPRINT C2%;" CALIBRATION CURVE DATA":LPRINT:LPRINT TAB(10);
      "SLOPE";S1;TAB(50);"INTERCEPT";I1
2051 LPRINT A%;" CALIBRATION DATA":LPRINT:LPRINT TAB(10);"SLOPE";
      S2;TAB(50);"INTERCEPT";;I2
2052 LPRINT:LPRINT:LPRINT
2055 LPRINT TAB(82);"AB";TAB(113);"ABA"
2056 LPRINT
2060 LPRINT TAB(10);"Vri";TAB(20);"Hri";TAB(30);"Huv";TAB(40);
      "R";TAB(60);"WTF";TAB(75);"MWT";TAB(90);"WTF";TAB(105);"MWT",
2070 LPRINT TAB(120);"WTF"
2090 RETURN
2500 INPUT"DATE LIKE 17/5/83";E1$:PRINT
2505 INPUT"SOLVENT USED";E2$:PRINT
2510 INPUT"NAME OF A BLOCK";C2$:PRINT
2515 INPUT"NAME OF SECOND BLOCK UNIT";A$
2520 PRINT
2540 PRINT"WHAT ARE THE RESPONSE FACTORS FOR ";C2$
2560 INPUT"UV";U1:INPUT"RI";R1
2580 PRINT
2600 PRINT"WHAT ARE THE RESPONSE FACTORS FOR"; A$
2620 PRINT
2660 INPUT"UV";U2:INPUT"RI";R2
2680 GOSUB 3000
2700 PRINT"NB.Vuv=Vri-2mm"
2720 PRINT" REMEMBER THE SCALING FACTOR IN PEAK HEIGHT"
2740 GOSUB 2000
2760 INPUT"NO. OF RUNS REQUIRED";N
2780 DIM K(9,N)
2800 RETURN
3000 INPUT"MOL.WT.OF A BLOCK";M1
3020 PRINT"ENTER THE SLOPE AND INTERECEPT OF Pst.CALIBRATION
      CURVE FOR SOLVENT USED"
3040 INPUT"SLOPE";S1:INPUT"INTERCEPT";I1
3060 PRINT"ENTER CAL.DATA FOR"; A$
3080 INPUT"SLOPE";S2:INPUT"INTERCEPT";I2
3100 RETURN
4000 LETZ1=10^(S1*C+I1)
4020 LET Z2=LOG(Z1-M1)/2.303
4040 LET Z3=(S2/S1)*(Z2-I1)+I2
4060 LET Z4=EXP(Z3)*2.303
4080 LET W5=Z4/(Z4+M1)

```

```

4100 LET Z5=LOG(Z1-(2*M1))/2.303
4120 LET Z6=(S2/S1)*(Z5-I1)+I2
4140 LET Z7=EXP(Z6)^2.303
4160 LET W6=Z7/(Z7+(2*M1))
4180 RETURN
4200 CALL"DUMP",0,0,319,191,1
4220 GOTO1300
5000 FOR J=1TON
5020 CALL"PLOT",(28*F4*(K(1,J)-F1)+39),(160*F7*(K(5,J)-F5)+31),3
5040 NEXTJ
5060 RETURN
5080 END
6000 LET K(4,J)=K(3,J)/K(2,J)
6020 LET A2=K(4,J)*(R2-R1)
6040 LET K(5,J)=(K(4,J)*R1-U1)/(U2-U1-A2)
6060 PRINT"WEIGHT FRACTION OF";A$;"IS";K(5,J)
6080 LET L1=10^(S1*(K(1,J))+I1)
6090 IF(L1-M1)>0 THEN 6100 ELSE 6220
6100 LET L2=LOG(L1-M1)/2.303
6120 LET L3=(S2/S1)*(L2-I1)+I2
6140 LET K(6,J)=EXP(L3)^2.303
6160 PRINT
6180 PRINT"THE MOL.WT.OF";A$;"IS";K(6,J)
6200 LET K(7,J)=K(6,J)/(K(6,J)+M1)
6220 PRINT:PRINT
6240 PRINT"THE WEIGHT FRACTION OF";A$;"IS";K(7,J)
6250 IF (L1-(2*M1))>0 THEN 6260 ELSE6400
6260 LETL5=LOG(L1-(2*M1))/2.303
6280 LET L6=(S2/S1)*(L5-I1)+I2
6300 LET K(8,J)=EXP(L6)^2.303
6320 PRINT:PRINT
6340 PRINT"THE ABA MOL.WT OF";A$;"IS";K(8,J)
6360 LETK(9,J)=K(8,J)/(K(8,J)+(2*M1))
6380 PRINT:PRINT
6400 PRINT"THE ABA WT. FRACTION IS";K(9,J)
6420 IF B$="Y"THEN6440 ELSE6480
6440 LPRINT TAB(9);K(1,J);TAB(19);K(2,J);TAB(29);K(3,J);TAB(38);
      K(4,J);TAB(57);K(5,J);TAB(73);K(6,J),
6460 LPRINT TAB(87);K(7,J);TAB(103);K(8,J);TAB(117);K(9,J)
6480 RETURN
6500 PRINT"1. NO DATA FILE":PRINT
6520 PRINT"2. NEW DATA FILE":PRINT
6540 PRINT"3. READ OLD DATA FILE":PRINT
6560 INPUT"ENTER AS APPROPRIATE(1,2,3)";Z1
6580 ON Z1 GOTO 40,6600,8000
6600 INPUT"NAME OF NEW FILE";D1$
6620 CREATEE10,D1$
6640 GOSUB 2500
6660 PRINTE10,E1$:PRINTE10,E2$:PRINTE10,C2$:PRINTE10,A$
6665 LET U1$=STR$(U1):U2$=STR$(R1):U3$=STR$(U2):U4$=STR$(R2)
6668 LET U5$=STR$(M1):U6$=STR$(S1):U7$=STR$(I1):U8$=STR$(S2)
6671 LET U9$=STR$(I2):Z1$=STR$(N)
6674 PRINTE10,U1$:PRINTE10,U2$:PRINTE10,U3$:PRINTE10,U4$:PRINTE10,U5$
6677 PRINTE10,U6$:PRINTE10,U7$:PRINTE10,U8$:PRINTE10,U9$:PRINTE10,Z1$
6680 FOR J=1TON
6700 INPUT"ENTER ELUTION VOL.INC=";K(1,J):Z2$=STR$(K(1,J)):PRINTE10,Z2$

```

```

6720 INPUT"HEIGHT OF RI AT EL.VOL.INmm";K(2,J):Z3%=STR$(K(2,J)):PRINT#10,Z3%
6740 INPUT"HEIGHT OF RI AT EL.VOL.INmm";K(3,J):Z4%=STR$(K(3,J)):PRINT#10,Z4%
6760 GOSUB6000
6780 NEXT J
6790 CLOSE#10
6800 GOTO760
8000 INPUT"NAME OF FILE";D1%
8020 OPEN#10,D1%
8040 INPUT#10,E1%:INPUT#10,E2%:INPUT#10,C2%:INPUT#10,A%
8043 INPUT#10,U1%:INPUT#10,U2%:INPUT#10,U3%:INPUT#10,U4%:INPUT#10,U5%
8046 INPUT#10,U6%:INPUT#10,U7%:INPUT#10,U8%:INPUT#10,U9%:INPUT#10,Z1%
8049 LET U1=VAL(U1%):R1=VAL(U2%):U2=VAL(U3%):R2=VAL(U4%):M1=VAL(U5%)
8052 LET S1=VAL(U6%):I1=VAL(U7%):S2=VAL(U8%):I2=VAL(U9%):N=VAL(Z1%)
8060 DIM X(9,N)
8070 GOTO8300
8080 GOSUB2000
8100 FOR J=1TON
8120 INPUT#10,Z2%,Z3%,Z4%
8140 K(1,J)=VAL(Z2%):K(2,J)=VAL(Z3%):K(3,J)=VAL(Z4%)
8160 GOSUB6000
8180 NEXTJ
8200 GOTO760
8300 PRINT"DATE ";E1%
8320 PRINT"SOLVENT ";E2%
8340 PRINT"A BLOCK UNIT ";C2%
8360 PRINT"B BLOCK UNIT";A%
8380 CALL"CLEAR"
8400 GRAPH1
8420 CALL"RESOLUTION",0,2
8440 CALL"COLOUR",0,0,0,1
8460 CALL"COLOUR",2,7,7,0
8480 PLOT 20,56,"PARAMETERS DEFINED ARE"
8500 PLOT 20,52,"RESPONSE FACTORS"
8520 PLOT 18,47,"UV":PLOT35,47,"RI"
8540 PLOT 10,42,"A":PLOT 10,37,"B"
8560 PLOT 20,30,"CALIBRATION DATA"
8580 PLOT 18,27,"SLOPE":PLOT35,27,"INTERCEPT"
8600 PLOT10,22,"A":PLOT10,15,"B"
8620 X1%=STR$(U1):X2%=STR$(R1):X3%=STR$(U2):X4%=STR$(R2)
8640 CALL"STPLOT",55,135,VARADR(X1%),2
8660 CALL"STPLOT",122,135,VARADR(X2%),2
8680 CALL"STPLOT",55,115,VARADR(X3%),2
8700 CALL"STPLOT",122,115,VARADR(X4%),2
8720 X5%=STR$(S1):X6%=STR$(I1):X7%=STR$(S2):X8%=STR$(I2)
8740 CALL"STPLOT",50,67,VARADR(X5%),2
8760 CALL"STPLOT",125,67,VARADR(X6%),2
8780 CALL"STPLOT",50,44,VARADR(X7%),2
8800 CALL"STPLOT",125,44,VARADR(X8%),2
8820 PLOT2,7,"DO YOU WISH TA CHANGE ANY PARAMETERS"
8840 INPUT"TYPE(Y/N)";P1%
8860 GRAPH0
8880 IFP1%="N"THEN8080 ELSE IF P1%="Y"THEN8900 ELSE8820
8900 PRINT" DO YOU WISH TO CHANGE"
8920 PRINT
8940 PRINT"1. RESPONSE FACTORS"
8960 PRINT"2. CALIBRATION DATA"

```

```
8980 INPUT P1
9000 ON P1 GOTO9020,9280
9020 PRINT" DO YOU WISH TO CHANGE"
9040 PRINT"1 UV.OF A";PRINT"2. RI.OF A"
9060 PRINT"3.UV.OF B";PRINT"4. RI.OF B"
9080 INPUT P2
9100 ON P2 GOTO 9120,9160,9200,9240
9120 INPUT"TYPE IN NEW UV.OF A";U1
9140 GOTO8380
9160 INPUT"TYPE IN NEW RI.OFA";R1
9180 GOTO8380
9200 INPUT"TYPE IN NEW UV.OF B";U2
9220 GOTO8380
9240 INPUT"TYPE IN NEW RI.OF B";R2
9260 GOTO8380
9280 PRINT"1. SLOPE OF A";PRINT"2. INTERCEPT OF A"
9300 PRINT"3. SLOPE OF B";PRINT"4. INTERCEPT OF B"
9320 INPUT P3
9340 ON P3 GOTO 9360,9400,9440,9480
9360 INPUT"TYPE IN NEW SLOPE FOR A";S1
9380 GOTO8380
9400 INPUT"TYPE IN NEW INTERCEPT FOR A";I1
9420 GOTO8380
9440 INPUT"TYPE IN NEW SLOPE FOR B";S2
9460 GOTO8380
9480 INPUT"TYPE IN NEW INTERCEPT FOR B";I2
9550 GOTO8380
```